

**EFFECTIVENESS OF LOCAL COOLING ON ENHANCING TISSUE ISCHEMIA
TOLERANCE IN PEOPLE WITH SPINAL CORD INJURY**

by

Yi-Ting Tzen

Bachelor of Science, National Taiwan University, 2005

Master of Science, University of Pittsburgh, 2008

Submitted to the Graduate Faculty of
School of Health and Rehabilitation Science in partial fulfillment
of the requirements for the degree of
Doctor of Philosophy

University of Pittsburgh

2010

UNIVERSITY OF PITTSBURGH
SCHOOL OF HEALTH AND REHABILITATION SCIENCE

This dissertation was presented

by

Yi-Ting Tzen

It was defended on

July 28th, 2010

and approved by

George Carvell, Professor, Department of Physical Therapy

Patrick J. Loughlin, Professor, Departmental of Bioengineering

Patricia E. Karg, Assistant Professor, Department of Rehabilitation Science and Technology

Mary Jo Geyer, Assistant Professor, Department of Rehabilitation Science and Technology

Dissertation Advisor: David M. Brienza, Professor, Department of Rehabilitation Science
and Technology

Copyright © by Yi-Ting Tzen

2010

**EFFECTIVENESS OF LOCAL COOLING ON ENHANCING TISSUE ISCHEMIA
TOLERANCE IN PEOPLE WITH SPINAL CORD INJURY**

Yi-Ting Tzen, Ph.D.

University of Pittsburgh, 2010

People with spinal cord injury (SCI) are at risk of pressure ulcer development due to impaired mobility, sensation or changes in tissue properties. Increased skin temperature is one of the least explored risk factors for pressure ulcers. Since people with SCI also encounter thermoregulation deficits, investigation of the effectiveness of local skin cooling in this population is particularly important. Three groups of subjects were recruited: 1) 14 subjects with SCI at T6 and above, 2) 8 subjects with SCI below T6, and 3) 14 healthy controls. Reactive hyperemic response was the main study outcome and was measured after three different combinations of stimuli: 1) pressure only, 2) pressure with fast cooling ($-4^{\circ}\text{C}/\text{min}$) and 3) pressure with slow cooling ($-0.33^{\circ}\text{C}/\text{min}$). Spectral density of the skin blood flow (SBF) was used to investigate the underlying microcirculatory control mechanisms. Five of the subjects did not have reactive hyperemia in all test sessions and were excluded from statistical analysis. In the control group, the normalized peak SBF and perfusion area were close to significantly greater in pressure only as compared to fast cooling ($p=0.023$ and $p=0.023$, respectively) and slow cooling ($p=0.033$ and $p=0.016$, respectively). Although this phenomenon was not significant when analyzing subjects with SCI alone, significant changes were observed in the signal attributed to the metabolic control mechanism and were observed in this population with pressure only ($p=0.019$) and pressure with slow cooling ($p=0.041$).

Since the reactive hyperemic response is mediated by different control mechanisms, the less obvious changes in reactive hyperemia in people with SCI may be due to alterations in microcirculation after injury. Results from this study suggest that local skin cooling is beneficial to ischemic tissue by decreasing the metabolic demand, and this is generally consistent with previous animal studies and our pilot study. Findings from this study also suggest that investigating time domain parameters and time-dependent spectral analysis of the SBF signal is helpful in understanding circulatory control in people with different levels of neurological deficits. This study contributes toward justification for the development of support surfaces with microclimate controls to enhance tissue integrity.

TABLE OF CONTENTS

PREFACE.....	XX
1.0 INTRODUCTION	1
1.1 OBJECTIVES AND SPECIFIC AIMS	2
1.1.1 Hypothesis 1 and its rationale	2
1.1.2 Hypothesis 2 and its rationale	3
1.2 SIGNIFICANCE.....	6
2.0 BACKGROUND	7
2.1 PRESSURE ULCER DEFINITION AND PREVALENCE.....	7
2.2 ETIOLOGY OF PRESSURE ULCERS.....	8
2.2.1 Prolonged pressure	8
2.2.1.1 Tissue ischemia.....	10
2.2.1.2 Ischemic-reperfusion injury	10
2.2.1.3 Cell deformation	12
2.2.2 Pressure in combination with shear force.....	13
2.3 RISK FACTORS OF PRESSURE ULCERS.....	16
2.3.1 Impaired sensation	17
2.3.2 Decreased mobility and activity.....	17
2.3.3 Increased skin temperature.....	18

2.3.3.1	Findings from animal studies	19
2.3.3.2	Findings from human study.....	21
2.3.3.3	Impaired thermoregulation in people with SCI.....	23
(a)	Central control mechanisms	23
(b)	Local control mechanisms.....	25
2.3.4	Changes in tissue property	26
2.4	BENEFITS OF LOCAL SKIN COOLING	27
2.4.1	Reduced metabolic demand during tissue ischemia	28
2.4.2	Decreased ischemia-reperfusion injury	29
2.4.3	Selection of different cooling rates	30
2.5	INDIRECT MEASUREMENT OF TISSUE RESPONSE	32
2.5.1	Reactive hyperemia.....	32
2.5.1.1	Physiological control mechanisms of reactive hyperemia...	33
2.5.1.2	Parameters of reactive hyperemia	35
2.5.2	Laser Doppler flowmetry system.....	37
2.6	SKIN BLOOD FLOW SIGNAL PROCESSING	38
2.6.1	Exponential curve-fitting of the reactive hyperemia	38
2.6.2	Time-frequency analysis of the SBF signal.....	40
3.0	METHODS	44
3.1	RESEARCH DESIGN.....	44
3.2	SUBJECTS.....	45
3.3	PROCEDURES.....	45
3.3.1	Screening procedure	46

3.3.2	Experimental procedure.....	46
3.4	INSTRUMENTATION.....	49
3.4.1	Computer-controlled indenter.....	50
3.4.2	Cooling system.....	51
3.4.3	Laser Doppler flowmetry.....	52
3.5	OUTCOME MEASURES AND DATA ANALYSIS.....	53
3.5.1	Outcome measures and SBF signal processing.....	53
3.5.2	Statistical analysis.....	59
4.0	RESULTS.....	61
4.1	EXISTENCE OF REACTIVE HYPEREMIA.....	61
4.2	RANDOMIZATION OF THE ORDER OF TEST SESSIONS.....	64
4.3	DEMOGRAPHIC DATA.....	65
4.4	PRESSURE APPLIED ON THE SKIN.....	67
4.4.1	Results from subjects that had reactive hyperemia in pressure only test session.....	67
4.4.2	Results from subjects with no reactive hyperemic response in all test sessions.....	70
4.5	SKIN TEMPERATURE.....	73
4.5.1	Results from subjects that had reactive hyperemia in pressure only test session.....	73
4.5.2	Results from subjects with no reactive hyperemic response in all test sessions.....	77
4.6	SKIN BLOOD FLOW.....	79

4.6.1	Baseline SBF	80
4.6.2	Reactive hyperemic response compared within subjects	82
4.6.2.1	Hypothesis 1a) and 1b): normalized peak	82
4.6.2.2	Hypothesis 1c) and 1d): perfusion area	85
4.6.2.3	Other parameters: time to peak and half life.....	88
4.6.2.4	Normalized spectral densities	92
(a)	Metabolic spectral density.....	92
(b)	Neurogenic spectral density	95
(c)	Myogenic spectral density	97
4.6.3	Reactive hyperemic response compared among groups.....	99
4.6.3.1	Hypotheses 2 a) b) e) and f): decreased normalized peak SBF with local cooling.....	99
4.6.3.2	Hypotheses 2 c) d) g) and h): decreased perfusion area with local cooling	101
5.0	DISCUSSION	104
5.1	SUMMARY OF MAJOR FINDINGS.....	104
5.2	TEST CONDITIONS	105
5.3	EFFECTIVENESS OF DIFFERENT COOLING RATES IN CONTROL GROUP.....	105
5.4	EFFECTIVENESS OF DIFFERENT COOLING RATES IN PEOPLE WITH SCI.....	108
5.5	DIFFERENCES IN COOLING EFFECTS ON PEOPLE WITH VARIOUS LEVELS OF NEUROLOGICAL DEFICITS	111

5.6 SUBJECTS WITH NO REACTIVE HYPEREMIA IN ALL TEST SESSIONS.....	113
5.7 LIMITATIONS.....	113
6.0 CONCLUSION	115
APPENDIX A.....	116
APPENDIX B	171
BIBLIOGRAPHY	187

LIST OF TABLES

Table 1. 3x3 mixed factorial design.....	44
Table 2. Randomization of the order of test sessions.	47
Table 3. Details of existence of reactive hyperemic response in all subjects.	63
Table 4. Number of subjects within each group that underwent each order of the three test sessions.	64
Table 5. Number of subjects within each group that underwent each order of the three test sessions.	64
Table 6. Summary of subjects' demographic data.	65
Table 7. Detailed demographic information of all subjects.....	66
Table 8. Mean and standard deviation of applied pressure on the sacral skin during baseline.	68
Table 9. Mean and standard deviation of applied pressure on the sacral skin during 60mmHg of target pressure.....	68
Table 10. Mean and standard deviation of applied pressure on the sacral skin during reactive hyperemia.	68
Table 11. Mean and standard deviation of skin temperature during baseline.	74
Table 12. Mean and standard deviation of skin temperature at the end of 60mmHg pressure.	74

Table 13. Mean and standard deviation of skin temperature during reactive hyperemia.	75
Table 14. Mean and standard deviation of baseline SBF, and the results of the two-way repeated measures ANOVA.....	80
Table 15. Mean and standard deviation of normalized peak SBF and the results of the Friedman test (N=31).....	82
Table 16. Mean and standard deviation of normalized peak SBF and the results of the Friedman tests computed separately by group.....	84
Table 17. Mean and standard deviation of perfusion area and the results of the Friedman test (N=31).....	85
Table 18. Mean and standard deviation of perfusion area and the results of the Friedman tests computed separately by group.....	87
Table 19. Mean and standard deviation of time to peak and the results of the Friedman test (N=17).....	88
Table 20. Mean and standard deviation of time to peak and the results of the Friedman tests computed separately by group.....	89
Table 21. Mean and standard deviation of half life and the results of the Friedman test (N=17).....	90
Table 22. Mean and standard deviation of half life and the results of the Friedman tests computed separately by group.....	91
Table 23. Mean and standard deviation (SD) of normalized metabolic spectral densities during reactive hyperemia.....	93
Table 24. Mean and standard deviation (SD) of normalized neurogenic spectral densities during reactive hyperemia.....	96

Table 25. Mean and standard deviation (SD) of normalized myogenic spectral densities during reactive hyperemia..... 98

Table 26. Mean and standard deviation (SD) of percent change of normalized peak SBF in all subjects (excludes those with no reactive hyperemia in all test sessions). 100

Table 27. Mean and standard deviation (SD) of percent change of perfusion area in all subjects (exclude those with no reactive hyperemia in all test sessions)..... 102

LIST OF FIGURES

Figure 1. Reactive hyperemia time domain parameters.....	36
Figure 2. Physical model of reactive hyperemia.....	40
Figure 3. Test setting.....	48
Figure 4. Pressure application phases.	48
Figure 5. Computer control interface created with LabVIEW.	49
Figure 6. Computer-controlled indenter.	50
Figure 7. Thermoelectric cooling system at the tip of the indenter.	52
Figure 8. Schematic figure of outcome measures collected.	53
Figure 9. Schematic figure of steps of signal processing.....	54
Figure 10. Steps of skin blood flow signal processing.	55
Figure 11. Summary of the existence of reactive hyperemic response. RH = reactive hyperemia.....	62
Figure 12. Average applied pressure during three test sessions on subjects with reactive hyperemia in control group.....	69
Figure 13. Average applied pressure during three test sessions on subjects with reactive hyperemia in T6A group.....	69
Figure 14. Average applied pressure during three test sessions on subjects with reactive hyperemia in T6B group.....	70

Figure 15. Average applied pressure during three test sessions on the subject without reactive hyperemia in control group.	71
Figure 16. Average applied pressure during three test sessions on subjects without reactive hyperemia in T6A group.	72
Figure 17. Average applied pressure during three test sessions on subjects without reactive hyperemia in T6B group.	72
Figure 18. Averaged skin temperature during three test sessions on subjects with reactive hyperemia in control group.	75
Figure 19. Averaged skin temperature during three test sessions on subjects with reactive hyperemia in T6A group.	76
Figure 20. Averaged skin temperature during three test sessions on subjects with reactive hyperemia in T6B group.	76
Figure 21. Averaged skin temperature during three test sessions on the subject without reactive hyperemia in control group.	78
Figure 22. Averaged skin temperature during three test sessions on subjects without reactive hyperemia in T6A group.	78
Figure 23. Averaged skin temperature during three test sessions on subjects without reactive hyperemia in T6B group.	79
Figure 24. Box plots of baseline SBF in all subjects (excluding those without reactive hyperemia in all test sessions).....	81
Figure 25. Box plots of baseline SBF in subjects without reactive hyperemia in all test sessions.	81

Figure 26. Box plots of normalized peak SBF in all subjects (excluding those without reactive hyperemia in all test sessions)..... 83

Figure 27. Box plots of normalized peak SBF by group in all subjects (excluding those without reactive hyperemia in all test sessions)..... 84

Figure 28. Box plots of perfusion area in all subjects (excludes those without reactive hyperemia in all test sessions)..... 86

Figure 29. Box plots of perfusion area by group in all subjects (excludes those without reactive hyperemia in all test sessions)..... 87

Figure 30. Box plots of time to peak SBF in all subjects (excludes those without reactive hyperemia in all test sessions)..... 89

Figure 31. Box plots of time to peak by group in all subjects (excludes those without reactive hyperemia in all test sessions)..... 90

Figure 32. Box plots of half life in all subjects (excludes those without reactive hyperemia in all test sessions)..... 91

Figure 33. Box plots of half life by group in all subjects (excludes those without reactive hyperemia in all test sessions)..... 92

Figure 34. Box plots of normalized metabolic spectral density in all subjects (excludes those without reactive hyperemia in all three sessions)..... 94

Figure 35. Box plots of normalized metabolic spectral density in subjects with no reactive hyperemia in all test sessions..... 95

Figure 36. Box plots of normalized neurogenic spectral density in all subjects (excludes those without reactive hyperemia in all test sessions)..... 96

Figure 37. Box plots of normalized neurogenic spectral density in subjects with no reactive hyperemia in all test sessions.	97
Figure 38. Box plots of normalized myogenic spectral density in all subjects (excludes those without reactive hyperemia in all test sessions).	98
Figure 39. Box plots of normalized myogenic spectral density in subjects with no reactive hyperemia in all three test sessions.	99
Figure 40. Box plots of changes in normalized peak SBF from pressure only in all three groups.	101
Figure 41. Box plots of changes in perfusion area from pressure only in all three groups.	103

LIST OF EQUATIONS

Equation 1. Current 'I' in Figure 2 calculated based on Ohm's Law	40
Equation 2. Bi-exponential function of time simplified from Equation 1.	40
Equation 3. Fourier expansion of signal (addition of sinusoids, $e^{j\omega t}$, with different frequencies).....	42
Equation 4. Fourier analysis.	42
Equation 5. Fourier transform of signal $s(\tau)$ around time t , and $h(\tau-t)$ is the window function.	43
Equation 6. Bi-exponential equation for curve fitting.	56
Equation 7. Derivative of equation 5.	57
Equation 8. Time to peak SBF calculated from equation 6.	57
Equation 9. Peak SBF.	57
Equation 10. Normalized peak SBF. \bar{S} is the baseline SBF.	57
Equation 11. Perfusion area. \bar{S} is the baseline SBF.	57
Equation 12. Spectrogram.....	58
Equation 13. Normalized metabolic spectral density.	58
Equation 14. Normalized neurogenic spectral density.	58
Equation 15. Normalized myogenic spectral density.	58
Equation 16. Percent changes in normalized peak SBF with fast cooling.....	59

Equation 17. Percent changes in perfusion area with fast cooling.	59
Equation 18. Percent changes in normalized peak SBF with slow cooling.....	59
Equation 19. Percent changes in perfusion area with slow cooling.....	59

PREFACE

The process of completing this dissertation was a wonderful journey. It was not just reading articles and experimenting, but also networking with other professions and people that are in need of the technology to solve everyday problems, and constantly modifying the direction of the research. It is also a process of learning how to criticize logically and solving problems that I was faced with. There were ups and downs during this journey, and I always encouraged myself with Johannes Brahms' masterpiece: Symphony No. 1, Op. 68. With constant self-critics and self-expectations to be as great as Ludwig van Beethoven, Brahms spent 21 years to complete this great piece of artwork. To me, this five-year of pressure ulcer research is like composing a piece of symphonic music; all notes should be in perfect positions and each instrument had its own role. In addition, the goal of this work was to extend the findings from animal studies that was done 15 years ago to human research.

Throughout this process, I would like to thank so many people that made this dissertation a beautiful dream come true and a pleasant journey to remember. I would like to thank:

- Dr. David Brienza for funding my graduate study for the past five years and guiding/advising me the right direction to complete this work.

- Dr. Patrick Loughlin for endless support and guidance on signal processing, which is an extremely big portion of this study.
- Dr. George Carvell for challenging my logic all the time during the process of completing this project and guiding me to think and solve the problems.
- Professor Patricia Karg for supporting this project and guiding me to think and solve the problems.
- Dr. Mary Jo Geyer for supporting and guiding me in this project with a clinician's point of view.
- Mr. Erik Porach for endless technical support of this project from instrument development to maintenance during subject testing.
- Staff from Department of Physical Medicine and Rehabilitation, UPMC: Ms. Karen Greenwald, Ms. Tina Harrison and Mr. Ian Smith for assisting me in recruiting subjects for this study.
- Pittsburgh Steelwheeler Quad-Rugby team and Basketball team for disseminating the research information and participating in this research study.
- All participants in this study for actually making this project possible.
- Colleagues from Dept. of Rehabilitation Science and Technology Bakery Square Office: Ms. Debby Keelan, Ms. Cheryl Rohall, Mr. Joe Ruffing, Ms. Linda Szczepanski, Dr. Linda van Roosmalen, Dr. Ana Allegretti, Dr. Rich Schein for endless support throughout this five years.
- My "boys and girls": Krissy Glauser, AJ Malkiewicz, David Smeresky, Sean Douth, Chaz Vukotich for supporting me and keeping me company throughout different stages of my dissertation works.

- My beloved parents Kai-Yuan Tzen, and Shwu-Jen Chen, and the Tzen and Chen's relatives for continuous support both day and night, remotely from Taiwan.
- My family in Pittsburgh: Emily Chin Fair, Shawn Fair, baby Katherine, Faye Ho Wang, and Alex Wang for supporting me, be with me when I was in need, and pray with me when I was weak.
- The professors and my classmates from Department of Physical Therapy, National Taiwan University for supporting me remotely from Taiwan for the past five years.
- Last but not least, thank Lord Jesus for making all the good things and miracles happened throughout this unforgettable journey.

1.0 INTRODUCTION

People with SCI are susceptible to pressure ulcer development at weight bearing areas due to impaired mobility, sensation or changes in tissue properties. Increased skin temperature is one of the least explored risk factors for pressure ulcers. Previous studies found that when the skin was in close contact with support surfaces for a prolonged period of time, the skin temperature increased (Cochran, 1985; Fisher, Szymke, Aptem, & Kosiak, 1978; S. F. C. Stewart, Palmieri, & Cochran, 1980). Findings from previous animal studies suggested that local cooling provided a protective effect of the skin during prolonged pressure (Iaizzo, et al., 1995; Kokate, et al., 1995). However, there was limited information on the cooling effect for people in high-risk populations. In addition, there was no rationale for selecting the most effective cooling rate. Human thermoregulation is mediated through both central and local control mechanisms, and people with SCI may encounter impairments in thermoregulation due to central and/or the local control deficits. So far, there is limited information on the tissue response to local cooling in the SCI population. Reactive hyperemia is a non-invasive measurement widely used in examining tissue response to ischemia. For this study, reactive hyperemia is used to provide information on the various circulatory control mechanisms when the skin is stimulated with temperature and pressure changes and for people with different levels of neurological deficit and those without SCI.

1.1 OBJECTIVES AND SPECIFIC AIMS

The objective of this study was to investigate the effectiveness of local cooling on enhancing weight-bearing tissue tolerance on at-risk human skin. The three specific aims are: 1) to investigate the SBF response to local cooling at two different cooling rates in weight-bearing sacral tissues, 2) to investigate the difference in SBF response to local stimuli (pressure and cooling) on people with different degrees of neurological impairment, and 3) to investigate the underlying vascular control mechanisms to local stimuli on people with different degrees of neurological impairments.

1.1.1 Hypothesis 1 and its rationale

Previous animal and human studies showed that local skin cooling had a protective effect on ischemic tissue (Iaizzo, et al., 1995; Kokate, et al., 1995; Tzen, Brienza, Karg, & Loughlin, 2010), possibly by decreasing the tissue metabolic rate during ischemia (Rowell, 1974). A study on human vascular response during local skin cooling found that the decreased SBF with local cooling application was a combined result of vasodilation and vasoconstriction controlled by different mechanisms (Yamazaki, et al., 2006). They also found that the initial vasodilation response is significantly more obvious with fast cooling than with slow cooling. Given that the tissue metabolic rate depends on the tissue temperature, with less vasoconstriction response with fast cooling of the skin, less severe tissue ischemia was expected with fast cooling as compared to slow cooling.

Reactive hyperemia has been widely used to investigate the tissue viability non-invasively, and parameters such as normalized peak SBF and perfusion area each represent the

severity of tissue ischemia and metabolic repayment, respectively (Hagisawa, Ferguson-Pell, Cardi, & Miller, 1994). Therefore, this physiological response was selected as an outcome measurement of this study by inducing this response with tissue ischemia at 60 mmHg for 20 minutes. Local skin cooling (both fast and slow) was applied during the 20 minutes, and was removed at the end of the 20 minutes. The reactive hyperemic response was measured immediately after the release of 60 mmHg of pressure for 10 minutes for comparison among three test sessions. A detailed diagram of the pressure and temperature applications is in section 3.3.2.

Based on the specific aim 1 and previously described rationale, I hypothesize that:

- 1) In people with and without SCI, after cessation of 20 minutes of 60 mmHg pressure,
 - a) the skin without local cooling will have a greater normalized peak SBF as compared to the skin with fast cooling and skin with slow cooling.
 - b) the skin with slow cooling will have a greater normalized peak SBF as compared to the skin with fast cooling.
 - c) the skin without local cooling will have a greater perfusion area as compared to the skin with fast cooling and skin with slow cooling.
 - d) the skin with slow cooling will have a greater perfusion area as compared to the skin with fast cooling.

1.1.2 Hypothesis 2 and its rationale

People with SCI have decreased thermoregulation as compared to healthy controls (Sae-Sia, Wipke-Tevis, & Williams, 2007). This may be caused by impaired thermoregulation through both central and local nervous systems (Kellogg, 2006). People with complete injury level at T6

and above have impaired sensation as well as central control of the circulatory system. Although people with complete injury below T6 have intact central control of circulation, the impaired sensation after injury may cause decreased thermoregulation as compared to people without SCI. Since the initial vasoconstriction upon local skin cooling requires both intact sensory and autonomic functions (Johnson, Yen, Zhao, & Kosiba, 2005), subjects with injury level at T6 and above were expected to have less initial vasoconstriction upon cooling as compared to subjects with injury level below T6 and healthy controls. In addition, subjects with injury level below T6 were expected to have less vasoconstriction as compared to healthy controls. Therefore, cold induced vasodilation was expected to be greatest in subjects with injury level above T6 and least in healthy controls. Based on this, a slighter reactive hyperemic response was expected in subjects with injury level at T6 and above during fast cooling, and decreases in normalized peak SBF and perfusion area from pressure only were expected to be greatest in this group as compared to the other two groups.

Based on specific aim 2, we hypothesize that:

- 2) After the cessation of 20 minutes of 60 mmHg pressure,
 - a) the skin with local fast cooling during pressure application will have a greater decrease in normalized peak SBF from pressure only for people with injury level at T6 and above as compared to people with injury level below T6 and without SCI.
 - b) the skin with local fast cooling during pressure application will have a greater decrease in normalized peak SBF from pressure only for people with injury level below T6 as compared to people without SCI.

- c) the skin with local fast cooling during pressure application will have a greater decrease in perfusion area from pressure only for people with injury level at T6 and above as compared to people with injury level below T6 and without SCI.
- d) the skin with local fast cooling during pressure application will have a greater decrease in perfusion area from pressure only for people with injury level below T6 as compared to people without SCI.
- e) the skin with local slow cooling during pressure application will have a greater decrease in normalized peak SBF from pressure only for people with injury level at T6 and above as compared to people with injury level below T6 and without SCI.
- f) the skin with local slow cooling during pressure application will have a greater decrease in normalized peak SBF from pressure only for people with injury level below T6 as compared to people without SCI.
- g) the skin with local slow cooling during pressure application will have a greater decrease in perfusion area from pressure only for people with injury level at T6 and above as compared to people with injury level below T6 and without SCI.
- h) the skin with local slow cooling during pressure application will have a greater decrease in perfusion area from pressure only for people with injury level below T6 as compared to people without SCI.

1.2 SIGNIFICANCE

This study enhanced the understanding of the relationship between local cooling and weight-bearing tissue tolerance in two aspects. First, findings from this study reflected the physiological response of people at risk of pressure ulcer development. Previous studies that investigated the effect of local cooling under pressure were performed either on animals (Iaizzo, et al., 1995; Kokate, et al., 1995) or on young healthy adult human subjects (Tzen, et al., 2010). This study was the first to investigate the cooling effect on people with different levels of neurological deficit. Secondly, results from this study provided information for selecting the most effective cooling rate on enhancing tissue tolerance. Previous animal and human studies cooled the skin to target temperature as soon as pressure was applied (Iaizzo, et al., 1995; Kokate, et al., 1995; Tzen, et al., 2010). However, a study that investigated two different cooling rates showed that fast cooling caused smaller vasoconstriction as compared to slow cooling (Yamazaki, et al., 2006). This study considers the rate of local cooling instead of just the target temperature alone, and findings from this work may assist in future design of support surfaces (e.g., seat cushions, mattresses) with local cooling features.

2.0 BACKGROUND

2.1 PRESSURE ULCER DEFINITION AND PREVALENCE

Pressure ulcers are “localized injury to the skin and/or underlying tissue usually over a bony prominence, as a result of pressure, or pressure in combination with shear and/or friction” (National Pressure Ulcer Advisory Panel, 2007a). It is often found with people who have limited mobility or impaired sensation, such as people with spinal cord injury (Cardenas, Hoffman, Kirshblum, & McKinley, 2004; Haisma, et al., 2007; Paker, et al., 2006), hospitalized patients (Allman, 1997; Lindgren, Unosson, Fredrikson, & Ek, 2004), or the elderly population (Allman, 1989; Amlung, Miller, & Bosley, 2001).

Pressure ulcers occur in both acute and long-term care settings. The prevalence of pressure ulcers ranges from 14-17% in acute care settings (Whittington & Briones, 2004), and remains high in chronic immobilized individuals. In long-term care settings, the prevalence of pressure ulcers ranges from 15-30% in chronic SCI population (Gelis, et al., 2009; Raghavan, Raza, Ahmed, & Chamberlain, 2003). People with SCI are at high risk of developing pressure ulcers mainly due to the impaired sensation and motor function after their injuries (Bogie & Bader, 2005). The prevalence remains the same within 10 years of injury and increases slightly later on (Y. Chen, DeVivo, & Jackson, 2005). The high prevalence in the SCI population makes pressure ulcers one of the most common secondary complications in this population (36%) along

with urinary track infection (47-49%) (Haisma, et al., 2007; McKinley, Jackson, Cardenas, & DeVivo, 1999). They are also one of the most frequent causes for re-hospitalization in this population (17.9%) (Paker, et al., 2006), especially in people with complete injuries (Cardenas, et al., 2004).

2.2 ETIOLOGY OF PRESSURE ULCERS

To date, the etiology of pressure ulcer development is not yet fully understood nor fully explored (Bouten, Oomens, Colin, & Bader, 2005). However, most researchers agree that prolonged pressure and pressure in combination with shear force are the two main etiological factors causing pressure ulcers (Yarkony, 1994).

2.2.1 Prolonged pressure

Pressure ulcers are usually located at sites that are subjected to prolonged pressure, especially areas of bony prominence, including malleolus, elbow, sacrum, greater trochanter, ischial tuberosity and heel (Bansal, Scott, Stewart, & Cockerell, 2005). In early animal studies, researchers examined the effect of pressure by inducing pressure ulcers on the animals with different magnitudes and durations of pressure. For example, Kosiak (1961) applied seven different magnitudes of localized pressure at the hamstring muscles (ranging from 35-240 mmHg) on both normal and paraplegic rats for one to four hours. Microscopic examination found that there was no change to the tissue under 35 mmHg of pressure, but when pressure was increased to 70 mmHg, about 10% of the muscle fiber damage was noted within two hours of

pressure application in both normal and paraplegic rats. This suggests that the higher the amount of pressure applied to the skin, the shorter the time required to induce the tissue breakdown.

With the enhancements in technology, later studies investigated the effect of prolonged pressure on at risk populations with the use of pressure mapping systems to measure the interface pressure and functional magnetic resonance imaging (MRI) to measure the underlying tissue deformation. A study by Brienza et al. (2001) investigated the interface pressure in a group of at-risk elderly wheelchair users. They found that both the mean peak pressure and the average of the highest four pressures were significantly higher in the people that developed pressure ulcers. This indicated that a higher interface pressure is related to the higher incidence of ulceration in the at-risk population. To understand the effect of pressure on loading within the tissue, later studies from Linder-Ganz et al., quantified the compressive stress and strain of the muscle and fat tissues at the buttock area with the use of MRI and finite element approach (Linder-Ganz & Gefen, 2007; Linder-Ganz, Shabshin, Itzhak, & Gefen, 2007). They built the finite element models of the buttock by using MRI with and without weight-bearing sitting in healthy participants. They found that the tissue strain and stress were higher in the muscle tissue than the skin (Linder-Ganz, et al., 2007). In the same paper, they further compared the internal tissue loads between at risk population and healthy controls and found that people at risk of pressure ulcer development had higher strain and stress in the muscle. Findings from these noninvasive measurements all suggest that loading of the soft tissue is the main etiologic factor of pressure ulcer formation.

Prolonged pressure is believed to cause ulceration through three different pathways: tissue ischemia, ischemic-reperfusion injury, and cell deformation (Bouten, et al., 2005).

2.2.1.1 Tissue ischemia

Previous studies found the relationship between tissue ischemia and pressure ulcer development by inducing the tissue damage and comparing the results with changes in SBF before and during pressure application. Salcido et al. (1995) applied 19 kPa (145 mmHg) of pressure on rats for 5 consecutive days (6 hours daily). They found that the SBF decreased from a baseline value to biological zero (no flow as measured by the laser Doppler flowmeter) during the pressure application phase. After the five days of pressure application, 90% of the animals developed pressure ulcers. This indicated that tissue ischemia is one of the main pathways of ulceration. Two studies suggested that decreased tissue oxygenation caused by tissue ischemia might be the underlying mechanism of tissue damage (Bader, 1990; Newson & Rolfe, 1982). Newson and Rolfe (1982) increased the pressure gradually until the blood flow was occluded (up to 40-50 kPa), and they found that the skin surface oxygen decreased with the increase of pressure. Bader (1990) measured the skin oxygen level during repetitive loading on human subjects, and he found that the skin oxygen levels decreased during the loading periods and increased when the loads were removed. A later study by Knight et al. (2001) investigated the oxygen level and the sweat metabolites at the sacral area of 14 human subjects during 5.3-16 kPa of pressure, and they report that when the tissue oxygen level is reduced to 60% below the baseline value, there is a significant inverse relationship between the percent reduction of oxygen level and sweat metabolites (i.e., lactate, urea). This indicates that tissue oxygen is a critical factor of tissue metabolism and this may explain the pathway of ulceration by tissue ischemia.

2.2.1.2 Ischemic-reperfusion injury

Another explanation of skin breakdown is the ischemic-reperfusion injury. A review article summarized that in many instances tissue damage did not occur during the hypoxia;

instead, it happened after tissue ischemia was relieved (McCord, 1985). This type of injury was identified in different organs, including heart, brain, kidney and liver (McCord, 1985). Pretto defined that ischemia-reperfusion was caused by blood reperfusion to the previously ischemic tissue (Pretto, 1991). The main pathway of this type of injury is the oxidative stress caused by the release of reactive oxygen and nitrogen species, e.g., free radicals (Taylor & James, 2005). Cells have antioxidant mechanisms that maintain the balance and function of the cell. However, when the release of free radicals upon reperfusion exceeds the cell's "free radical scavenging" capacity, tissue damage occurs (Pretto, 1991).

Researchers suspected that pressure ulcers might be caused by skin reperfusion as well, and they applied different reperfusion cycles on mice and compared the histological data afterwards (Peirce, Skalak, & Rodeheaver, 2000; Tsuji, Ichioka, Sekiya, & Nakatsuka, 2005). Peirce et al. (2000) investigated the effect of reperfusion by applying eight combinations of tissue ischemia and reperfusion (I/R) cycles on rats by compressing the dorsal skin at 50 mmHg. They measured the SBF, transcutaneous oxygen tension, and full-thickness biopsies 11.5 hours after the relief of the last compression cycle. They found that with the same durations of tissue ischemia, increased number of I/R cycles significantly increased the necrotic area, and decreased the SBF and oxygen tension 11.5 hours after the last compression cycle. They also discovered that with the same total amount of tissue ischemia (i.e. duration of ischemia per cycle times I/R cycles), the greater the number of I/R cycles, the greater the necrotic area. The group of rats with only one I/R cycle had the least damage and decreased SBF as compared to sites with more I/R cycles. This indicated that repeated ischemia-reperfusion were more harmful than prolonged ischemia alone (Peirce, et al., 2000). Tsuji et al. (2005) investigated the microcirculatory injury by using similar pressure application method. They divided mice into two groups. Each group

of mice had dorsal skin compression for 8 hours in total; one group had four cycles of compression and release (i.e. two hours of compression and one hour of reperfusion per cycle), and the other group had eight hours of continuous compression. Functional capillary density (FCD: total length of capillaries with red blood cell flow) was measured before (FCD_{pre}) and 35 hours after (FCD_{post}) the compression and release cycles, and the ratio of microcirculatory injury ($[1-(FCD_{post}/FCD_{pre})]*100\%$) was the outcome. They found that the group with four cycles of reperfusion had a significantly greater ratio as compared to continuous compression only. Findings of this study suggest that repetitive ischemia-reperfusion damages the microcirculation more than prolonged pressure alone, and this might contribute to the formation of pressure ulcers.

2.2.1.3 Cell deformation

Tissue damage also may be caused by compression-induced cell deformation. Several studies have investigated this effect by applying different amount of compressive strains on individual cells (Bouten, Knight, Lee, & Bader, 2001; Breuls, Bouten, Oomens, Bader, & Baaijens, 2003). Bouten et al. (2001) applied compressive strains of 0, 10, 20, 30, and 40% on mouse skeletal myoblasts that were seeded within agarose constructs, and 20% of compressive strain corresponding to 4.3 kPa of compressive stress. They measured the cell deformation by comparing the strained vs. unstrained diameters of the cell with a laser scanning microscope and assessed the cell damage by counting the percentage of membrane disruption or fragmentation to total cell number. They found that all myoblasts and 90% of myotubes deformed with 20% of compressive strain, while all myoblasts and myotubes deformed with 40% of compressive strain. They also discovered that with 20% of compressive strain, the percentage of cell damage was significantly higher than the unstrained group with cell compression for as short as one hour.

The percentage of cell damage increased significantly with longer period of cell compression. Breuls et al. (2003) used a similar pressure application protocol on skeletal muscle myotubes embedded in gel constructs, and measured the percentage of cell damage between three different compressive strains: 0, 30, and 50% (30-50% corresponded to the straining levels of muscle tissue near bony prominences as measured with animal MRI). They found 13.6% of cell death occurred immediately after 50% strain application; and four hours after strain relief, the percentage of cell damage was significantly greater in 50% strain than in 30% and 0% respectively. This suggested that a clinically relevant amount of compression alone could induce tissue damage, and greater compression caused more cell injury. A later study examined tissue deformation on a rat model with MRI (Stekelenburg, Oomens, Strijkers, Nicolay, & Bader, 2006). They applied 150 kPa of indentation on the tibialis anterior muscle on rats, and the pressure simulated the indentation of muscle tissue at bony prominences. T2-weighted (transverse relaxation time) MR images were taken during pressure application and up to 20 hours after pressure removal, and histology of the tissue was examined at 1, 4, and 20 hours after pressure removal. They found that the signal intensity of MR images increased immediately upon pressure relief, and histological data showed large tissue necrosis at one and four hours after pressure release. Since increased T2 has been widely recognized as a measurement for tissue damage, results from this study indicated that the tissue damage occurred right after pressure relief, and histological data supports this finding.

2.2.2 Pressure in combination with shear force

Shear force in combination with pressure is another etiological factor noted for causing pressure ulcers. Reuler and Cooney (1981) suggested that shear force could be caused easily by lying in a

semi-recumbent position in the bed. Shear is “the force per unit area exerted parallel to the plane of interest” (National Pressure Ulcer Advisory Panel, 2007b), and shear force alone does not induce skin breakdown (Bennett, Kavner, Lee, & Trainor, 1979).

An early study from Dinsdale (1974) investigated the effect of frictional force in combination with pressure on ulceration. Frictional force is “the resistance to motion in a parallel direction relative to the common boundary of two surfaces” (National Pressure Ulcer Advisory Panel, 2007b) and can be categorized as a type of shear force generated at the skin and superficial fascia (Wang & Sanders, 2005). Dinsdale’s study contained two parts; the first part of the study examined the tissue lesion after applying different amounts of prolonged pressure (ranging from 160 to 1100 mmHg) for three hours with and without frictional force, and the second part of the study investigated the tissue damage after applying 159 mmHg of pressure for three 1.5 hour periods on pigs’ posterior superior iliac spines with and without frictional force. For the first part of the study, he found that there were no tissue damage with pressure below 480 mmHg only, and animals with pressure and friction had more tissue damage. However, there were no significant differences when the pressure was greater than 500 mmHg. In the second part of the study, he found that there was significantly more tissue damage with frictional force in all 14 animals. Findings from this study suggested that frictional force is a risk factor of ulceration and lower pressure is required to induce tissue damage with the existence of frictional force. Goldstein and Sanders (1998) later investigated the effect of shear force extensively on ulceration by inducing tissue damage with different combination of pressure and shear. The study applied different combinations of pressure (ranging from 1-16 N) and shear force (ranging from 1-6 N) on the greater trochanters of the pigs. The pressure in combination with shear force was applied on the skin for 10-minute intervals repeatedly until tissue damage was observed or

up to a total of 40 minutes of load. They found that when the tissue was loaded with the same amount of pressure, higher shear stress caused tissue breakdown to occur earlier. In addition, they found that the highest shear stress caused the most severe tissue damage.

The most possible pathway that explains the tissue damage caused by shear force in combination with pressure is tissue ischemia and hypoxia. Bennett et al. (Bennett, et al., 1979) hypothesized that shear force in combination with pressure occluded the blood vessels more easily as compared to pressure only. They measured the SBF at the palm of four human participants under two conditions: 1) pressure only and 2) pressure in combination with shear force. In the first condition, the pressure was increased until the blood flow was totally occluded. In the second condition, the shear force was increased incrementally with the least amount of pressure required to prevent the loading device from slipping from the skin. They found that the amount of pressure required to occlude the blood flow with pressure alone was about 100-120 mmHg, while the amount of pressure required to occlude the blood flow with shear force was about 60-80 mmHg. From their results, they suggest that 2.7 g/cm² of shear force may be equivalent to 1 mmHg of pressure to occlude the SBF. Goossens et al. (1994) hypothesized that shear force in combination with pressure cut off oxygen supply more easily as compared to pressure only. They investigated the skin oxygen tension at the sacrum of young healthy human participants under different combinations of five levels of pressure (0, 4.6, 7.7, 10.8 and 13.9 kPa) and two levels of shear stress (0 and 3.1 kPa). They found that the cut-off pressure without shear force was 11.6 kPa, and the cut-off pressure with shear force (3.1 kPa) was 8.7 kPa.

2.3 RISK FACTORS OF PRESSURE ULCERS

In addition to pressure and shear force, several other risk factors contribute to pressure ulcer development. A conceptual scheme from Braden and Bergstrom (2000) suggested that the risk factors causing pressure ulcers could be divided into two categories: 1) the amount and duration of pressure exposure and 2) the tissue tolerance toward pressure. Given that pressure is the main cause of pressure ulcers, factors that increase the amount and duration of pressure exposure elevate the risk of pressure ulcer formation. Lack of sensation, decreased mobility and activity all affect the amount and duration of pressure exposure. The tissue tolerance toward pressure, by definition, is the tissue's ability to withstand the pressure without developing ulcers (Bergstrom, 2005). Several intrinsic and extrinsic factors affect tissue tolerance to pressure. The main intrinsic factor is changes in tissue properties due to aging or neurological deficits and the main extrinsic factor is increased skin temperature.

People with SCI are at extremely high risk of developing pressure ulcers. Spinal cord injury can cause different degrees of damage to the motor, sensory and autonomic functions. Several factors increase the risk of pressure ulcer development after SCI, including impaired sensation, decreased activity and immobility, changes in tissue condition and autonomic dysreflexia after injury (Bogie & Bader, 2005; Byrne & Salzberg, 1996). All these deficits could be grouped under the two categories of the conceptual scheme described above (Braden & Bergstrom, 2000), and will be explained in each of the following subsections.

2.3.1 Impaired sensation

Sensory perception has been used in risk assessment scales for years to predict the development of pressure ulcers (Braden & Bergstrom, 1988). Spinal cord injury causes sensory paralysis below injury level, and this may result in lack of detection of the uncomfortable area exposed to prolonged pressure (Bergstrom, 2005). Studies on SCI related risk factors in pressure ulcer development suggested that impaired sensation is one of the leading causes of pressure ulcers in this population. Bryne & Salzberg found that completeness of injury is a major risk factor in this population (Byrne & Salzberg, 1996). By definition, complete injury (American Spinal Injury Association (ASIA) Grade A) means no sensation or motor function at the sacral segments (S4-S5) (American Spinal Injury Association, 2006). Researchers found that people with complete injury had higher incidence of pressure ulcer development from one to 20 years post-injury (McKinley, et al., 1999), and a vast majority of veterans with SCI that developed pressure ulcers had complete injury (69%) (Garber & Rintala, 2003).

2.3.2 Decreased mobility and activity

Decreased level of activity and mobility are associated with ulceration in people with SCI (Byrne & Salzberg, 1996) and hospitalized patients (Lindgren, et al., 2004). Previous studies found that reduced spontaneous movements (Exton-smith & Sherwin, 1961) and attenuated movement frequency and magnitude (Nicholson, Leeman, Dobbs, Denham, & Dobbs, 1988) during sleeping increased the risk of ulcer development. In addition, people who require assistance with their activities of daily living tend to have more pressure ulcers than those who did not (Berlowitz & Wilking, 1989). In people with SCI, immobility and decreased activity

levels result from motor paralysis below injury level. This leads to prolonged loading of the skin during sitting and lying. Researchers found that level of mobility/activity is a risk factor in people with both acute (Salzberg, Byrne, Kabir, van Niewerburgh, & Cayten, 1999) and chronic SCI (Niazi, Salzberg, Byrne, & Viehbeck, 1997; Salzberg, et al., 1996). In addition, the higher incidence of pressure ulcer development in people with complete SCI also indicates that the absence of motor function below the injury level plays an important role in ulceration (Garber & Rintala, 2003; McKinley, et al., 1999).

2.3.3 Increased skin temperature

Previous studies found that skin temperature increased over time when the skin is in close contact with support surfaces. Researchers examined the changes in skin temperature by asking healthy participants to sit on different types of seat cushions and measured their skin temperature for a prolonged period of time (varied from 30 minutes to two hours) (Cochran, 1985; Fisher, et al., 1978; Seymour & Lacefield, 1985). All three studies only reported the changes in skin temperature from the baseline, and they found that the skin temperature increased immediately when the skin is in close contact with rubber (Fisher, et al., 1978), foam and air bladder (Cochran, 1985; S. F. C. Stewart, et al., 1980) cushions. On the contrary, they found that the skin temperature decreased immediately with the gel and water floatation cushions but increased thereafter in ten minutes (Cochran, 1985; Fisher, et al., 1978; S. F. C. Stewart, et al., 1980). The skin temperature reached the baseline value by the end of the two hours sitting on the gel cushion but remained below the baseline value with the use of water floatation cushions (Cochran, 1985; S. F. C. Stewart, et al., 1980). The time until skin temperature increase might be extended due to the high heat sink capacity of the gel and the water floatation cushions (S. F. C. Stewart, et al.,

1980). Similar findings were discovered in people with SCI, and the mean temperature was significantly higher in people with SCI regardless of the type of the cushions (Seymour & Lacefield, 1985). A recent study investigating the sacral skin temperature in the lying position at the acute care setting also found that the skin temperature increased within the two-hour turning intervals in patients with acute SCI and orthopedic trauma (Sae-Sia, et al., 2007). Findings of these studies all suggested that increased skin temperature is inevitable in all health care settings.

To date, only three animal studies and one human research study investigated the relative effect of increased skin temperature on pressure ulcer development. Although researchers generally believe that an increased tissue metabolism causes the ischemic tissue to breakdown faster (Rowell, 1974), the underlying mechanism of elevated skin temperature on pressure ulcer development is not yet fully discovered. Findings from the animal and human studies are described in details in the following two subsections: section 2.3.3.1 and 2.3.3.2.

2.3.3.1 Findings from animal studies

Kokate et al. (1995) first investigated the relationship between the skin temperature and pressure ulcer development on a swine model. They applied localized prolonged pressure of 100 mmHg on the backs of swine for five hours under four different temperatures: 25, 35, 40, and 45°C. Sixteen animals were tested, and a laser Doppler perfusion monitor system was used to measure SBF after the operation for 28 days. In addition, a histological evaluation was made after pressure removal for up to 21 days. Histological investigation at 7 days post-operation showed that all tissue layers were normal under 25°C, while moderate muscle damage was found at sites with 35°C, and tissue necrosis at all layers were found at sites with 45°C. The results were consistent with the pattern of cutaneous blood perfusion after pressure was relieved. The

SBF measured at 25°C and 35°C remained the same as the baseline value during the 28 days after pressure removal, while SBF measured at 45°C was absent during the whole 28 days. These results indicated that temperatures as high as 45°C could result in tissue damage immediately, whereas temperatures at 25°C could preserve the tissue viability under the same amount of localized pressure.

A further study from Iaizzo et al. (1995) adopted the similar research protocol and performed an advanced animal study in two parts. First they tested the same four temperatures with a localized pressure of 100 mmHg on the back of swine for three different amounts of time: two, five and ten hours. Histological assessments were performed seven days after pressure removal. They found that temperature as high as 45°C could cause tissue damage under localized pressure for as short as 2 hours, while sites with 25°C showed no indication of any tissue damage. In addition, the severity of tissue damage increased progressively with longer periods of pressure applied on the skin in all temperatures above 25°C. The second part of the study aimed to find the threshold temperature to prevent pressure ulcers. They tested the effect of different temperatures within a smaller range (25, 27, 30, and 32°C) under 100 mmHg pressure for ten hours. Histological assessment showed that the tissue damage was significantly lower in this range as compared to that with 35°C. They found that the lowest temperature induced the least amount of damage in all layers, while the higher temperature induced tissue damage in more layers. In addition, their findings suggested that deep tissue layers tend to be more sensitive to injury at higher temperatures. Since they did not find any significant differences on tissue damage within the range of 25 to 30°C, they suggested that cooling skin to a temperature below 30°C might minimize the tissue damage caused by prolonged pressure.

Patel et al. (1999) investigated temperature effects on skin perfusion response under localized pressure. They measured the skin perfusion response under three different localized pressures: 3.7, 18, and 73 mmHg, and two different temperatures: 28 and 36°C. They found that heating the skin caused a 25% increase in perfusion under 18 mmHg of pressure, but not under 73 mmHg pressure. The authors further investigated the skin perfusion by applying pressure incrementally from 3.7 to 62 mmHg under the two different temperatures. They found that the skin perfusion dropped to zero when the pressure reached 55 mmHg, and that the skin perfusion increased from 3.7 to 18 mmHg with 36°C but not for pressure exceeding more than 18 mmHg. The results indicated that the application of local heating increased the skin perfusion through more vasodilation and reduced vascular resistance, however this did not occur when the vessels were mechanically occluded under higher pressure (Lachenbruch, 2005). Based on the data collected by Patel et al., Lachenbruch (2005) analyzed the effect of pressure in combination with temperature on skin perfusion. He found that the same amount of perfusion deficit occurred at both 56 mmHg with 28°C, and at 40 mmHg with 36°C. This suggested that the presence of cooling preserved the tissue by reducing 29% of the pressure applied on the skin.

Findings from all three previous animal studies suggested that local skin cooling provided a protective effect on ischemic tissue. Temperature as low as 25°C is beneficial to the ischemic tissue on animals, however the underlying protective mechanism with local skin cooling was not clear.

2.3.3.2 Findings from human study

Our research team first investigated the effect of temperature on clinically relevant pressure on human subjects (Tzen, et al., 2010). Ten young healthy adults aging from 18 to 40 years old were recruited in this study. The study was a repeated measures design, and each

subject was tested under two conditions: pressure only, and pressure with local cooling. The pressure applied on the skin contained three phases: 0.4 kPa for 10 minutes, 8 kPa for 30 minutes, and 0.4 kPa for 20 minutes. Reactive hyperemia was the main outcome measure of the study, which is a normal physiological phenomenon of increased SBF after a period of tissue ischemia. We found that the reactive hyperemic response was greater in non-cooling than in cooling, and the normalized peak SBF was significantly larger in non-cooling than in cooling. The normalized peak SBF represents the amount of vascular response after the release of tissue ischemia (Hagisawa, et al., 1994), and previous study also suggested that the more severe the tissue ischemia (i.e. longer period of tissue ischemia), the higher peak SBF was discovered (Matsubara, et al., 1998). Given that the duration of tissue ischemia was the same in cooling and non-cooling, the significant decrease in normalized peak SBF indicated that local cooling provided a protective effect of the tissue ischemia (Tzen, et al., 2010). We further analyzed the underlying mechanism using time-dependent spectral analysis. Although not statistically significant, we found that the myogenic activity remained elevated throughout the hyperemic response with cooling, while the myogenic activity elevated initially and returned to baseline without cooling. A previous study suggested that the decreased myogenic response during and after heating of the skin was the result of decreased smooth muscle tone (Geyer, Jan, Brienza, & Boninger, 2004). Therefore, our finding implied that local cooling increased the smooth muscle tone and caused local vasoconstriction. This study provided pilot results of the temperature effect on ischemic tissue in human subjects, however due to the small sample size, we were not able to distinguish the underlying mechanism of temperature on ischemic tissues.

2.3.3.3 Impaired thermoregulation in people with SCI

Sae-sia et al. (2007) measured the sacral skin temperature of people with SCI at the acute care clinic and found that people with higher skin temperature had higher incidence of pressure ulcer development. To date there is no direct linkage between thermoregulation and pressure ulcer development; however, given that increased temperature causes the skin to be more vulnerable to tissue damage under prolonged pressure, changes in thermoregulation in people with SCI may affect the tissue tolerance toward pressure during weight-bearing conditions.

Both central and local control mechanisms modulate human thermoregulation through the peripheral circulation system (Kellogg, 2006). The central vascular control mechanism is mediated via the sympathetic nervous system (Holowatz, et al., 2003; Johnson, et al., 2005; Kellogg, et al., 1995; Scremin & Kenney, 2004), and the local vascular control mechanism is mediated through different local neural and non-neural responses (Johnson, et al., 2005; Kellogg, 2006; Minson, Berry, & Joyner, 2001; Pergola, Johnson, Kellogg, & Kosiba, 1996). Depending on the level and type of injury, SCI may result in impairments in sensation and/or autonomic function. Impairments in either sensory or autonomic function may affect the peripheral circulatory control system through the central or local control mechanisms.

(a) Central control mechanisms

The central control of the thermoregulation contains two pathways: active vasodilation during heat stress and noradrenergic vasoconstriction during cold stress (Holowatz, et al., 2003; Johnson, et al., 2005; Kellogg, et al., 1995; Scremin & Kenney, 2004). Previous studies found that the cholinergic nerves release acetylcholine (Hokfelt, Johansson, Ljungdahl, Lundberg, & Schultzberg, 1980) and another cotransmitter (Kellogg, et al., 1995), possibly vasoactive intestinal peptide, during heating. Acetylcholine mainly caused the sweating response, while the

vasoactive intestinal peptide caused the vasodilation of the cutaneous arterioles. However, the interactions of the two neurotransmitters and vasodilation were not completely identified. Later studies discovered that acetylcholine modulated the vasodilation response through the nitric oxide synthase mechanism (Shibasaki, Wilson, Cui, & Crandall, 2002), and a functional nitric oxide synthase played an important role in active vasodilation (Kellogg, Crandall, Chrarkoudian, & Johnson, 1998; Shastry, Dietz, Halliwill, Reed, & Joyner, 1998). The sympathetic noradrenergic nerve releases two neurotransmitters causing active vasoconstriction of the cutaneous arterioles during cooling (Kellogg, 2006). The two neurotransmitters are norepinephrine and neuropeptide Y (NPY), and they induce the vasoconstriction through the α_1 , α_2 receptors (Flavahan, 1991; Johnson, et al., 2005) and postjunctional NPY Y_1 receptors of the vascular smooth muscles, respectively (Stephens, Aoki, Kosiba, & Johnson, 2001; Stephens, Saad, Bennett, Kosiba, & Johnson, 2004).

People with SCI level at T6 and above usually encounter impaired central control over the circulation system (Bogie & Bader, 2005). This could lead to the condition of autonomic dysreflexia, which is an increased autonomic reflex response to various irritating stimuli (Byrne & Salzberg, 1996). Petrofsky (1992) investigated the aural temperature of people with and without SCI. Four people without any neurological deficits and twelve people with complete SCI (six with injury level between T7-T12 and another six with injury level between C6-C8) were recruited. The core temperature and the sweat rate were measured with and without upper extremity exercise under three different environmental temperatures (30, 35, and 40°C). He found that people with injury level between C6-8 had higher core temperature regardless of the environmental temperature and the exercise condition. In addition, this group had the lowest sweating rate and the difference from control group was especially obvious with higher

environmental temperature. This indicated that people with a higher level of injury have a limited capacity for thermoregulation, and this may be due to inability to sweat after the autonomic function impairment.

(b) Local control mechanisms

Local heating of the skin induces two local control mechanisms: the sensory reflex (neural), and the local nitric oxide generation (non-neural) mechanism (Minson, et al., 2001). Studies found that increased in SBF with local heating was mediated by sensory reflex (Minson, et al., 2001) and local nitric oxide production (Kellogg, Liu, Kosiba, & O'Donnell, 1999). In addition, the two local control mechanisms are independent of the function of the adrenergic system (central control mechanism) (Pergola, Kellogg, Johnson, Kosiba, & Solomon, 1993). Local cooling of the skin induces two phases of vasoconstriction (Johnson, et al., 2005). The initial decrease in SBF is a result of combined noradrenergic vasoconstriction and non-neurogenic vasodilation (Johnson, 2007). The noradrenergic vasoconstriction requires intact sensory and autonomic functions (Johnson, et al., 2005), while the non-neurogenic vasodilation depends on the cooling rate of the skin (Yamazaki, et al., 2006). The prolonged phase of vasoconstriction is mediated through another non-neurogenic mechanism, and the Rho-Rho kinase system is partially attributed to this mechanism (Thompson, Holowatz, Flavahan, & Kenney, 2007).

To date, there is limited literature that examines the local thermoregulatory response in people with SCI. Price (2006) reviewed articles that investigated thermoregulation during exercise in people with different degrees of SCI. As compared to people without SCI, people with thoracic or lumbar spinal lesions showed similar core temperature but greater heat storage in the lower limbs during exercise regardless of the environmental temperature. The results

suggested a lower heat dissipating rate in this population, however, the underlying mechanisms causing this difference remain unclear.

2.3.4 Changes in tissue property

One common characteristic of the high-risk population is changes in tissue property. Researchers found that elderly people and people with SCI had several differences in tissue property as compared to populations not at-risk of pressure ulcer development. A recent survey showed that more than 50% of the people with pressure ulcers are over 70 years old (Amlung, et al., 2001). Studies found the elasticity and subcutaneous fat of the skin decrease with normal aging (Garcia & Thomas, 2006); and the epidermis, dermis and the vessel walls become thinner as compared to younger population (Witkowski & Parish, 2000).

In people with SCI, there are several changes in tissue property that may cause the skin to become more vulnerable to ulceration, including disuse muscle atrophy and changes in body composition. Castro et al. (1999) did biopsies at the right vastus lateralis muscle in fifteen people with complete SCI at three time points: 6, 11, and 24 weeks after injury. They found that the average fiber cross-sectional area declined significantly (27-56%) from week 6 to week 24. In addition, the relative percentage of type IIa fiber decreased significantly during this period of time, while type IIax+IIx increased. They suggested that the muscle atrophy recognized in all fiber types might be due to the loss of contractile protein within the skeletal muscles. A review article from Giangreporio and McCartney (2006) identified several soft tissue composition changes after SCI. The total fat mass and the percentage of fat mass in the lower limbs were higher in people with SCI. However these studies didn't show a direct linkage between changes of body composition and ulcer formation. A recently study from Linder-Ganz et al. (2008)

investigated the sub-dermal tissue of the buttocks in people with SCI under both weight-bearing and non-weight-bearing conditions. They found that the gluteal muscle thickness was generally thinner in people with SCI as compared to healthy controls at non-weight-bearing condition. In addition, the computer model built from integrating images formed by MRI showed a significantly higher strain and stress in both muscle and fat tissue in people with SCI. Since the test protocol was the same for all subjects, the differences in strain and stress during the weight-bearing condition might be due to the anatomical changes in people after injury. They used the same test protocol to measure the strain and stress on people with SCI while sitting on commercially available pressure redistribution cushions (Linder-Ganz, et al., 2008). The peak gluteal stress was 3-5 times greater in people with SCI than controls, and the integrated peak compression stress over time was 35-50 times greater in people with SCI than controls. Results of this study were consistent with their previous finding that anatomical changes after injury caused higher stress on the tissue during the weight-bearing situation.

2.4 BENEFITS OF LOCAL SKIN COOLING

Since increased skin temperature is one of the risk factors causing pressure ulcers, local skin cooling is believed to be a potential method to prevent ulceration. Cooling has been used in various fields for tissue preservation, including organ transplants, stroke (Erecinska, Thoresen, & Silver, 2003; Zhao, Steinberg, & Sapolsky, 2007), bypass surgery (Q. Chen, et al., 2002; Riess, Camara, Kevin, An, & Stowe, 2004) and free-flap surgery (Diederich, et al., 2009). Several mechanisms contribute to the protective effect of cooling including reduced metabolic demand

during tissue ischemia, decreased ischemic-reperfusion injury and diminished inflammation response.

2.4.1 Reduced metabolic demand during tissue ischemia

Decreased temperature causes the metabolic-arresting effect (Hochachka, 1986), which is a protective effect of reducing tissue metabolism by cooling. This effect has been recognized in different tissues, including skeletal muscles (Segal & Faulkner, 1985; Seiyama, Kosaka, Maeda, & Shiga, 1996), cutaneous tissue, and even heart (Q. Chen, et al., 2002; Chitwood, Sink, Hill, Wechsler, & Sabiston, 1979; Riess, et al., 2004) and brain (Rosomoff & Holaday, 1954).

Seiyama et al. (1996) examined the metabolic-arresting effect of hypothermia on isolated rat skeletal muscle by measuring the O₂ consumption (difference of influent and effluent O₂ concentration) under different tissue temperature. They found that with the same influent oxygen concentration, the muscle at higher temperature had more O₂ uptake. In addition, they measured the myoglobin and cytochrome oxygenation with a spectrophotometer and found that lower temperature increased oxygenation of myoglobin and cytochrome of the muscle cell. Findings from this study indicate that hypothermia decreases the metabolic rate of the skeletal muscle, and diminishes the respiratory rate of the mitochondria or electron flow of the cell respiratory chain. Michenfelder and Milde (1991) examined the changes of metabolism and cerebral function with mild hypothermia. They investigated the cerebral metabolism on adult dogs by measuring the ratio of two rates of oxygen consumption measured over a 10°C range. They cooled the brain from 37°C to 14°C, and found that the rate of oxygen consumption decreased about 55-60% for every 10°C of brain tissue temperature reduction. Results from this

study suggested that hypothermia had a potential protective effect for the brain. However, they did not report any data on brain function when the temperature decreased.

Erecinska et al. (2003) reviewed articles that investigated hypothermia on energy metabolism in mammalian brain. In addition to the oxygen metabolic rate, they reviewed previous studies that investigated the cerebral metabolic rate of glucose and lactate. From eight previous studies that measured the cerebral metabolic rates ranging from 18 to 41°C, they found that both the metabolic rates of glucose and lactate were reduced when the tissue temperature is lower. Calculations derived from data collected in eight previous studies suggest that the cerebral metabolic rate of glucose and lactate is reduced about two to four fold when the tissue temperature is reduced 10°C.

2.4.2 Decreased ischemia-reperfusion injury

The other explanation of hypothermia on tissue survival is to reduce the ischemia-reperfusion injury, which is one of the etiological factors of pressure ulcer development. Choi et al. (2005) investigated the hepatic injury after 24 hours of reperfusion in the rat liver. Tissue ischemia was induced for 75 minutes under two conditions: normothermia (37°C) and mild-hypothermia (34°C). Histological assessment was performed 24 hours after ischemia relief to measure the hepatic injury. They found that there was more than 75% of necrosis in normothermic condition, whereas the mild hypothermia reduced the tissue necrosis about 25 to 50%. In addition, after 24 hours of reperfusion, the survival rate was significantly lower in the normothermic group. Diederich et al. (2009) investigated the protective effect of hypothermia on dissected rat rectus femoris muscles. Tissue ischemia was induced for one hour to simulate the procedure of free flap transfer, and the skin temperature was controlled at three different

levels during tissue ischemia: local cooling at 10°C, exposing to room temperature (23°C) and local heating at 30°C. They found that there is significantly less muscle necrosis following local cooling compared to the other two temperature conditions. Results from both studies indicated that there is a protective effect of cooling that reduces ischemia-reperfusion tissue injury.

In light of the beneficial effect of cooling on reperfusion injury described in previous paragraph, other studies investigated the timing of the cooling intervention during ischemia and reperfusion. Mowlavi et al. (2003) investigated the muscle tissue viability and muscle edema under four conditions: 10°C local cooling during 1) four hours of tissue ischemia only, 2) the initial three hours of reperfusion, 3) four hours of tissue ischemia and the initial three hours of reperfusion, and 4) no local cooling. They found that the muscle viability was significantly higher in all three hypothermia groups as compared to no cooling. In addition, the muscle edema was significantly reduced in all three hypothermia groups as compared to no cooling. The results indicated local cooling intervention during early reperfusion could provide a protective effect on reperfusion injury. Another study investigated the myocardial tissues with the cooling intervention given continuously before, during and after tissue ischemia (Kanemoto, et al., 2009). They found that all groups with cooling intervention significantly reduced the infarct size of the myocardial tissues as compared to group without cooling intervention. In addition, they discovered that the tissue temperature at reperfusion is correlated with the size of infarction. The results also suggested that hypothermia provided a protective effect on tissue during reperfusion.

2.4.3 Selection of different cooling rates

Given that local cooling might provide a protective effect on skin under localized pressure, there is no rationale on selecting the cooling rate. Kellogg reviewed the physiological

response of the vessels during local cooling (Kellogg, 2006). He summarized that the vascular response mechanisms during local cooling could be explained in two phases. The initial decrease of SBF is the combined result of two mechanisms: sympathetic vasoconstriction, and a vasodilation that is not modulated by the nervous system. The prolonged phase of decreased SBF is mediated by another non-neural vasoconstriction. Yamazaki et al. (2006) investigated the initial cold induced vasodilation with two different cooling rates and found that this mechanism was rate dependent. They cooled the forearm skin at two different rates: fast cooling ($-4^{\circ}\text{C}/\text{min}$) and slow cooling ($-0.33^{\circ}\text{C}/\text{min}$). To unmask the initial vasodilation response, the initial sympathetic vasoconstriction was blocked with bretylium tosylate (adrenergic transmitter blocker). The initial vasodilation response was observed in the fast cooling but not in slow cooling. To further understand the control mechanism of this initial vasodilation, nitric oxide synthase inhibitor was applied during the process of local cooling. They found that nitric oxide synthase inhibitor did not significantly decrease the SBF during the early stage of local skin cooling. The results suggest that the initial cold-induced vasodilation is rate dependent, however the control mechanism of this response remains unclear but does not appear to be primarily mediated by nitric oxide. In addition, there was no evidence on how long the vasodilation lasted during the period of local cooling.

Literature reviews from section 2.4.1 suggest that the local cell metabolic rate depends on surrounding tissue temperature. Since there was a limitation of increasing SBF with heating when the vessels were mechanically constricted by high pressure (Patel, et al., 1999), application of fast cooling might cause less vasoconstriction of the skin as compared with slow cooling under the same amount of mechanical pressure on the skin. Since the tissue metabolic rate depends on the tissue temperature, with the same tissue metabolic rate (skin cooled to the same

temperature with both fast and slow cooling) and more blood flow supply to the target tissue (fast cooling induced initial vasodilation), we might be able to preserve the tissue tolerance under localized pressure with fast cooling.

2.5 INDIRECT MEASUREMENT OF TISSUE RESPONSE

To investigate the cooling effect on human subjects, a non-invasive measurement method should be used to test the differences. Previous pressure ulcer studies in the lab setting used numerous non-invasive measurement tools to investigate the effect of risk factors (e.g. pressure, shear, smoking, and changes in tissue conditions) on pressure ulcer development. The outcome measures used most often in the literatures were arterial oxygen tension and reactive hyperemia. To measure the arterial oxygen tension, a transcutaneous oximetry (TcPO₂) should be used (Jan & Brienza, 2006; Newson & Rolfe, 1982). It is a reliable method to measure tissue viability by assessing the blood gas that is permeated to the surface of the skin (Togawa, Tamura, & Öberg, 1997a). Since the skin is not permeable to gas, heating the skin up to 40-45°C is required to obtain an accurate reading of the oxygen tension (Bongard & Bounameaux, 1993; Jan & Brienza, 2006). Given that a cooling intervention was provided in this study, it was not appropriate to use TcPO₂ as an outcome measurement tool.

2.5.1 Reactive hyperemia

The reactive hyperemic response was selected as an outcome measurement tool for this research. It has been adopted in several pressure ulcer studies that tested human subjects (Hagisawa, et al.,

1994; V. Schubert & Fagrell, 1991b; Sprigle, Linden, & Riordan, 2002), and it has also been used in numerous studies that investigate the micro-vascular function in people that are smokers (Noble, Voegeli, & Clough, 2003), the elderly population (V. Schubert & Fagrell, 1991a), and for people at high risk for developing cardiovascular diseases (Matsubara, et al., 1998; Ruano, et al., 2005; Skrha, Prazn, Haas, Kvasnicka, & Kalvodova, 2001; J. Stewart, et al., 2004).

Reactive hyperemia is a normal physiological response that occurs after a period of tissue ischemia in many different organs of the human body (Levick, 2003; Wilkin, 1987), including but not limited to the skin, liver, heart, and brain. A reactive hyperemic response is a sudden increased blood flow that appears immediately after the release of vessel occlusion. The blood flow rises from biological zero (blood flow during vessel occlusion) to a peak then gradually descends to the baseline value (blood flow before vessel occlusion). It can be induced easily by blocking the SBF for as short as three minutes (Cracowski, Minson, Salvat-Melis, & Halliwill, 2006), and it lasts about one half of the time of the tissue ischemia (Sprigle, et al., 2002).

2.5.1.1 Physiological control mechanisms of reactive hyperemia

Researchers to date agree that the main explanation for the occurrence of reactive hyperemia is to erase/correct the oxygen and nutritional debt accumulated during tissue ischemia (Hagisawa, et al., 1994; Levick, 2003). However, the underlying mechanisms are not completely understood. There are three main mechanisms that contribute to the hyperemic response, including accumulation of metabolic vasodilators, neurogenic and myogenic responses (Cracowski, et al., 2006).

Two previous studies have identified several metabolic substances that contribute to vasodilation during the reactive hyperemic response. These substances included prostaglandin and adenosine. Studies that investigated the contribution of the metabolic substances tested the

reactive hyperemia under the condition with and without the inhibitor or drug that blocks the release of these metabolic substances. Kilbom and Wennmalm (1976) investigated the effect of prostaglandin (metabolic substance generated by endothelial cells) on reactive hyperemia at human forearms. They measured the reactive hyperemic response with and without indomethacin (an inhibitor of prostaglandin), and found that the reactive hyperemic response was smaller with the use of indomethacin. This indicated that prostaglandin is one of the metabolic substances released during reactive hyperemia. Carlsson, Sollevi and Wennmalm (1987) measured the effect of adenosine on reactive hyperemia with and without theophylline (adenosine receptor antagonist). Adenosine is a degradation product of adenosine triphosphate, which is a substance of cell metabolism. They found that theophylline reduces 35% of the reactive hyperemia, indicating that adenosine plays a role in the reactive hyperemic response and proved that tissue metabolism contributes to the response.

Myogenic control mechanism of blood flow is caused by the changes in transmural pressure of the vessel (R. Schubert & Mulvany, 1999). This control mechanism was first investigated about a century ago by inducing the reactive hyperemic response on denervated dog femoral arteries with short period of blood flow occlusion (Bayliss, 1902). Bayliss suggested that the response was independent of the central nervous system, since the animals were anesthetized, however, the contribution of metabolic and peripheral nervous system to reactive hyperemia was not completely blocked in this early study. A recent study investigated the myogenic response by measuring the reactive dilation under the stimuli of changing hemodynamic forces, including pressure and flow (Koller & Bagi, 2002). Reactive dilation is the change in the diameter of the vessel, and it is the outcome measure of the study to simulate the reactive hyperemia *in vivo*. To eliminate other factors that might affect the reactive

hyperemia, they performed the tests on isolated rat skeletal muscle arterioles. They found that when the pressure was changed, the peak reactive dilation increased but not the duration. They also found that when the pressure and flow were changed, both the peak and duration of the reactive dilation increased. To distinguish the substances that contributed to the response, they further performed the same protocol after endothelium removal and inhibition of nitric oxide synthase. They found that inhibition of NO synthase and endothelium removal significantly reduced the peak, this indicated that deformation of the endothelial cell releases the nitric oxide, therefore causing the vasodilation. This study suggested that the stretch, deformation, pressure and changes in flow induced the reactive hyperemia, and this response was mediated partly by the release of nitric oxide.

The reactive hyperemic response is also mediated through sensory nerves. Larkin and Williams (1993) investigated the skin reactive hyperemic response by blocking the sensory nerves with local anesthesia. They found that the reactive hyperemic response was significantly reduced with the anesthesia, however the neurotransmitter that is responsible for this response was not identified. A later study investigated the neurogenic response and its interaction with the calcium activated potassium (BK_{Ca}) channels (Lorenzo & Minson, 2007). BK_{Ca} channel regulates the vascular tone and is activated by increased concentration of Ca²⁺ and depolarization of the cell membrane (Jackson, 2000). They found that the reactive hyperemia was significantly reduced with both blockers independently and in combination. Therefore they suggested that both the sensory nerves and the BK_{Ca} channels mediated the reactive hyperemic response.

2.5.1.2 Parameters of reactive hyperemia

To quantify the hyperemic response and characterize the underlying mechanisms, several parameters were identified in previous studies (Hagisawa, et al., 1994; V. Schubert & Fagrell,

1991a; Sprigle, et al., 2002). The most commonly used parameters of reactive hyperemia include baseline SBF, peak SBF, time to peak SBF, half-life of SBF and perfusion area, and each parameter corresponds to different mechanisms. Figure 1 is a typical reactive hyperemia response collected from subject CTRL_06 in this study, baseline SBF is the SBF measured before tissue ischemia; peak SBF is the maximum value of SBF that occurs after the end of tissue ischemia; time to peak SBF is the time period between the end of tissue ischemia and the peak SBF; the half-life is the time period between peak SBF and the half-way of SBF descending from the peak SBF; and the perfusion area is the area for the reactive hyperemia curve above the baseline value.

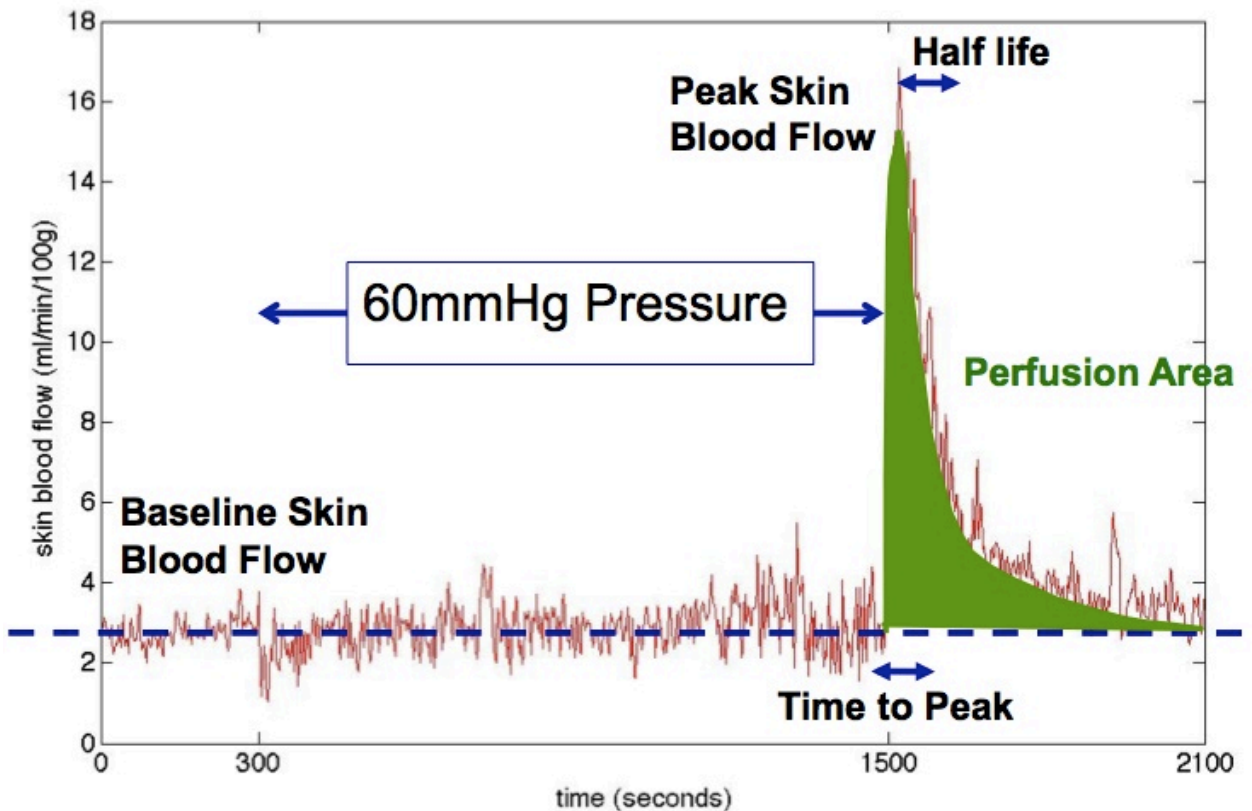


Figure 1. Reactive hyperemia time domain parameters.

Peak SBF is the most widely used parameter of the reactive hyperemia. It represents how extensively the vessels react to ischemia (Hagisawa, et al., 1994); in addition, it indicates the severity of tissue ischemia since longer duration of tissue ischemia induces higher peak SBF (Matsubara, et al., 1998). Time to peak SBF is another broadly adopted parameter. It represents how fast the vessel reacts to tissue ischemia (Hagisawa, et al., 1994) and is thought to reflect the cutaneous vascular resistance of the measured sites (Sprigle, et al., 2002; Yvonne-Tee, Rassol, Halim, & Rahman, 2005). Both the peak SBF and the time to peak SBF are highly reproducible measures (Yvonne-Tee, et al., 2005). Half-life represents the gradual decrease in vasodilation response after the peak SBF (Hagisawa, et al., 1994) and the duration of reactive hyperemia (Noble, et al., 2003). A study on smokers and non-smokers suggested that this vasodilation response is nitric oxide dependent since the endothelial nitric oxide synthase was inhibited with smoking (Noble, et al., 2003). Perfusion area represents the metabolic repayment after the tissue ischemia (V. Schubert & Fagrell, 1991b). Details and definition of each parameter are described in section 3.5.

2.5.2 Laser Doppler flowmetry system

To detect the reactive hyperemic response, the laser Doppler flowmetry (LDF) was selected. LDF is a method to measure SBF continuously and non-invasively (Togawa, Tamura, & Öberg, 1997b). The mechanism of using LDF to measure skin microcirculation is through projecting a laser beam to the skin, then collect the scattered light through the optical fibers (Togawa, et al., 1997b). It has been used in many studies on pressure ulcers risk assessment (V. Schubert & Fagrell, 1991b), endothelial function (Cracowski, et al., 2006), and tissue viability after free flap surgery (Holzle, Loeffelbein, Nolte, & Wolff, 2006). LDF has been shown to be a reliable tool

for monitoring skin perfusion (Kind, et al., 1998; Yuen & Feng, 2000). In addition, Ghazanfari et al. (2002) found that LDF had high test-retest reliability ($r = .81, p < .01$).

2.6 SKIN BLOOD FLOW SIGNAL PROCESSING

Skin blood flow signals obtained from the laser Doppler flowmetry contain information regarding the physiological response of the skin during and after tissue ischemia. Signal processing of the SBF in time and frequency domains provides information on the physiological response after the release of tissue ischemia. Skin blood flow signal was analyzed using two signal processing methods to characterize the reactive hyperemic response in both time and frequency domains. An exponential curve-fitting technique was used to select the time-domain parameters of the reactive hyperemia, while time-frequency analysis was used to examine the different control mechanisms of the SBF during the reactive hyperemia.

2.6.1 Exponential curve-fitting of the reactive hyperemia

To identify the parameters of the reactive hyperemia for statistical analysis, the reactive hyperemic response has to be recognized in the first place. Previous studies that used laser Doppler flowmetry to measure the SBF showed that there were oscillations of the SBF during baseline and reactive hyperemia (Cracowski, et al., 2006; Rossi, et al., 2007; J. Stewart, et al., 2004). Researchers examined the SBF in frequency domain and suggested that these very low frequency oscillations (ranging from 0.008-0.15Hz) represented three physiological control mechanisms: metabolic, neurogenic and myogenic mechanisms (Azman-Juvan, Bernjak,

Urbancic-Rovan, Stefanovska, & Stajer, 2007; Bracic & Stefanovska, 1998; Stefanovska, Bracic, & Kvernmo, 1999). Details of each frequency band are described in section 2.6.2. Given that the oscillation of SBF provided information of underlying control mechanisms, the low frequency of blood flow oscillation should not be filtered for the purpose of selecting the time domain parameters of the reactive hyperemia.

All previous studies that used reactive hyperemia as outcome measures selected the parameters by visually detecting the blood flow. However, the accuracy of each parameter might be questionable since there was no rationale on selecting from several blood flow points and visually selecting parameters is subjective and may vary from person to person (Humeau, Saumet, & L'Huillier, 2000). Nevertheless, studies to date still select parameters with this method. In contrast, a physical model of the post-occlusive reactive hyperemia has been developed by simulating the flow response with a circuit, containing voltage as the pressure, resistor as time-varying resistance of the capillary and current as the flow (de Mul, Morales, Smit, & Graaff, 2005). Figure 2 shows a circuit that simulate the blood flow response during reactive hyperemia developed by de Mul and colleagues. V_0 and V_1 represent the aortic pressure and arterial pressure, respectively. R_1 , R_2 , R_3 and R_4 represent the flow resistance, and C_1 and C_2 represent the compliance of the vessel (ratio of changes in blood volume to pressure). Current 'I' is the peripheral blood flow. Based on Ohm's Law, $I=V/R$, current 'I' in Figure 2 can be derived as Equation 1. In Equation 1, p_1 , p_2 are constants, and t is time. This reactive hyperemia flow model has the characteristic of starting from zero at the beginning of reactive hyperemia ($t=0$) and reaches the resting blood flow when time approaches infinity ($t \rightarrow \infty$). Equation 1 could be simplified to Equation 2, which is a simple bi-exponential function of time t . Symbol $y(t)$ is the blood flow curve (function of time t), and A_1 , A_2 , B , τ_1 , τ_2 are constants. To objectively select

the time domain parameters of the reactive hyperemia, a least-squares curve fit of this bi-exponential function (Equation 2) to the blood flow data in this study was performed (details described in section 3.5.1).

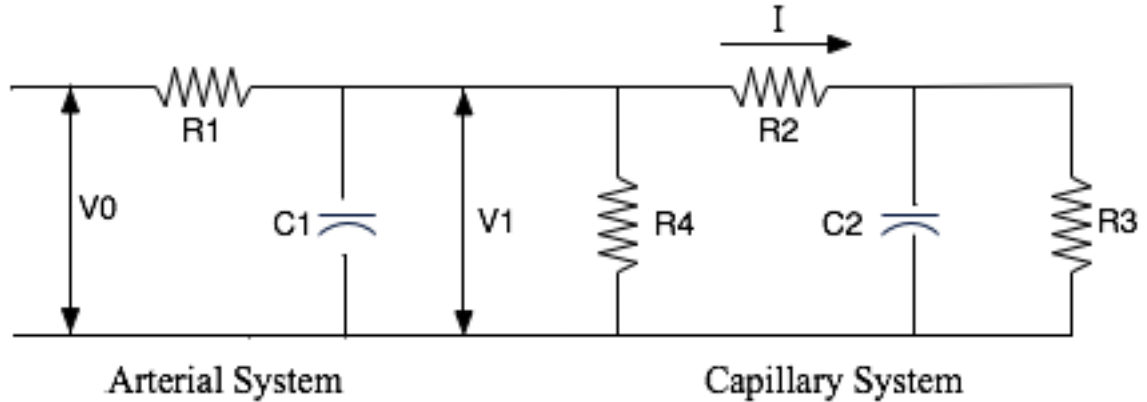


Figure 2. Physical model of reactive hyperemia.

V_0 and V_1 represent the aortic pressure and arterial pressure, respectively. R_1 , R_2 , R_3 and R_4 represent the flow resistance, and C_1 and C_2 represent the compliance of the vessel (ratio of changes in blood volume to pressure). Current ' I ' is the peripheral blood flow.

Equation 1. Current ' I ' in Figure 2 calculated based on Ohm's Law.

$$I = \frac{V_0}{R_4(R_1 + R_2 + R_3) + R_1(R_2 + R_3)} \left[1 + \frac{1}{p_2 - p_1} \left\{ (C_2 R_3 p_1 p_2 - p_2) e^{-p_1 t} - (C_2 R_3 p_1 p_2 - p_1) e^{-p_2 t} \right\} \right]$$

Equation 2. Bi-exponential function of time simplified from Equation 1.

$$y(t) = A_1 e^{-t/\tau_1} + A_2 e^{-t/\tau_2} + B$$

2.6.2 Time-frequency analysis of the SBF signal

In addition to the parameters of reactive hyperemia described previously, SBF signals can also be analyzed in the frequency domain (Bracic & Stefanovska, 1998, 1999; Stefanovska, et al., 1999). Five frequency bands were identified in previous studies, and each frequency band corresponds to a specific mechanism that controls the SBF. They are the metabolic (0.008-0.02

Hz), neurogenic (0.02-0.05 Hz), myogenic (0.05-0.15 Hz), respiratory (0.15-0.4 Hz), and cardiac (0.4-2.0Hz) mechanisms. An early study computed spectral analysis of the heart rate variability signal and identified two characteristic peaks centered around the heart beat (1 Hz) and the respiratory frequency (0.3 Hz) (Di Renzo, Marnica, Parati, Pedott, & Zanchetti, 1995). Based on this finding, Bracic and Stefanovska (1999) examined the energy densities using wavelet transform between the SBF signal and the heart rate variability signal. They found that there were also two characteristic peaks that centered at the two frequencies identified in the previous studies, and these two frequencies corresponded to the cardiac and the respiratory control mechanisms of the SBF. Another characteristic peak centered around 0.1Hz was identified in the blood-pressure signal (Bracic & Stefanovska, 1998). Since smooth muscle movement was activated through the changes of intravascular pressure and is primarily responsible for the blood-pressure regulation, this frequency band was identified as the myogenic response of the SBF (Cracowski, et al., 2006). Kastrup et al. (Kastrup, Bülow, & Lassen, 1989) applied local and ganglionic nerve blockers on the skin. They found that the peak centered about 0.025 Hz was diminished significantly with the nerve blockers. This indicated that this frequency band represented the neurogenic control mechanism of the SBF. Stefanovaska et al. (1999) examined the characteristic peak about 0.0095-0.02Hz of the spectra with and without the endothelium-dependent vasodilators. They found that the energy densities increased significantly with the use of the vasodilators. This indicated this frequency band corresponded to the metabolic control mechanism of the SBF.

Frequency analysis of signals has been used in various fields for decades. Frequency description of a signal helps us learn about the source of the signal and simplifies our understanding of the waveform (Cohen, 1995c). Traditional Fourier analysis, as an example,

transforms the signal into frequency domain and shows the different aspects of the signal (Cohen, 1995c). A signal could be expressed as addition of sinusoids with different frequencies (Equation 3). The spectrum (Fourier transform) of the signal $s(t)$ is $S(\omega)$, and it can be obtained by Equation 4.

Equation 3. Fourier expansion of signal (addition of sinusoids, $e^{j\omega t}$, with different frequencies).

$$s(t) = \frac{1}{\sqrt{2\pi}} \int S(\omega) e^{j\omega t} d\omega$$

Equation 4. Fourier analysis.

$$S(\omega) = \frac{1}{\sqrt{2\pi}} \int s(t) e^{-j\omega t} dt$$

The SBF signal, like many other biomedical signals, is non-stationary (Jan, Brienza, & Geyer, 2005). This means the frequency characteristics of the SBF change over time. Traditional Fourier transform is able to analyze the signal in the frequency domain, however, it cannot distinguish when these frequencies occur during the measurement period (Cohen, 1995a). Short-time Fourier transform (STFT) is a method most widely used to overcome this difficulty by breaking the signal into short-time segments (windows), then a Fourier analysis is computed within each segment (Cohen, 1995b). Equation 5 is the Fourier transform of signal $s(\tau)$ around time t , and $h(\tau-t)$ is the window function. Spectral density, $S_t(\omega)$, is the outcome of the short time-Fourier transform. It represents the energy at specific time and within specific frequency bands. By analyzing the SBF data in both time and frequency domains, we could better understand the changes in control mechanisms with the cooling intervention.

Equation 5. Fourier transform of signal $s(\tau)$ around time t , and $h(\tau-t)$ is the window function.

$$S_t(\omega) = \frac{1}{\sqrt{2\pi}} \int e^{-j\omega\tau} s_t(\tau) d\tau = \frac{1}{\sqrt{2\pi}} \int e^{-j\omega\tau} s(\tau) h(\tau - t) d\tau$$

3.0 METHODS

3.1 RESEARCH DESIGN

A 3x3 mixed factorial design was used to test the interaction between types of local stimuli and levels of injury (Table 1). The independent variable between groups was determined by the level of injury. The three levels are: 1) injury level at T6 and above (T6A), 2) injury level below T6 (T6B), and 3) control (CTRL). The independent variable within the subjects was determined by the test condition. The three test conditions are: 1) pressure only, 2) pressure with slow cooling (-.33°C/min), and 3) pressure with fast cooling (-4°C/min). All subjects were tested under the three conditions in a random order. The Institutional Review Board (IRB) of University of Pittsburgh has approved the protocol of this study (IRB #PRO08060015).

Table 1. 3x3 mixed factorial design.

The numbers listed in each group/condition are the subject IDs.

		Test condition		
		Pressure only	Pressure + slow cooling	Pressure + fast cooling
Level of injury	T6A	T6A01...T6A14	T6A01...T6A14	T6A01...T6A14
	T6B	T6B01...T6B14	T6B01...T6B14	T6B01...T6B14
	CTRL	CTRL01...CTRL14	CTRL01...CTRL14	CTRL01...CTRL14

3.2 SUBJECTS

A total of 36 adult subjects between 18 and 65 years old were recruited: 14 of them had no history of any neurological deficit, 14 had traumatic SCI with an injury level at T6 and above, and 8 had traumatic SCI with an injury level below T6. All subjects were free of any cardiovascular, pulmonary diseases, diabetes mellitus, or hypertension. Subjects with SCI did not have any current pressure ulcers at the sacral area, and experienced the injury at least one year prior to the experiment. They were all wheelchair users and had no motor function at the sacral level. To ensure that we tested the hypotheses of this study, only people with impaired autonomic function were recruited in the group of injury level at T6 and above. The subjects were recruited through the Department of Physical Medicine and Rehabilitation, and Center of Rehabilitation Services at the University of Pittsburgh Medical Center (UPMC). In addition, the research flyers were sent to the Human Engineering Research Laboratory, UPMC Center of Assistive Technology, Three Rivers Center of Independent Living, Keystone Paralyzed Veterans of America, Hope Network, Office of Vocational Rehabilitation and Three Rivers Adaptive Sports to distribute to potential subjects.

3.3 PROCEDURES

The study contained two parts: the screening and the experimental procedures. The purpose of the screening procedure was to ensure that only people who meet the inclusion criteria of the study were recruited. The purpose of the experimental procedure was to perform the three test sessions on the subjects.

3.3.1 Screening procedure

The screening procedure contained two parts: telephone screening and face-to-face screening procedures. Potential participants underwent the telephone screening process first, and the following information was obtained: age, gender, general health status (history of hypertension, diabetes mellitus, cardiovascular, pulmonary disease), level of injury, duration of injury, autonomic function (symptoms of autonomic dysreflexia, awareness of need to empty bladder and sensation of bowel movement) and history of pressure ulcers and smoking. Potential participants that met the criteria proceeded to a face-to-face screening procedure. After completing the consent form, several measurements were taken to determine the eligibility of the participants, including blood pressure, heart rate, motor function, and questionnaires (for injury level at T6 and above only) on other autonomic functions (i.e. sensation of changes in temperature and ability to sweat). The face-to-face screening procedure was performed in the Tissue Integrity Management (TIM) Laboratory at the Department of Rehabilitation Science and Technology, University of Pittsburgh. All caffeinated food and drinks were prohibited 12 hours prior to the face-to-face screening procedure, and smokers refrained from smoking for at least 4 hours prior to and during the experiment.

3.3.2 Experimental procedure

Once qualified for the study, the subject proceeded with the experimental procedure, which was performed in the TIM lab as well. Room temperature was controlled at $22\pm 1^{\circ}\text{C}$ ($71.6\pm 1.8^{\circ}\text{F}$). Subjects were kept relaxed for at least 30 minutes in the laboratory to acclimate to the room temperature. All subjects were randomly assigned to the order of the three experiment sessions

by allowing them to select one of six envelopes that contained one of the six different orders of the experiment sessions (Table 2).

Table 2. Randomization of the order of test sessions.

This table gives the six different orders of the three test sessions.

Envelop	Test session I	Test Session II	Test Session III
A	Pressure + Slow Cooling	Pressure + Fast Cooling	Pressure Only
B	Pressure Only	Pressure + Slow Cooling	Pressure + Fast Cooling
C	Pressure + Fast Cooling	Pressure Only	Pressure + Slow Cooling
D	Pressure + Slow Cooling	Pressure Only	Pressure + Fast Cooling
E	Pressure Only	Pressure + Fast Cooling	Pressure + Slow Cooling
F	Pressure + Fast Cooling	Pressure + Slow Cooling	Pressure Only

During the experiment, the subjects lay prone on the mat table, and the tests were performed on the skin at the sacrum (Figure 3). All three sessions had identical pressure application phases (Figure 4). A pressure of 0.4 kPa (3 mmHg) was applied to the skin for the first five minutes, then the pressure was increased to 8 kPa (60 mmHg) for 20 minutes, and the pressure dropped back to 0.4 kPa of pressure for another 10 minutes. Pressure of 0.4 kPa is equal to a light contact of the skin, while 8 kPa of pressure induced reactive hyperemia after pressure relief. Local cooling was applied to the skin during the 20-minute interval of 8 kPa pressure. A 30-60 minute washout period was given between each test session to avoid measuring the reactive hyperemic response from the previous test session (lasts about half of the time of tissue ischemia (Sprigle, et al., 2002)) as the baseline SBF for the next test session. To ensure the safety of the subject, blood pressure and heart rate were measured before and after each test session, and the skin was checked after each session to see if any blanching occurred.

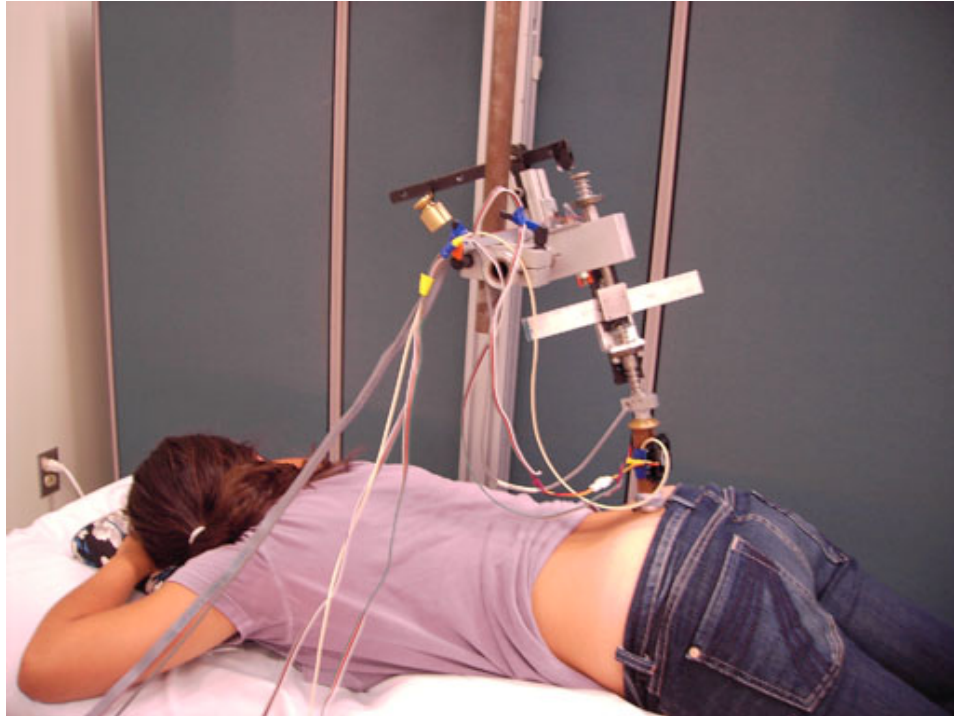


Figure 3. Test setting.

The subjects lay prone on the mat table, and the tests were performed on the skin at the sacrum.

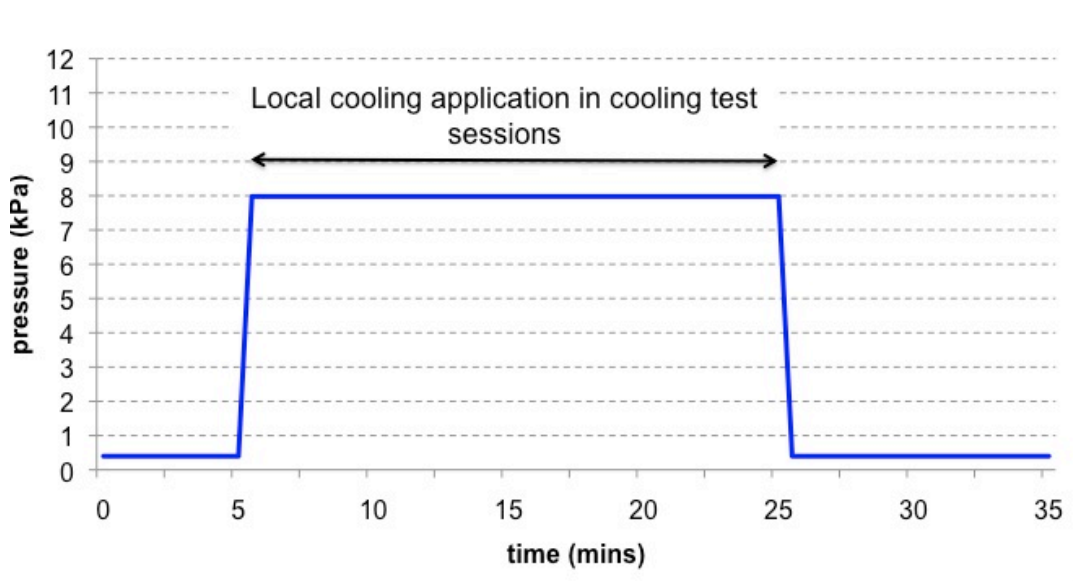


Figure 4. Pressure application phases.

A pressure of 0.4 kPa was applied to the skin for the first five minutes, then the pressure was increased to 8 kPa for 20 minutes, and the pressure dropped back to 0.4 kPa of pressure for another 10 minutes. Local cooling was applied to the skin during the 20-minute interval of 8 kPa pressure.

3.4 INSTRUMENTATION

The instruments that were used in this study include: 1) computer-controlled indenter, 2) cooling system, and 3) laser Doppler flowmetry (LDF). A computer interface created by the LabVIEW program (version 7.3, National Instrument, Austin, TX) was used to control both temperature and pressure (Figure 5) and displayed the SBF and temperature data in real-time for easy monitoring.

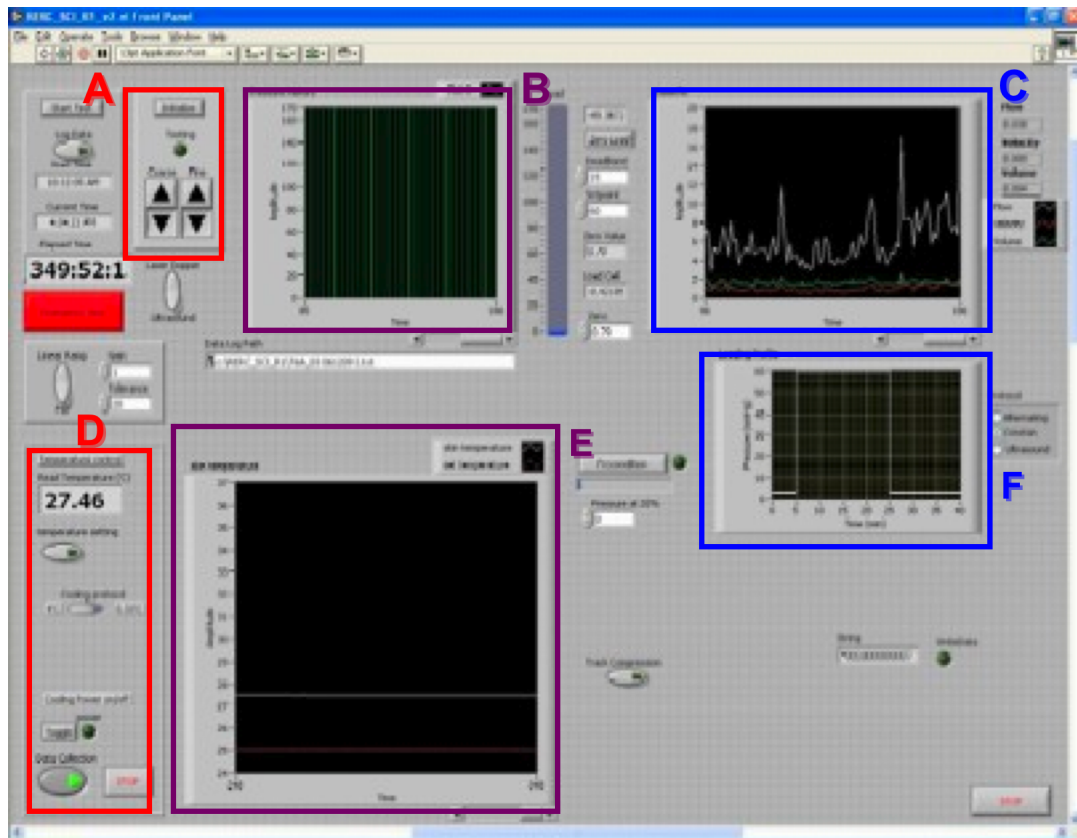


Figure 5. Computer control interface created with LabVIEW.
(A) pressure control panel, (B) pressure monitor, (C) SBF monitor, (D) temperature control, (E) temperature monitor, and (F) display of pressure control phase.

3.4.1 Computer-controlled indenter

A computer-controlled indenter was used to maintain the pressure applied on the skin (Figure 6). From bottom to the top, it consists of a load cell (LC703, Omegadyne Inc., Sunbury, OH), a stage (MTR-13-E, National Aperture Inc., Salem, NH), a motor, and a lever system. A strain gauge was located within the load cell. Deformation of the strain gauge provided readings of the force that was applied on the skin. A proportional-integral-derivative (PID) controller was embedded in the LabVIEW program. The force read by the load cell was compared to the target value, and the moving speed of the stage was adjusted through the motor to maintain the pressure applied on the skin. The lever system was counter-weighted to allow the indenter to accommodate the respiratory movement of the subjects during the test.

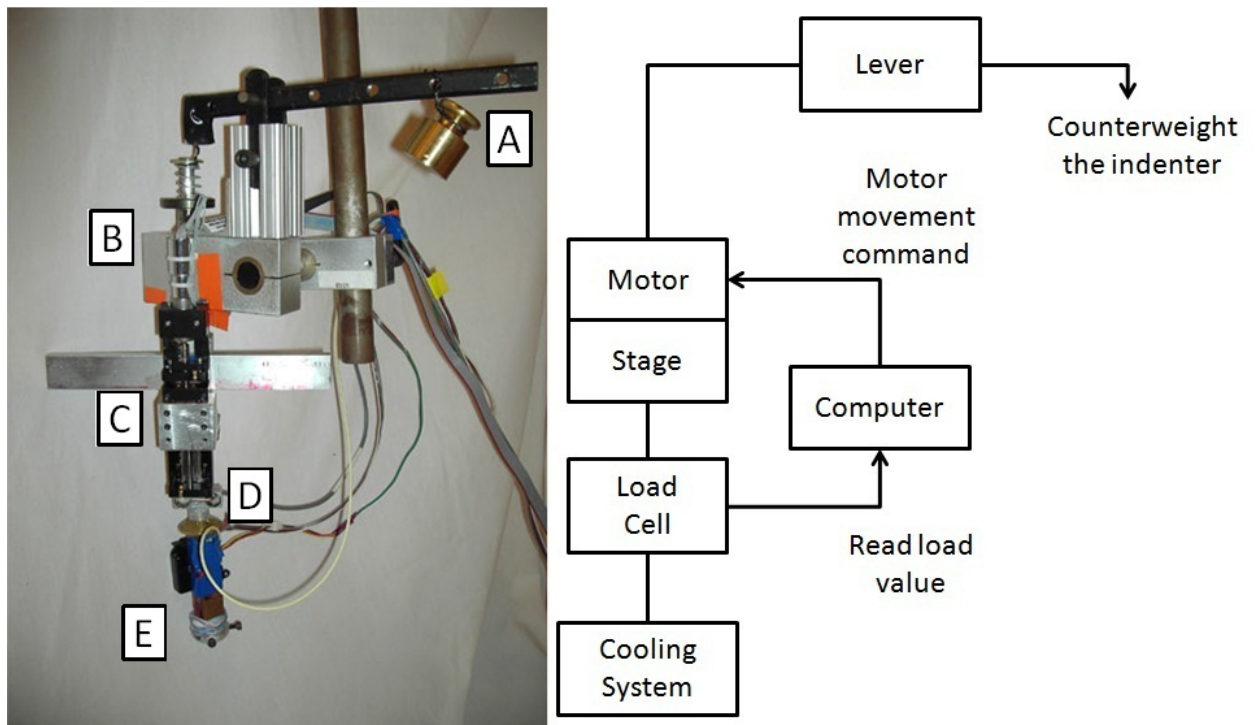


Figure 6. Computer-controlled indenter.

Left side: picture of computer controlled indenter (A) lever, (B) motor, (C) stage, (D) load cell, and (E) cooling system; Right side: schematic figure of the loading system.

3.4.2 Cooling system

A thermoelectric (TE) cooling system (TE Technology, Traverse City, MI) was used to measure the skin temperature and apply local cooling at two different rates (Figure 7). It was located below the load cell of the computer-controlled indenter, and it was the only component that contacted the skin directly. A ball-and-socket joint was used to connect the cooling system to the load cell to provide more range of motion for the respiratory movement of the subjects. The total cooling area of the skin was 1.8 cm^2 , and an opening (.2 cm in diameter) was located in the center of the cooling system to hold the LDF probe.

The cooling system consists of four parts: the thermistor (modified from model MP2444), TE module (CH-38-1.0-0.8), heat radiator, and temperature controller board (TC-36-25 RS232). The TE module actively transfers heat from its cold side to the heat side through the Peltier effect. The thermistor was attached to the cold side of the module, and the heat radiator was attached to the heat side with a conductive glue (TSE3941, Toshiba, Japan). A mini fan was attached to the side of the radiator to assist the process of heat radiation. Another PID controller embedded within the temperature controller board was used to control the skin temperature. The parameters of the PID controller were set up as: proportional bandwidth = 1°C , integral gain = 0.1 repeat/minute, and derivative gain = 0.1 minute. The skin temperature measured by the thermistor was compared to the target value within the temperature controller, and the electrical power supplied to the TE module was adjusted based on the difference.

Since the thermoelectric module was not thermally insulated and the cooling system was mainly made from copper, the thermoelectric module was preheated to 36°C for 20 minutes prior to the test to prevent cooling effect caused by the large heat sink capacity of the cooling system. After the thermoelectric module was preheated for 20 minutes, the preheating procedure was

turned off for 10 minutes before the probe was attached to the skin. During the 10 minutes, the temperature was able to reach to a steady state temperature of 26°C (slightly lower than the normal skin temperature). The probe was attached to the skin for another 10 minutes before the collection of any experimental data to ensure the thermistor was reading the actual skin temperature. The experimental procedure did not start until the skin temperature reached a steady state (changes within 0.001°C/sec).

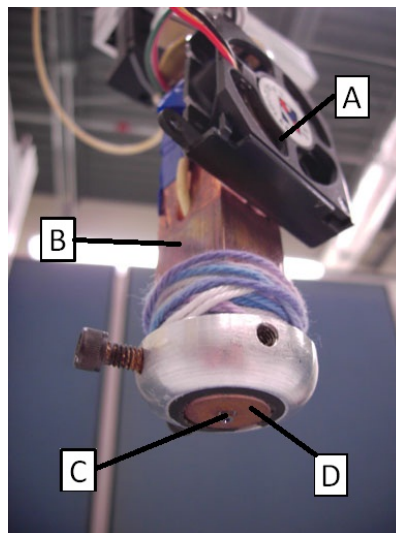


Figure 7. Thermoelectric cooling system at the tip of the indenter.
(A) mini fan, (B) heat sink, (C) opening for LDF probe, and (D) thermistor.

3.4.3 Laser Doppler flowmetry

Laserflo Blood Perfusion Monitor 2 (Vasamedics, Eden Prairie, MN) was used in the study to collect the SBF data. The Softip pencil probe (P-435) was located in the center of the cooling system to measure the SBF throughout each test session (Figure 7). This FDA-approved device provided non-invasive measurements of SBF at about 1 mm deep.

3.5 OUTCOME MEASURES AND DATA ANALYSIS

3.5.1 Outcome measures and SBF signal processing

The outcome measures collected in this study include demographic data and experimental data. The demographic data collected included: age, body mass index [weight (kg)/ (height (m))²], autonomic function, injury level, years post-injury, and mean blood pressure (2/3 diastolic pressure + 1/3 systolic pressure). The experimental data collected in this study included pressure applied on the skin, skin temperature and skin blood flow. Figure 8 is a schematic figure showing all the outcome measures collected for statistical analysis in this study. A signal processing procedure was performed to the skin blood flow data to get the time-domain parameters of the reactive hyperemia and the normalized spectral densities for statistical analyses. The steps of signal processing are broken down in Figure 9.

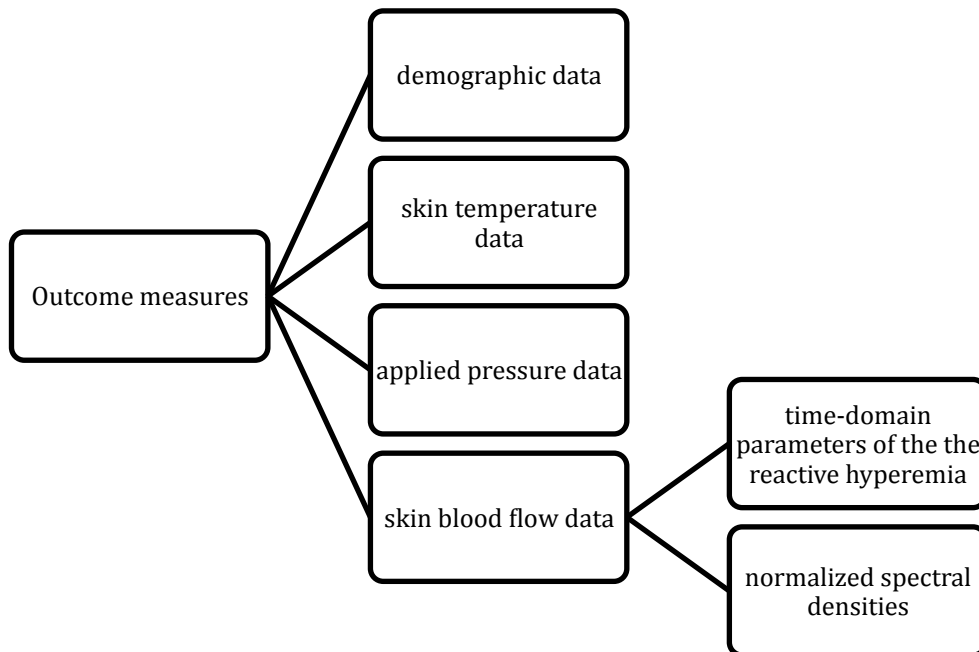


Figure 8. Schematic figure of outcome measures collected.

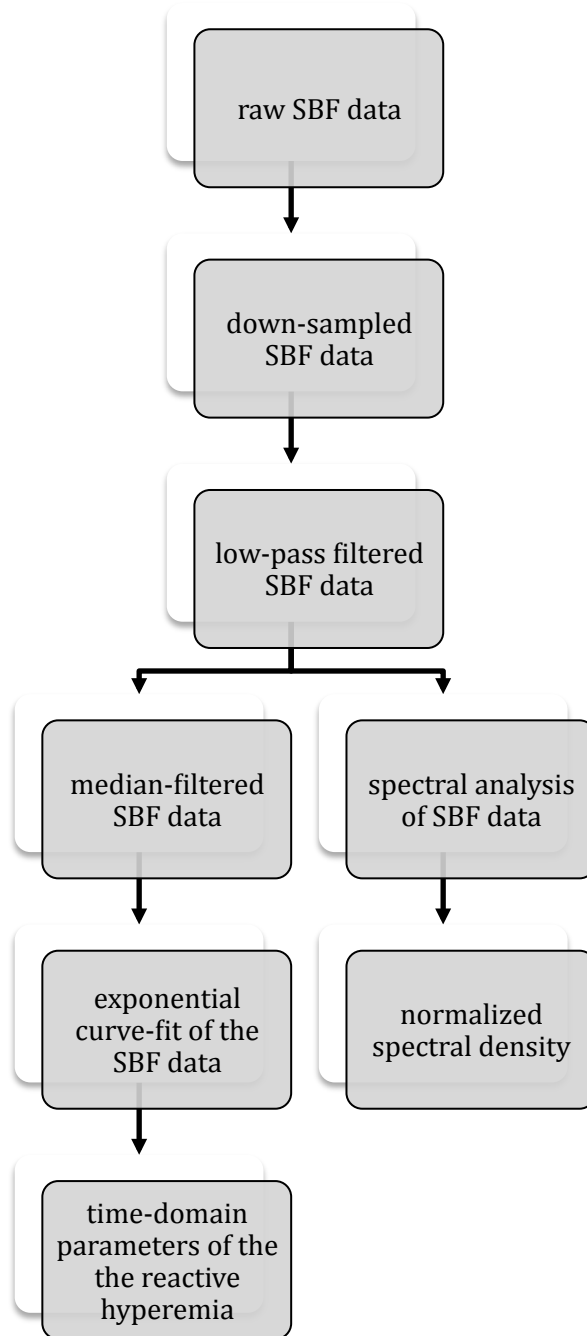


Figure 9. Schematic figure of steps of signal processing.

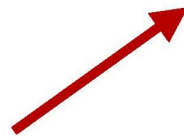
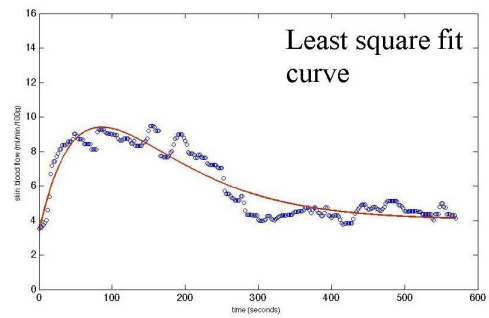
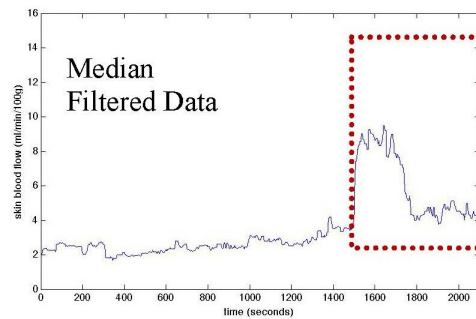
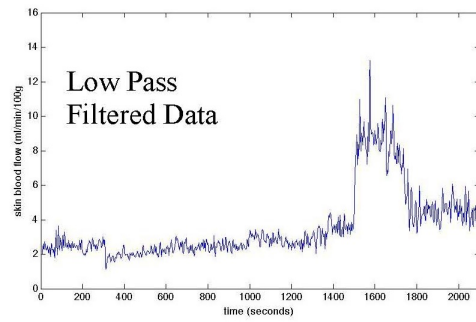
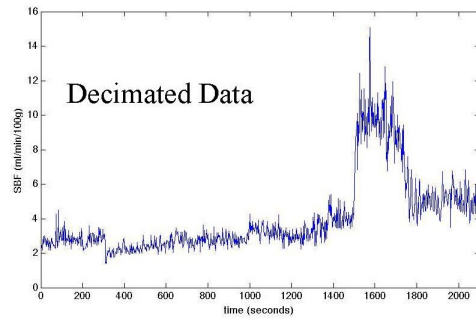
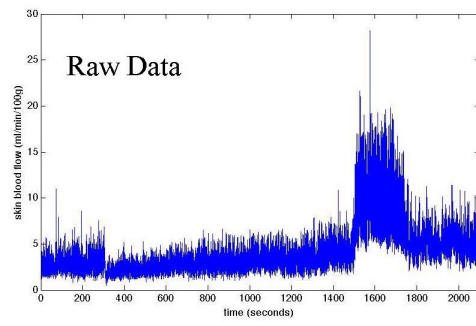


Figure 10. Steps of skin blood flow signal processing.

Figure 9 is the schematic figure of signal processing, and Figure 10 shows the steps of SBF signal processing in one of the subjects' data. The MatLab program (The MathWorks, Natick, MA) was used to perform the signal processing. The raw SBF data were sampled at a rate of 20 Hz. The data were then digitally down-sampled to 0.5 Hz (with anti-aliasing filter [Matlab routine: decimate]). Since we were not interested in the vasomotion caused by heart rate and respiration, a tenth-ordered Chebyshev I low-pass filter (with the cut-off frequency at 0.15Hz) was applied to the down-sampled SBF data. The SBF data was then processed into two pathways, one was to select the time domain parameters of the reactive hyperemia and the other was to calculate the normalized spectral densities. In order to remove large outliers (spikes) from the time series data, before selecting any time domain parameters of the reactive hyperemia, an 11-point-window (22 seconds) median filter was applied to the low-pass-filtered SBF data. Least-squared model fit was used to fit a bi-exponential curve (Equation 6) to the filtered SBF data to calculate parameters: A_1 , A_2 , τ_1 , τ_2 and B . The five time-domain parameters of the reactive hyperemia were then calculated based on the fit equation. The five time-domain parameters were the baseline, normalized peak SBF, time to peak SBF, half life and the perfusion area. By taking derivative of Equation 6, time to peak (Equation 8) can be calculated when Equation 7 equals zero. Peak SBF can be calculated by plugging Equation 8 into Equation 6, and it's shown in Equation 9. To normalize the peak SBF and calculate the perfusion area and half life, baseline SBF should be calculated first. Baseline SBF is the averaged value of skin blood flow data collected at the first five minutes of the test sessions, and it is given symbol \bar{S} for following equations.

Equation 6. Bi-exponential equation for curve fitting.

$$y(t) = A_1 e^{-t/\tau_1} + A_2 e^{-t/\tau_2} + B$$

Equation 7. Derivative of equation 5.

$$y'(t) = A_1 \left(\frac{-1}{\tau_1} \right) e^{-t/\tau_1} + A_1 \left(\frac{-1}{\tau_2} \right) e^{-t/\tau_2}$$

Equation 8. Time to peak SBF calculated from equation 6.

$$t = \frac{\ln \left(-\frac{A_2}{\tau_2} \times \frac{\tau_1}{A_1} \right)}{\left(\frac{1}{\tau_2} - \frac{1}{\tau_1} \right)}$$

Equation 9. Peak SBF.

$$\begin{aligned} y_{peak} &= A_1 e^{\frac{\ln(-A_2\tau_1/A_1\tau_2)}{1-\tau_1/\tau_2}} + A_2 e^{\frac{\ln(-A_2\tau_1/A_1\tau_2)}{-1+\tau_2/\tau_1}} + B \\ &= A_1 \left(\frac{-A_2\tau_1}{A_1\tau_2} \right)^{\frac{\tau_2}{\tau_2-\tau_1}} + A_2 \left(\frac{-A_2\tau_1}{A_1\tau_2} \right)^{\frac{\tau_1}{\tau_2-\tau_1}} + B \end{aligned}$$

Equation 10. Normalized peak SBF. \bar{S} is the baseline SBF.

$$y_{normalized-peak} = \left[\left(y_{peak} - \bar{S} \right) / \bar{S} \right] \times 100\%$$

Equation 11. Perfusion area. \bar{S} is the baseline SBF.

$$\begin{aligned} area &= \int_{t=0}^{\infty} (y(t) - \bar{S}) dt = A_1 \int_{t=0}^{\infty} e^{-t/\tau_1} dt + A_2 \int_{t=0}^{\infty} e^{-t/\tau_2} dt + \int_{t=0}^{\infty} (B - \bar{S}) dt \\ &= A_1 (0 - (-\tau_1)) + A_2 (0 - (-\tau_2)) = A_1\tau_1 + A_2\tau_2 \end{aligned}$$

To obtain the normalized spectral densities of the SBF data, spectrogram was computed. Spectrogram is the magnitude-square of short-time Fourier transform (Equation 12) (Cohen, 1995b). A 256-sample Hanning window (512 seconds) was used to compute the spectrogram. This window length was selected so that the spectral main lobe of the window ($\sim 4/T$, $T=512$ seconds) was narrower than the width of the narrowest physiologic band (0.012 Hz,

corresponding to the metabolic band), thereby guarding against significant leakage of power from one physiologic band into its neighboring band. For statistical purposes, the spectrogram was integrated within the three target frequency bands: 1) metabolic: 0.008-0.02 Hz, 2) neurogenic: 0.02-0.05 Hz, 3) myogenic: 0.05-0.15 Hz, and within two time intervals: 1) the five minutes prior to 8 kPa pressure application, and 2) the first five minutes after 8 kPa pressure removal. The integrated spectrogram was normalized to the spectrogram at baseline (five minutes prior to 8 kPa pressure application) for the metabolic (Equation 13), neurogenic (Equation 14), and myogenic (Equation 15) frequency bands.

Equation 12. Spectrogram.

$S_t(\omega)$ is the Fourier transform of signal $s(\tau)$, and $h(\tau-t)$ is the window function.

$$P_{SP}(t, \omega) = |S_t(\omega)|^2 = \left| \frac{1}{\sqrt{2\pi}} \int e^{-j\omega\tau} s(\tau) h(\tau - t) d\tau \right|^2$$

Equation 13. Normalized metabolic spectral density.

The metabolic spectral density (frequency range: 0.008-0.02Hz) during time period 1500-1800 seconds is normalized to that during time period 0-300 seconds.

$$P_{sp-\omega} = \left[\left(\int_{\omega=0.008 \text{ Hz}}^{0.02 \text{ Hz}} \int_{T=1500 \text{ sec}}^{1800 \text{ sec}} (T, \omega) dT d\omega \right) / \left(\int_{\omega=0.008 \text{ Hz}}^{0.02 \text{ Hz}} \int_{T=0 \text{ sec}}^{300 \text{ sec}} (T, \omega) dT d\omega \right) \right] \times 100\%$$

Equation 14. Normalized neurogenic spectral density.

The neurogenic spectral density (frequency range: 0.02-0.05Hz) during time period 1500-1800 seconds is normalized to that during time period 0-300 seconds.

$$P_{sp-\omega} = \left[\left(\int_{\omega=0.02 \text{ Hz}}^{0.05 \text{ Hz}} \int_{T=1500 \text{ sec}}^{1800 \text{ sec}} (T, \omega) dT d\omega \right) / \left(\int_{\omega=0.02 \text{ Hz}}^{0.05 \text{ Hz}} \int_{T=0 \text{ sec}}^{300 \text{ sec}} (T, \omega) dT d\omega \right) \right] \times 100\%$$

Equation 15. Normalized myogenic spectral density.

The myogenic spectral density (frequency range: 0.05-0.15Hz) during time period 1500-1800 seconds is normalized to that during time period 0-300 seconds.

$$P_{sp-\omega} = \left[\left(\int_{\omega=0.05 \text{ Hz}}^{0.15 \text{ Hz}} \int_{T=1500 \text{ sec}}^{1800 \text{ sec}} (T, \omega) dT d\omega \right) / \left(\int_{\omega=0.05 \text{ Hz}}^{0.15 \text{ Hz}} \int_{T=0 \text{ sec}}^{300 \text{ sec}} (T, \omega) dT d\omega \right) \right] \times 100\%$$

To compare the difference among subjects with different levels of neurological deficits, outcome measures generated from the time domain parameters were calculated. The outcome measures for each cooling condition were calculated as percent changes in reactive hyperemia parameters from the pressure only condition. The four parameters are listed as followed:

Equation 16. Percent changes in normalized peak SBF with fast cooling.

$$\Delta normalized_peak_{Fast} = \left[\left(NpSBF_{Non-cooling} - NpSBF_{Fast-cooling} \right) / NpSBF_{Non-cooling} \right] \times 100\%$$

Equation 17. Percent changes in perfusion area with fast cooling.

$$\Delta area_{Fast} = \left[\left(area_{Non-cooling} - area_{Fast-cooling} \right) / area_{Non-cooling} \right] \times 100\%$$

Equation 18. Percent changes in normalized peak SBF with slow cooling.

$$\Delta normalized_peak_{Slow} = \left[\left(NpSBF_{Non-cooling} - NpSBF_{Slow-cooling} \right) / NpSBF_{Non-cooling} \right] \times 100\%$$

Equation 19. Percent changes in perfusion area with slow cooling.

$$\Delta area_{Slow} = \left[\left(area_{Non-cooling} - area_{Slow-cooling} \right) / area_{Non-cooling} \right] \times 100\%$$

3.5.2 Statistical analysis

Descriptive analysis was used to see the distribution of the data and to determine the statistical analysis to use. Parametric tests were used for normally distributed variables, while non-parametric tests were used for non-normally distributed variables (Portney & Watkins, 2000). To ensure the consistency of the test instrument, two way repeated measures analysis of variance (ANOVA) was used to compare the applied pressure on the three test sessions and among the three groups of subjects. In addition, to ensure the cooling capacity of the test system and that

skin temperature was the same before any temperature controls, two way repeated measures ANOVA was used to compare the skin temperature among all three test sessions and three groups of subjects before and at the end of the cooling application. For hypotheses 1 a) and b), the variables to be compared within subjects included the four parameters of the reactive hyperemia (normalized peak SBF, perfusion area, time to peak SBF, half life) and the integrated spectrum during two intervals (baseline and the first 5 minutes of reactive hyperemia) within each of the three frequency bands. To compare the four parameters of the reactive hyperemia, one way repeated measures ANOVA or Friedman test was used for parametric or nonparametric variables. A p value $<.05$ was recognized as significant and Pair-wise comparison with Bonferroni correction was used if the repeated measures ANOVA or Friedman tests showed significant results. To compare the integrated spectral densities change over time, paired t -test or Wilcoxon signed rank test was used to compare the difference between baseline and the first five minutes of reactive hyperemia with each group of subjects and each of the three test sessions. For hypotheses 2), one way ANOVA or Kruskal-Wallis test was used to compare the difference of percent changes with fast and slow cooling application from pressure only in normalized peak SBF, perfusion area, time to peak, and half life among the three subject groups.

4.0 RESULTS

A total of 36 adult subjects between 18 and 65 years old were recruited: 14 of them had no history of any neurological deficit, 14 had traumatic SCI with an injury level at T6 and above, and 8 had traumatic SCI with an injury level below T6. Since the reactive hyperemic response was the main outcome measurement of the study, the existence of reactive hyperemia was determined before any statistical analysis was computed.

4.1 EXISTENCE OF REACTIVE HYPEREMIA

According to the definition of reactive hyperemia, which is an increase in blood flow after ischemia relief that returns to the baseline value (Levick, 2003), the SBF after pressure relief that did not exceed the baseline value was considered as no reactive hyperemic response.

Figure 11 is the summary of percentage of existence of reactive hyperemia in all three groups, and Table 3 provides details of each subject. The reactive hyperemic response was not observed in the pressure only test session in one subject in the control group (CTRL_19), two subjects in T6A group (T6A_04 and T6A_11), and two subjects in the T6B group (T6B_01 and T6B_06). These five subjects also did not have reactive hyperemia in both the fast and slow cooling test sessions. For the rest of the subjects, five out of 13 subjects (38.46%) in control group, four out of 12 subject (33.33%) in T6A group, and two out of six subjects (33.33%) in

T6B group had no reactive hyperemic response with fast cooling. One out of 13 subjects (7.69%) in control group, two out of 12 subjects (16.67%) in T6A group, and one out of six subjects (16.67%) in T6B group had no reactive hyperemic response with slow cooling.

Since the reactive hyperemic response was not induced in five subjects, the results of these five subjects were reported separately from the rest of the subjects. In addition, data from the five subjects were not included for statistical analysis.

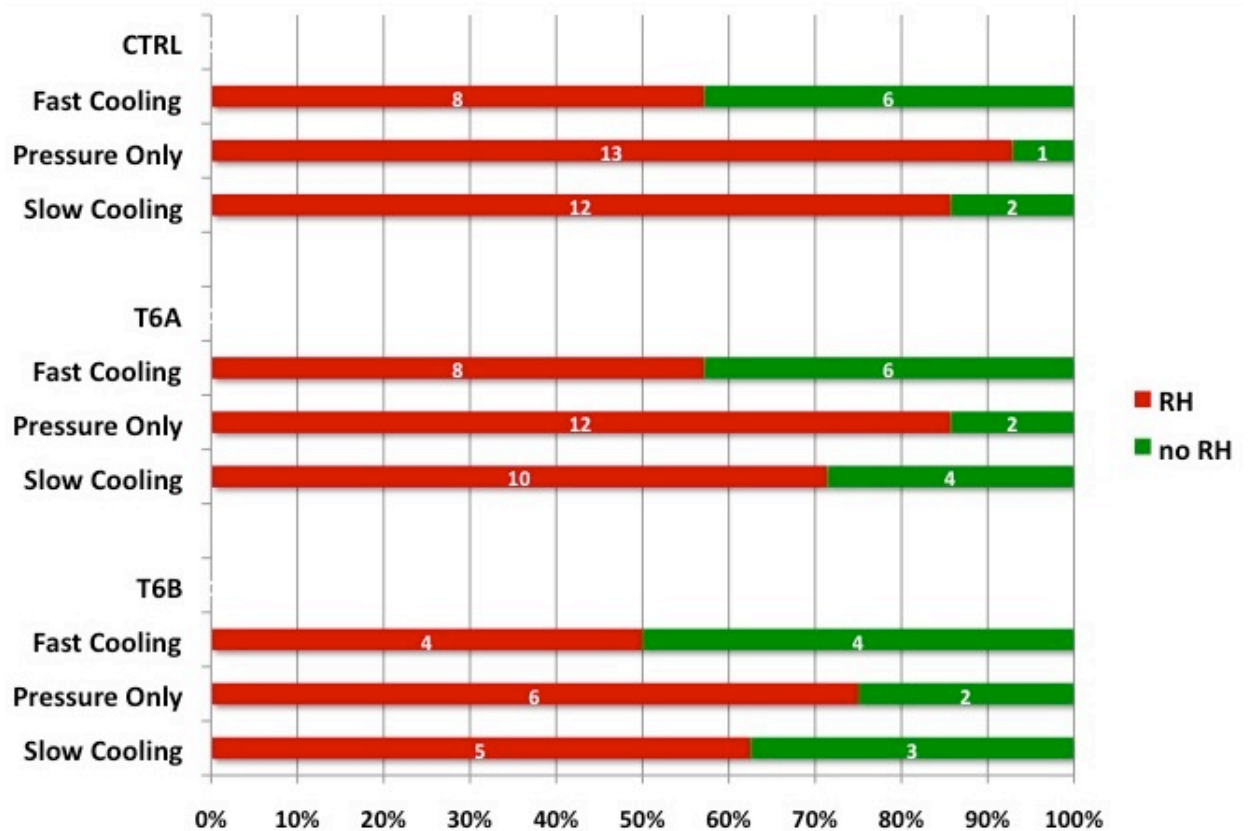


Figure 11. Summary of the existence of reactive hyperemic response. RH = reactive hyperemia.

Table 3. Details of existence of reactive hyperemic response in all subjects.

Subject ID	Test Session	Reactive Hyperemia	Subject ID	Test Session	Reactive Hyperemia	Subject ID	Test Session	Reactive Hyperemia
CTRL_01	PF	+	T6A_01	PF	-	T6B_01	PF	-
	PO	+		PO	+		PO	-
	PS	+		PS	+		PS	-
CTRL_03	PF	-	T6A_03	PF	-	T6B_02	PF	+
	PO	+		PO	+		PO	+
	PS	+		PS	+		PS	+
CTRL_04	PF	+	T6A_04	PF	-	T6B_03	PF	+
	PO	+		PO	-		PO	+
	PS	+		PS	-		PS	+
CTRL_05	PF	+	T6A_05	PF	+	T6B_04	PF	-
	PO	+		PO	+		PO	+
	PS	+		PS	-		PS	+
CTRL_06	PF	+	T6A_06	PF	-	T6B_05	PF	+
	PO	+		PO	+		PO	+
	PS	+		PS	+		PS	-
CTRL_07	PF	+	T6A_07	PF	+	T6B_06	PF	-
	PO	+		PO	+		PO	-
	PS	+		PS	+		PS	-
CTRL_09	PF	-	T6A_08	PF	+	T6B_07	PF	+
	PO	+		PO	+		PO	+
	PS	-		PS	+		PS	+
CTRL_10	PF	-	T6A_09	PF	-	T6B_09	PF	-
	PO	+		PO	+		PO	+
	PS	+		PS	+		PS	+
CTRL_11	PF	+	T6A_10	PF	+	/		
	PO	+		PO	+			
	PS	+		PS	+			
CTRL_13	PF	-	T6A_11	PF	-			
	PO	+		PO	-			
	PS	+		PS	-			
CTRL_14	PF	+	T6A_12	PF	+			
	PO	+		PO	+			
	PS	+		PS	+			
CTRL_16	PF	-	T6A_13	PF	+			
	PO	+		PO	+			
	PS	+		PS	+			
CTRL_17	PF	+	T6A_14	PF	+			
	PO	+		PO	+			
	PS	+		PS	-			
CTRL_19	PF	-	T6A_15	PF	+			
	PO	-		PO	+			
	PS	-		PS	+			

PF= pressure + fast cooling, PO= pressure only, PS= pressure + slow cooling. '+' represents existence of reactive hyperemia, and '-' represents no reactive hyperemia.

4.2 RANDOMIZATION OF THE ORDER OF TEST SESSIONS

All subjects selected one of the six envelopes for the purpose of randomizing the order of the three test sessions. Table 4 shows the number of subjects within each group that underwent the six different orders of the test sessions. The five subjects that did not have reactive hyperemia in all three test sessions were excluded in this table. The order of the test sessions of these five subjects is presented in Table 5.

Table 4. Number of subjects within each group that underwent each order of the three test sessions.
This table excludes the subjects that did not have reactive hyperemia in all three test sessions.

Order of Tests \ Group	CTRL	T6A	T6B	Total
A: PS→PF→PO	1	2	2	5
B: PO→PS→PF	-	4	1	5
C: PF→PO→PS	4	2	1	7
D: PS→PO→PF	3	3	2	8
E: PO→PF→PS	2	-	-	2
F: PF→PS→PO	4	3	2	9

PS = pressure + slow cooling test session, PF = pressure + fast cooling test session, PO = pressure only test session, CTRL = control group, T6A = subjects with injury level at T6 and above, and T6B = subjects with injury level below T6. ‘-’ = no subjects with that order of the test sessions.

Table 5. Number of subjects within each group that underwent each order of the three test sessions.
This table only contains the five subjects that did not have reactive hyperemia in all three test sessions.

Order of Tests \ Group	CTRL	T6A	T6B	Total
A: PS→PF→PO	-	-	-	0
B: PO→PS→PF	-	1	-	1
C: PF→PO→PS	-	-	-	0
D: PS→PO→PF	1	-	1	2
E: PO→PF→PS	-	-	-	0
F: PF→PS→PO	-	1	1	2

PS = pressure + slow cooling test session, PF = pressure + fast cooling test session, PO = pressure only test session, CTRL = control group, T6A = subjects with injury level at T6 and above, and T6B = subjects with injury level below T6. ‘-’ = no subjects with that order of the test sessions.

4.3 DEMOGRAPHIC DATA

Table 6 is the summary of the subjects' demographic data (excludes the five subjects that did not have reactive hyperemia in all three test sessions) and Table 7 shows the details of each subject's demographic information. There were more male subjects than female subjects in both T6A and T6B groups, and the averaged age of the two SCI groups were slightly higher than the control group. The body mass index and the skinfold thickness were similar in all three groups. The mean blood pressure was slightly higher in the T6B group, while it was slightly lower in the T6A group. The 14 subjects in group T6A all had symptoms of autonomic dysreflexia, no awareness of the need to empty bladder or bowel movement. Although three of these 14 subjects had sensation preserved below the injury level, these 14 subjects self reported that they had no sensation of changes in temperature and reduced ability to sweat below the injury level.

Table 6. Summary of subjects' demographic data.

The results were presented in mean \pm one standard deviation. This table excludes the subjects that did not have reactive hyperemia in all three test sections.

Group	Number of Subjects Recruited	Gender	Age	Body Mass Index (kg/m ²)	Injury Duration (yrs)	Mean Blood Pressure (mmHg)	Skinfold Thickness (cm)
CTRL	13	6 Male 7 Female	34.22 \pm 11.45	22.77 \pm 3.34	NA*	84.85 \pm 8.48	0.71 \pm 0.26
T6A	12	11 Male 1 Female	37.69 \pm 11.20	22.13 \pm 3.68	13.00 \pm 9.78	77.92 \pm 7.74	0.69 \pm 0.17
T6B	6	5 Male 1 Female	36.81 \pm 10.02	26.35 \pm 4.05	10.50 \pm 6.83	95.56 \pm 8.48	0.85 \pm 0.19

*NA= not applicable.

Table 7. Detailed demographic information of all subjects.

The five subjects that did not have reactive hyperemic response in all three test sessions were highlighted in **bold**.

Subject	Gender	Age	Body Mass Index (kg/m ²)	Race	Injury Level	Injury Duration (yrs)	ASIA Grade	Sensation	Mean Blood Pressure (mmHg)	Skinfold Thickness (cm)	Smoker
CTRL_01	Male	36.36	28.69	Caucasian	-	-	-	+	102.22	1.33	-
CTRL_03	Male	48.17	23.01	Caucasian	-	-	-	+	87.56	0.51	-
CTRL_04	Male	27.23	24.03	Asian	-	-	-	+	76.78	0.55	-
CTRL_05	Male	49.93	24.41	Caucasian	-	-	-	+	88.00	0.63	-
CTRL_06	Female	29.26	20.12	Asian	-	-	-	+	80.56	0.57	-
CTRL_07	Female	19.43	24.13	Caucasian	-	-	-	+	77.33	0.81	-
CTRL_09	Female	50.62	24.63	Caucasian	-	-	-	+	78.11	0.67	-
CTRL_10	Male	19.82	20.64	Caucasian	-	-	-	+	84.11	0.74	-
CTRL_11	Female	21.37	21.48	Caucasian	-	-	-	+	91.56	0.54	-
CTRL_13	Male	25.14	27.26	Caucasian	-	-	-	+	91.56	0.66	-
CTRL_14	Female	35.67	17.80	Asian	-	-	-	+	69.56	0.77	-
CTRL_16	Female	44.03	22.66	Asian	-	-	-	+	90.67	1.12	-
CTRL_17	Female	37.84	17.23	Caucasian	-	-	-	+	85.11	0.39	-
CTRL_19	Male	28.14	23.01	Caucasian	-	-	-	+	88.44	0.50	-
T6A_01	Male	20.71	16.82	A-A	C5-C6	3	A	-	81.56	0.52	-
T6A_03	Male	43.29	26.17	Caucasian	C7	18	A	-	83.78	0.94	-
T6A_04	Male	47.93	20.09	A-A	T4-5	14	A	-	94.44	0.95	-
T6A_05	Female	26.71	20.34	Caucasian	T4	2	A	-	74.00	1.04	-
T6A_06	Male	34.94	24.33	Caucasian	C4	6	A	-	73.78	0.62	-
T6A_07	Male	48.27	23.67	Caucasian	C5-6	23	A	-	85.00	0.64	-
T6A_08	Male	37.26	19.58	Caucasian	C5-7	5	A	-	71.11	0.51	-
T6A_09	Male	50.27	25.63	Caucasian	C5-6	31	A	-	80.22	0.71	-
T6A_10	Male	27.30	17.63	Caucasian	C7	7	A	-	66.89	0.49	-
T6A_11	Male	28.90	26.58	Caucasian	C6-T5	4	A	-	79.11	0.66	-
T6A_12	Male	32.07	20.63	Caucasian	C6-7	4.5	B	+	74.67	0.64	-
T6A_13	Male	60.33	28.89	Caucasian	C6	25	B	+	70.00	0.74	-
T6A_14	Male	35.42	22.38	Caucasian	T4-6	16.5	A	-	94.67	0.70	-
T6A_15	Male	35.73	19.49	Caucasian	C7-8	15	B	+	79.33	0.74	-
T6B_01	Male	52.59	25.09	Caucasian	T7-8	34	B	+	95.44	0.75	-
T6B_02	Female	47.44	29.12	A-A	T7	2	B	+	106.22	0.87	+
T6B_03	Male	41.84	22.04	Caucasian	T11-12	17	A	-	103.11	0.80	-
T6B_04	Male	27.81	24.78	Caucasian	T8	9	A	-	98.67	0.59	-
T6B_05	Male	45.85	30.54	Caucasian	T6-7	16	A	-	92.00	0.75	+
T6B_06	Male	57.86	33.38	A-A	T12	22	B	+	106.67	0.86	-
T6B_07	Male	22.75	29.98	Caucasian	T8-9	3	A	-	84.67	1.17	+
T6B_09	Male	35.15	21.62	A-A	T7	16	A	-	88.67	0.91	-

A-A = African-American. ASIA Grade is the grading standard of spinal cord injury from American Spinal Injury Association. ASIA Grade A = Complete: No motor or sensory function is preserved in the sacral segments S4-S5. ASIA Grade B = Incomplete: Sensory but not motor function is preserved below the neurological level and includes the sacral segments S4-S5. (American Spinal Injury Association, 2006)

4.4 PRESSURE APPLIED ON THE SKIN

4.4.1 Results from subjects that had reactive hyperemia in pressure only test session

Figure 12, Figure 13, and Figure 14 are the average applied pressure on the skin of all subjects (excludes those without reactive hyperemia in all three test sessions) in the control, T6A and T6B groups for the three test sessions, respectively. To show the comparison among the three different test sessions, the data was averaged every 30 seconds to plot the three figures. By observing the three figures, the applied pressure was maintained at 3 mmHg during the first five minutes and the last 10 minutes of the test in all three test sessions of all three groups of subjects. From the fifth to the 25th minute of the test, the applied pressure was maintained at 60 mmHg during the 20 minutes in all three test sessions of all three groups of subjects. Although the applied pressure oscillated slightly above and below the target value in subject groups T6A and T6B throughout the test, the applied pressure rapidly reached the target value.

To compare the pressure applied on the skin, especially to ensure that the pressure applied on the skin to induce the reactive hyperemic response was the same in all participants, a two-way repeated measures ANOVA was used to compare the pressure during the three phases of the test (averaged during the first 5 minutes, the 20 minutes of 60 mmHg pressure application period, and the last 10 minutes of the test). Table 8, Table 9 and Table 10 show the results of descriptive analysis (mean and standard deviation) and two-way repeated measures ANOVA of the applied pressure on the skin in the three groups during the three pressure application phases. The results showed that the pressure applied on the skin during the 60 mmHg pressure application was not significantly different among the three test sessions and the three groups of subjects (Table 9). The applied pressure during baseline and reactive hyperemia were

significantly higher in the T6A and T6B groups, however the differences were small (within 1 mmHg). This may be due to the slight oscillation of pressure in the two SCI groups.

Table 8. Mean and standard deviation of applied pressure on the sacral skin during baseline.

Test Session Group	PF	PO	PS	Comparisons (<i>p</i>)	
				Within Subject	Between Group
CTRL	3.00 ± 0.45	3.02 ± 0.41	3.11 ± 0.48	.271	<.001*
T6A	3.97 ± 0.62	3.77 ± 0.70	3.52 ± 0.53		
T6B	3.64 ± 0.15	3.72 ± 0.26	3.60 ± 0.11		

PS = pressure + slow cooling test session, PF = pressure + fast cooling test session, PO = pressure only test session.

Table 9. Mean and standard deviation of applied pressure on the sacral skin during 60mmHg of target pressure.

Test Session Group	PF	PO	PS	Comparisons (<i>p</i>)	
				Within Subject	Between Group
CTRL	57.36 ± 1.89	57.85 ± 2.46	57.48 ± 1.53	.144	.177
T6A	58.65 ± 4.35	59.38 ± 5.05	59.84 ± 4.45		
T6B	60.05 ± 4.45	61.12 ± 2.89	60.54 ± 3.98		

PS = pressure + slow cooling test session, PF = pressure + fast cooling test session, PO = pressure only test session.

Table 10. Mean and standard deviation of applied pressure on the sacral skin during reactive hyperemia.

Test Session Group	PF	PO	PS	Comparisons (<i>p</i>)	
				Within Subject	Between Group
CTRL	3.05 ± 0.53	2.98 ± 0.37	3.06 ± 0.42	.670	<.001*
T6A	3.86 ± 0.78	3.92 ± 0.63	3.62 ± 0.60		
T6B	3.64 ± 0.21	3.73 ± 0.32	3.72 ± 0.19		

PS = pressure + slow cooling test session, PF = pressure + fast cooling test session, PO = pressure only test session.

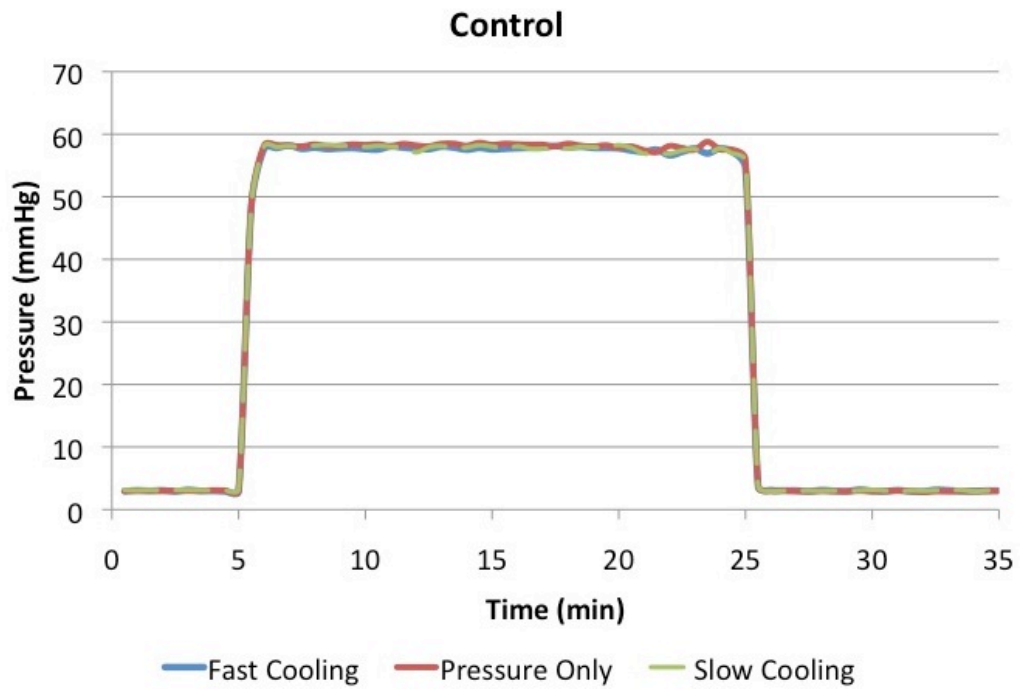


Figure 12. Average applied pressure during three test sessions on subjects with reactive hyperemia in control group.

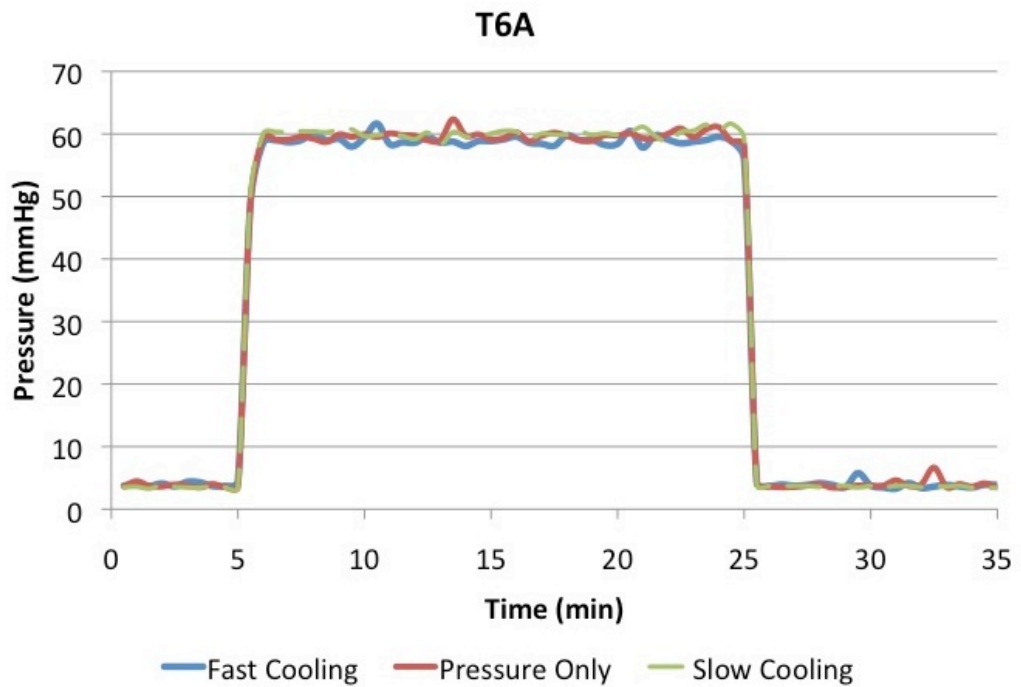


Figure 13. Average applied pressure during three test sessions on subjects with reactive hyperemia in T6A group.

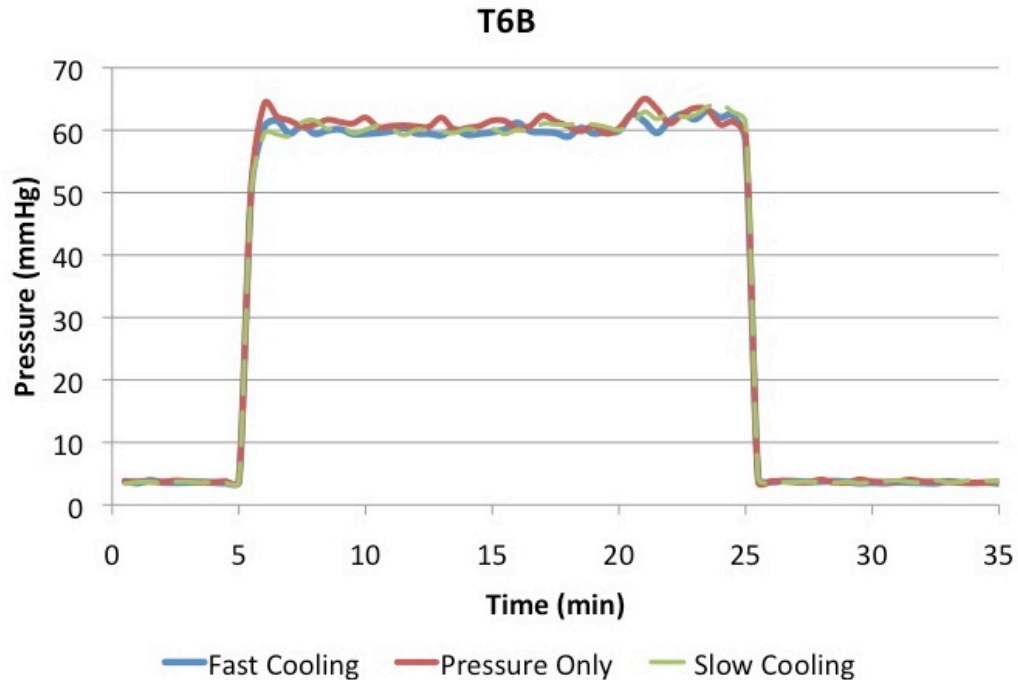


Figure 14. Average applied pressure during three test sessions on subjects with reactive hyperemia in T6B group.

4.4.2 Results from subjects with no reactive hyperemic response in all test sessions

Figure 15, Figure 16 and Figure 17 are the average applied pressure on the skin of subjects with no reactive hyperemia in all three test sessions in the control, T6A and T6B groups for the three test sessions, respectively. To show the comparison among the three different test sessions, the data was also averaged every 30 seconds to plot the three figures. By observing the three figures, the applied pressure was maintained at 3 mmHg during the first five minutes and the last 10 minutes of the test in all three test sessions of all three groups of subjects. From the fifth to the 25th minute of the test, the applied pressure was slightly higher in the control group than in the other two test sessions; the average applied pressure was slightly lower than 60 mmHg in all three test sessions in the T6B group. However, the applied pressure was maintained at 60 mmHg

during the 20 minutes in all three test sessions in the T6A group. The applied pressure oscillated around the target value in all three groups, and the oscillation range of all three groups is slightly greater than that in the other 31 subjects (Figure 12, Figure 13 and Figure 14).

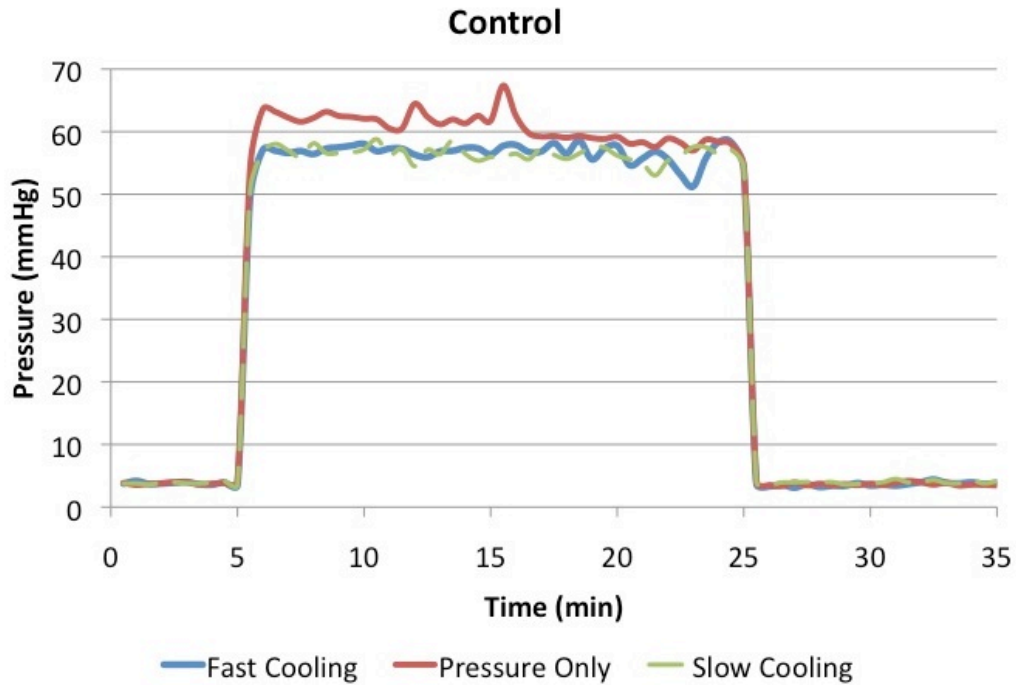


Figure 15. Average applied pressure during three test sessions on the subject without reactive hyperemia in control group.

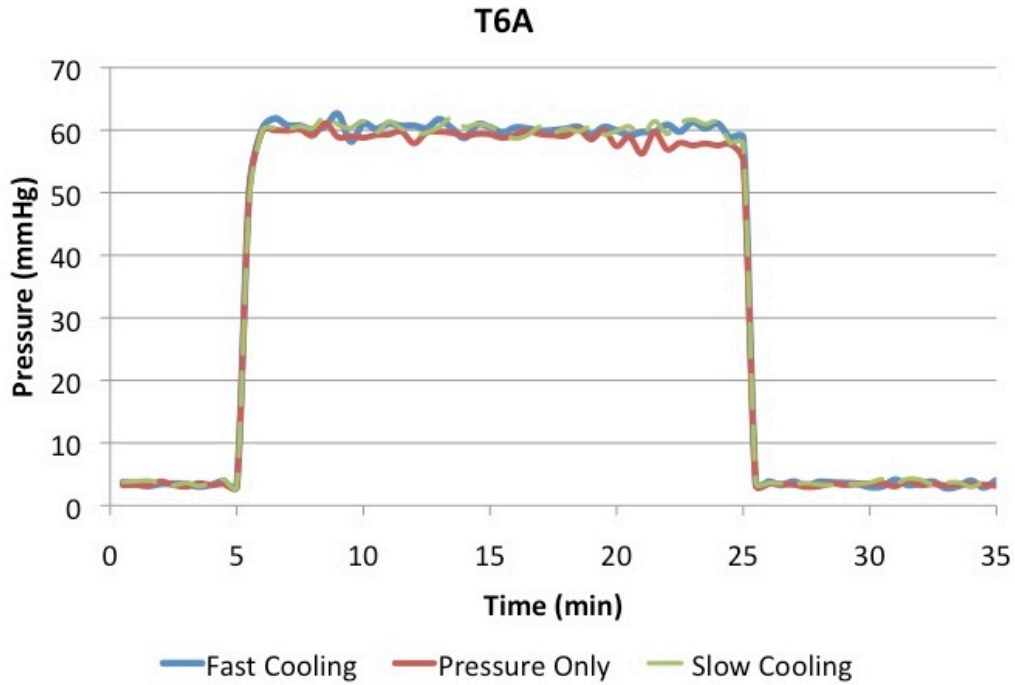


Figure 16. Average applied pressure during three test sessions on subjects without reactive hyperemia in T6A group.

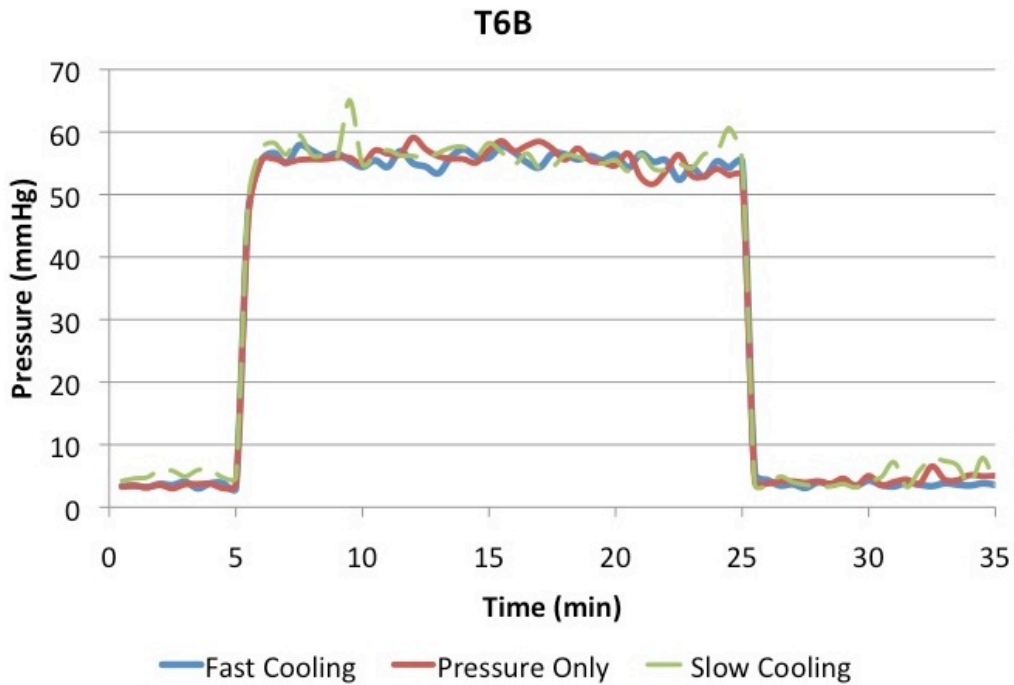


Figure 17. Average applied pressure during three test sessions on subjects without reactive hyperemia in T6B group.

4.5 SKIN TEMPERATURE

4.5.1 Results from subjects that had reactive hyperemia in pressure only test session

Figure 18, Figure 19, and Figure 20 are the average skin temperature from all subjects (excludes those without reactive hyperemia in all three test sessions) in the control, T6A, and T6B groups in all three test sessions, respectively. To show the comparison among the three different test sessions, the data was averaged every 30 seconds to plot the three figures. By observing the three figures, the skin temperature decreased about 0.5°C during the first five minutes in all three test sessions of all three groups of subjects. The skin temperature reached 25°C within one minute of cooling application in the fast cooling test session in all three groups, and the skin temperature decreased at a slower rate and reached 25°C after 15 minutes of cooling application in the slow cooling test session in all three groups. The skin temperature reached the baseline skin temperature rapidly after removal of cooling application in both fast and slow cooling test sessions in all three groups.

To compare the skin temperature, especially to ensure the capability of the local cooling system on subjects with different levels of neurological deficit, a two-way repeated measures ANOVA was used to compare the skin temperature during the three phases of the test (the skin temperature averaged during the first 5 minutes, the skin temperature after 20 minutes of 60 mmHg pressure application, and the skin temperature averaged during the last 10 minutes of the test). Table 11, Table 12 and Table 13 show the results of descriptive analysis (mean and standard deviation) and two-way repeated measures ANOVA of the skin temperature in the three groups during the three pressure application phases. The results showed that the skin temperature after 20 minutes of 60 mmHg of pressure application was significantly different

among test sessions; however, there was no significant difference among test groups (Table 12). Pair-wise comparisons showed that skin temperature after 20 minutes of 60 mmHg pressure application without cooling was significantly higher than for both fast ($p<0.001$) and slow cooling ($p<0.001$). Although the skin temperature at the end of 60 mmHg pressure application was also significantly higher in slow cooling as compared to fast cooling ($p<0.001$), the differences were small (within 0.05°C). The results showed that the baseline skin temperature was significantly different among test sessions and subject groups (Table 11). However, the differences were small ($0.5\text{-}1^{\circ}\text{C}$), and the baseline skin temperature did not affect the capacity of local cooling application to the subjects. The results also showed that the skin temperature during reactive hyperemia was significantly different among test sessions, but not among subject groups (Table 13). However, the differences were small ($0.5\text{-}1^{\circ}\text{C}$).

Table 11. Mean and standard deviation of skin temperature during baseline.

Test Session Group	PF	PO	PS	Comparisons (p)	
				Within Subject	Between Group
CTRL	28.34 ± 1.17	28.03 ± 0.58	27.83 ± 0.78	.030*	.037*
T6A	28.24 ± 1.58	28.14 ± 0.94	27.94 ± 1.60		
T6B	29.86 ± 1.13	28.96 ± 0.79	29.09 ± 1.54		

PS = pressure + slow cooling test session, PF = pressure + fast cooling test session, PO = pressure only test session.

Table 12. Mean and standard deviation of skin temperature at the end of 60mmHg pressure.

Test Session Group	PF	PO	PS	Comparisons (p)	
				Within Subject	Between Group
CTRL	24.97 ± 0.02	28.16 ± 0.64	25.00 ± 0.01	<.001*	.123
T6A	24.97 ± 0.02	27.78 ± 0.98	25.00 ± 0.01		
T6B	24.97 ± 0.02	28.61 ± 0.74	25.00 ± 0.00		

PS = pressure + slow cooling test session, PF = pressure + fast cooling test session, PO = pressure only test session.

Table 13. Mean and standard deviation of skin temperature during reactive hyperemia.

Test Session Group	PF	PO	PS	Comparisons (<i>p</i>)	
				Within Subject	Between Group
CTRL	28.00 ± 1.00	27.59 ± 0.69	27.54 ± 0.60	.039*	.121
T6A	27.43 ± 0.91	27.21 ± 1.04	27.53 ± 1.20		
T6B	28.29 ± 0.88	28.04 ± 0.70	28.52 ± 1.03		

PS = pressure + slow cooling test session, PF = pressure + fast cooling test session, PO = pressure only test session.

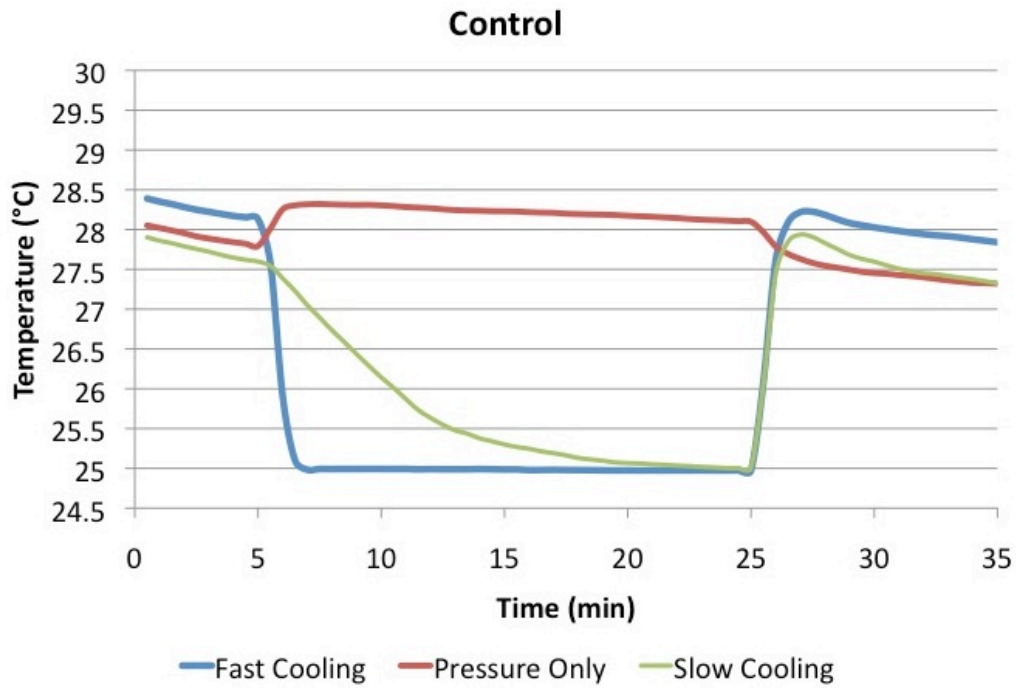


Figure 18. Averaged skin temperature during three test sessions on subjects with reactive hyperemia in control group.

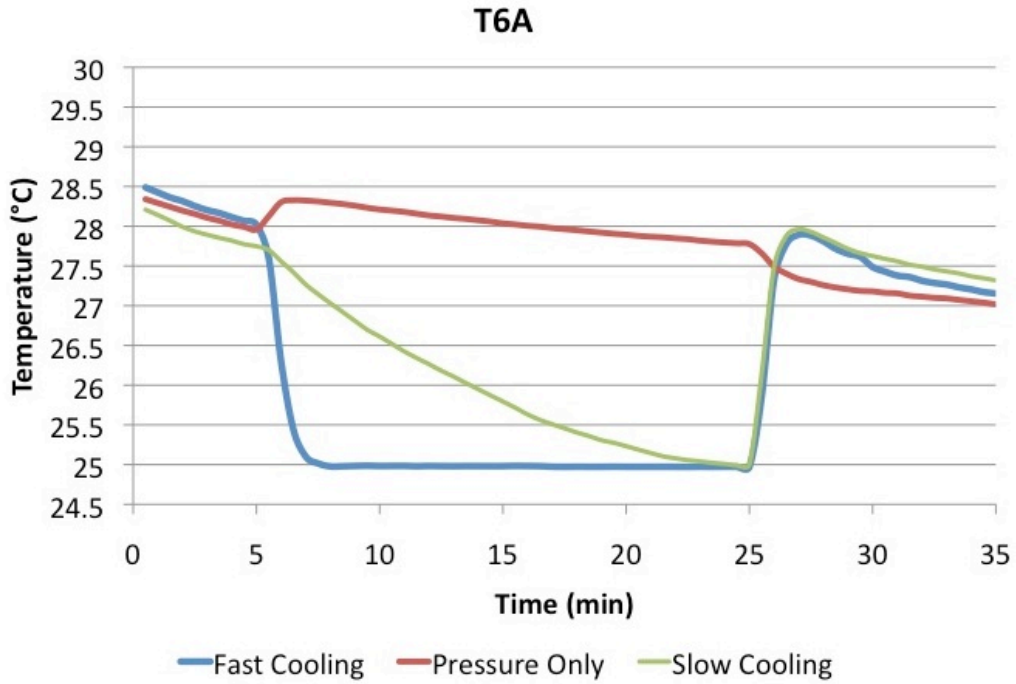


Figure 19. Averaged skin temperature during three test sessions on subjects with reactive hyperemia in T6A group.

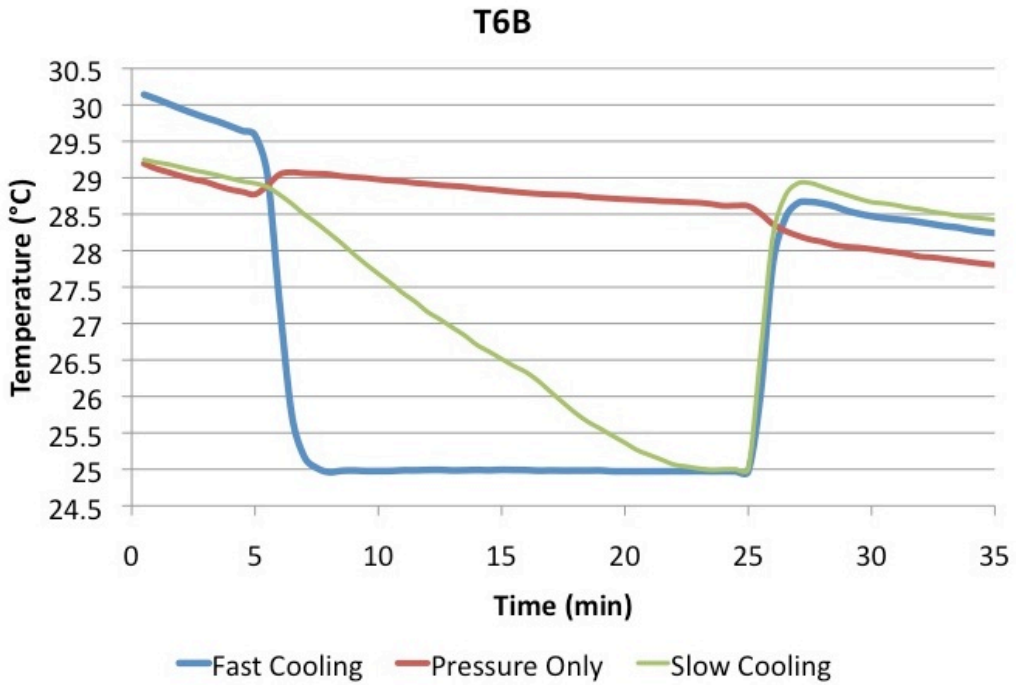


Figure 20. Averaged skin temperature during three test sessions on subjects with reactive hyperemia in T6B group.

4.5.2 Results from subjects with no reactive hyperemic response in all test sessions

Figure 21, Figure 22 and Figure 23 are the average skin temperature of subjects with no reactive hyperemia in all three test sessions in the control, T6A and T6B groups for the three test sessions, respectively. To show the comparison among the three different test sessions, the data was also averaged every 30 seconds to plot the three figures. By observing the three figures, all three figures showed similar trend of skin temperature changes as compared to the other 31 subjects shown previously. The skin temperature also decreased about 0.5°C during the first five minutes in all three test sessions of all three groups of subjects. The skin temperature reached 25°C within one minute of cooling application in the fast cooling test session in all three groups. The skin temperature decreased at a slower rate and reached 25°C after 15 minutes of cooling application in the slow cooling test session in T6A and T6B groups. Since the baseline skin temperature was lower for the subject in the control group (Figure 21) as compared to the other subjects that had reactive hyperemia in the same group (Figure 18), the skin temperature reached 25°C in a shorter period of time in the slow cooling test session. The skin temperature reached the baseline skin temperature rapidly after removal of cooling application in both fast and slow cooling test sessions in all three groups.

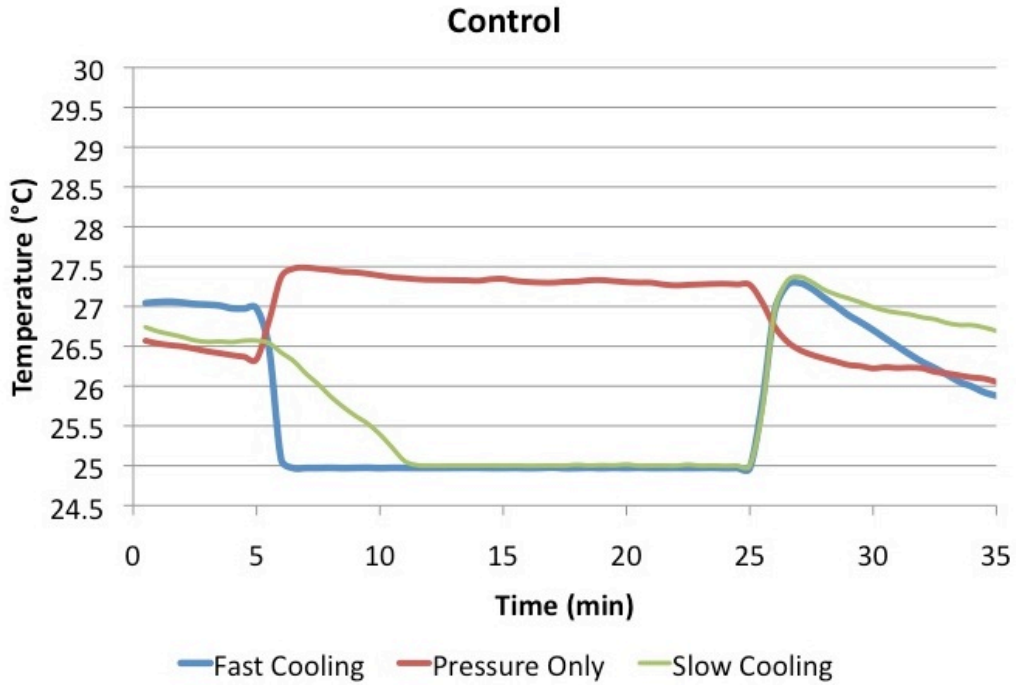


Figure 21. Averaged skin temperature during three test sessions on the subject without reactive hyperemia in control group.

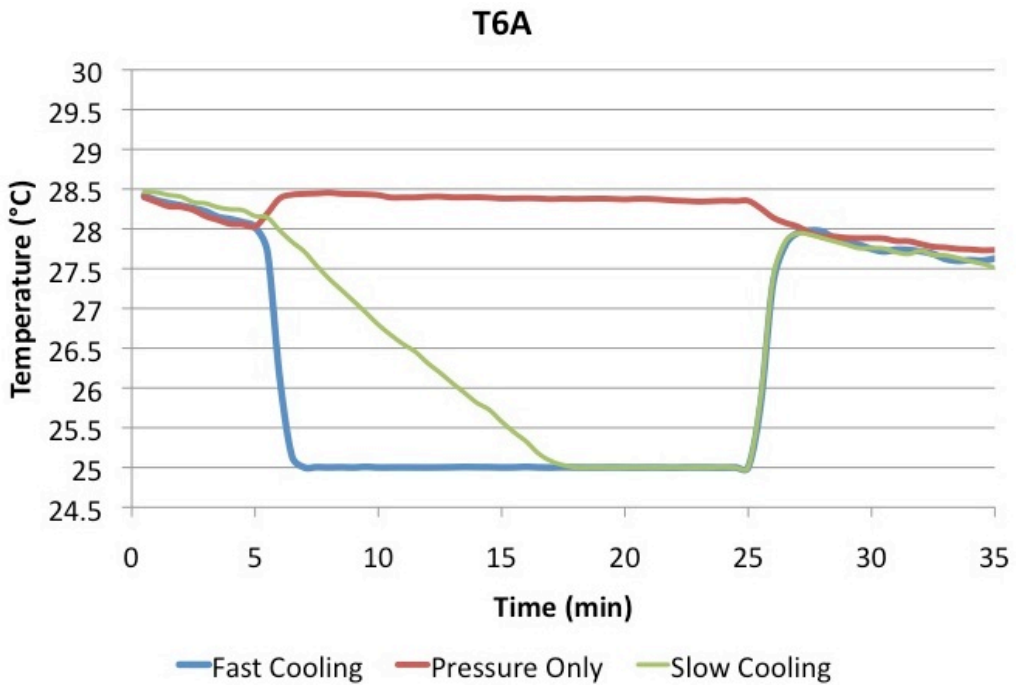


Figure 22. Averaged skin temperature during three test sessions on subjects without reactive hyperemia in T6A group.

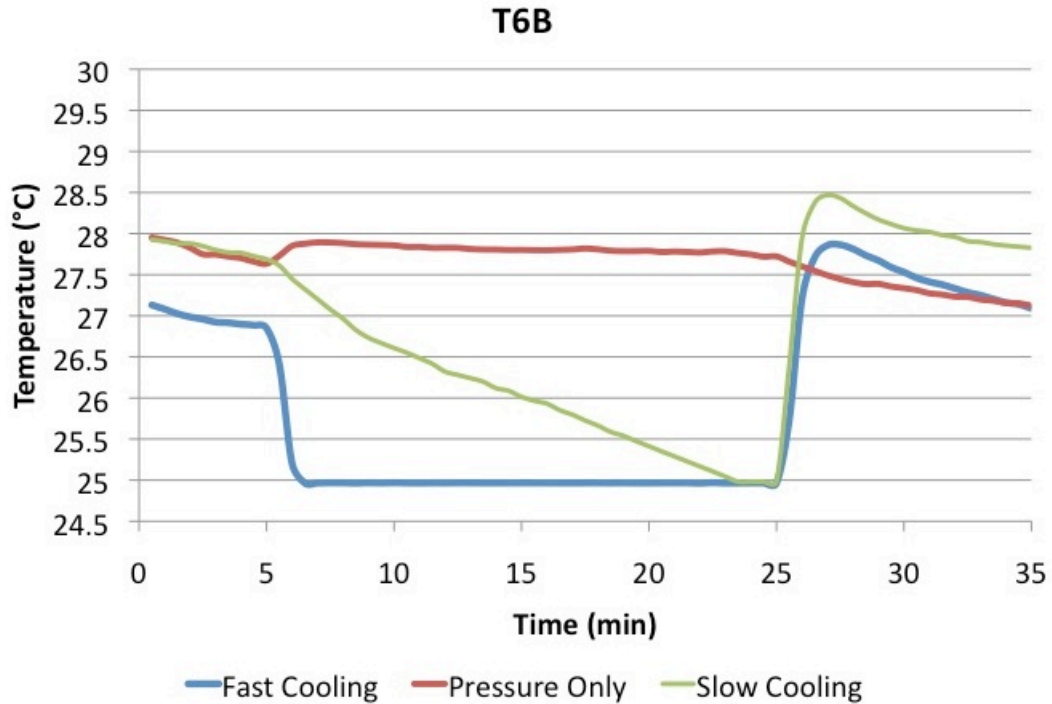


Figure 23. Averaged skin temperature during three test sessions on subjects without reactive hyperemia in T6B group.

4.6 SKIN BLOOD FLOW

Since breaking down the skin blood flow data into the target parameters provides more information to answer the research questions of this study, the data shown in this section contains only the parameters of the reactive hyperemia. The filtered skin blood flow data with the least-squared fit curves of all 36 subjects were plotted and attached as Appendix A of this dissertation.

4.6.1 Baseline SBF

Figure 24 is the box plot (displays the median, quartiles, extreme values, and labels the outliers) of the baseline SBF in all subjects (excludes those without reactive hyperemia in all three test sessions). To ensure that the baseline SBF is not a factor among test sessions and the three groups of subjects, a two-way repeated measures ANOVA was used to compare the baseline SBF. The results showed that the baseline SBF was not significantly different among the three test sessions and the three groups of subjects (Table 14). Figure 25 is the box plot of the baseline SBF in subjects with no reactive hyperemia in all three test sessions. The baseline SBF of the subject in the control group was higher than those in the T6A and T6B group. The baseline SBF of the subject in the control group was also higher when compared to the other subject in the same group that had reactive hyperemia, but this phenomenon was not observed in the T6A and T6B groups.

Table 14. Mean and standard deviation of baseline SBF, and the results of the two-way repeated measures ANOVA.

Test Session Group	PF	PO	PS	Comparisons (<i>p</i>)	
				Within Subject	Between Group
CTRL (N=13)	6.78 ± 3.18	5.86 ± 3.14	6.58 ± 3.43	.530	.146
T6A (N=12)	5.85 ± 2.97	6.13 ± 3.34	5.87 ± 2.85		
T6B (N=6)	3.59 ± 0.82	3.54 ± 1.20	4.84 ± 1.59		

PS = pressure + slow cooling test session, PF = pressure + fast cooling test session, PO = pressure only test session.

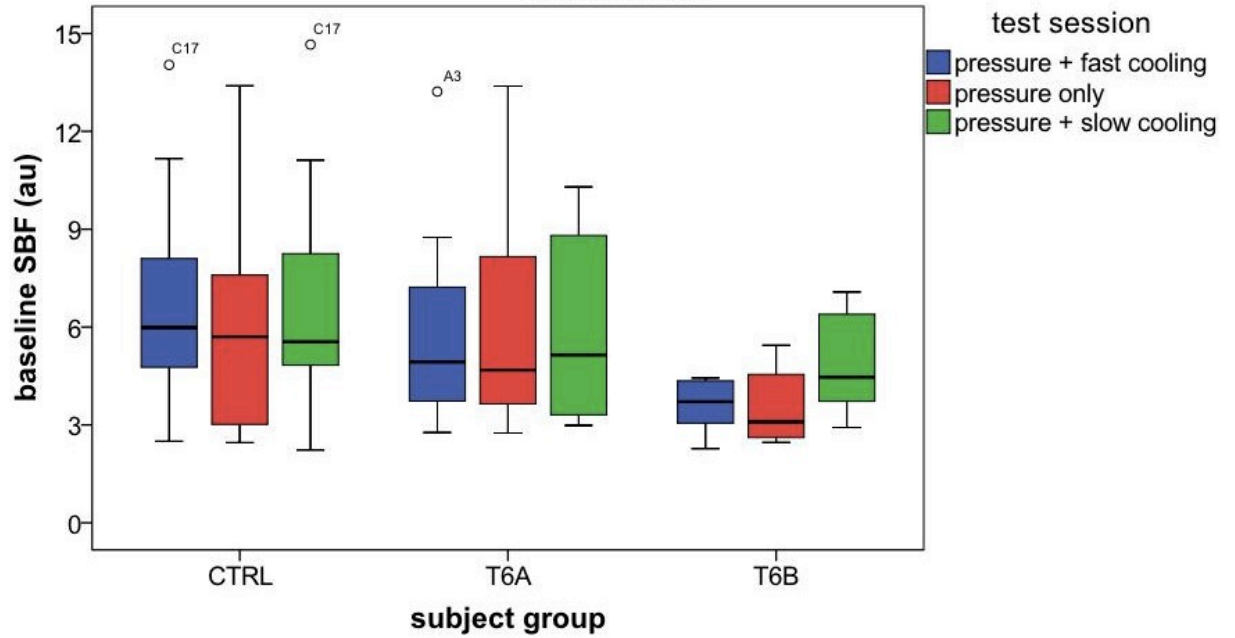


Figure 24. Box plots of baseline SBF in all subjects (excluding those without reactive hyperemia in all test sessions).

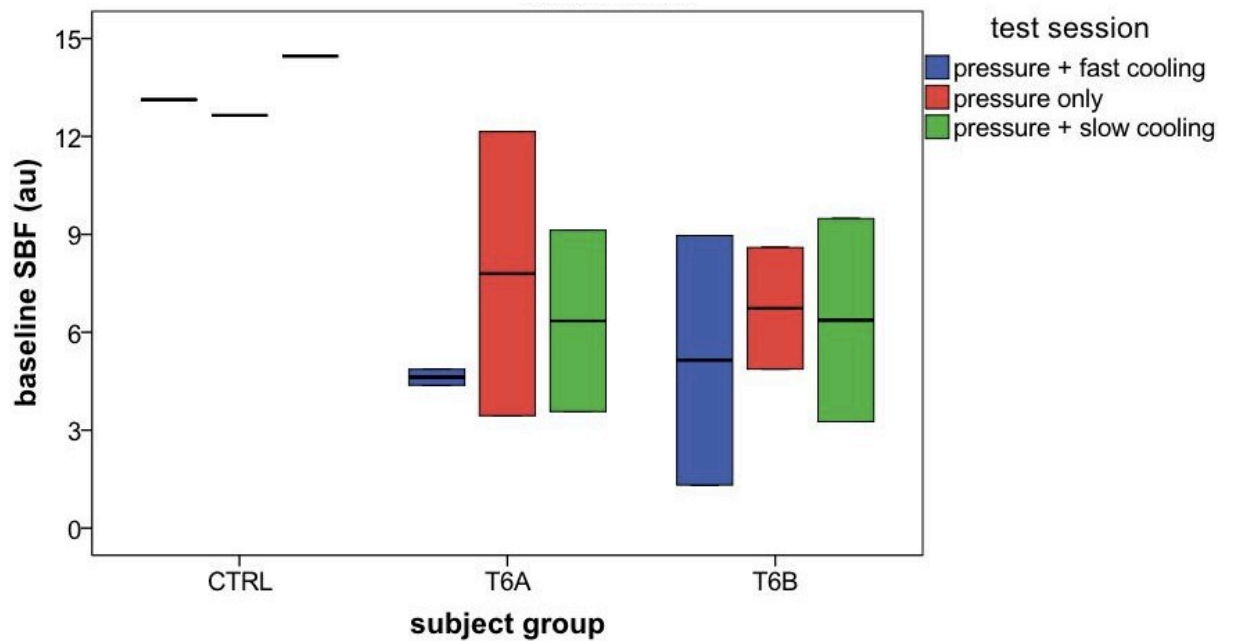


Figure 25. Box plots of baseline SBF in subjects without reactive hyperemia in all test sessions.

4.6.2 Reactive hyperemic response compared within subjects

4.6.2.1 Hypothesis 1a) and 1b): normalized peak

Since descriptive analysis showed that the normalized peak SBF was not normally distributed, a Friedman test was used to compare the differences among the three test sessions. Figure 26 is the box plot of normalized peak among three test sessions from all subjects (excluding those without reactive hyperemia in all test sessions). When comparing the three test sessions from all 31 subjects (Table 15), the Friedman test showed a significant difference among test sessions. Pair-wise comparison showed that the normalized peak SBF in pressure only was significantly greater than that in pressure with fast cooling ($p=0.014$) but not with slow cooling ($p=0.240$). In addition, the normalized peak SBF in pressure with slow cooling was close to significantly greater than that in pressure with fast cooling ($p=0.057$).

Table 15. Mean and standard deviation of normalized peak SBF and the results of the Friedman test (N=31).

Test Session Group	PF	PO	PS	Within Subject Comparisons (p)
Mean \pm Standard Deviation	61.18 \pm 84.18	114.08 \pm 108.12	89.88 \pm 105.01	.015*

PS = pressure + slow cooling test session, PF = pressure + fast cooling test session, PO = pressure only test session.

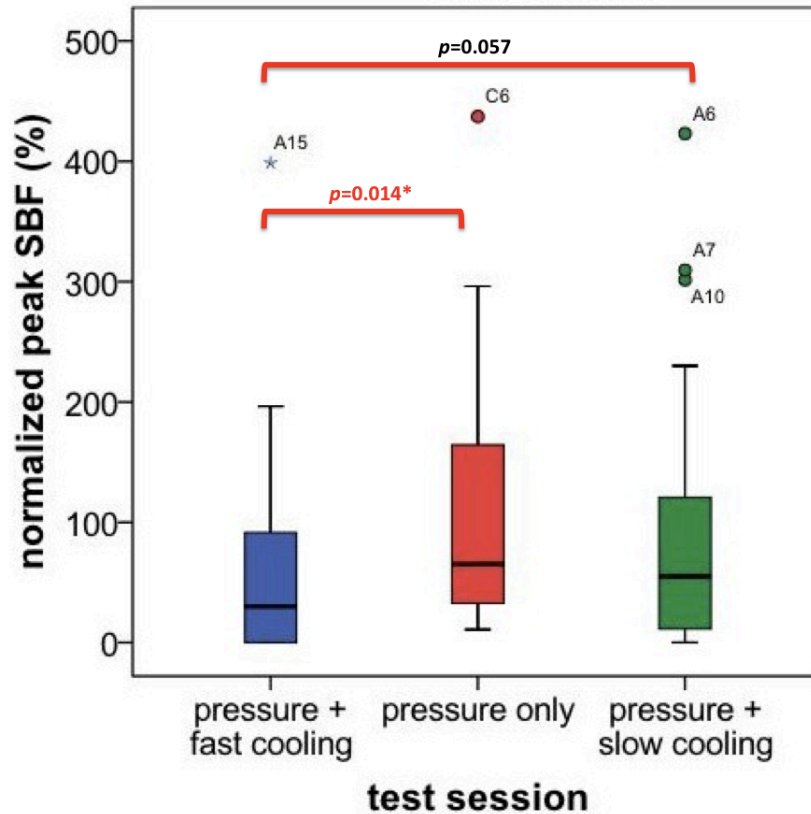


Figure 26. Box plots of normalized peak SBF in all subjects (excluding those without reactive hyperemia in all test sessions).

To further investigate the difference among test sessions in all three subject groups, the Friedman test was computed on three groups separately. Figure 27 is the box plot of the normalized peak among three test sessions plotted by groups. Table 16 shows the results of descriptive statistics and the Friedman tests of three groups. Although pressure with fast cooling had the lowest mean rank in all three groups, Friedman tests did not show significant differences among test sessions in all three groups. The differences among test sessions were close to significant in the control group, and the pair-wise comparison (with Bonferroni correction: $p < 0.016$ considered significant) showed that the normalized peak SBF in pressure only was close to significantly greater than that in pressure with fast cooling ($p = 0.023$) and pressure with slow

cooling ($p=0.033$). However, there was no significant difference in normalized peak SBF while comparing pressure with fast cooling and pressure with slow cooling.

Table 16. Mean and standard deviation of normalized peak SBF and the results of the Friedman tests computed separately by group.

Test Session \ Group	PF	PO	PS	Within Subject Comparisons (p)
CTRL (N=13)	43.80 ± 62.93	117.15 ± 127.31	47.06 ± 48.87	.052
T6A (N=12)	82.27 ± 110.66	108.36 ± 90.04	140.18 ± 139.02	.338
T6B (N=6)	56.62 ± 64.74	118.84 ± 115.26	82.07 ± 83.66	.513

PS = pressure + slow cooling test session, PF = pressure + fast cooling test session, PO = pressure only test session.

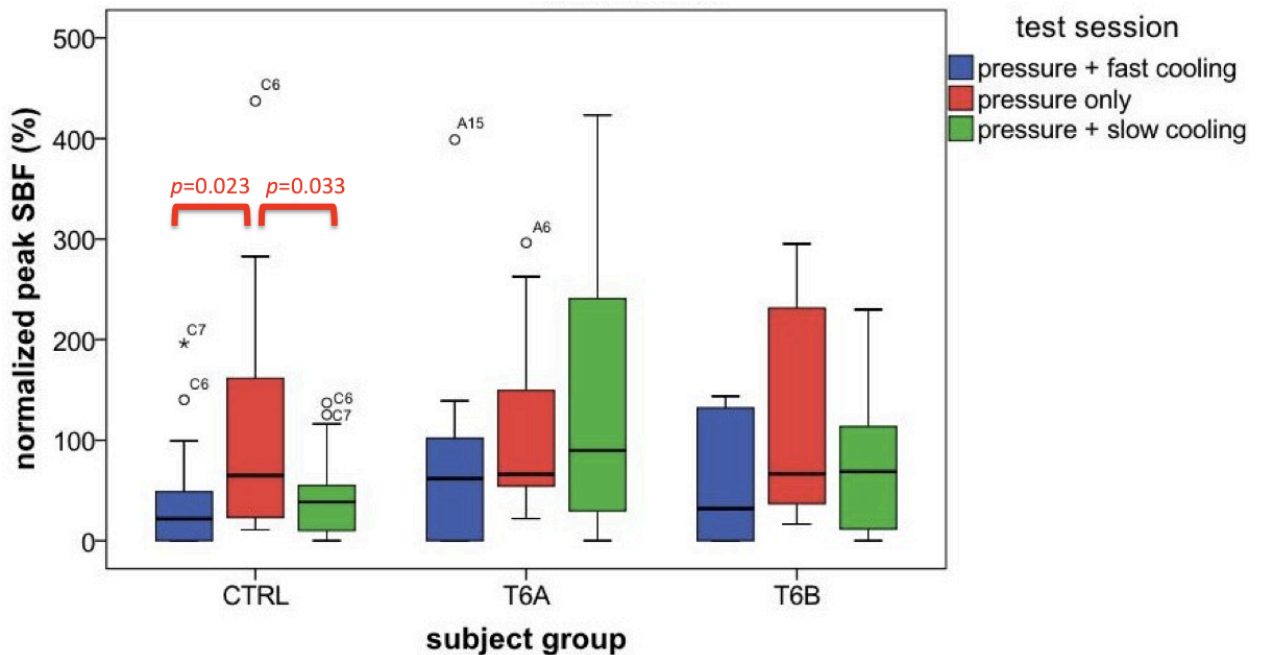


Figure 27. Box plots of normalized peak SBF by group in all subjects (excluding those without reactive hyperemia in all test sessions).

4.6.2.2 Hypothesis 1c) and 1d): perfusion area

Since descriptive analysis showed that the perfusion area was not normally distributed, a Friedman test was used to compare the differences among the three test sessions. Figure 28 is the box plot of perfusion area among three test sessions from all subjects (excludes those without reactive hyperemia in all test sessions). When comparing the three test sessions from all 31 subjects (Table 17), the Friedman test showed a significant difference among test sessions. Pair-wise comparison showed that the perfusion area in pressure only was significantly greater than that in pressure with fast cooling ($p=0.004$) but not with slow cooling ($p=0.065$). In addition, the perfusion area in pressure with slow cooling was not significantly greater than that in pressure with fast cooling ($p=0.131$).

Table 17. Mean and standard deviation of perfusion area and the results of the Friedman test (N=31).

Test Session Group	PF	PO	PS	Within Subject Comparisons (p)
Mean \pm Standard Deviation	143.28 \pm 262.12	311.25 \pm 278.25	215.17 \pm 311.39	.003*

PS = pressure + slow cooling test session, PF = pressure + fast cooling test session, PO = pressure only test session.

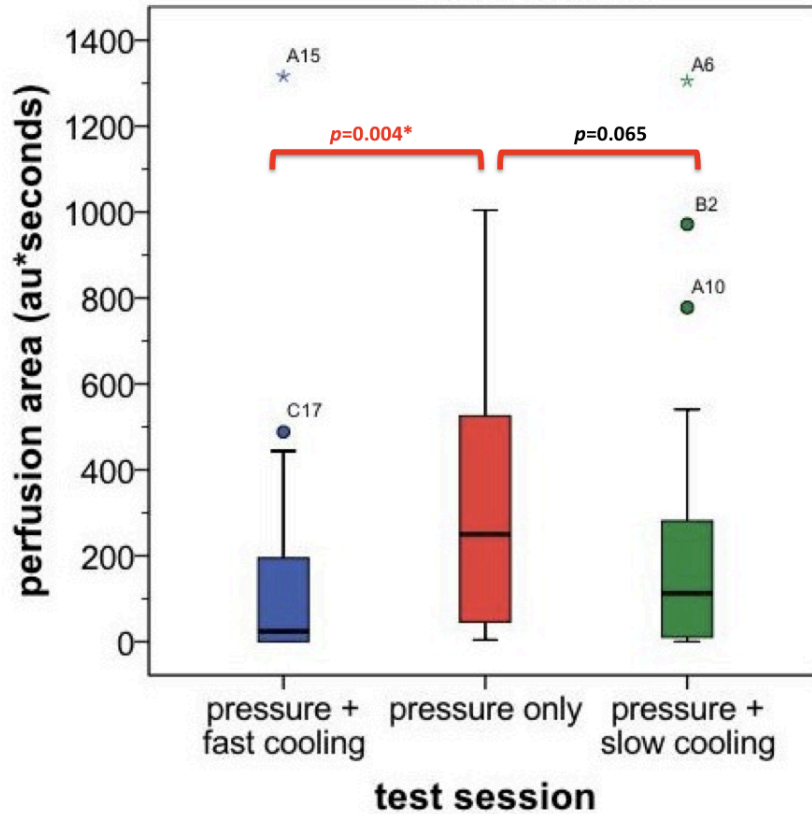


Figure 28. Box plots of perfusion area in all subjects (excludes those without reactive hyperemia in all test sessions).

To further investigate the difference among test sessions in all three groups, the Friedman test was computed on three groups separately. Figure 29 is the box plot of the perfusion area among three test sessions plotted by groups. Table 18 shows the results of descriptive statistics and the Friedman tests of three groups. Friedman test showed that there was a significant difference among three test sessions only in the control group, and pair-wise comparison (with Bonferroni correction: $p < 0.016$ considered significant) showed that the perfusion area of pressure only was significantly greater than that with slow cooling ($p = 0.016$), and was close to significantly greater as compared to pressure with fast cooling ($p = 0.023$). The perfusion area was also not significantly different between fast cooling and slow cooling ($p = .937$). Although

pressure with fast cooling had the lowest mean rank of perfusion area in all three groups, the Friedman test did not show significant differences among test sessions in the two SCI groups.

Table 18. Mean and standard deviation of perfusion area and the results of the Friedman tests computed separately by group.

Test Session \ Group	PF	PO	PS	Within Subject Comparisons (<i>p</i>)
CTRL (N=13)	101.13 ± 175.69	261.94 ± 213.04	67.61 ± 78.30	.019*
T6A (N=12)	212.11 ± 364.93	367.10 ± 300.51	370.04 ± 378.42	.174
T6B (N=6)	96.93 ± 163.18	306.88 ± 378.33	225.11 ± 371.12	.513

PS = pressure + slow cooling test session, PF = pressure + fast cooling test session, PO = pressure only test session.

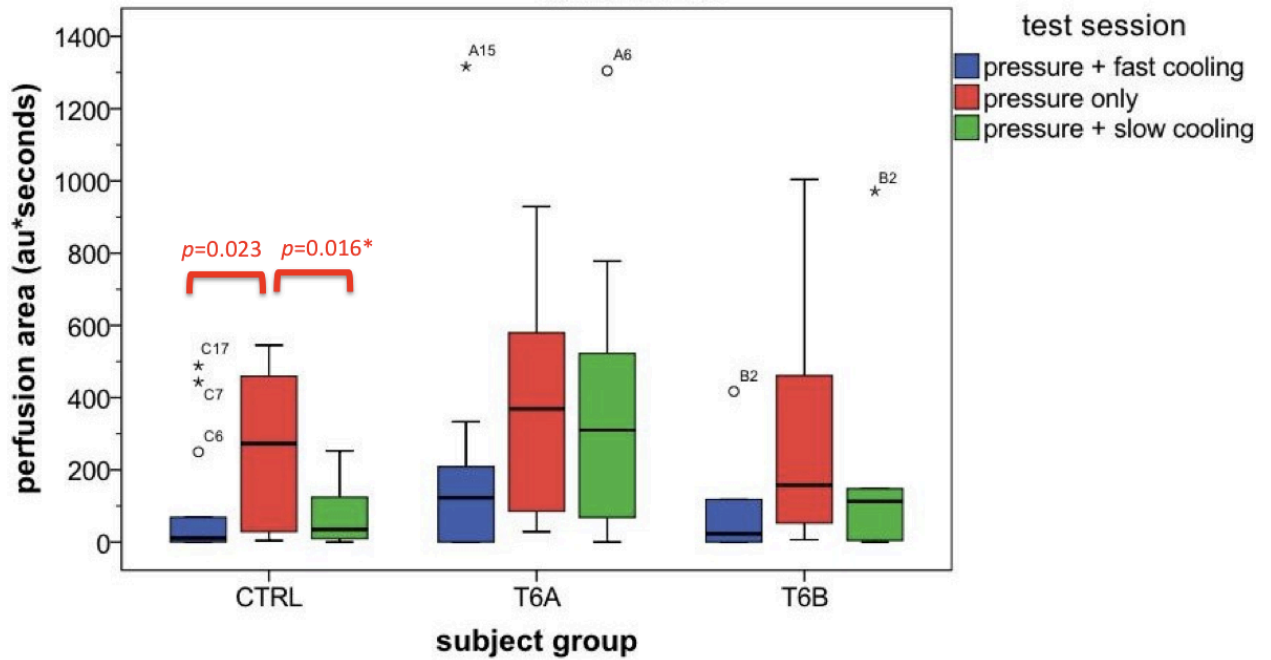


Figure 29. Box plots of perfusion area by group in all subjects (excludes those without reactive hyperemia in all test sessions).

4.6.2.3 Other parameters: time to peak and half life

To further characterize and understand the nature of the reactive hyperemia, time to the peak SBF and half life of the reactive hyperemia were compared among the three test sessions. Since both data sets were not normally distributed, the Friedman test was used to compare the differences among the three test sessions. Figure 30 and Figure 32 are the box plots of the time to peak SBF and half life among the three test sessions from all subjects (excludes those without reactive hyperemia in all test sessions), respectively. Only 17 subjects had reactive hyperemia in all three test sessions, and Friedman test did not show any significant differences among the three test sessions in either the time to peak SBF (Table 19) or half life (Table 21). Figure 31 and Figure 33 are the box plots of the time to peak and half life among three test sessions plotted by groups, respectively. Table 20 and Table 22 show the results of descriptive statistics and Friedman tests of the time to peak and half of three groups, respectively. There was also no significant difference among the test sessions with the subject groups analyzed separately.

Table 19. Mean and standard deviation of time to peak and the results of the Friedman test (N=17).

Test Session Group	PF	PO	PS	Within Subject Comparisons (<i>p</i>)
Mean ± Standard Deviation	41.88 ± 27.99	60.00 ± 44.86	49.65 ± 32.27	.481

PS = pressure + slow cooling test session, PF = pressure + fast cooling test session, PO = pressure only test session.

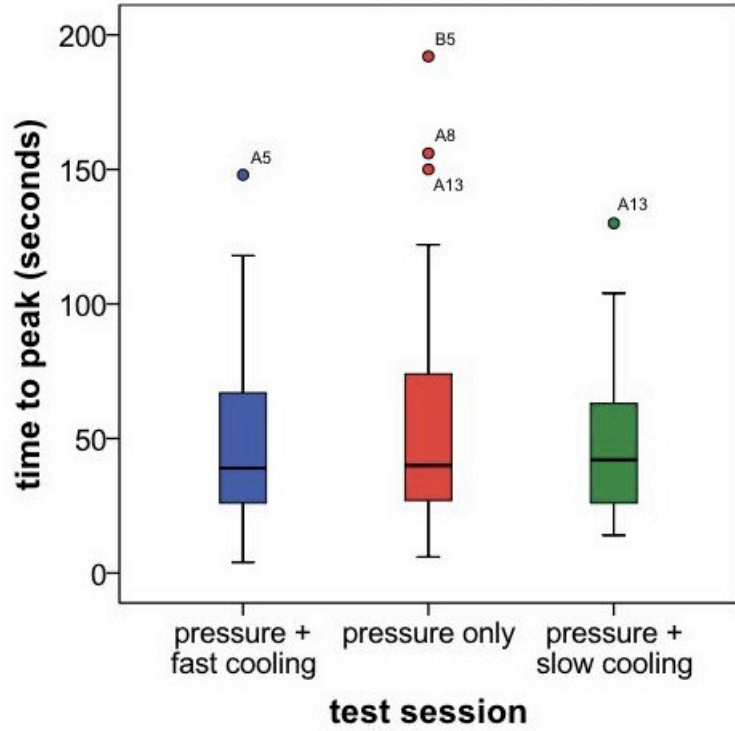


Figure 30. Box plots of time to peak SBF in all subjects (excludes those without reactive hyperemia in all test sessions).

Table 20. Mean and standard deviation of time to peak and the results of the Friedman tests computed separately by group.

Test Session \ Group	PF	PO	PS	Within Subject Comparisons (<i>p</i>)
CTRL (N=8)	41.00 ± 36.63	34.25 ± 19.34	42.25 ± 19.32	.607
T6A (N=6)	48.33 ± 20.49	80.33 ± 60.44	60.67 ± 40.07	.568
T6B (N=3)	31.33 ± 15.01	88.00 ± 24.25	47.33 ± 49.17	.264

PS = pressure + slow cooling test session, PF = pressure + fast cooling test session, PO = pressure only test session.

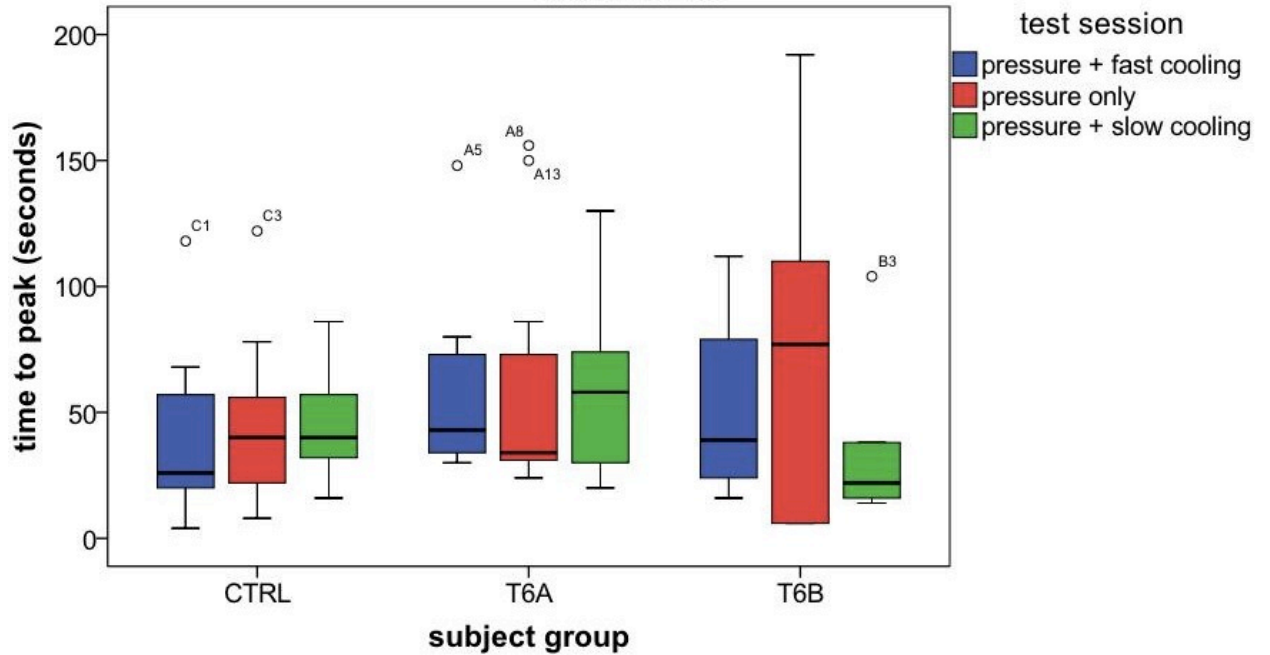


Figure 31. Box plots of time to peak by group in all subjects (excludes those without reactive hyperemia in all test sessions).

Table 21. Mean and standard deviation of half life and the results of the Friedman test (N=17).

Test Session \ Group	PF	PO	PS	Within Subject Comparisons (<i>p</i>)
Mean ± Standard Deviation	542.00 ± 49.40	498.12 ± 122.03	451.53 ± 166.53	.080

PS = pressure + slow cooling test session, PF = pressure + fast cooling test session, PO = pressure only test session.

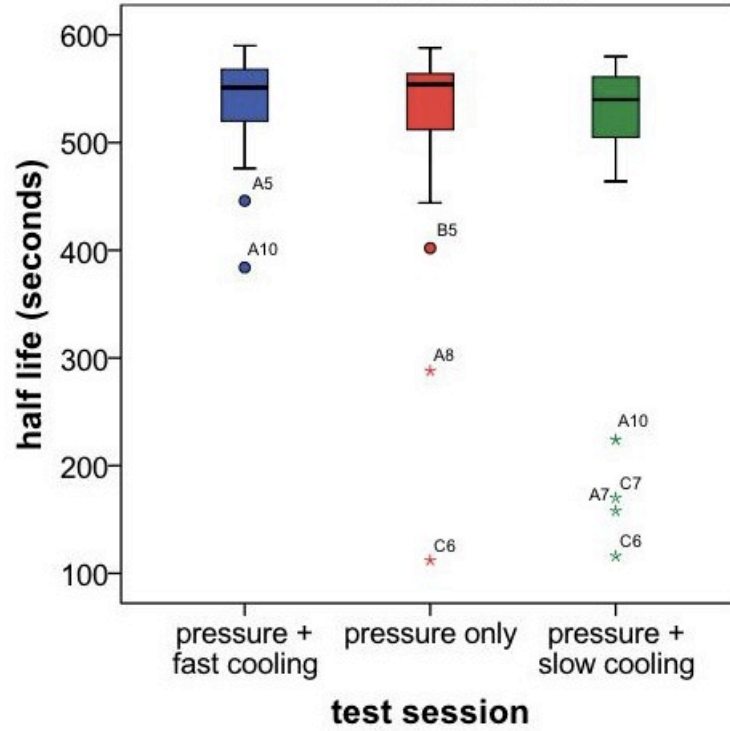


Figure 32. Box plots of half life in all subjects (excludes those without reactive hyperemia in all test sessions).

Table 22. Mean and standard deviation of half life and the results of the Friedman tests computed separately by group.

Test Session / Group	PF	PO	PS	Within Subject Comparisons (<i>p</i>)
CTRL (N=8)	553.00 ± 36.63	502.25 ± 158.79	445.50 ± 187.91	.223
T6A (N=6)	517.00 ± 68.11	488.67 ± 109.29	412.00 ± 176.00	.311
T6B (N=3)	562.67 ± 15.01	506.00 ± 24.25	546.67 ± 49.17	.264

PS = pressure + slow cooling test session, PF = pressure + fast cooling test session, PO = pressure only test session.

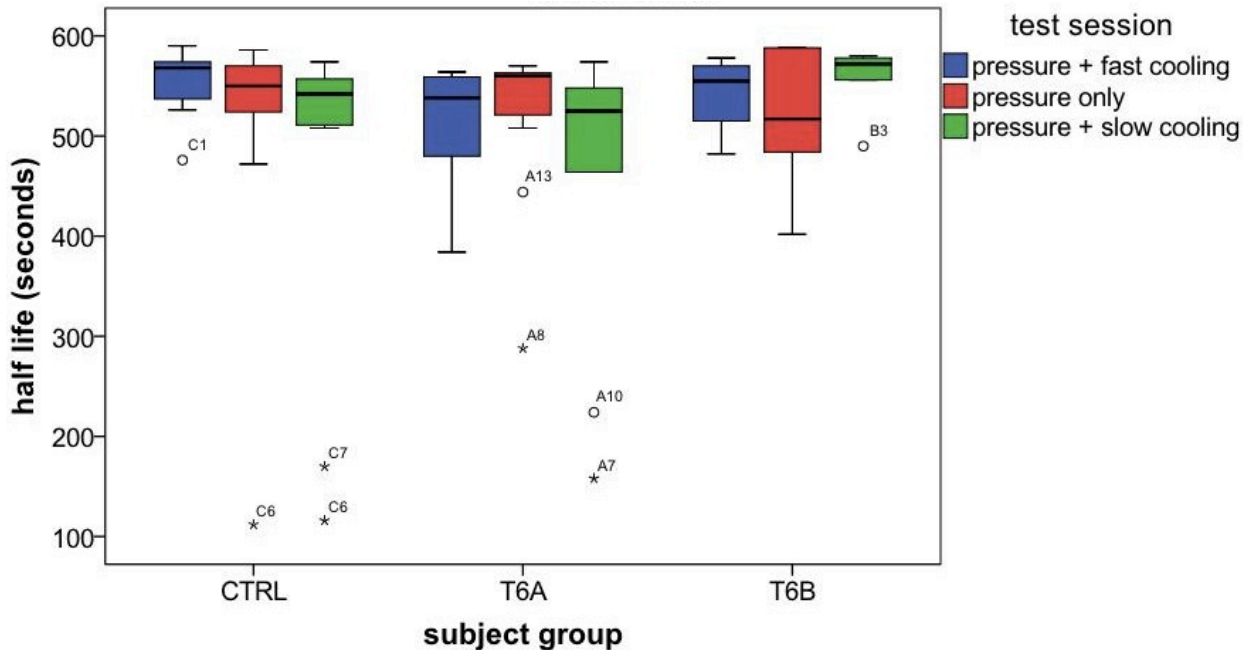


Figure 33. Box plots of half life by group in all subjects (excludes those without reactive hyperemia in all test sessions).

4.6.2.4 Normalized spectral densities

To understand the underlying vessel control mechanisms during reactive hyperemia, the SBF was broken down into three different frequency bands: metabolic, neurogenic, and myogenic. Since the spectral density in all three frequency bands were not normally distributed, the Wilcoxon signed rank test was used to compare the changes in spectral density during reactive hyperemia as compared to the blood flow at baseline (before application of pressure).

(a) Metabolic spectral density

Figure 34 is the box plot of normalized metabolic spectral densities of all three test sessions from all subjects (excludes those with no reactive hyperemia in all test sessions). Table 23 shows the results of descriptive analysis and Wilcoxon signed rank tests on the normalized metabolic spectral densities. The control group did not show any significant increase in

metabolic spectral density in all three test sessions. In people with injury level above T6, the metabolic spectral density increased significantly in both the pressure only and pressure with slow cooling test sessions, but not in the pressure with fast cooling. In people with injury level below T6, there was no significant increase in metabolic spectral density in all three test sessions. Figure 35 is the box plot of metabolic spectral densities in subjects with no reactive hyperemia in all test sessions. All five subjects had greater normalized metabolic spectral densities in pressure with fast cooling.

Table 23. Mean and standard deviation (SD) of normalized metabolic spectral densities during reactive hyperemia.

The *p* values were the results of Wilcoxon signed rank tests that compared the spectral densities during reactive hyperemia to that during baseline.

Test Session Group	PF		PO		PS	
	Mean ± SD	<i>p</i>	Mean ± SD	<i>p</i>	Mean ± SD	<i>p</i>
CTRL	132.43 ± 207.14	.552	417.54 ± 912.01	.279	110.47 ± 92.83	.701
T6A	809.09 ± 1492.76	.136	622.40 ± 1044.40	.019*	335.32 ± 382.62	.041*
T6B	436.78 ± 832.09	.463	379.37 ± 446.12	.345	289.40 ± 482.15	.600

PS = pressure + slow cooling test session, PF = pressure + fast cooling test session, PO = pressure only test session.

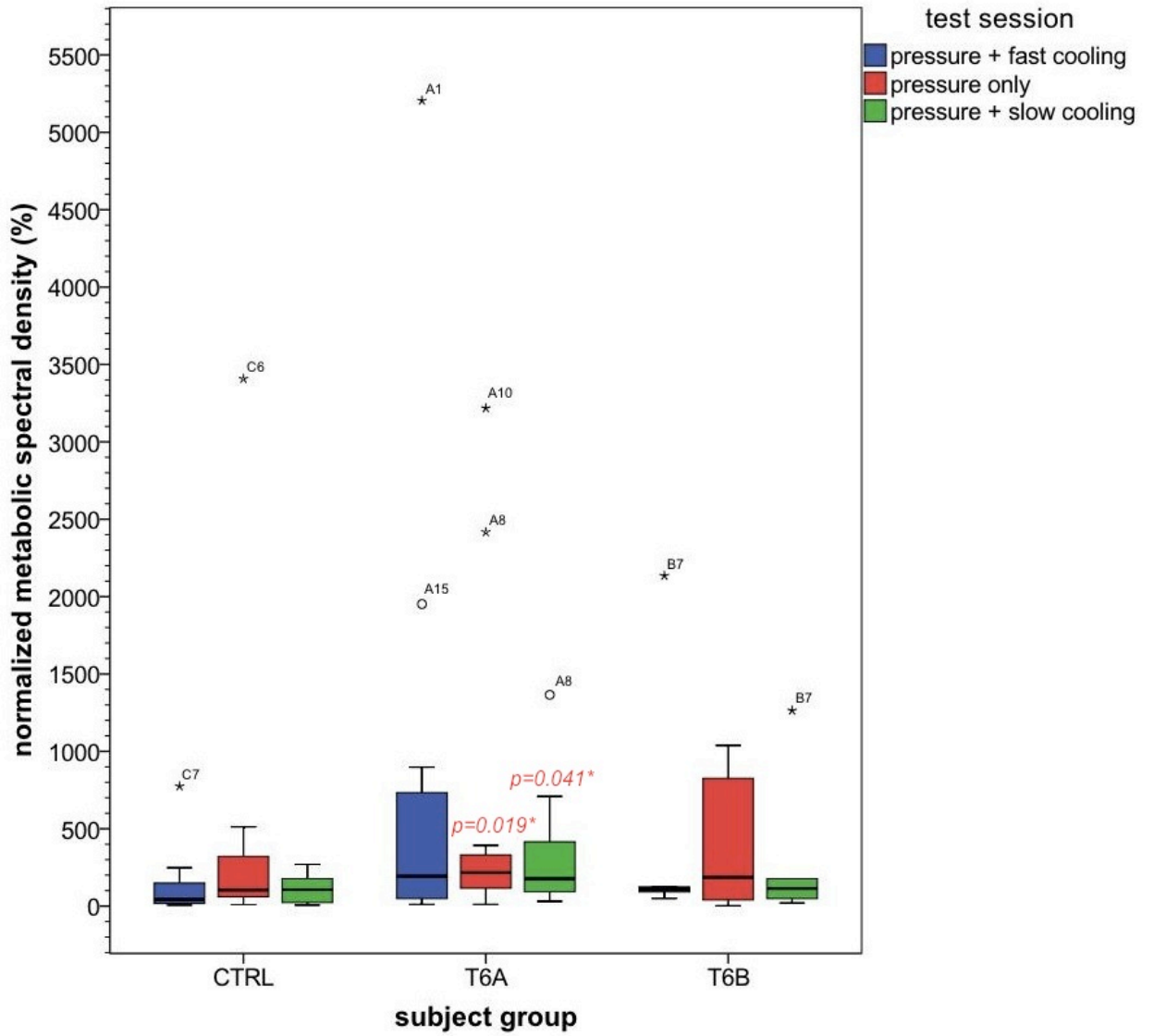


Figure 34. Box plots of normalized metabolic spectral density in all subjects (excludes those without reactive hyperemia in all three sessions).

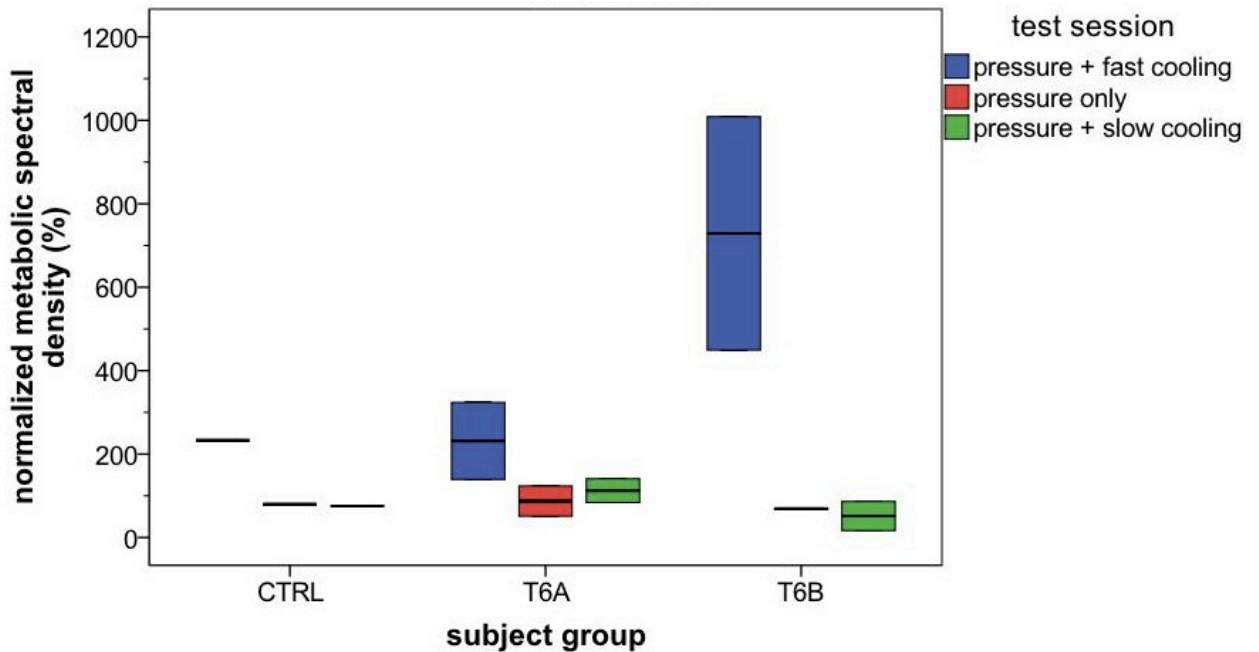


Figure 35. Box plots of normalized metabolic spectral density in subjects with no reactive hyperemia in all test sessions.

(b) Neurogenic spectral density

Figure 36 displays the normalized neurogenic spectral densities of from all subjects (excludes those with no reactive hyperemia). Table 24 shows the results of descriptive analysis and Wilcoxon signed rank tests on the normalized neurogenic spectral densities. The control group showed a significant increase with pressure only but not with pressure with fast or slow cooling. In people with injury level above T6, the neurogenic spectral density increased significantly in pressure with slow cooling but not in pressure with fast cooling, and it is close to significant in pressure only. In people with injury level below T6, there was no significant increase in neurogenic spectral density in all three test sessions. Figure 37 is the box plot of neurogenic spectral densities in subjects with no reactive hyperemia in all test sessions. Subjects in the control and T6B groups had greater normalized neurogenic spectral densities in pressure with fast cooling.

Table 24. Mean and standard deviation (SD) of normalized neurogenic spectral densities during reactive hyperemia.

The *p* values were the results of Wilcoxon signed rank tests that compared the spectral densities during reactive hyperemia to that during baseline.

Test Session Group	PF		PO		PS	
	Mean ± SD	<i>p</i>	Mean ± SD	<i>p</i>	Mean ± SD	<i>p</i>
CTRL	83.53 ± 78.35	.345	323.06 ± 413.57	.046*	181.03 ± 225.17	.650
T6A	355.18 ± 609.82	.530	317.97 ± 305.51	.071	259.83 ± 225.99	.006*
T6B	405.97 ± 678.18	.345	291.84 ± 362.25	.753	166.61 ± 207.83	.753

PS = pressure + slow cooling test session, PF = pressure + fast cooling test session, PO = pressure only test session.

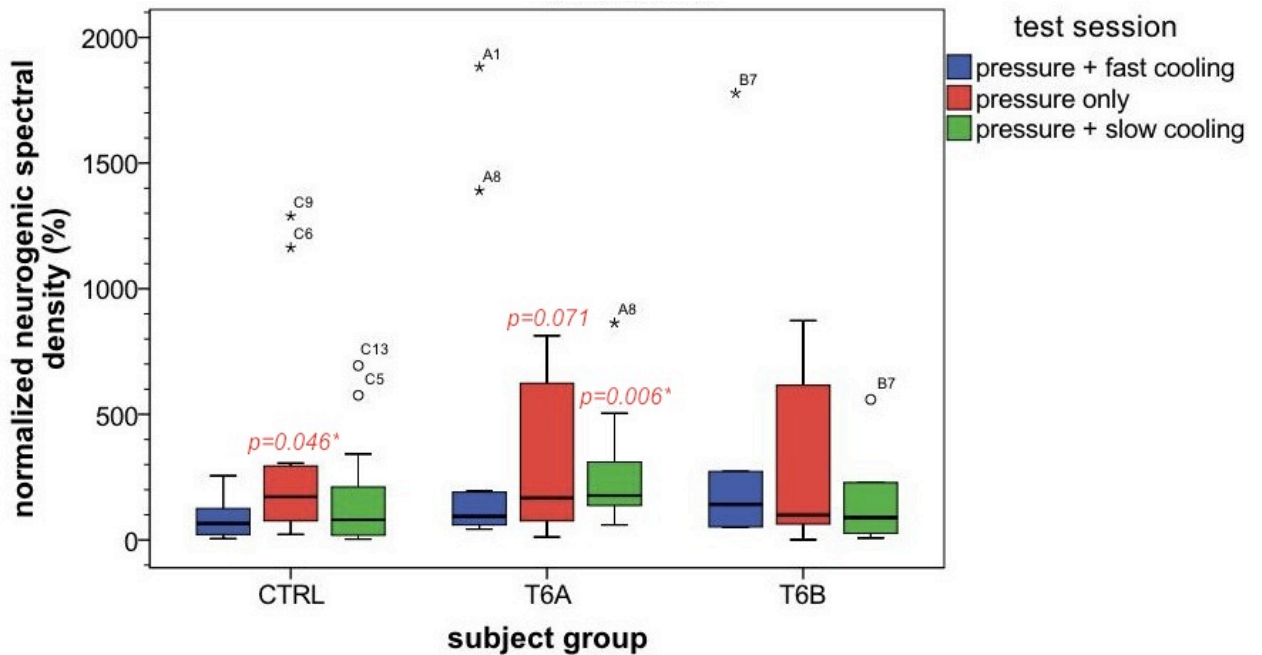


Figure 36. Box plots of normalized neurogenic spectral density in all subjects (excludes those without reactive hyperemia in all test sessions).

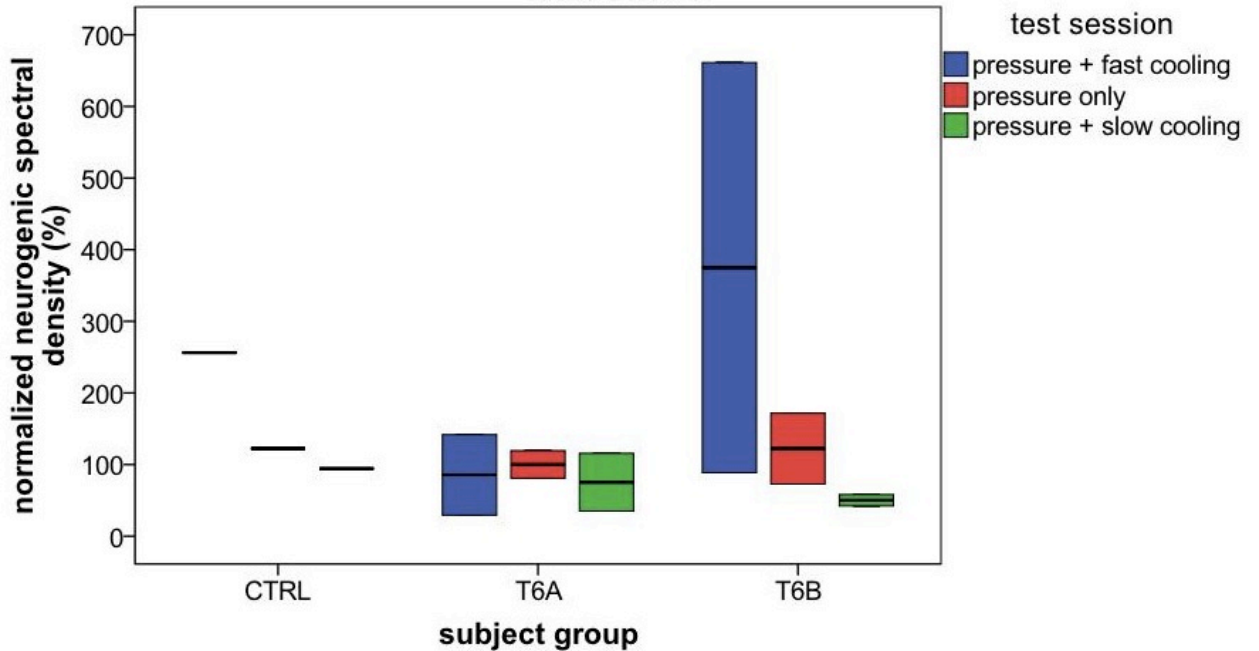


Figure 37. Box plots of normalized neurogenic spectral density in subjects with no reactive hyperemia in all test sessions.

(c) Myogenic spectral density

Figure 38 is the box plot of normalized myogenic spectral densities of all subjects (excludes those with no reactive hyperemia in all test sessions). Table 25 shows the results of descriptive analysis and Wilcoxon signed rank tests of the normalized myogenic spectral densities of the normalized myogenic spectral densities. The control group showed that the increase in myogenic spectral density is close to significant in pressure only, but not in pressure with fast or slow cooling. In people with injury level above T6, the myogenic spectral density increased significantly in pressure only and pressure with slow cooling but not in pressure with fast cooling. In people with injury level below T6, there was no significant increase in myogenic spectral density in all three test sessions. Figure 39 is the box plot of myogenic spectral densities in subjects with no reactive hyperemia in all test sessions. One of the subjects in each group had greater normalized myogenic spectral densities in pressure with fast cooling.

Table 25. Mean and standard deviation (SD) of normalized myogenic spectral densities during reactive hyperemia.

The *p* values were the results of Wilcoxon signed rank tests that compared the spectral densities during reactive hyperemia to that during baseline.

Test Session Group	PF		PO		PS	
	Mean ± SD	<i>p</i>	Mean ± SD	<i>p</i>	Mean ± SD	<i>p</i>
CTRL	105.04 ± 112.89	.650	298.93 ± 321.57	.064	125.85 ± 119.70	.552
T6A	258.51 ± 340.87	.308	326.32 ± 318.41	.034*	208.99 ± 101.54	.008*
T6B	291.31 ± 423.76	.345	213.08 ± 188.81	.345	145.80 ± 181.66	.917

PS = pressure + slow cooling test session, PF = pressure + fast cooling test session, PO = pressure only test session.

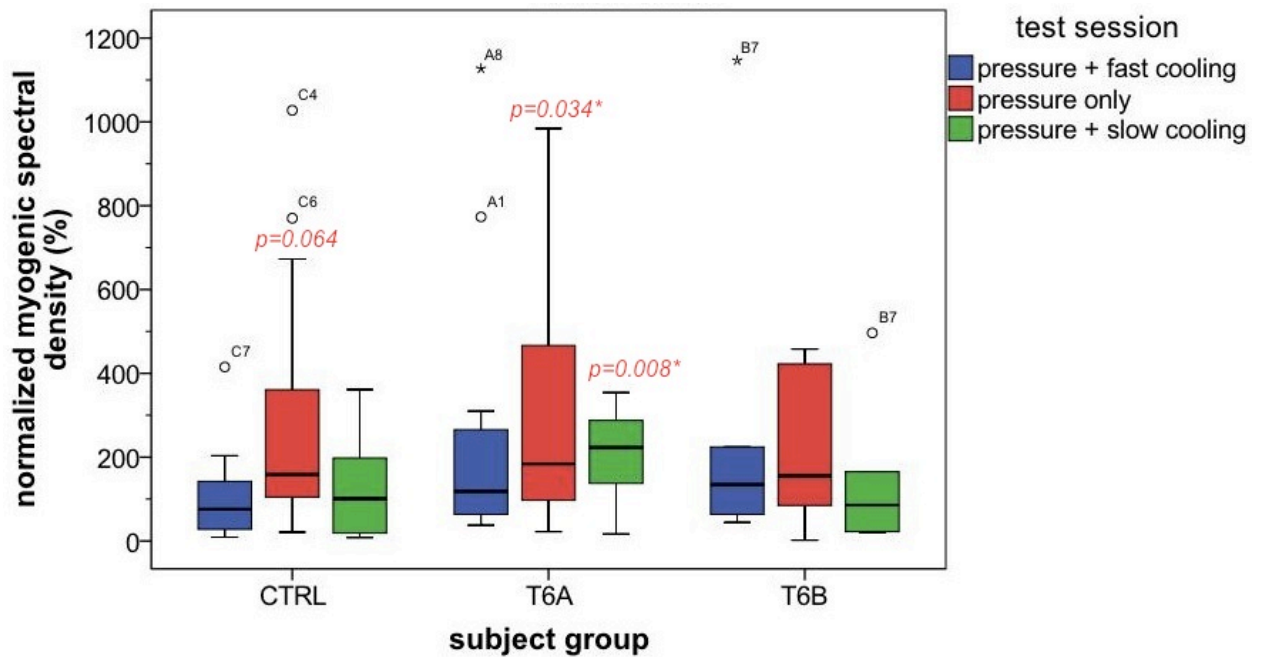


Figure 38. Box plots of normalized myogenic spectral density in all subjects (excludes those without reactive hyperemia in all test sessions).

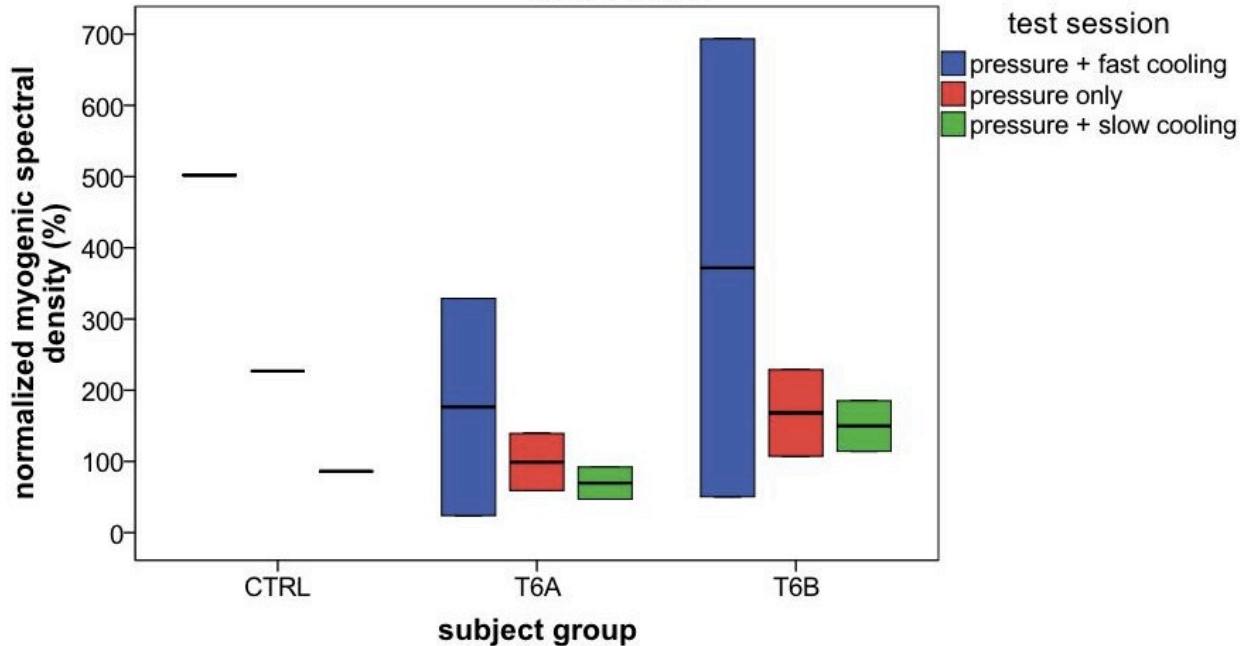


Figure 39. Box plots of normalized myogenic spectral density in subjects with no reactive hyperemia in all three test sessions.

4.6.3 Reactive hyperemic response compared among groups

Since the percentage decrease of normalized peak SBF, perfusion area, time to peak SBF and half life were not normally distributed, the Kruskal-Wallis test was used to compare the differences among the three subject groups. Due to the fact that there was no significant changes in time to peak SBF and half life with the local cooling application, no further statistical analysis was computed for the percent decrease of these two parameters to compare among groups.

4.6.3.1 Hypotheses 2 a) b) e) and f): decreased normalized peak SBF with local cooling

Figure 40 is the box plot of the percentage change of normalized peak SBF in pressure with fast and slow cooling subtracted from pressure only in all three groups. Table 26 shows the results of descriptive analysis and Kruskal-Wallis tests in all subjects (excludes those with no

reactive hyperemia in all test sessions). There was no significant difference among the three test groups in the percent change of normalized peak SBF.

Table 26. Mean and standard deviation (SD) of percent change of normalized peak SBF in all subjects (excludes those with no reactive hyperemia in all test sessions).

The *p* values were the results of Kruskal-Wallis tests.

Test Session Group	(PO-PF)/PO (%)		(PO-PS)/PO (%)	
	Mean ± SD	<i>p</i>	Mean ± SD	<i>p</i>
CTRL (N=13)	29.63 ± 125.06	.800	5.89 ± 126.26	.543
T6A (N=12)	-105.90 ± 507.67		-59.41 ± 164.99	
T6B (N=6)	-6.61 ± 151.34		-44.45 ± 153.72	

PS = pressure + slow cooling test session, PF = pressure + fast cooling test session, PO = pressure only test session.

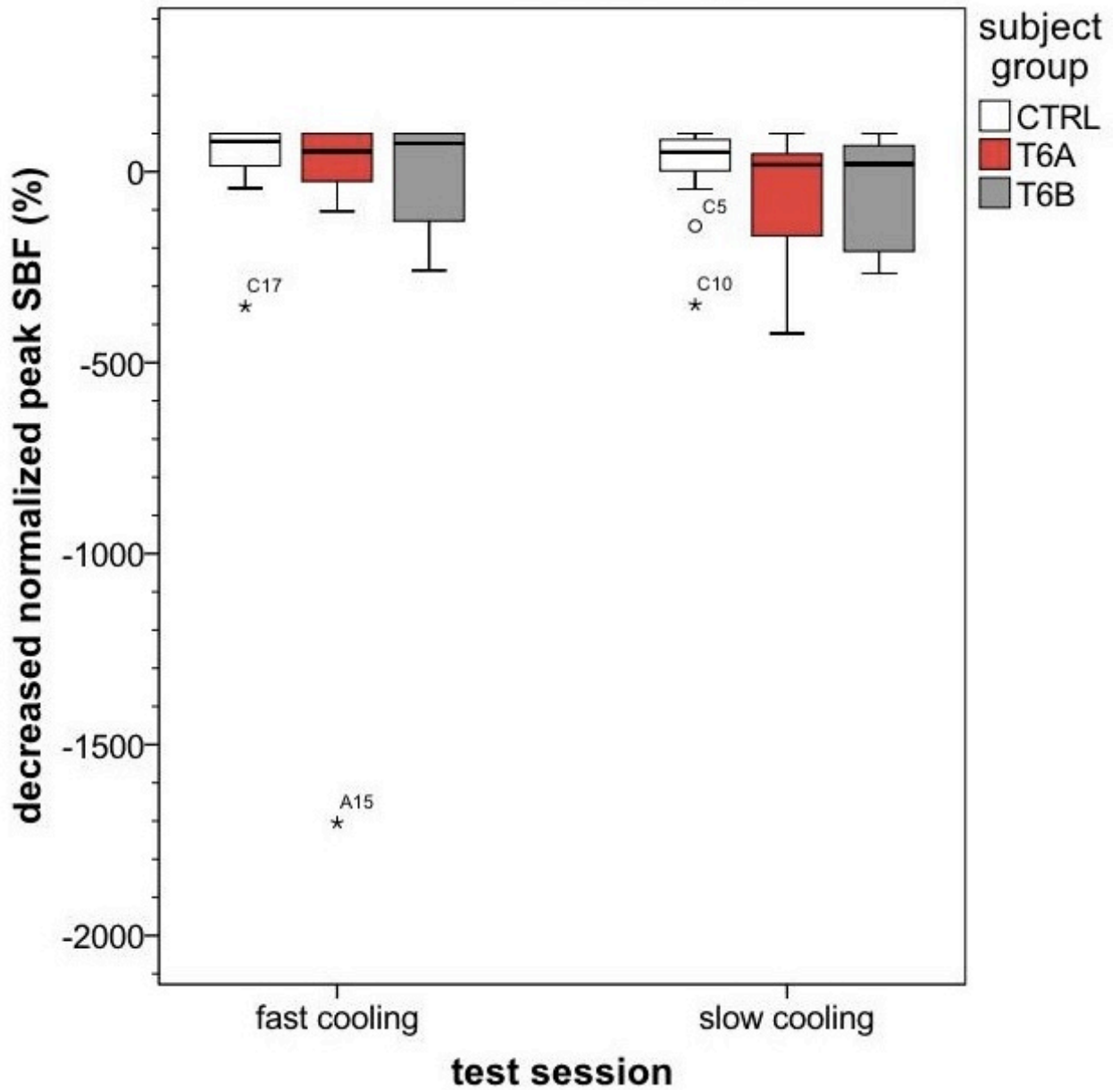


Figure 40. Box plots of changes in normalized peak SBF from pressure only in all three groups.

4.6.3.2 Hypotheses 2 c) d) g) and h): decreased perfusion area with local cooling

Figure 41 is the box plot of the percentage change of perfusion area in pressure with fast and slow cooling subtracted from pressure only in all three groups. Table 27 shows the results of descriptive analysis and Kruskal-Wallis tests in all subjects (excludes those with no reactive

hyperemia in all test sessions). There was no significant difference among the three test groups in the percent change of perfusion area.

Table 27. Mean and standard deviation (SD) of percent change of perfusion area in all subjects (exclude those with no reactive hyperemia in all test sessions).
The *p* values were the results of Kruskal-Wallis tests.

Test Session Group	(PO-PF)/PO (%)		(PO-PS)/PO (%)	
	Mean ± SD	<i>p</i>	Mean ± SD	<i>p</i>
CTRL (N=13)	-136.23 ± 745.39	.782	-159.67 ± 575.67	.514
T6A (N=12)	-356.34 ± 1309.43		-79.35 ± 230.82	
T6B (N=6)	-6.57 ± 171.51		-114.48 ± 362.44	

PS = pressure + slow cooling test session, PF = pressure + fast cooling test session, PO = pressure only test session.

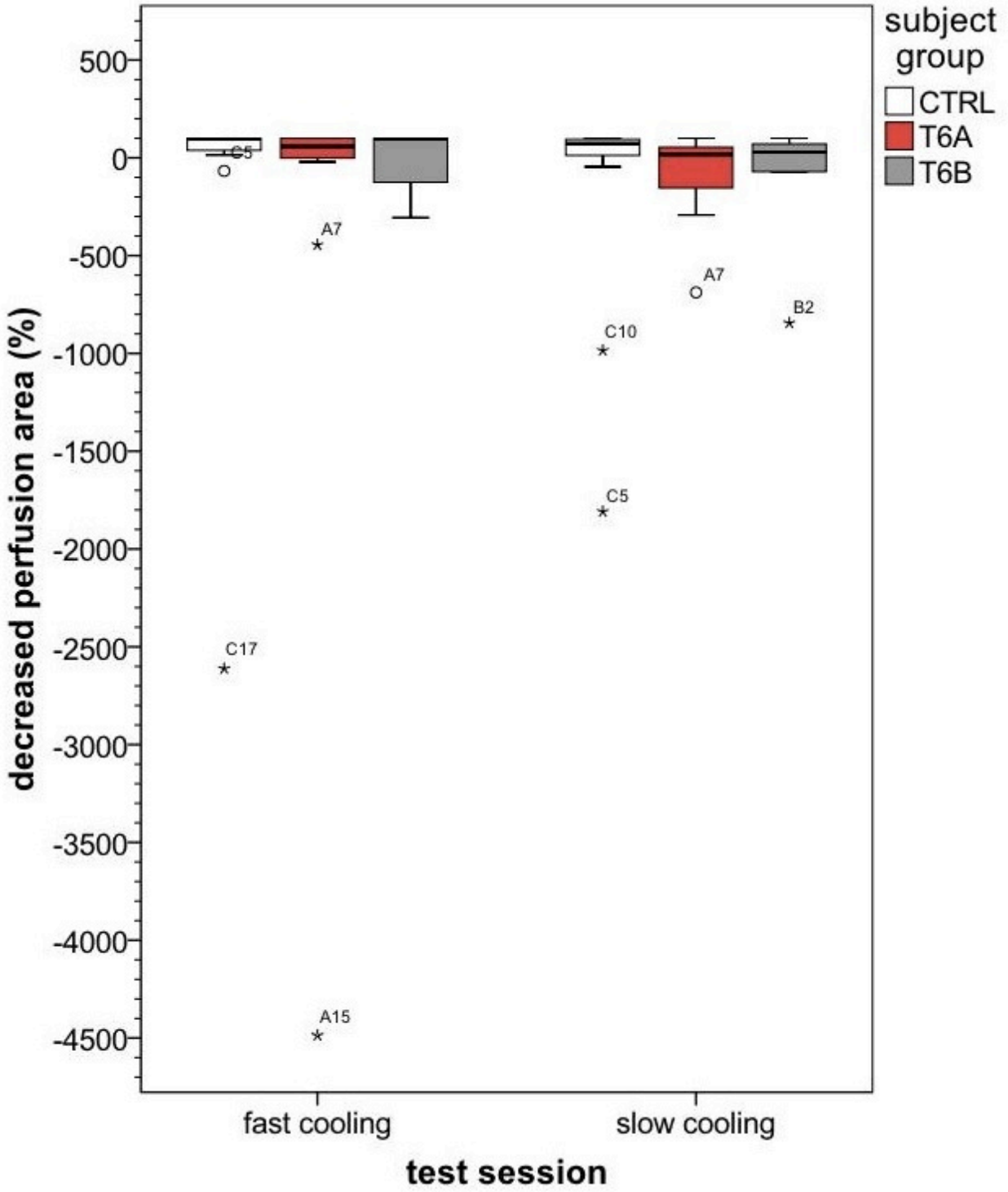


Figure 41. Box plots of changes in perfusion area from pressure only in all three groups.

5.0 DISCUSSION

5.1 SUMMARY OF MAJOR FINDINGS

Major findings from this study fall under four main categories: 1) the capability of controlling and maintaining the test conditions (section 5.2), 2) the effectiveness of different cooling rates on healthy controls (section 5.3), 3) the effectiveness of different cooling rates on people with SCI (section 5.4), and 4) the differences in cooling effects on people with different levels of neurological deficit (section 5.5). Results from this study suggest that the instruments used in this study were capable of providing pressure and temperature control on the skin. In addition, the integrated system was capable of measuring the reactive hyperemic response for comparison among subjects and test sessions. Results from the reactive hyperemic response suggest that local skin cooling provides a protective effect on the skin during ischemia in people without SCI. In people with injury level at T6 and above, this phenomenon was not observed in the time domain parameters of the reactive hyperemia, but was observed in the spectral densities. For comparisons among groups of changes in reactive hyperemia with local skin cooling, the lack of difference might be due to the small changes of reactive hyperemia with cooling application in people with SCI and the reduced hyperemic response after injury. Details of each main category are listed in the following sections.

5.2 TEST CONDITIONS

This study recruited a convenient sample of people with different levels of SCI. The majority of the subjects were males, and the recruitment sample is consistent with that reported by the CDC (Centers for Disease Control and Prevention, 1998). The test instrument of this study was modified from our previous pilot study that tested only young healthy adults (Tzen, et al., 2010). The consistent pressure control in all three test sessions and subject groups indicated that this system is capable of maintaining the same amount of pressure on people with different levels of neurological deficits. The movement artifacts (oscillation in pressure) by subjects with SCI were corrected quickly throughout the tests. The thermoelectric cooling system used in this study is the same as the one used in our pilot study as well. Results from this study show that the modified test system is capable of controlling the skin temperature at two different cooling rates in all subjects. In addition, both fast and slow cooling significantly reduces skin temperature as compared to that with pressure only.

5.3 EFFECTIVENESS OF DIFFERENT COOLING RATES IN CONTROL GROUP

Reactive hyperemia has been widely used in previous studies (Hagisawa, et al., 1994; V. Schubert & Fagrell, 1991b; Sprigle, et al., 2002) to investigate tissue viability and microvascular function. Time domain parameters including normalized peak SBF and perfusion area have been proven to represent different characteristics of this physiological response. The normalized peak SBF is the maximum percent increase of SBF after pressure relief. It was related to the extent of vasodilation during the reactive hyperemia (Hagisawa, et al., 1994). A

previous study suggested that this parameter provided information of the severity of tissue ischemia. Matsubara et al. (1998) induced the reactive hyperemic response with the same amount of pressure but with different amounts of time. They found that the peak SBF was significantly higher with longer period of tissue ischemia. The perfusion area was the total increase in SBF after the tissue ischemia. Previous studies suggested that this increase in blood flow was to erase the oxygen/nutrition debt of the ischemic tissue (Levick, 2003) and this parameter could represent the metabolic repayment of the tissue (Hagisawa, et al., 1994).

Results from people without SCI showed that both fast and slow cooling reduced the reactive hyperemic response. Thirteen of the subjects had reactive hyperemia in the pressure only test session. Given that the pressure application phase was consistent and the baseline SBF was not significantly different among test sessions, the absence of a reactive hyperemic response in the fast and/or slow cooling sessions of these subjects was mainly due to the local cooling application. Results of decreased normalized peak SBF with both fast and slow cooling suggests that the tissue ischemia was less severe with local skin cooling. This result was consistent with our pilot study that compared the normalized peak SBF after cooling (25°C) and non-cooling on young healthy adults (Tzen, et al., 2010) and another animal study that compared the normalized peak SBF after mild hypothermia (34°C) and with core temperature (37°C) on pig coronary artery (Olivecrona, Gotberg, Harnek, Van der Pals, & Erlinge, 2007). In addition, results of decreased perfusion area with both fast and slow cooling suggested that the metabolic demand during both cooling sessions was smaller as compared with no cooling. This finding is consistent with that for the normalized peak SBF. A previous study found that the tissue metabolic rate depends on the surrounding temperature of the tissue (Ruch & Patton, 1965), and a 1°C decrease of temperature causes about a 10% reduction in tissue metabolic rate. Results

from this study support the finding that tissue metabolism depends on tissue temperature. Although another previous study found that local skin fast cooling but not slow cooling induced an initial vasodilation (Yamazaki, et al., 2006), findings from this study did not show any significant differences in reactive hyperemia response between two cooling rates. One possible explanation may be that the initial vasodilation was not obvious when the skin was loaded. Another possible explanation may be that the initial cold-induced vasodilation does not last for a long period of time as compared to the time with loading. In the study that discovered the differences in initial vasodilation between two cooling rates, the researchers did not discover how long the initial vasodilation lasted. Finding from this study suggest that the blood supply during mechanical loading was not significantly different between the two cooling rates.

The underlying mechanism of blood flow mediation in the control group may be the result of neurogenic mechanisms. The metabolic spectral density did not show any significant changes during reactive hyperemia in the control group; this was consistent with the findings in our pilot study (Tzen, et al., 2010). However, the results conflict with a previous study using wavelet analysis to examine the blood flow signal in frequency domain. Li et al. investigated the spectrum of the reactive hyperemic response in people with and without SCI. They found that the normalized power spectrum increased significantly in metabolic, neurogenic and myogenic frequency bands in healthy controls, but only in metabolic frequency bands in SCI (Li, Leung, Tam, & Mak, 2006). The different findings from this study and the previous study may be due to different amount of external pressure that is applied on the skin (Li et al. used twice the amount of pressure than this study).

5.4 EFFECTIVENESS OF DIFFERENT COOLING RATES IN PEOPLE WITH SCI

There was no significant difference in normalized peak SBF and perfusion area among test sessions in people with spinal cord injury. This finding is in contrast with that in the control group and may be due to a reduced reactive hyperemic response after injury. Schubert and Fagrell (1991b) investigated the reactive hyperemic response in people with and without SCI and found that people with SCI had significantly lower perfusion area at the sacrum as compared to the healthy controls. Hagisawa et al. (1994) also investigated the reactive hyperemic response in people with SCI and found that the increase in blood content was significantly reduced in people with SCI as compared to the control group. Olive, McCully & Dudley (2002) investigated the reactive hyperemic response on people with incomplete SCI. They found that the normalized peak flow after 2 and 4 minutes of ischemia was significantly lower in people with SCI as compared with the control groups. The reduced reactive hyperemic response suggested that the vascular capacity of dilation was decreased in this population (Hagisawa, et al., 1994), and the tissue sensitivity of ischemia may decrease after injury (Olive, et al., 2002).

The changes in vascular responses in people with SCI may be caused by increased vascular resistance after the injury. Kooijman (2008) found that the structural changes and functional adaptation of the vascular response after injury cause the alteration in vascular response in people with SCI. The reactive hyperemic response is mediated by several physiological mechanisms, including the accumulation of endothelial vasodilators (Engelke, Halliwill, Proctor, Dietz, & Joyner, 1996), sensory reflex (Larkin & Williams, 1993; Lorenzo & Minson, 2007), and smooth muscle activity (Koller & Bagi, 2002) that modulate this local vascular response. The reduced reactive hyperemic response in people with SCI might be caused by the impaired β -adrenergic vasodilation, reduced nitric oxide release or endothelium sensitivity

of the nitric oxide (Olive, et al., 2002). However, there were no studies provide information of how much (e.g. percentage) each physiological mechanism contributes to the reactive hyperemic response. Furthermore, there are no studies that investigated ‘how much the reactive hyperemia changes’ when another stimulus in addition to pressure was added during the tissue ischemia in this population. Due to the reduced vasodilation during reactive hyperemia and the unknown percentage of each physiological mechanism that contributes to the reactive hyperemic response, the effectiveness of local cooling on tissue viability in this population may be masked by a combination of changes in different physiological responses.

The analysis of time domain parameters of the reactive hyperemia is augmented by the analysis of spectral density to provide information on specific physiological control mechanisms of the SBF. Time frequency analysis has been used in previous studies to investigate the control mechanisms of vascular response during different pressure application patterns (Jan, Brienza, Geyer, & Karg, 2008) and thermoregulation (Geyer, et al., 2004).

The metabolic spectral density is related to the vasodilation response caused by the accumulation of endothelial vasodilators (Stefanovska, et al., 1999). The increased metabolic spectral density only in people with injury level at T6 and above during pressure only and pressure with slow cooling suggested that the accumulation of the endothelial vasodilator during this two sessions may be more obvious than that observed in fast cooling. One possible explanation that the metabolic spectral density increased significantly in people with injury level at T6 and above might be because the tissue metabolism in people with SCI is different from that in healthy controls. To date, studies that investigated the risk of people with SCI in developing pressure ulcers focused mainly on how much the interface pressure (Brienza & Karg, 1998) or the sub-dermal tissue stress differ from those that are not at risk of pressure ulcers (Linder-Ganz,

et al., 2008). One study that investigated the resting metabolic rate of people with paraplegia showed that the resting metabolic rate of this population without pressure ulcers was significantly lower than that with pressure ulcers (Alexander, Spungen, Liu, Losada, & Bauman, 1995). In addition, the resting metabolic rate in healthy people with paraplegia was lower than the ambulatory individuals. Findings from this study raised a question that the tissue metabolism during prolonged pressure and changes in skin temperature might be different in people with SCI, and further investigation in this topic may contribute to the understanding of physiological changes of soft tissue under prolonged pressure.

The increased neurogenic spectral density in this population, however, was unexpected. Bracic and Stefanovska (Bracic & Stefanovska, 1998) found that the power spectrum within the neurogenic frequency band was absent with local anesthesia and sympathectomy. The changes in the neurogenic spectral density indicated that the part of the local nerve response on vascular control was preserved in people with SCI. A previous study blocked the α -adrenoceptor on people with and without SCI and found that the vascular resistance was reduced significantly in both population (Kooijman, Rongen, Smit, & Hopman, 2003). This suggested that the α -adrenergic tone was preserved after injury, and this response may be caused by the local reflex (probably the spinal sympathetic reflex and venoarteriolar reflex).

The myogenic spectral density reflects the smooth muscle activity caused by changes in vascular tone. Results of this study suggested that the endothelial vasodilation response in people with impaired autonomic nervous systems could still induce the smooth muscles surrounding the capillaries to maintain the vascular tone. Further investigation of the percentage of the myogenic control mechanism may help to understand why the changes during reactive

hyperemia were observed in the spectral density but this difference was not as evident in the time domain parameters.

5.5 DIFFERENCES IN COOLING EFFECTS ON PEOPLE WITH VARIOUS LEVELS OF NEUROLOGICAL DEFICITS

There was no significant difference in the reduction of reactive hyperemia with cooling application among the three groups. The lack of differences may be due to two reasons. First, from the results of hypotheses 1, the differences among test sessions were not obvious in subjects with SCI; therefore comparison of the percentage changes from pressure only did not show any differences among the groups with different levels of neurological deficit. Secondly, the percent decrease of reactive hyperemia with local cooling stimuli might be affected by the reduced reactive hyperemic response in people with SCI. As described in previous paragraphs, the reactive hyperemic response may be reduced after injury due to changes in vessel structures and functional adaptation (Kooijman, 2008). In addition, the percentage of different vascular control mechanisms may alter after injury. For example, Kooijman et al. (2007) found that the myogenic control mechanism dominated the local vasoconstriction response in people with SCI. They examined the vascular resistance of lower limb under two conditions: limb dependency and cuff inflation. The vasoconstriction response during limb dependency depends on the myogenic vasoconstriction and the venoarteriolar reflex, while the response during cuff inflation depends on venoarteriolar reflex only. They found that the vascular resistance of the lower limb increased significantly in people with SCI during limb dependency, however this phenomenon was not recognized during cuff inflation. This suggested that the myogenic controlled

vasoconstriction dominated the local vasoconstriction response in people with SCI. Nevertheless, to date, there are no data on how much the myogenic response contributes to the vascular control during reactive hyperemia, and there are also no data on how much the myogenic control mechanism increases in the vascular control as compared to the other physiological mechanisms.

The main differences observed among groups were in the time domain parameters and the spectral densities of the reactive hyperemia. Findings from the control group suggested that both cooling rates decreased the severity of tissue ischemia and the metabolic demand. In the control group, the significant changes in SBF after the release of tissue ischemia in the test session without cooling was mainly mediated by the neurogenic and myogenic control mechanisms. On the contrary, in subjects with injury level at T6 and above, although changes in skin blood flow during reactive hyperemia was not obvious, spectral densities showed that the endothelial-related vasodilation (possibly nitric oxide and endothelium-derived hyperpolarizing factor (Bellien, et al., 2006; Lorenzo & Minson, 2007)) during reactive hyperemia increased with pressure only and pressure with slow cooling test sessions. Results from this study suggest that local skin cooling provided a protective effect on people without SCI and people with SCI at T6 and above. Investigation of skin blood flow using time domain parameters and spectral densities provided more information on the tissue response to ischemia. In addition, use of the two analysis approaches together improves the understanding of vascular control in people who encounter physiological changes due to disease and injury.

5.6 SUBJECTS WITH NO REACTIVE HYPEREMIA IN ALL TEST SESSIONS

In general, reactive hyperemic response could be induced at pressure above 50 mmHg for about 3 to 15 minutes on the human forearm (Cracowski, et al., 2006). However, the amount of pressure used to induce the reactive hyperemic response differed from person to person. For example, Schubert and Fagrell (1991b) investigated the reactive hyperemic response on people with and without SCI and showed that the amount of pressure required to occlude the sacral SBF in people with SCI was significantly lower than that in the control group. The goal of this study was not to occlude the sacral SBF completely. Instead, this study created a pressure application phase that was similar to the clinical setting with slightly lower amount of pressure (Brienza, et al., 2001) to prevent any harmful effect caused by prolonged pressure. Pressure of 60 mmHg was used in our pilot study on young healthy adults, and it was sufficient to induce reactive hyperemic response in all subjects (Tzen, et al., 2010). Since the amount of pressure required to induce reactive hyperemic response differs from person to person, 60 mmHg of pressure may not be enough to induce the reactive hyperemic response in the five subjects in this study that did not have reactive hyperemia in all three test sessions.

5.7 LIMITATIONS

There were several limitations of this study. The sample size of the T6B group did not reach the target number of recruitment, and the differences within or between groups may be affected. There were no test performed on the subjects to ensure that caffeinated food were not consumed 12 hours prior to the test, and there were also no test to check if the smokers actually refrained

from smoking four hours prior to the test. In addition, all medical history was self-reported and there may be recall bias involved when subjects reported the information. Last, although the possible mechanisms that contribute to vascular controls were discovered, the exact substances or neurotransmitters of each mechanism were not fully identified. Future studies investigating the percentage of each substance that contributes to the vascular control in subjects with different levels of neurological deficit will help to understand the changes that occur after spinal cord injury.

6.0 CONCLUSION

This study is the first to investigate the effectiveness of local fast and slow cooling on people that are at risk of pressure ulcer development. The results suggest that local fast and slow cooling both had a protective effect on the skin during ischemia in healthy controls. In subjects with injury level at T6 and above, spectral density data suggest that the endothelial vasodilation was most obvious during pressure only and pressure with slow cooling; indicating that the accumulation of endothelial vasodilators increased significantly during ischemia in these two sessions but not with fast cooling.

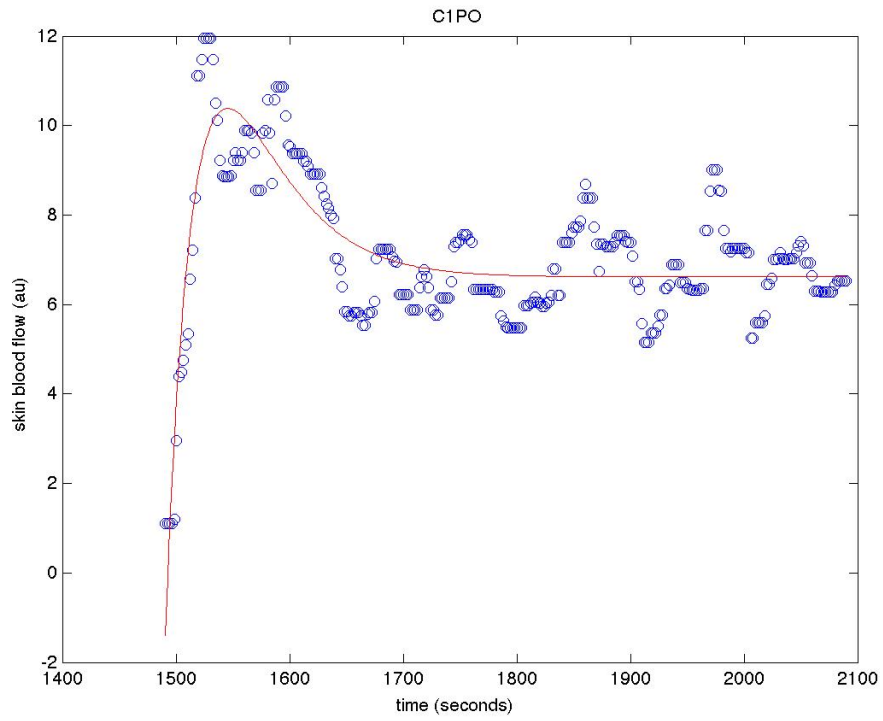
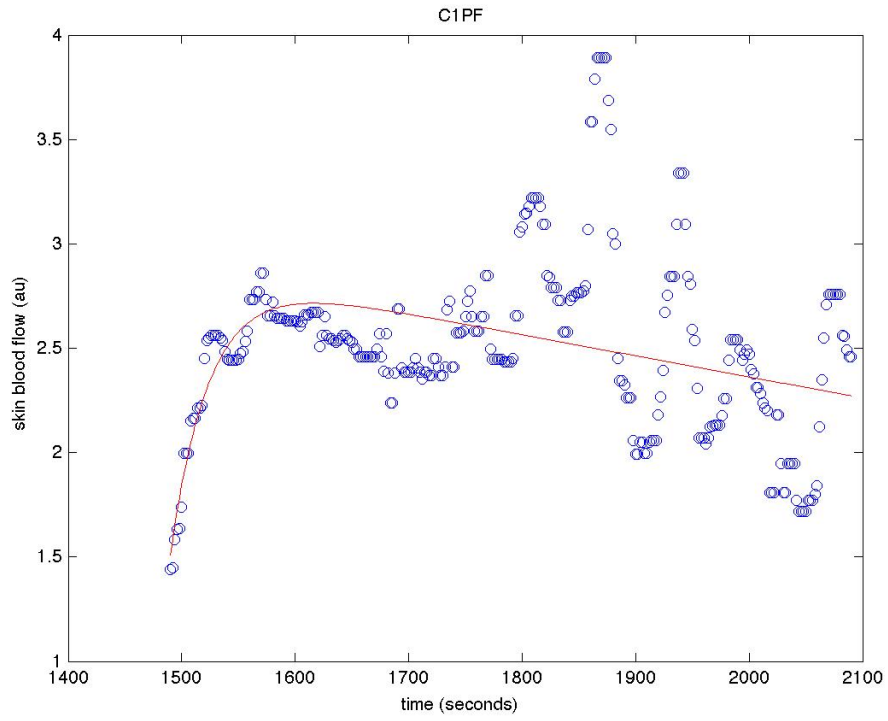
The results from this research support previous animal and human study findings that local skin cooling is beneficial to the tissue during prolonged pressure. In addition, this study supports that analyzing the SBF signal in the frequency domain using time-frequency analysis is helpful in understanding the underlying mechanisms of circulatory control in people with different levels of neurological deficits. Findings from this study will help to justify the development of support surfaces with microclimate controls for weight-bearing soft tissues. In addition, investigation of the changes in tissue metabolism during tissue loading and the local smooth muscle control of the microcirculation may contribute to the understanding of the risk of pressure ulcer development in people with SCI.

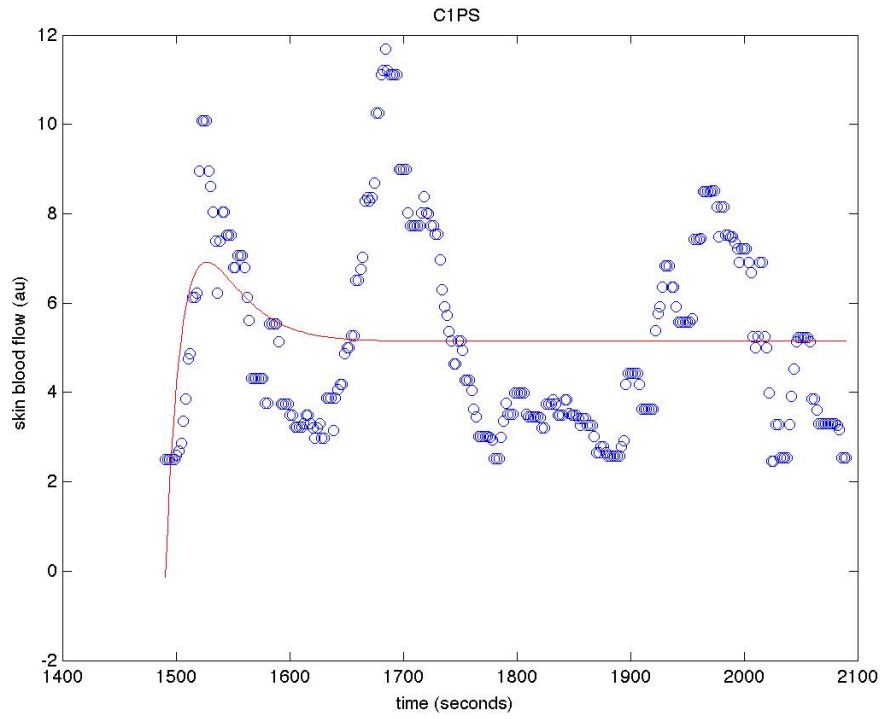
APPENDIX A

SKIN BLOOD FLOW EXPONENTIAL CURVE FITTING

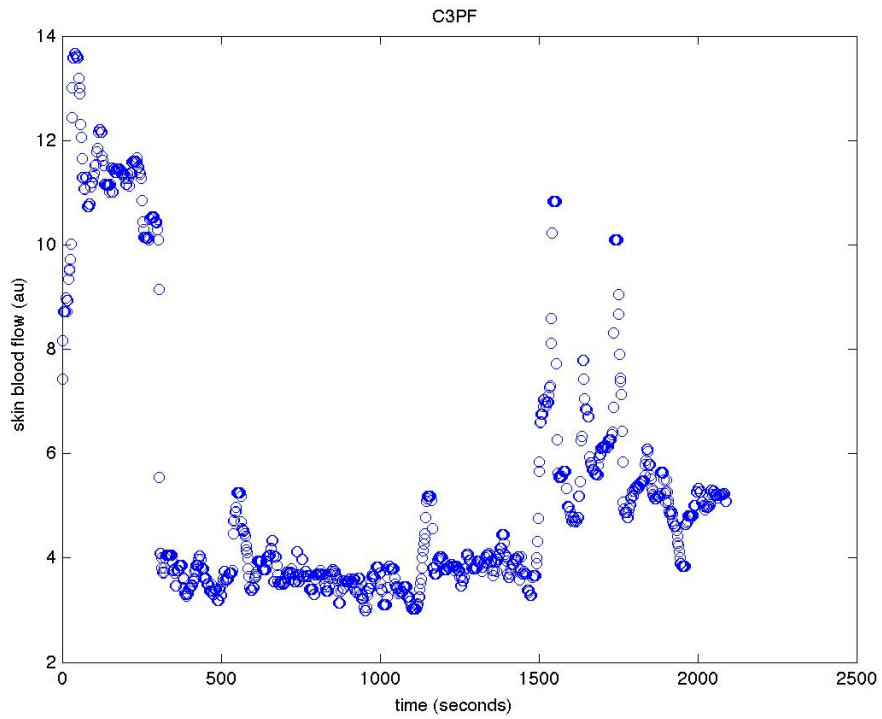
All figures are labeled with subject ID and test sessions (e.g. C=Control, A=T6A, B=T6B, PF=fast cooling, PO= pressure only, PS=slow cooling). Blue dots show the filtered SBF data, and the red line show the fit curve of the data. Baseline SBF of each test session and subject was listed for comparison. Test sessions with no reactive hyperemic response are plotted with the full length of the test to show that there was actually no hyperemic response as compared with baseline value.

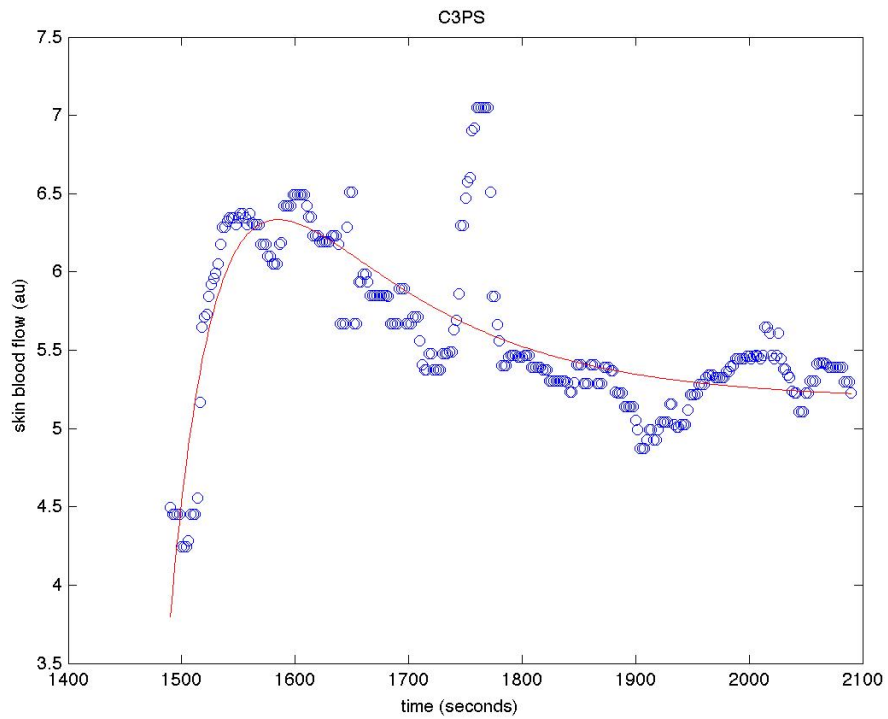
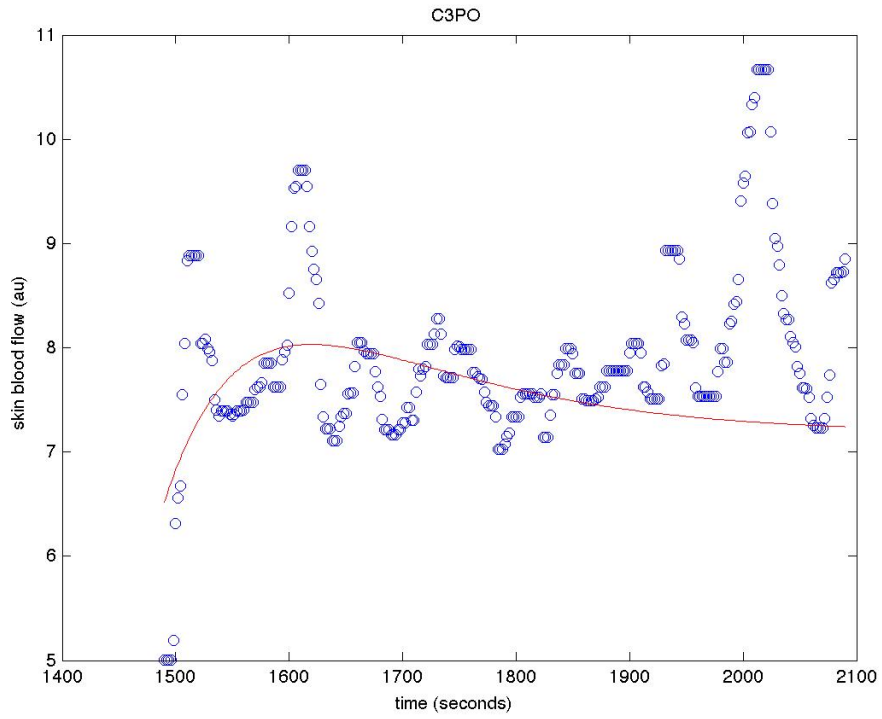
Subject CTRL_01: baseline SBF: PF= 2.50, PO= 4.13, PS= 4.83



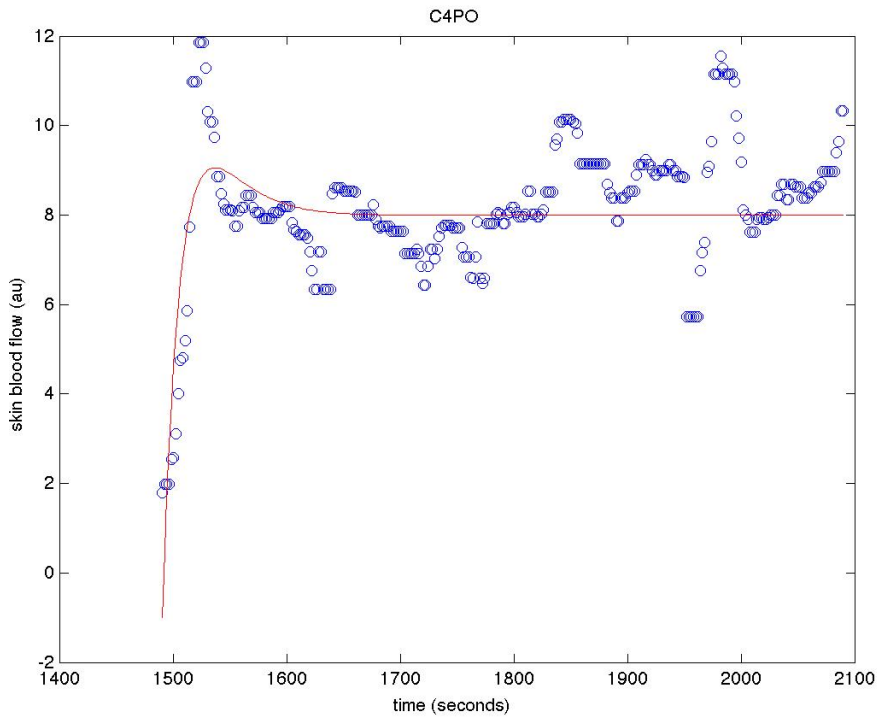
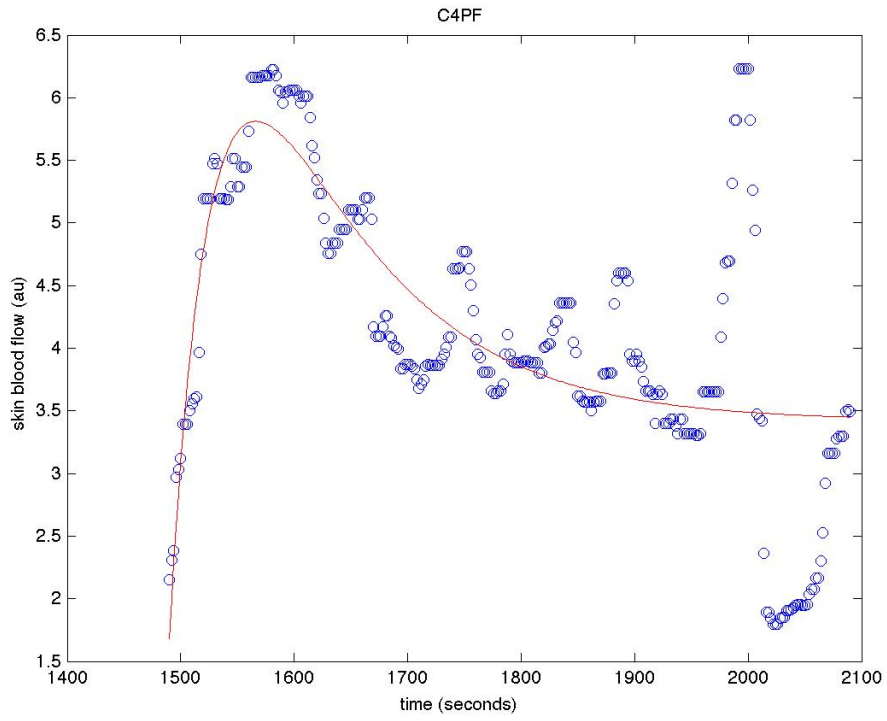


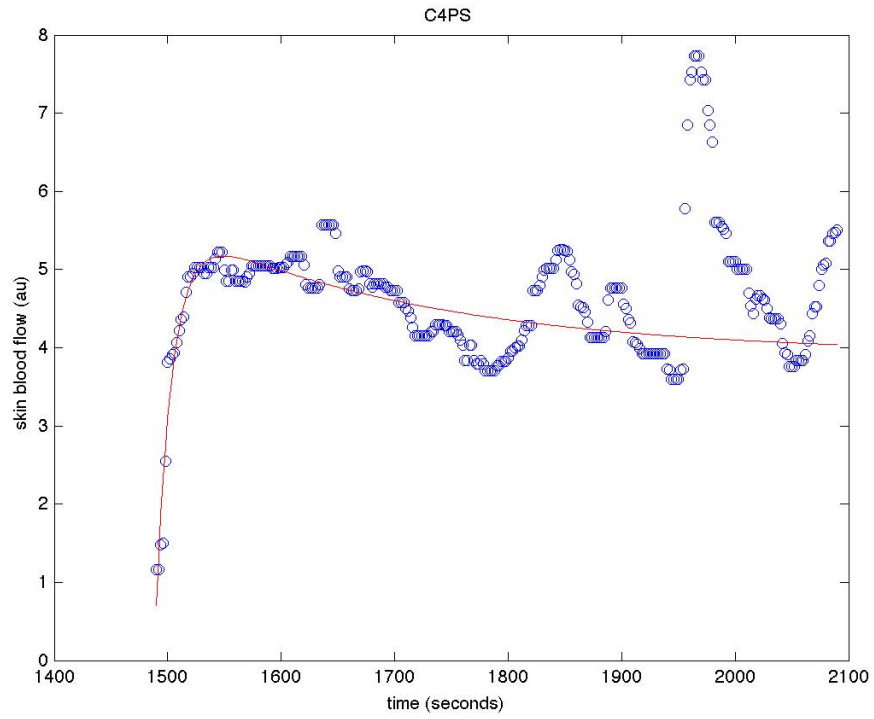
Subject CTRL_03: baseline SBF: PF=11.16, PO= 5.70, PS= 3.78



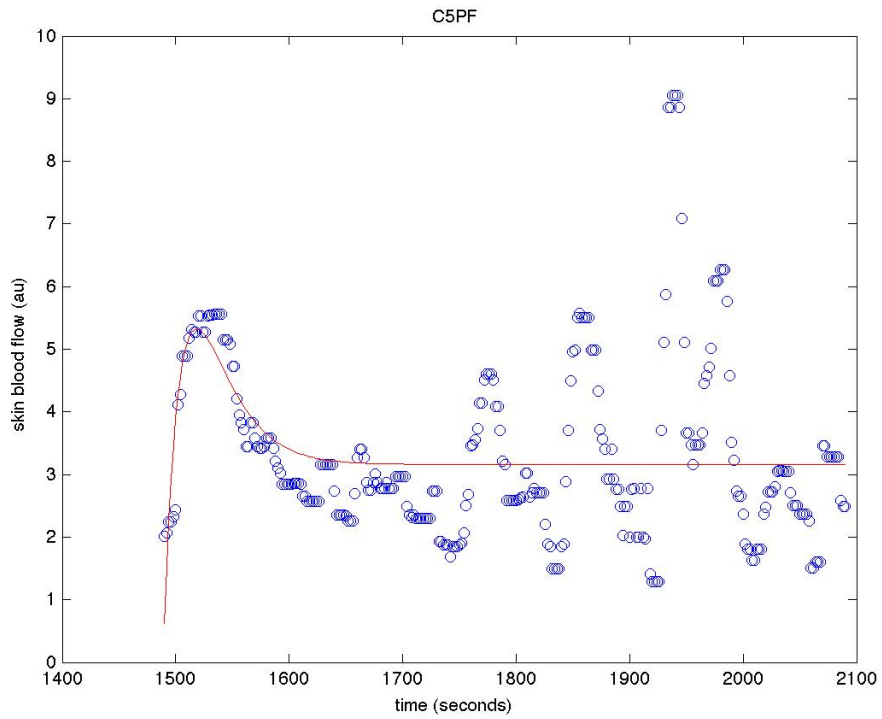


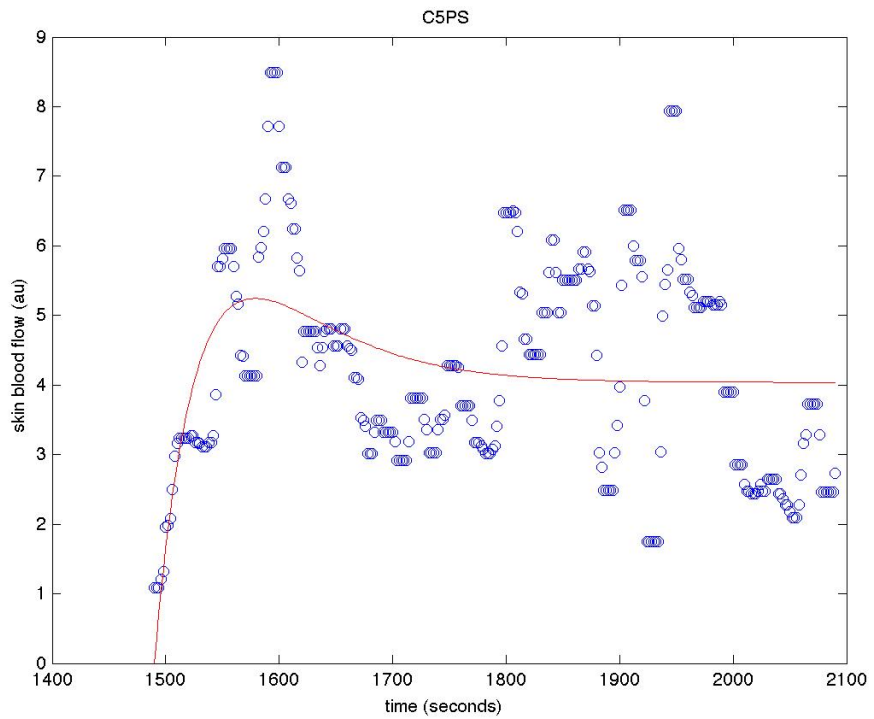
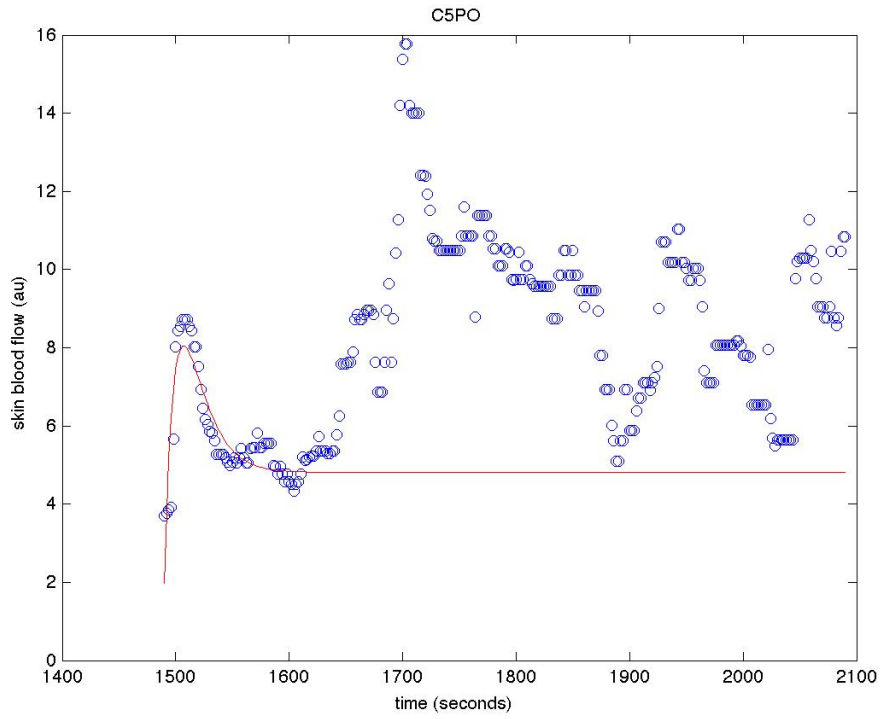
Subject CTRL_04: baseline SBF: PF=4.77, PO= 4.38, PS= 4.97



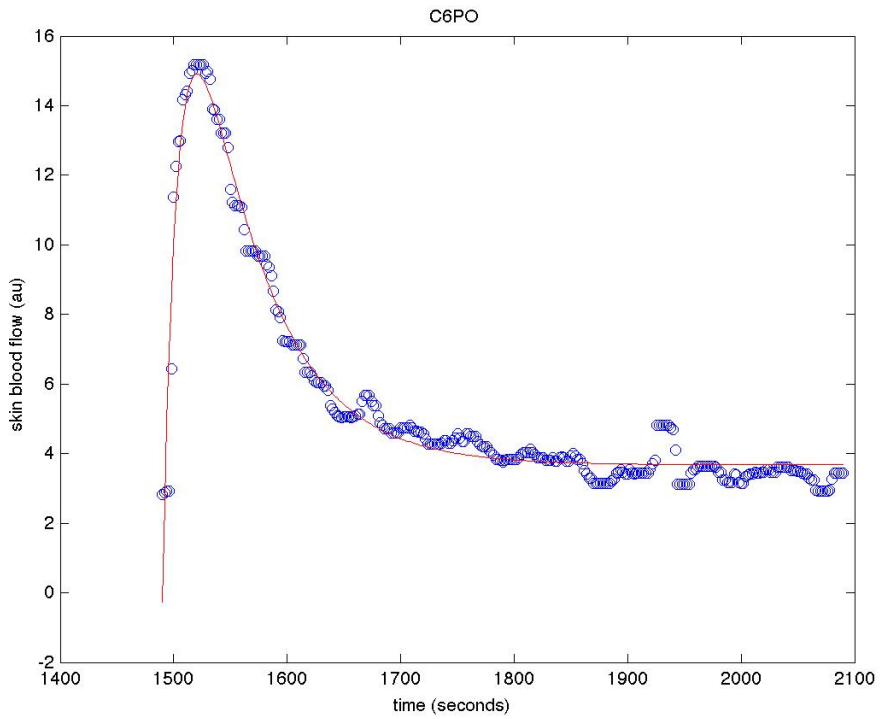
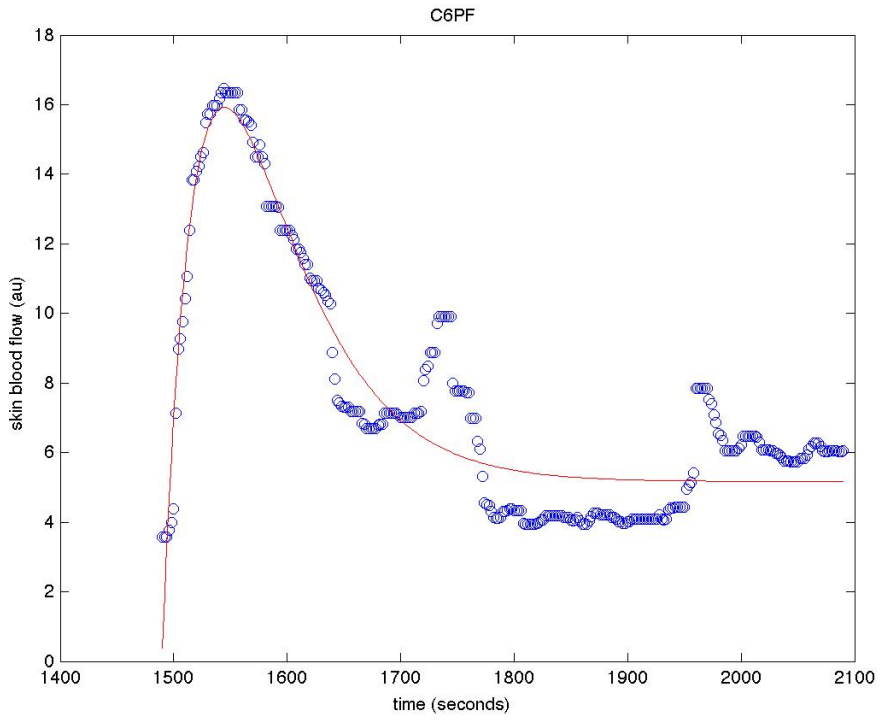


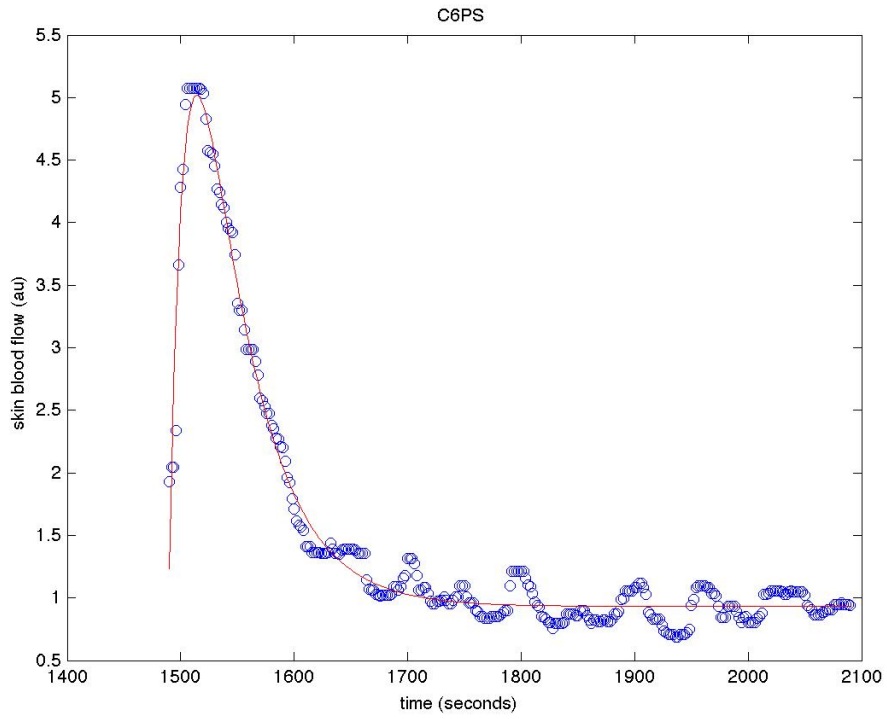
Subject CTRL_05: baseline SBF: PF=4.09, PO= 6.65, PS= 3.47



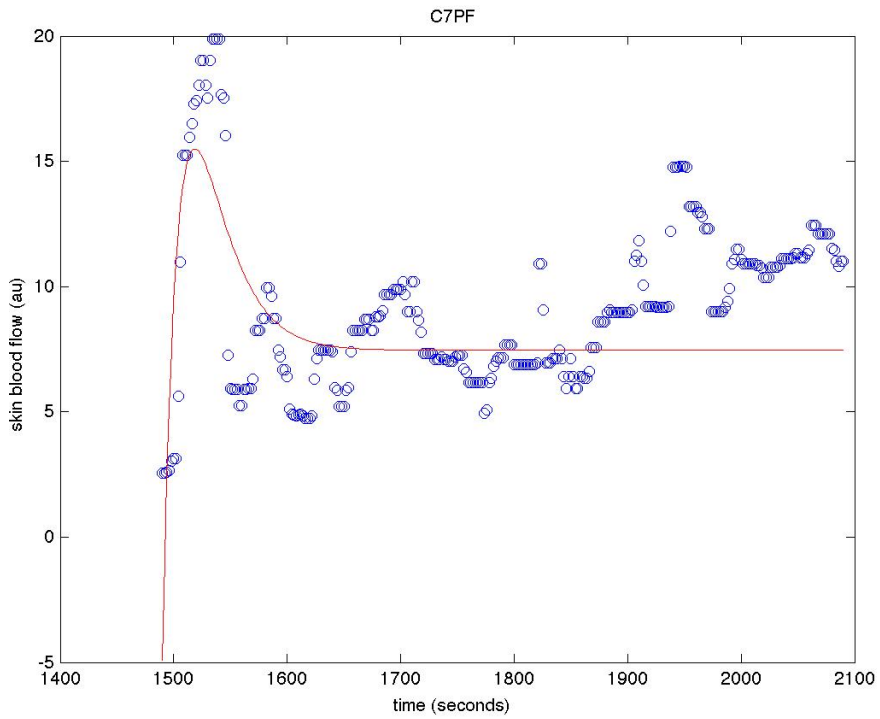


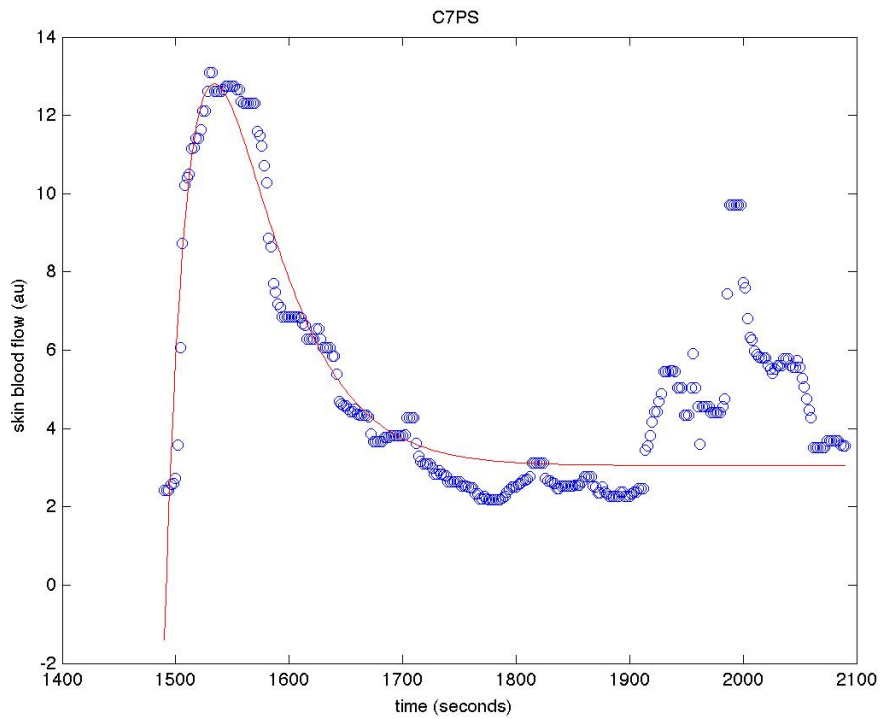
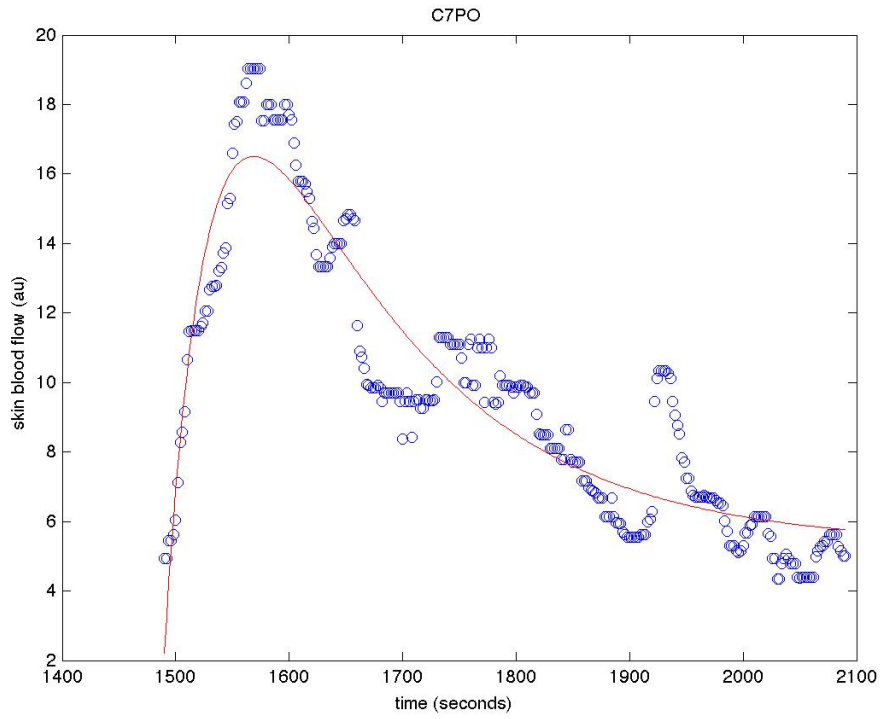
Subject CTRL_06: baseline SBF: PF=6.63, PO= 2.78, PS= 2.23



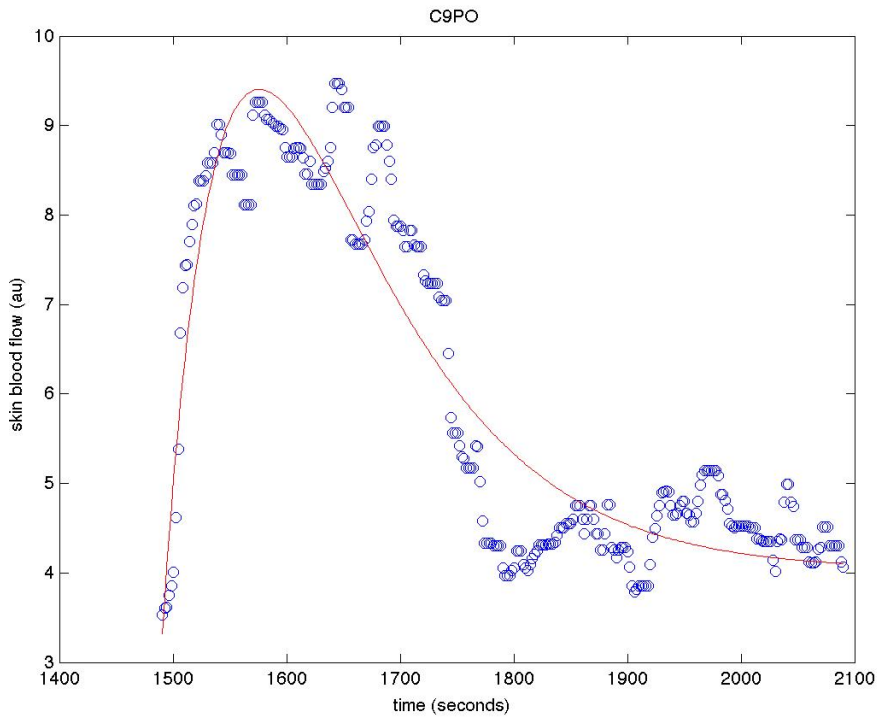
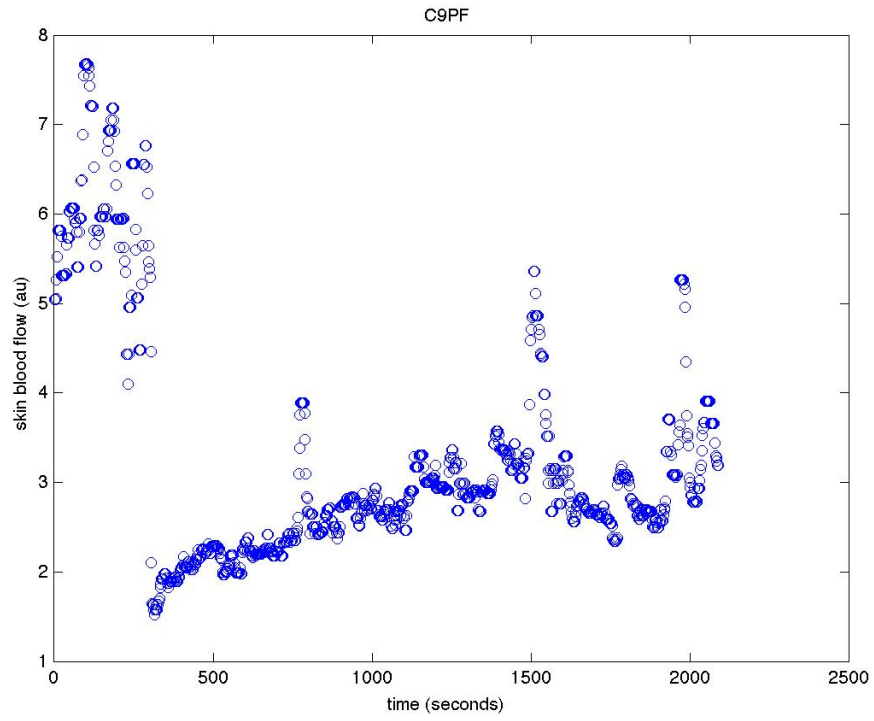


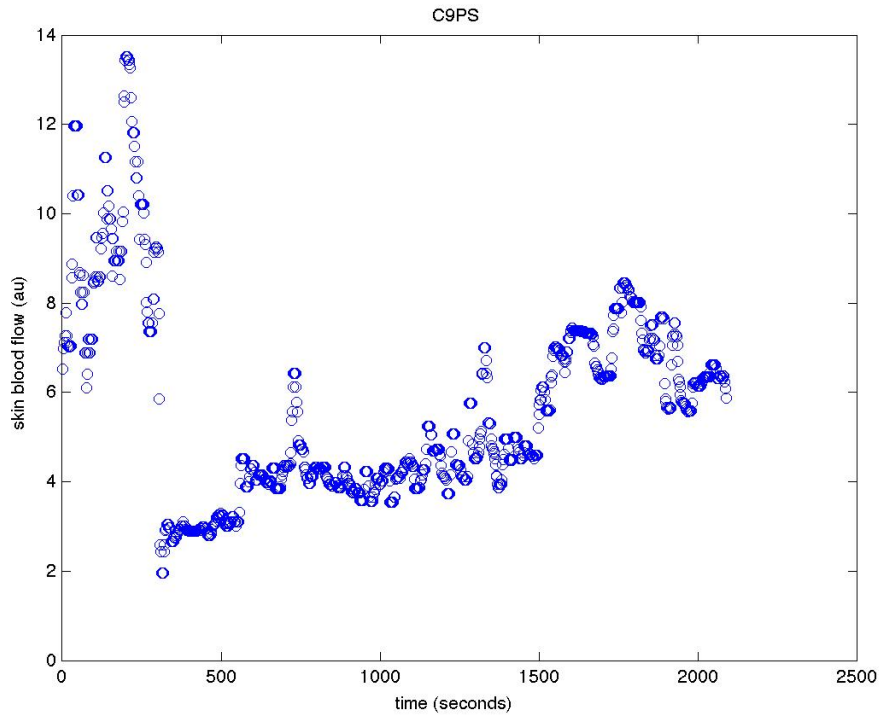
Subject CTRL_07: baseline SBF: PF=5.23, PO= 6.31, PS= 5.40



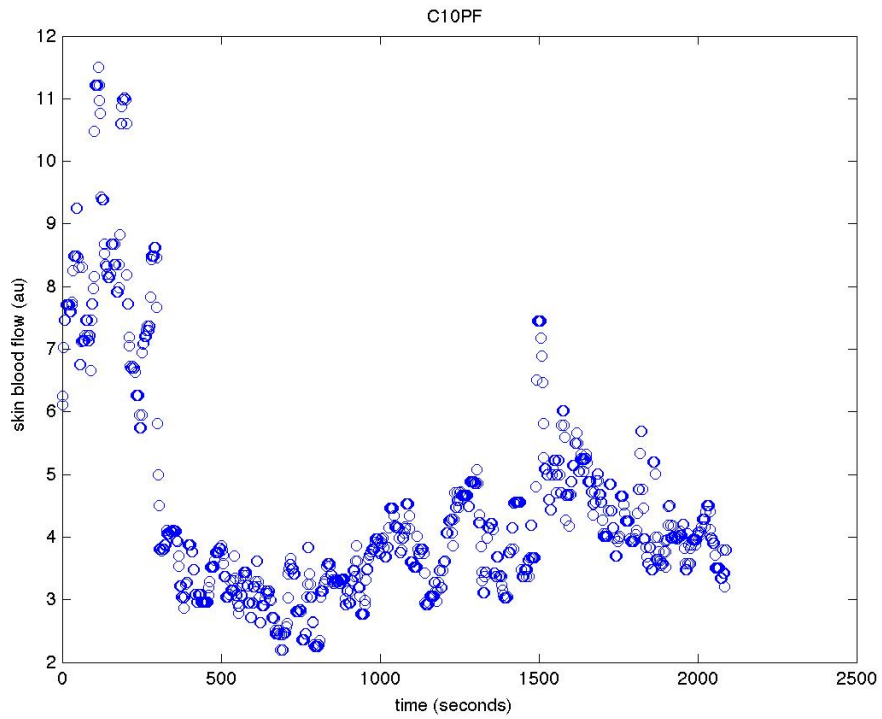


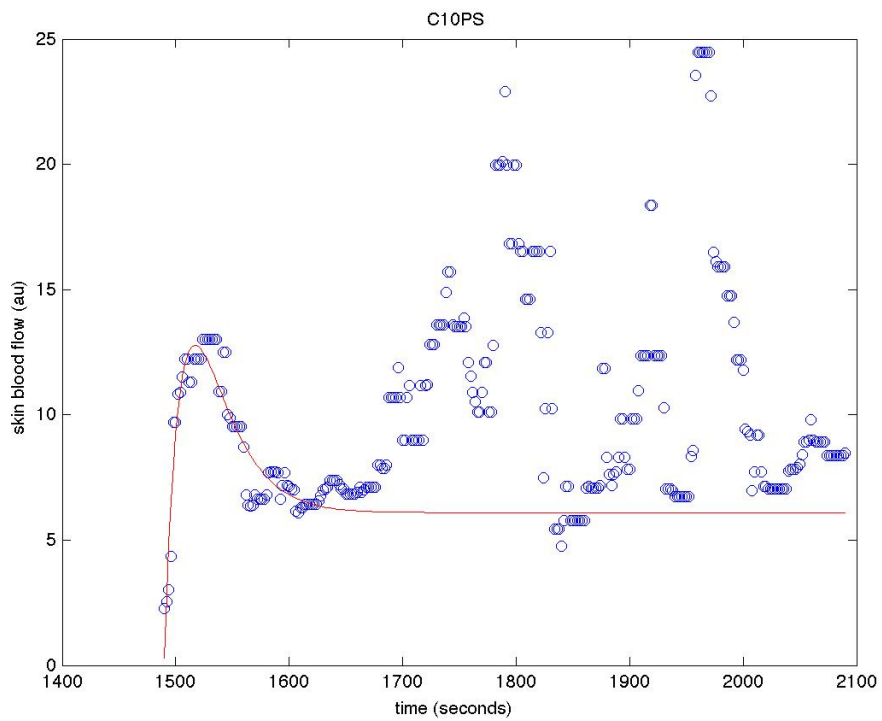
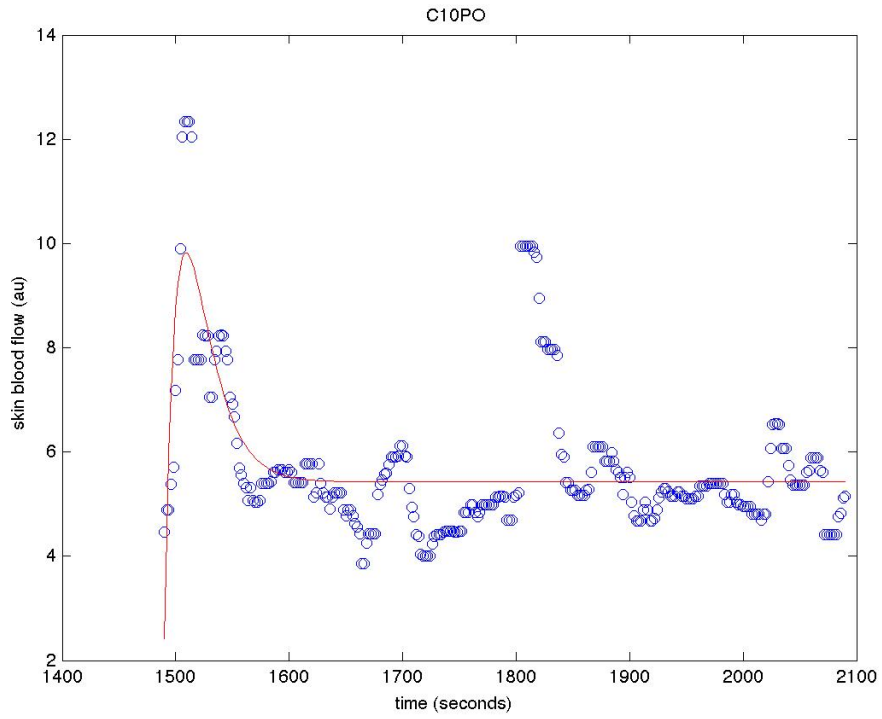
Subject CTRL_09: baseline SBF: PF=5.98, PO= 2.46, PS= 9.33



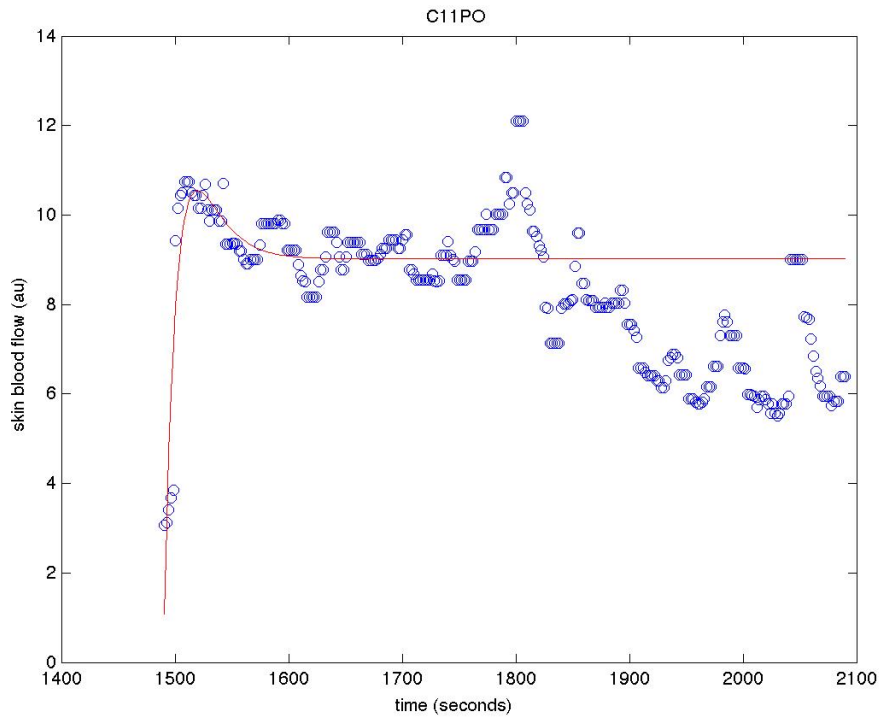
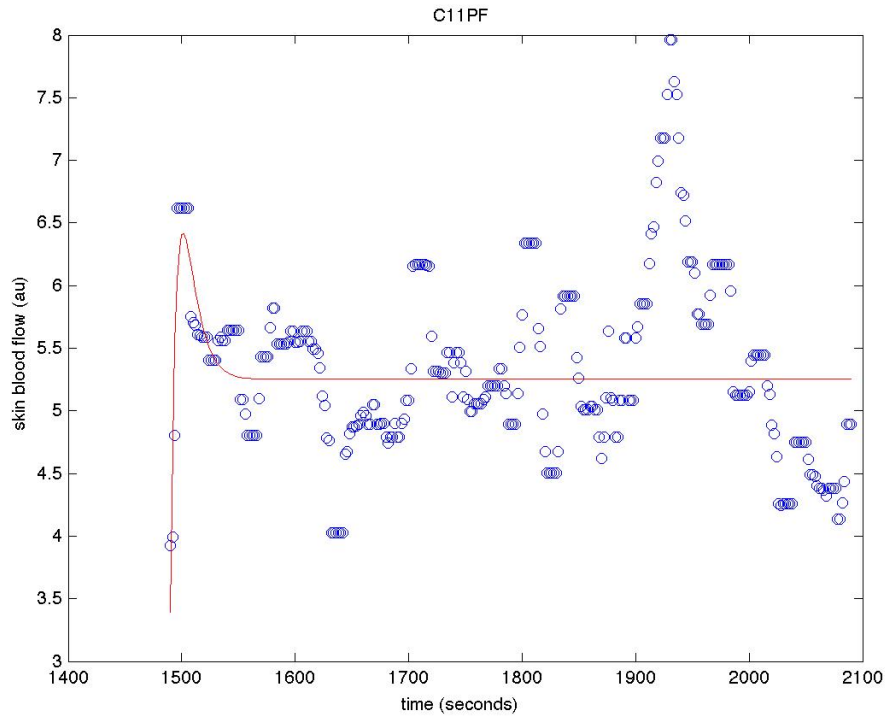


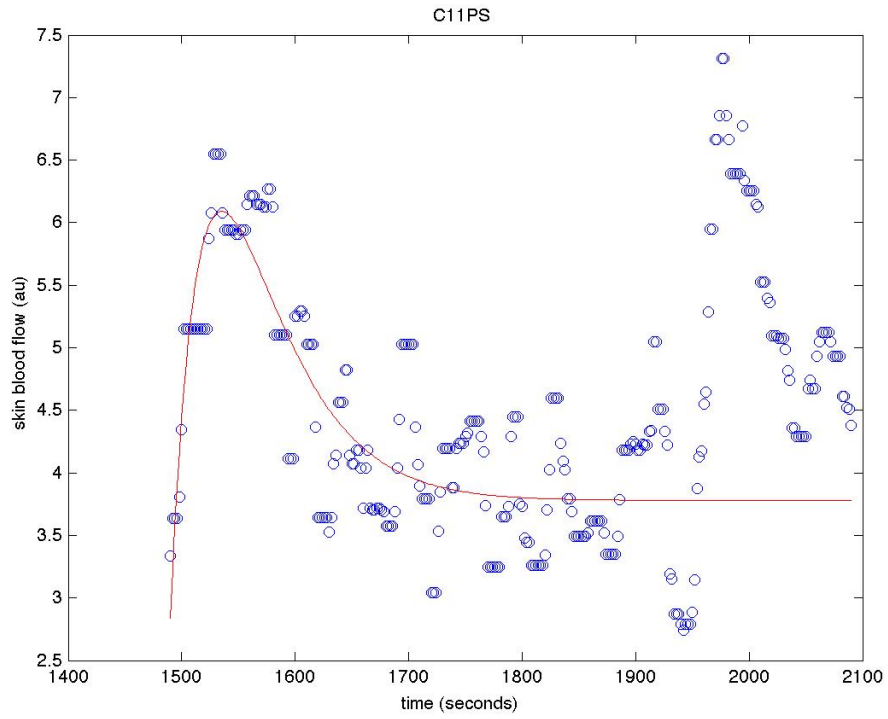
Subject CTRL_10: baseline SBF: PF=8.10, PO= 8.75, PS= 8.25



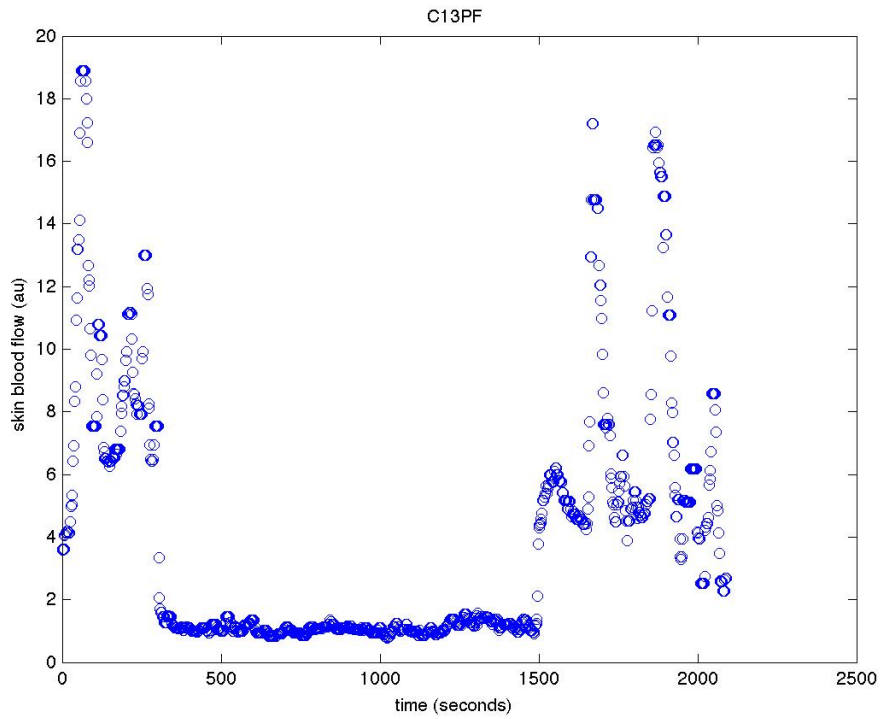


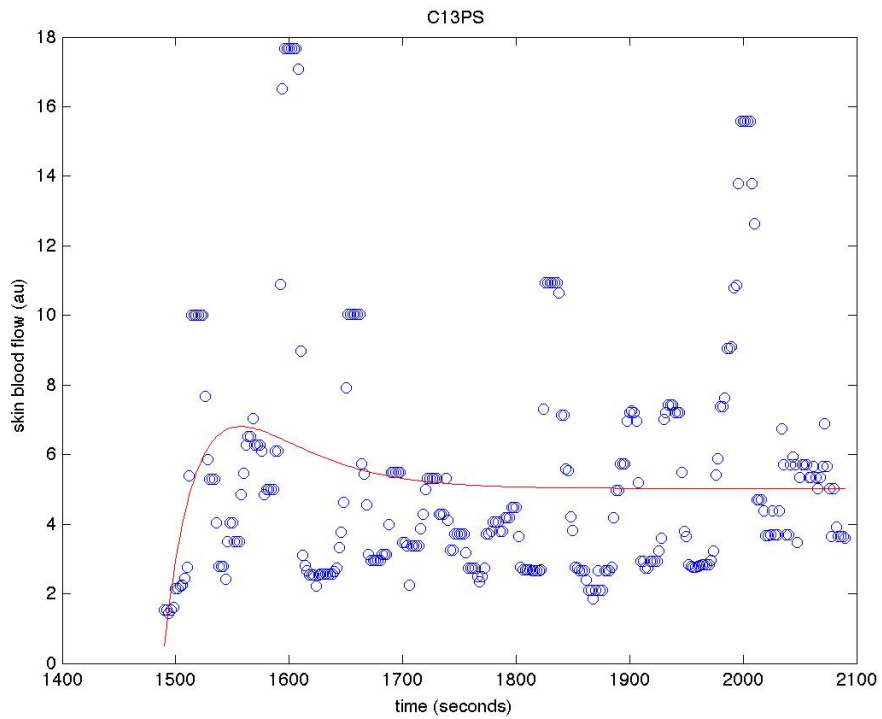
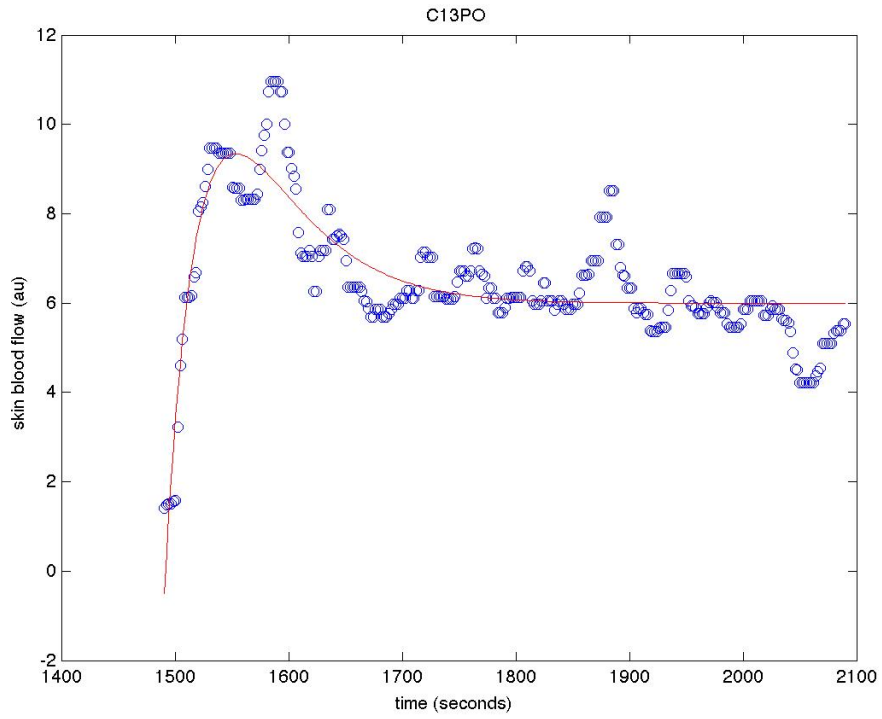
Subject CTRL_11: baseline SBF: PF=5.17, PO= 8.20, PS= 5.83



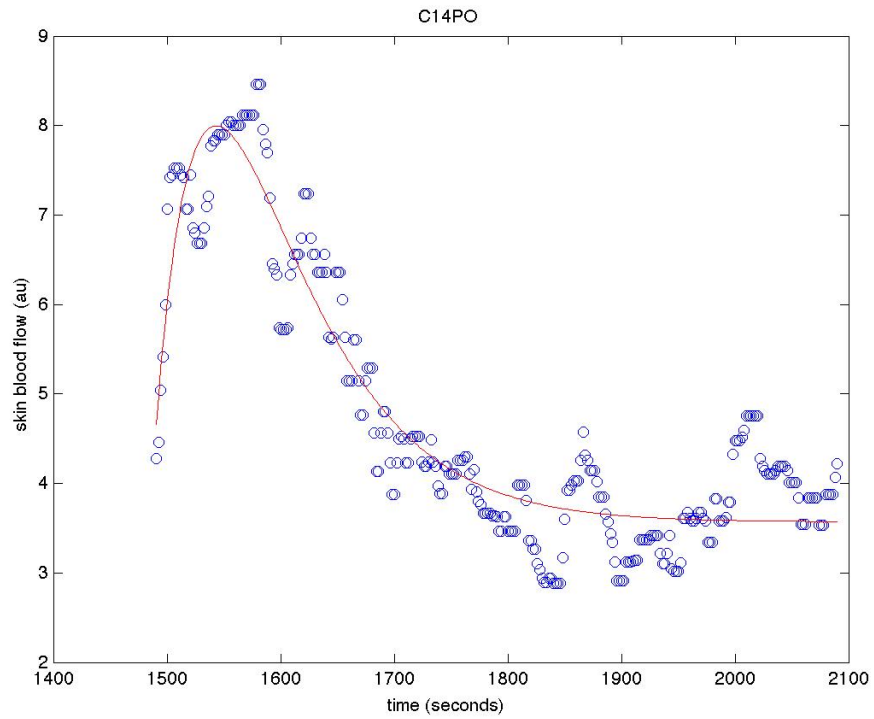
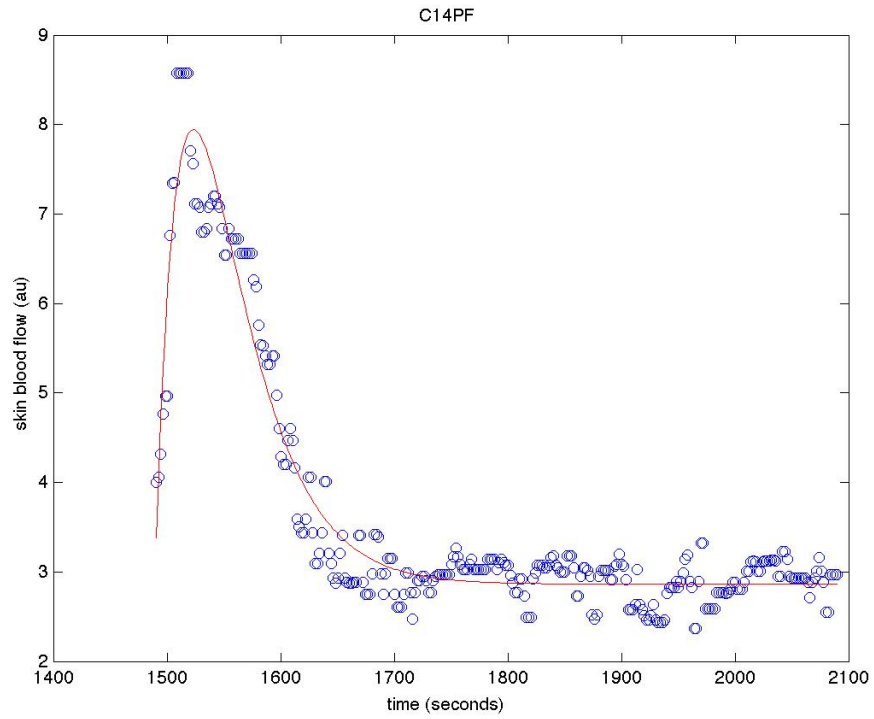


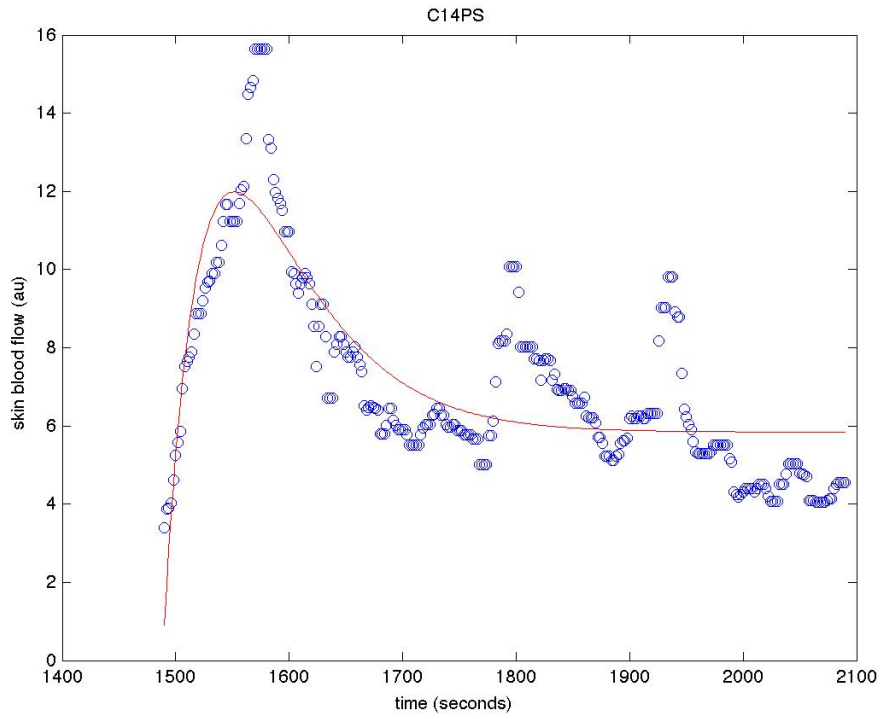
Subject CTRL_13: baseline SBF: PF=8.47, PO= 7.59, PS= 6.11



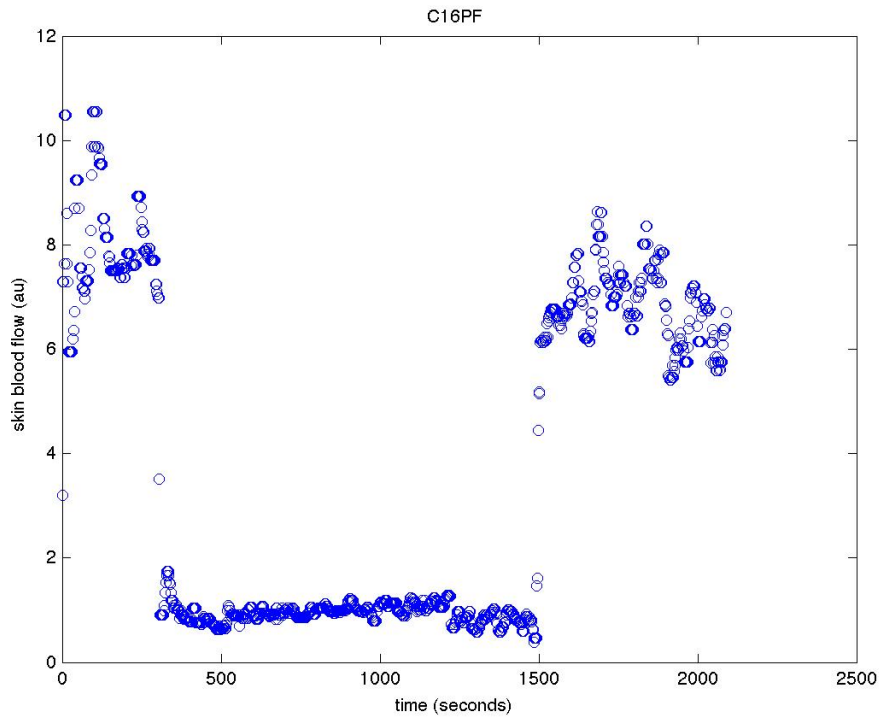


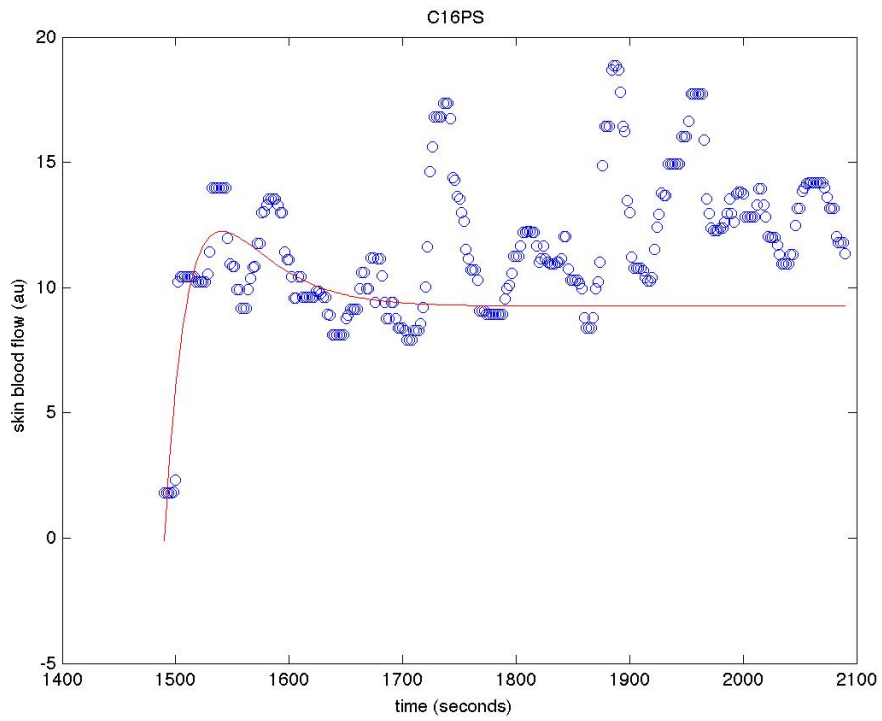
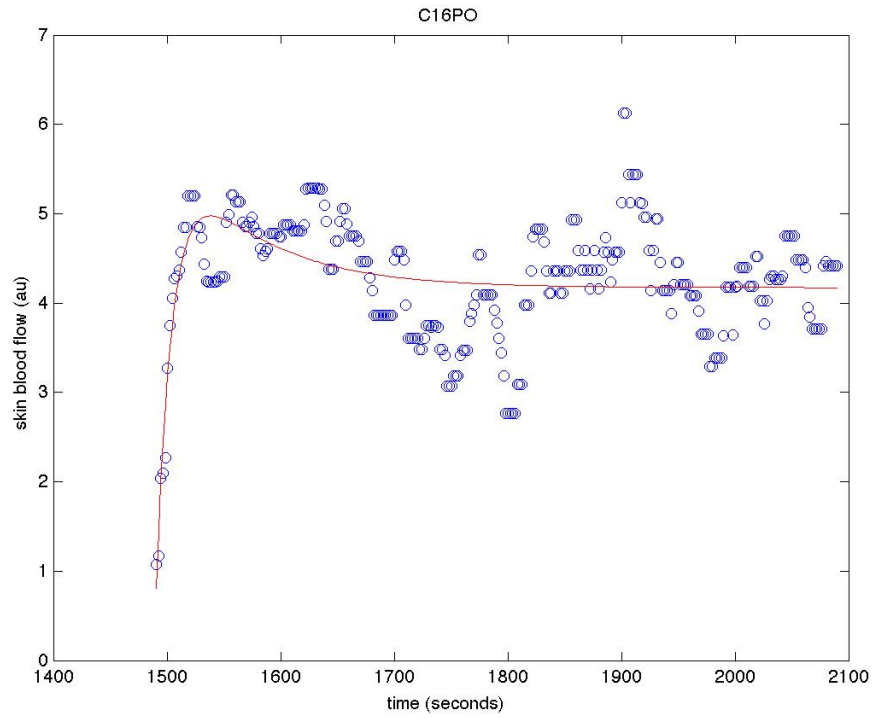
Subject CTRL_14: baseline SBF: PF=3.99, PO= 2.82, PS= 5.55



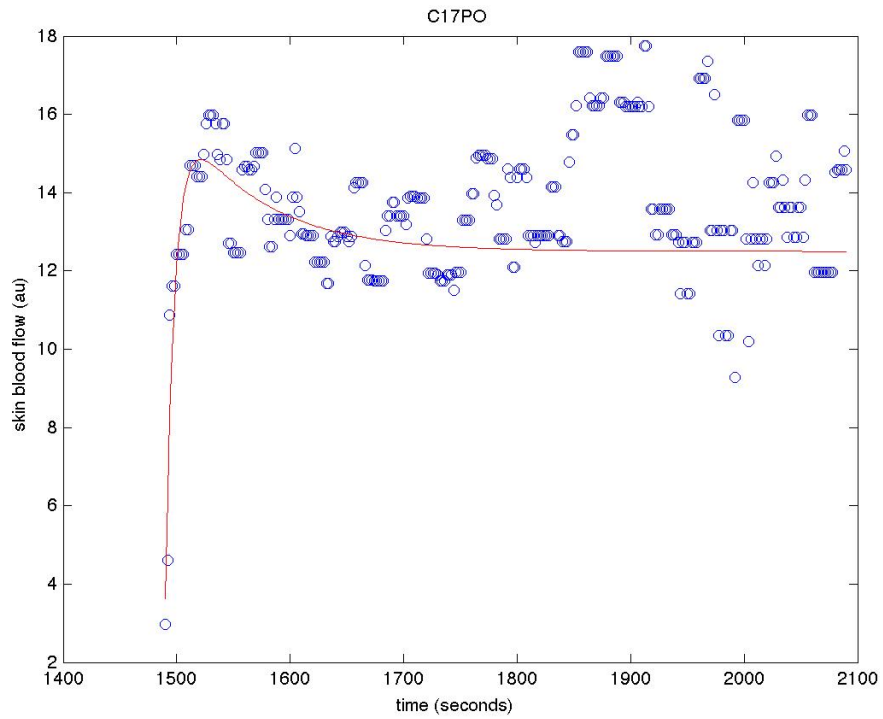
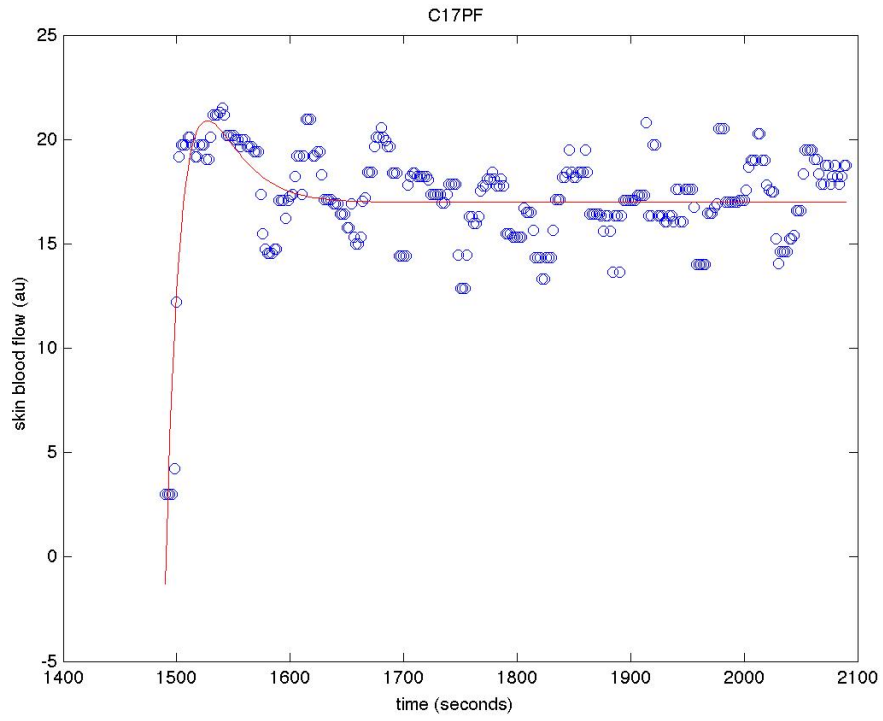


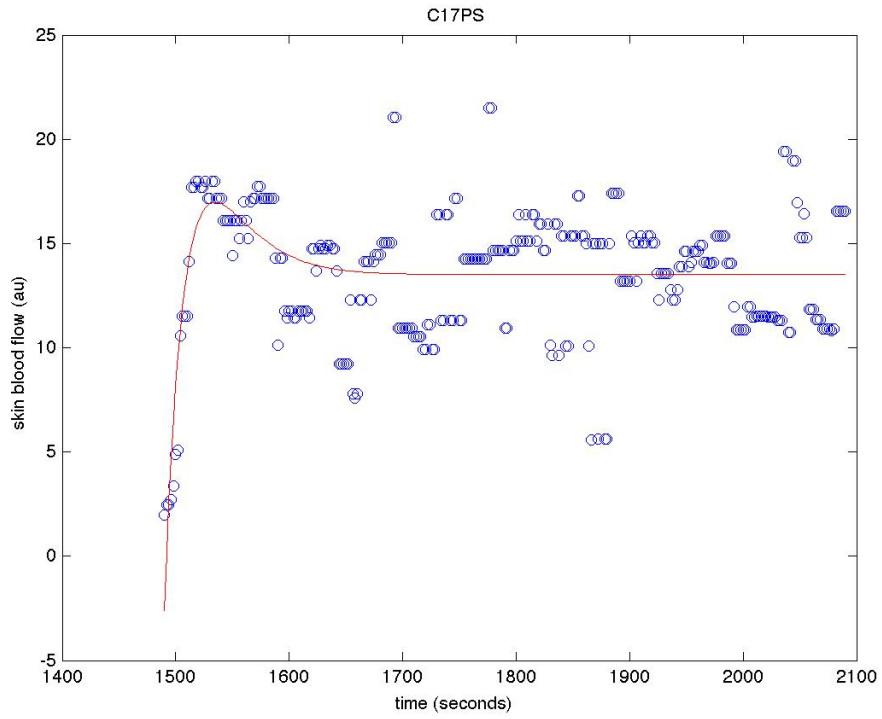
Subject CTRL_16: baseline SBF: PF=8.00, PO= 3.02, PS= 11.11



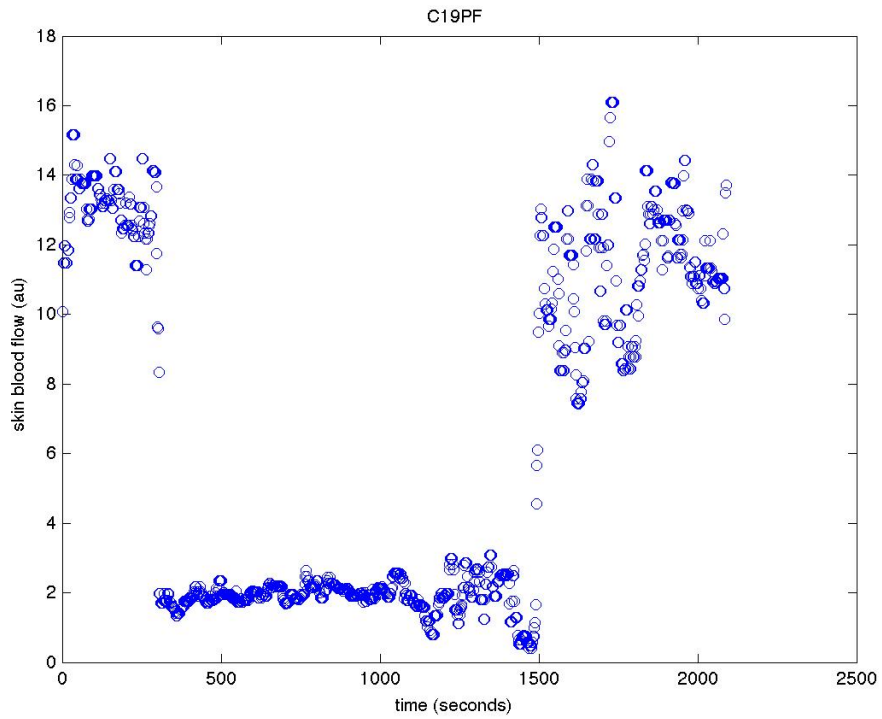


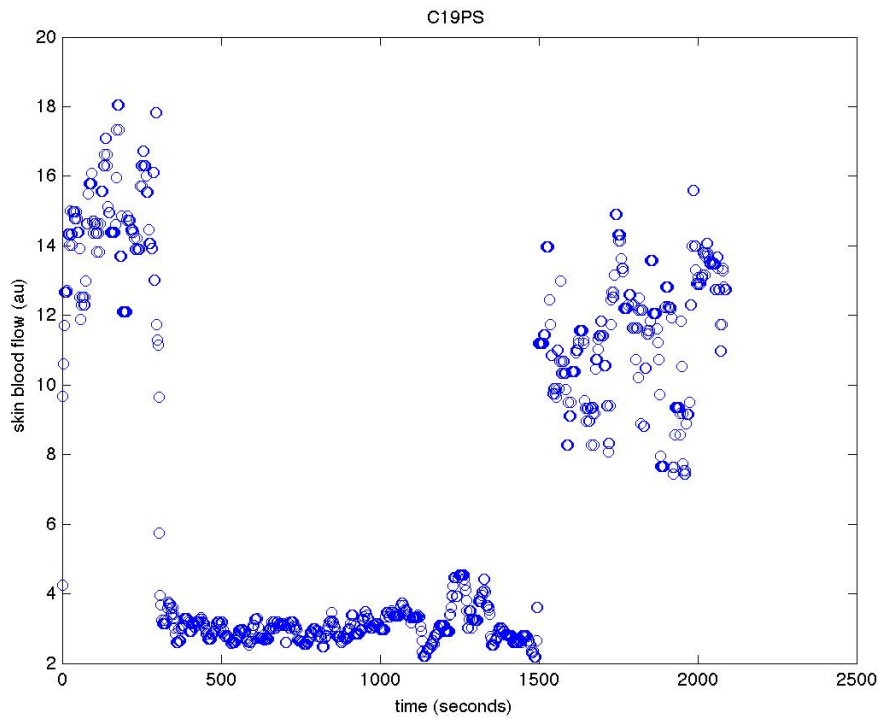
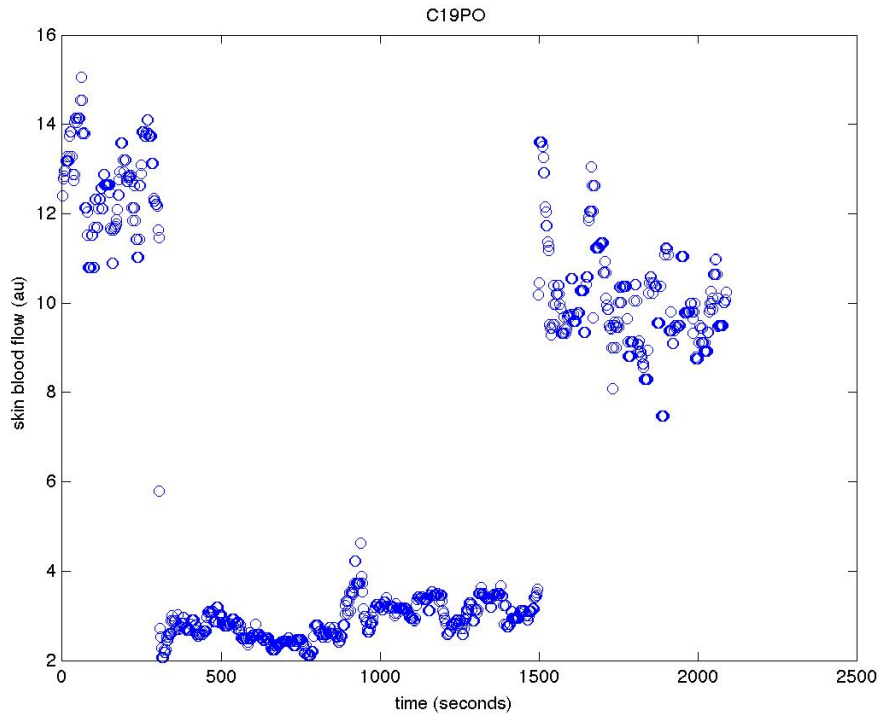
Subject CTRL_17: baseline SBF: PF=14.04, PO= 13.40, PS= 14.66



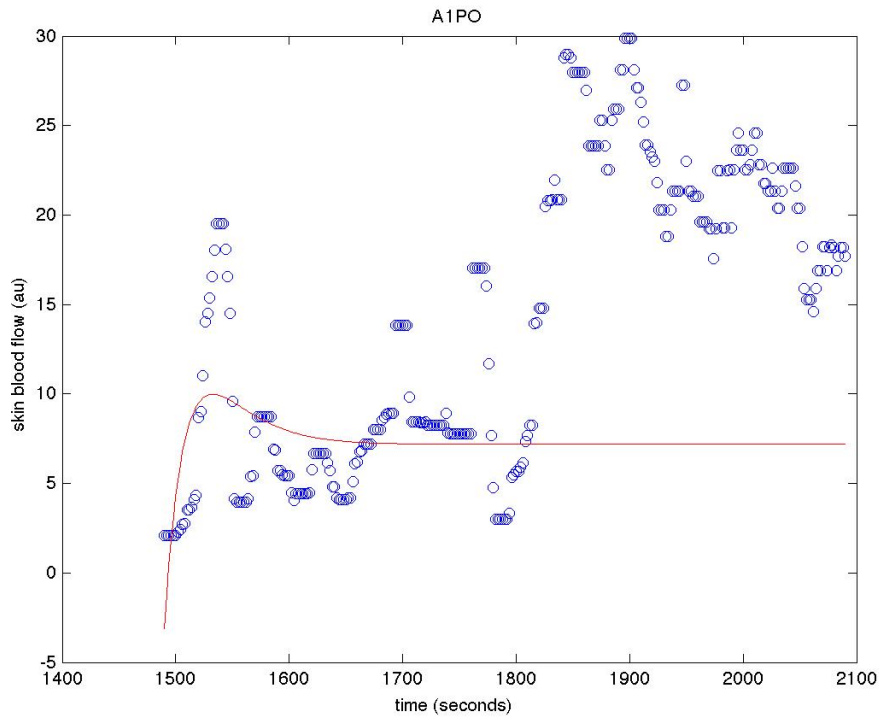
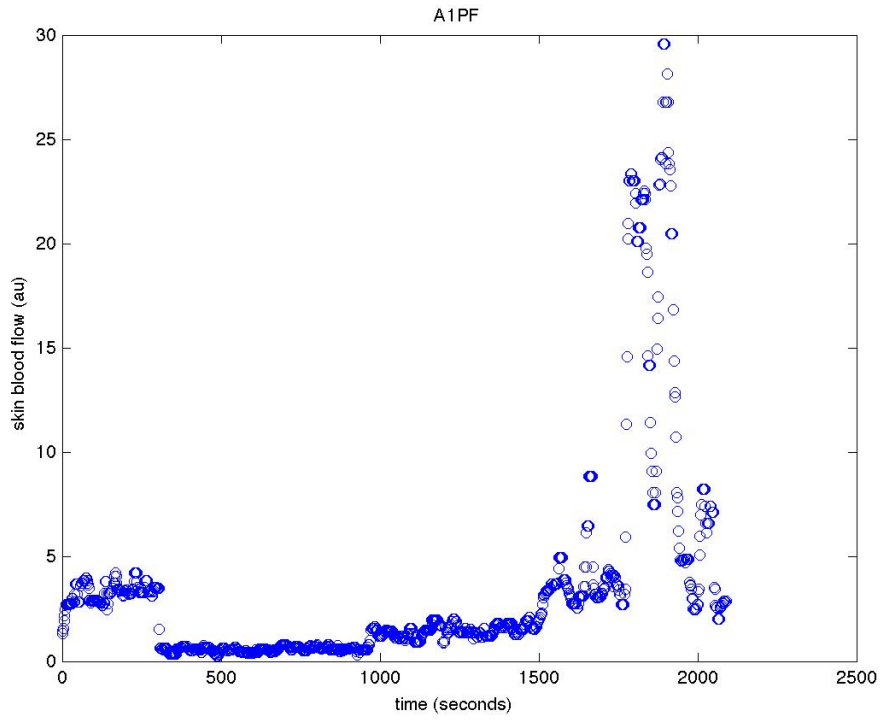


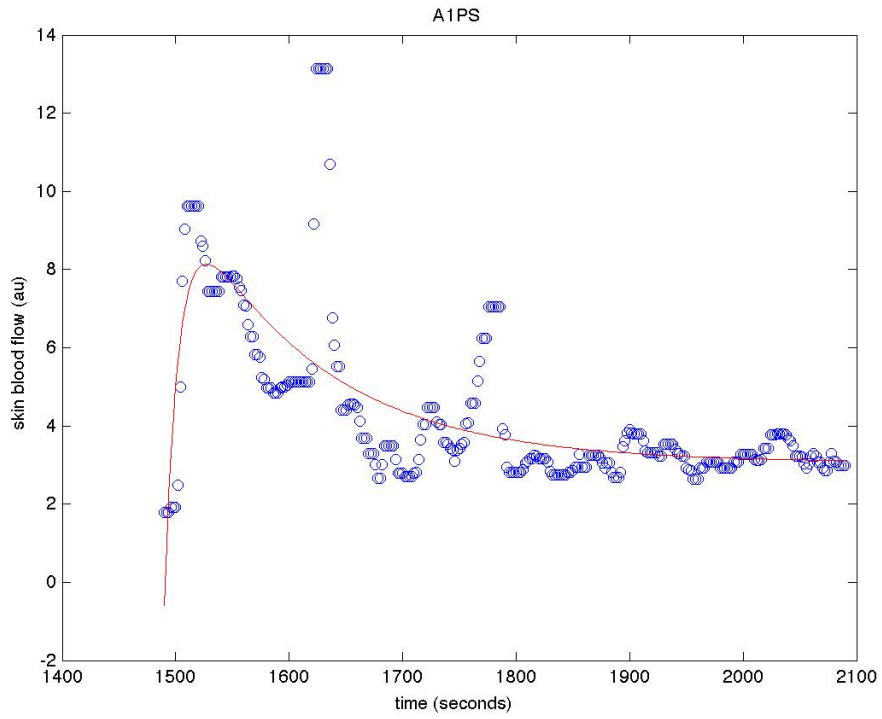
Subject CTRL_19: baseline SBF: PF=13.13, PO= 12.65, PS= 14.46



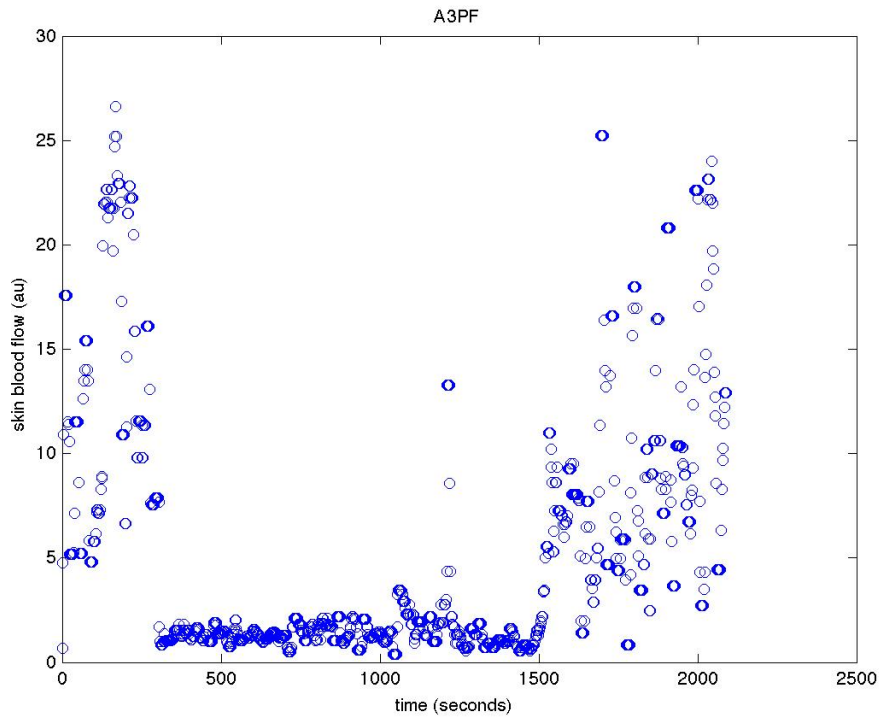


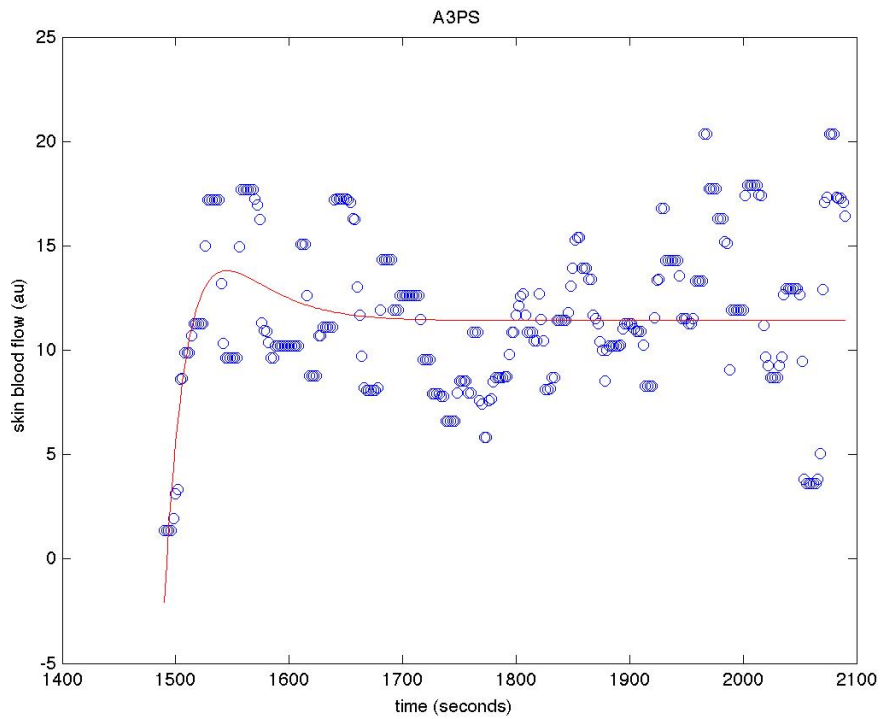
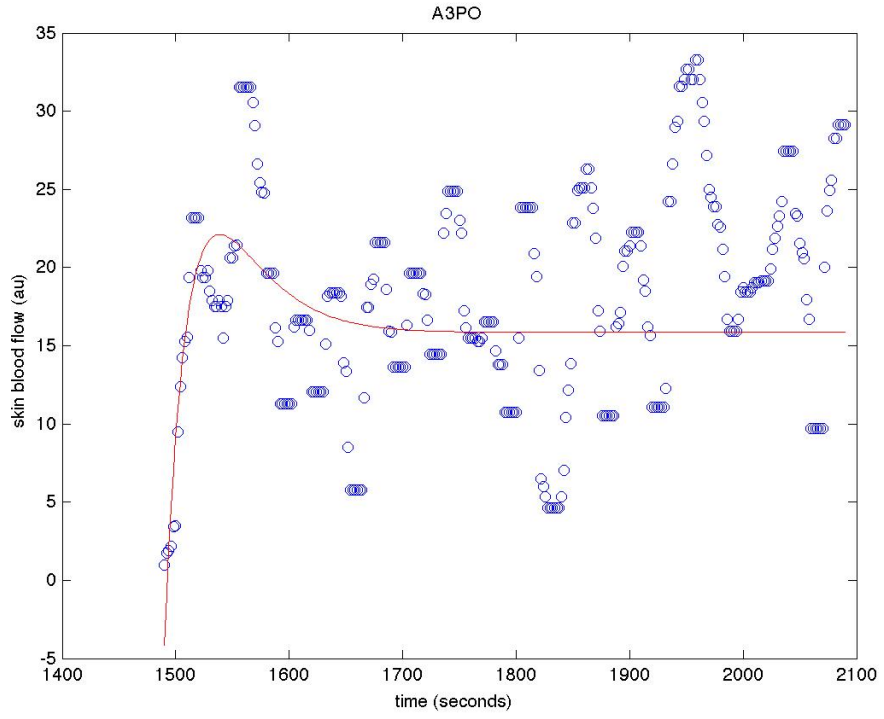
Subject T6A_01: baseline SBF: PF=3.25, PO= 7.79, PS= 3.97



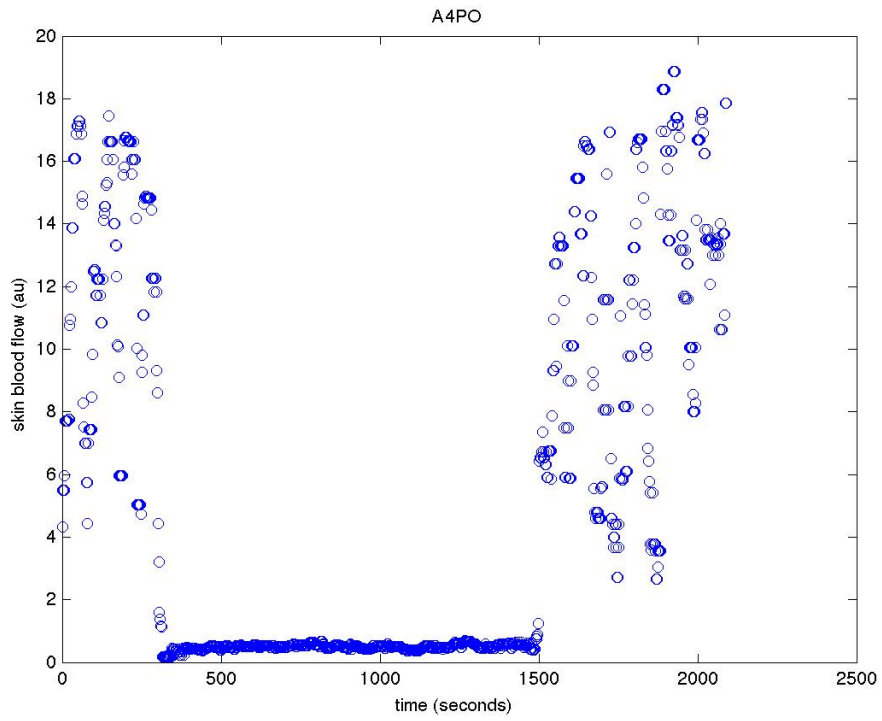
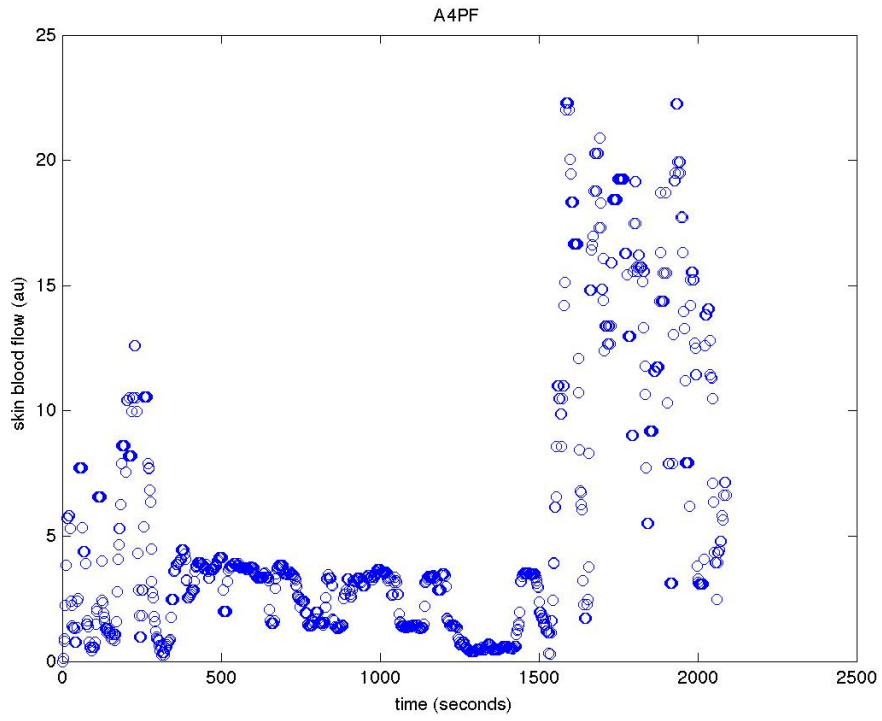


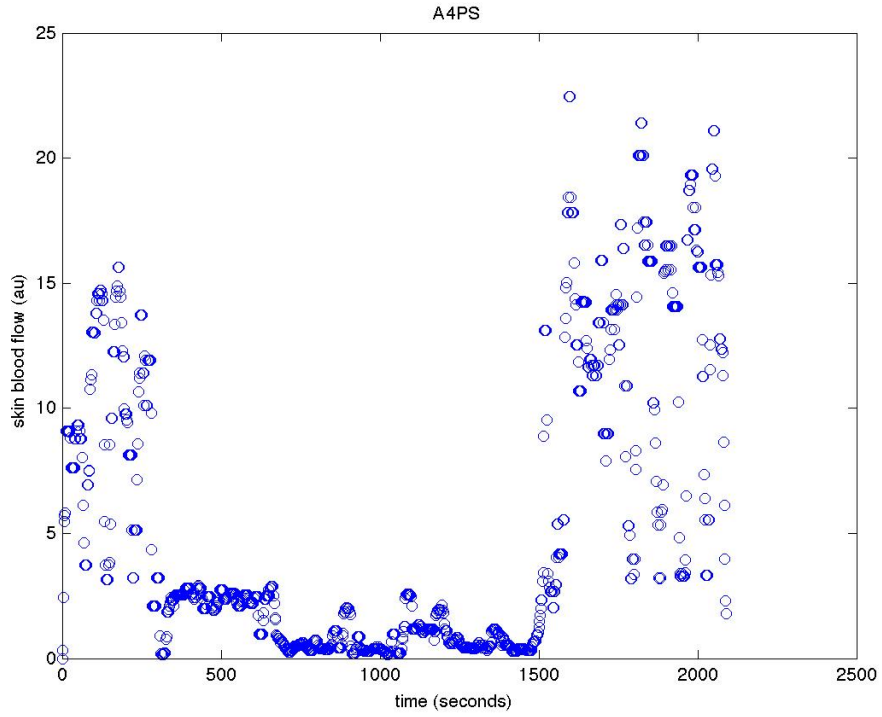
Subject T6A_03: baseline SBF: PF=13.22, PO= 13.39, PS= 9.54



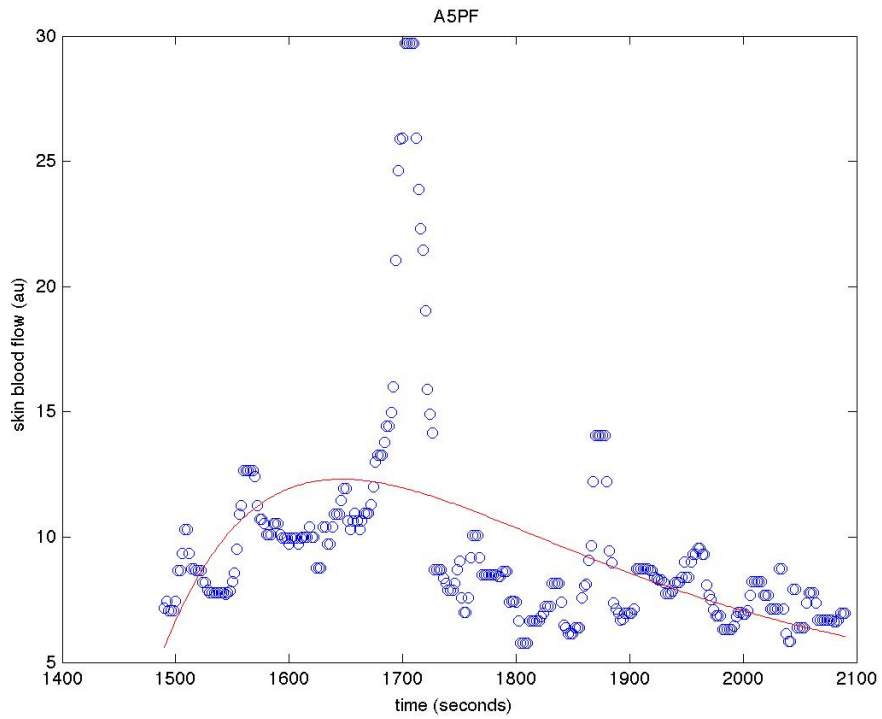


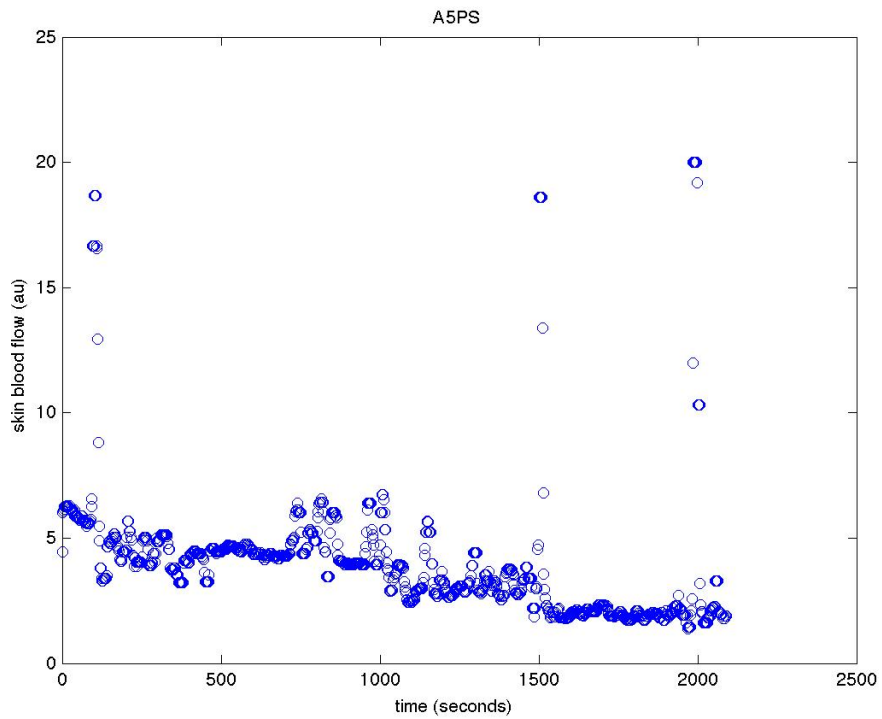
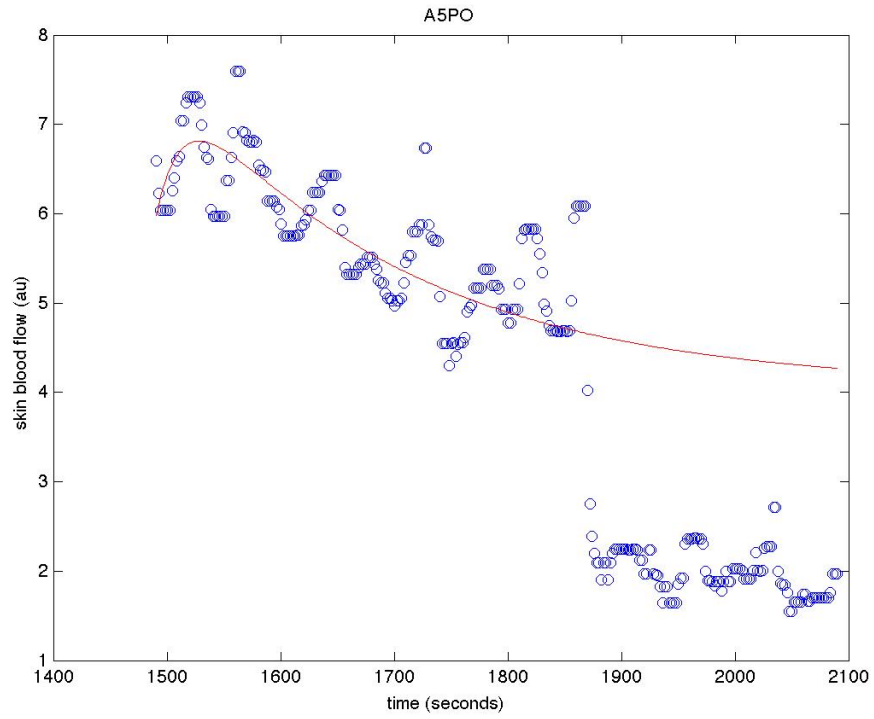
Subject T6A_04: baseline SBF: PF=4.38, PO= 12.15, PS= 9.13



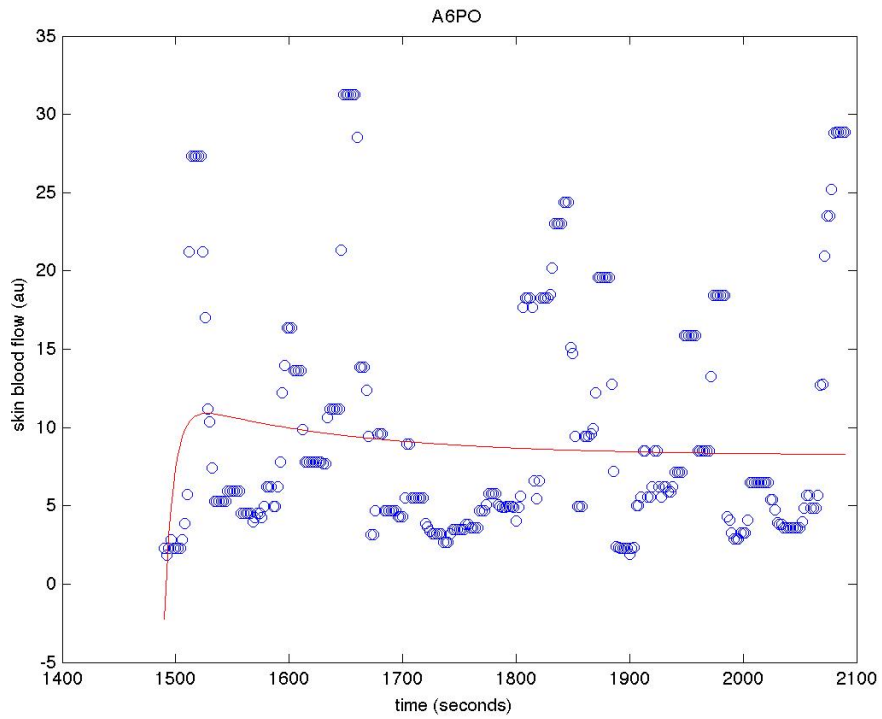
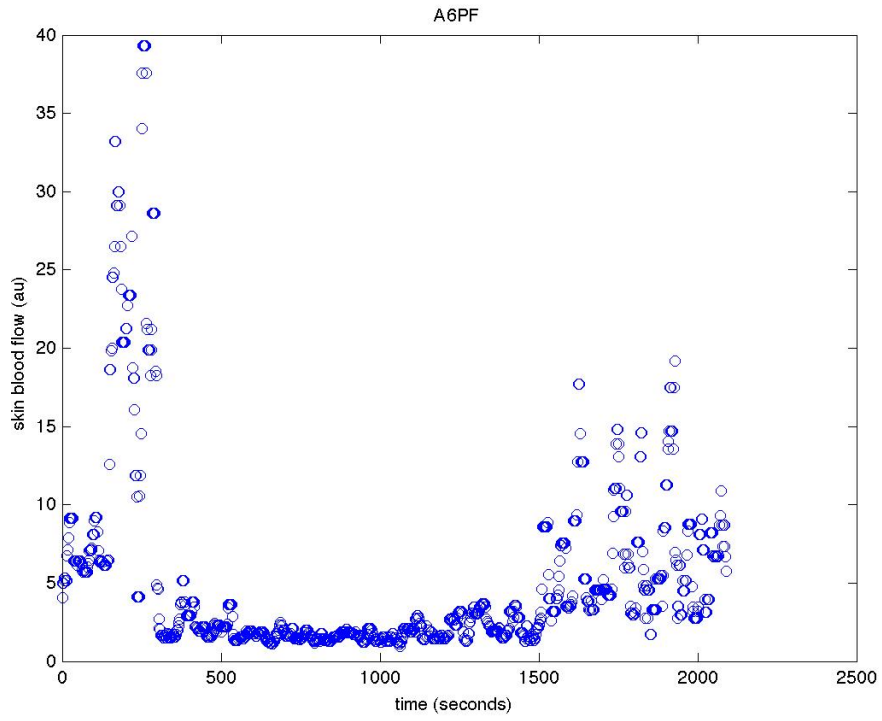


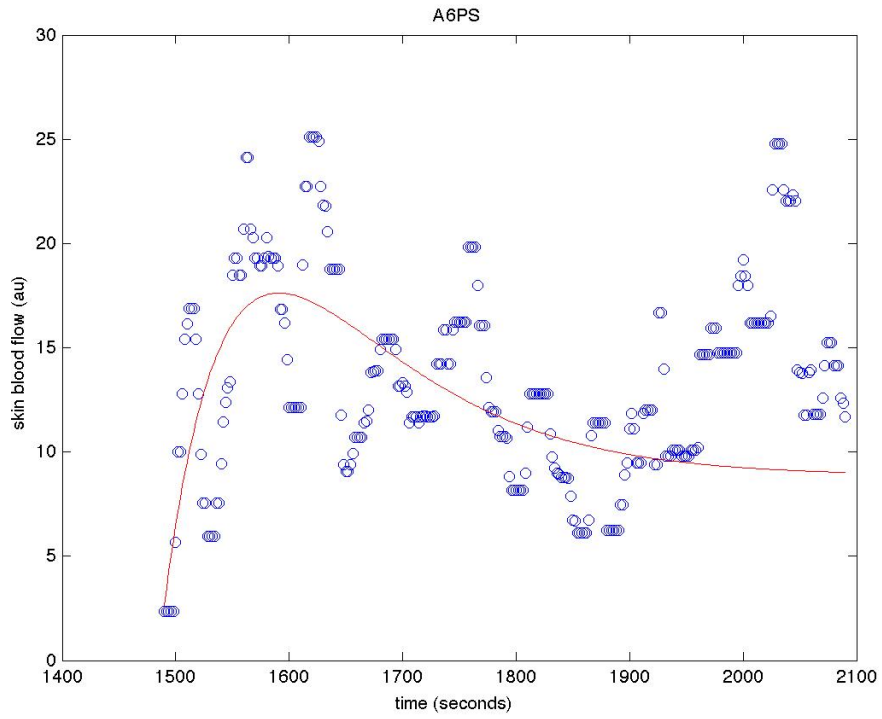
Subject T6A_05: baseline SBF: PF=8.75, PO= 3.54, PS= 5.69



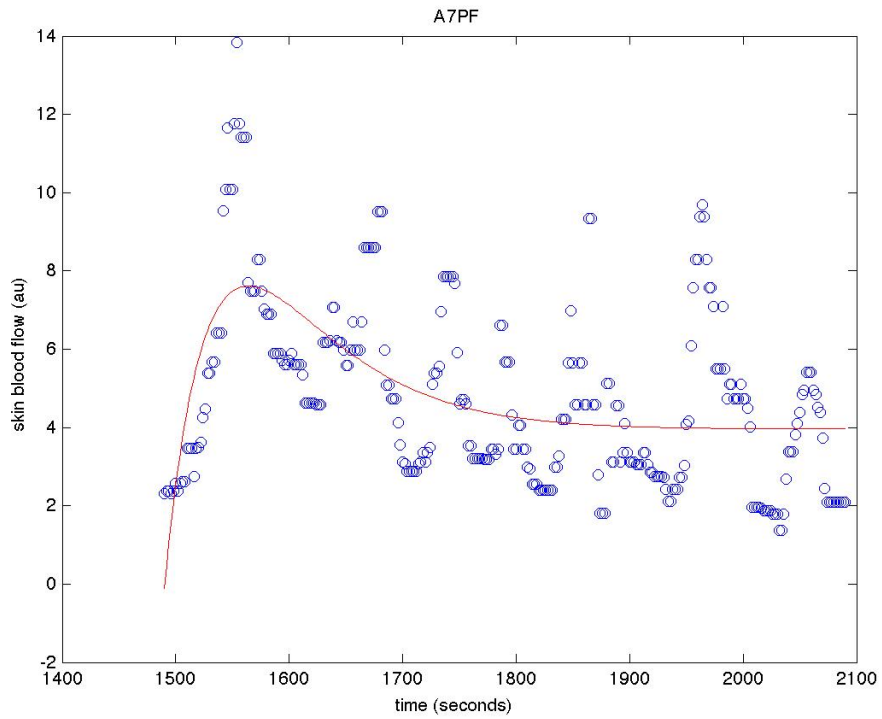


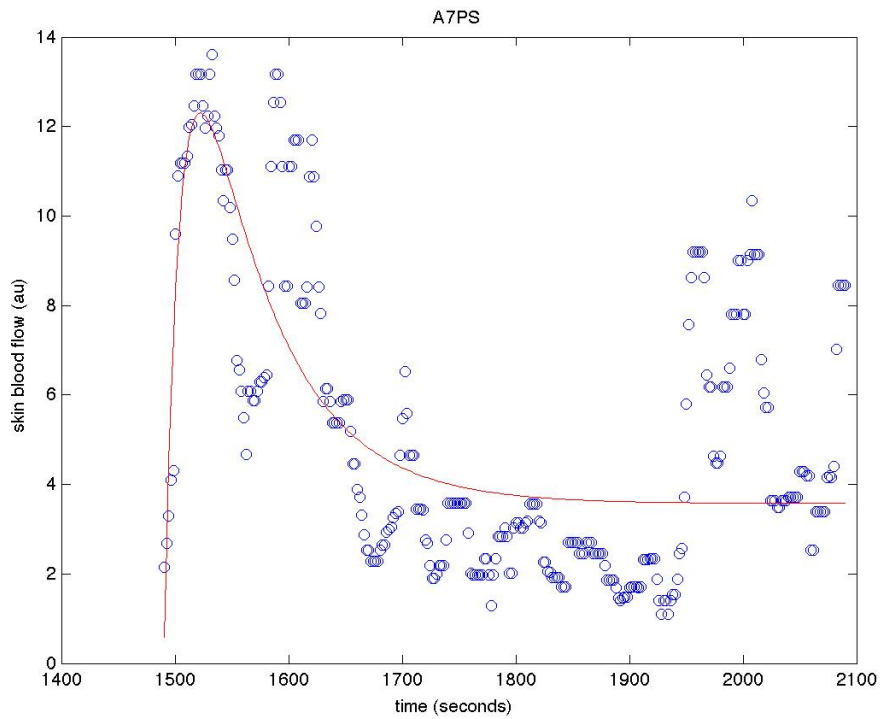
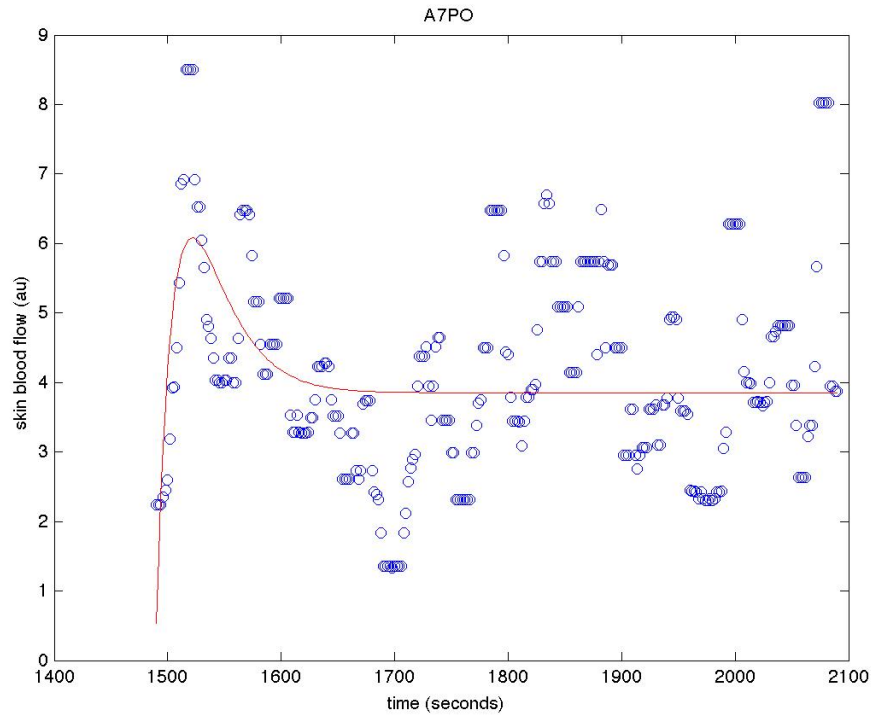
Subject T6A_06: baseline SBF: PF=6.77, PO= 2.75, PS= 3.37



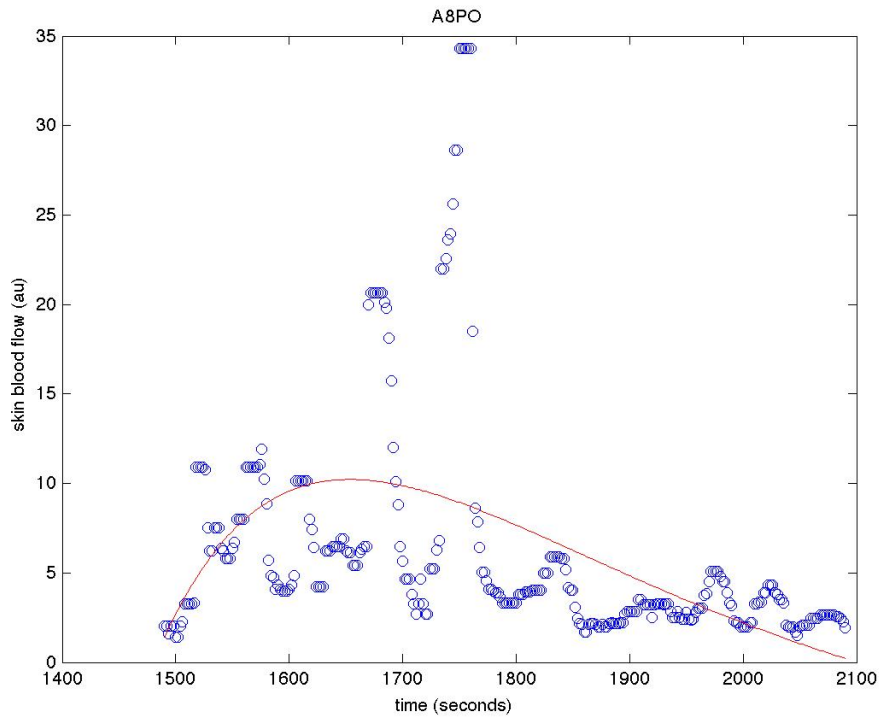
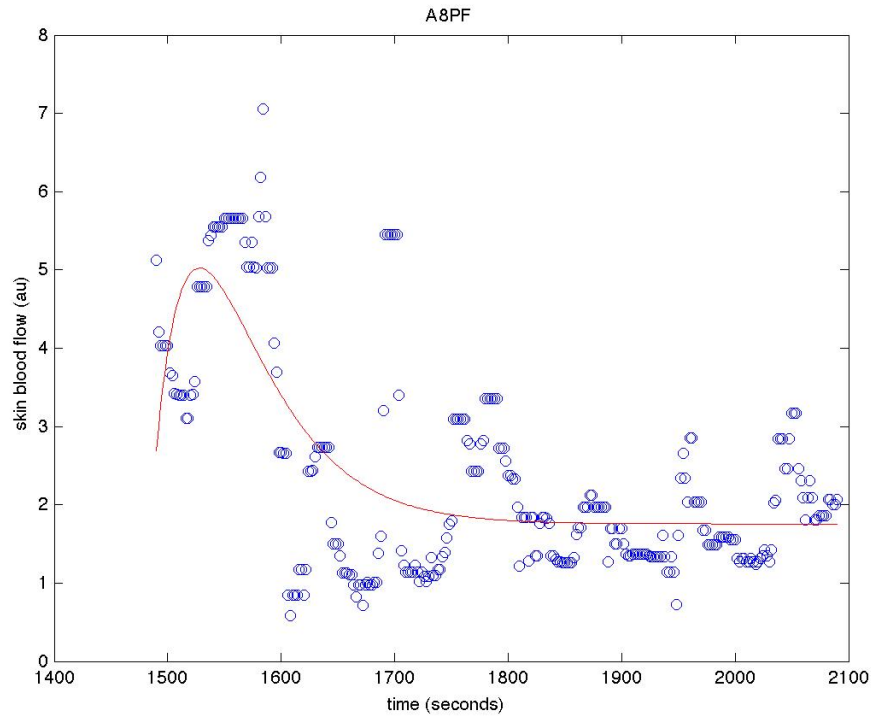


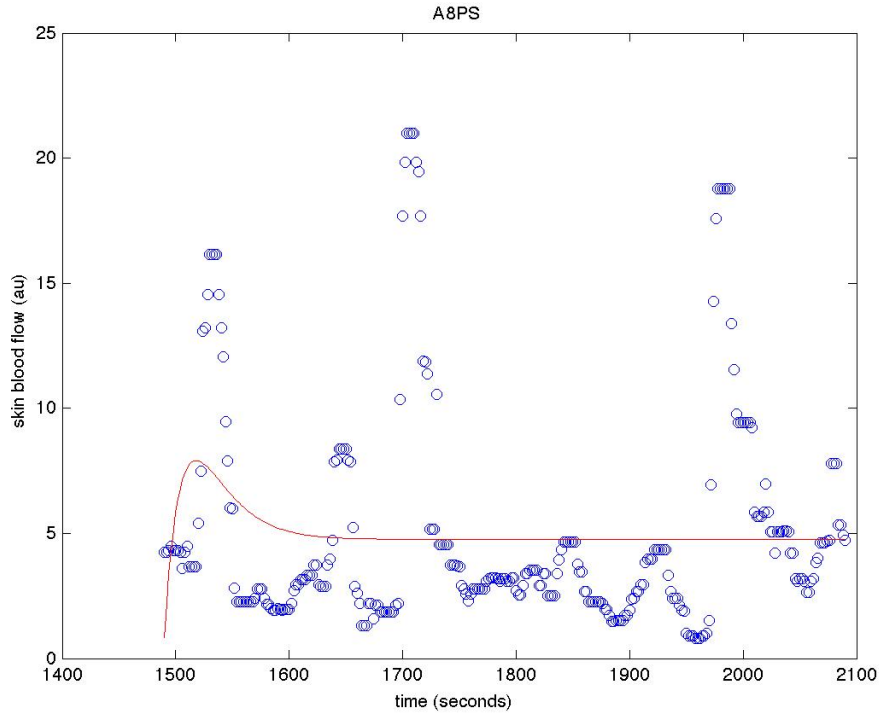
Subject T6A_07: baseline SBF: PF=3.45, PO= 3.82, PS= 3.00



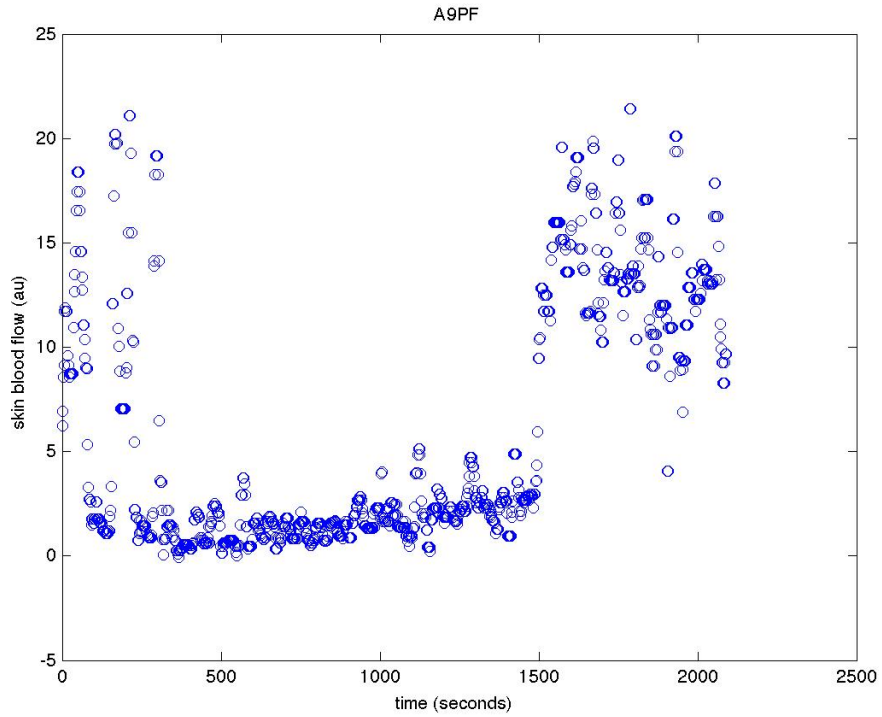


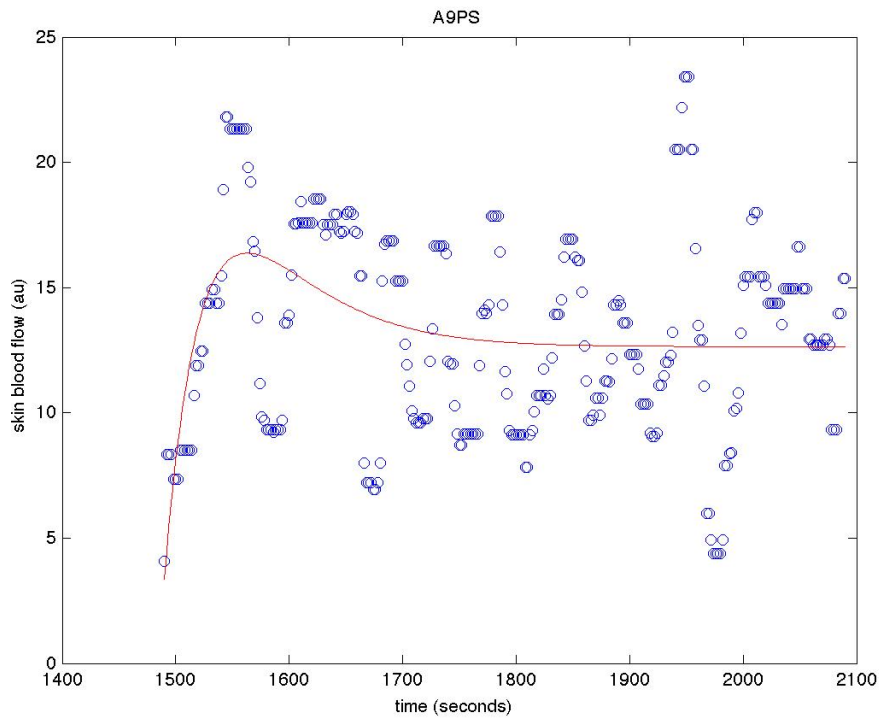
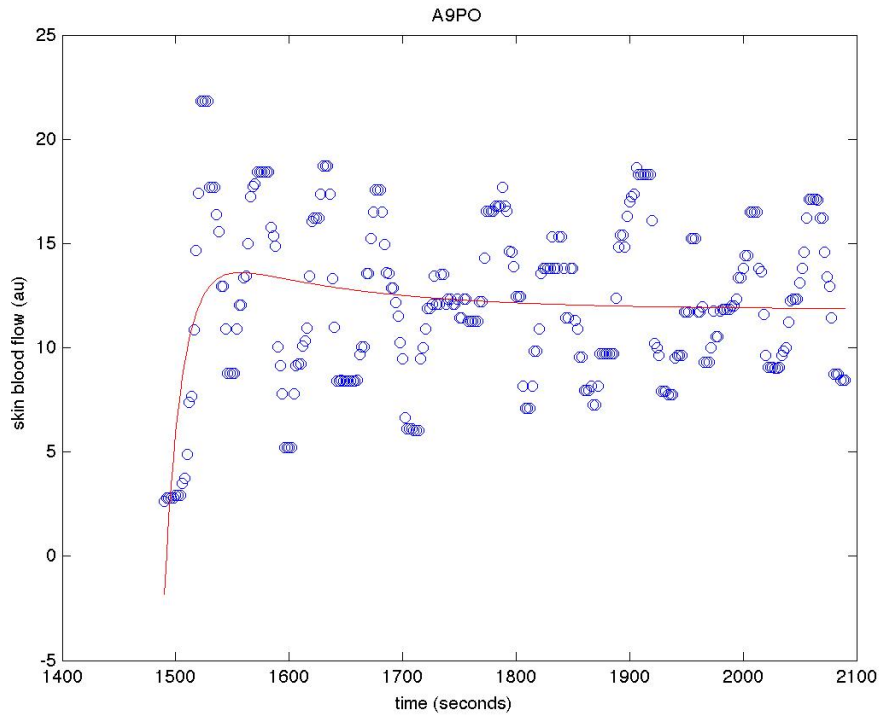
Subject T6A_08: baseline SBF: PF=2.77, PO= 2.82, PS= 2.98



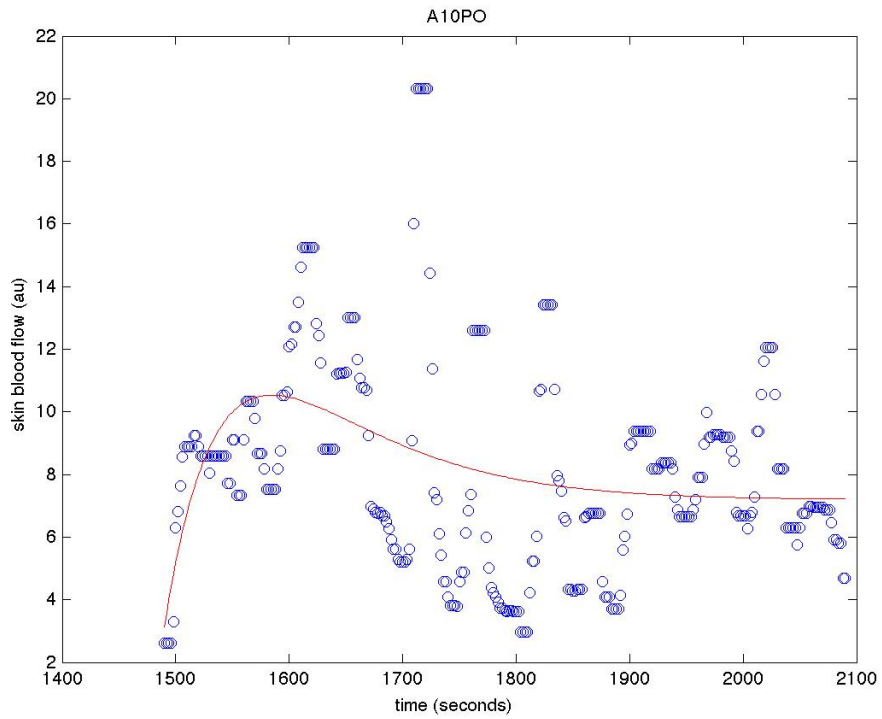
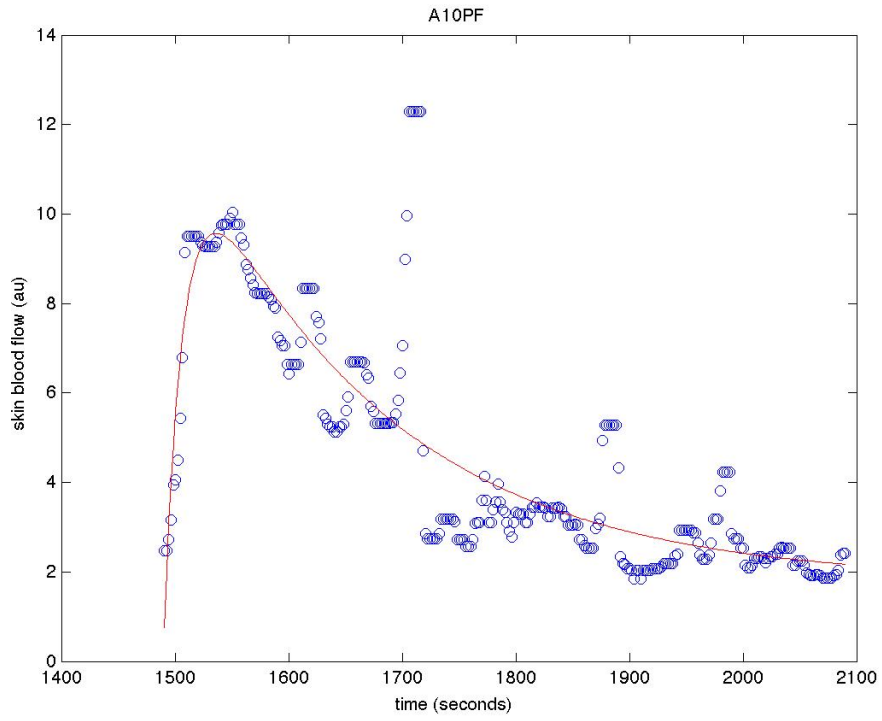


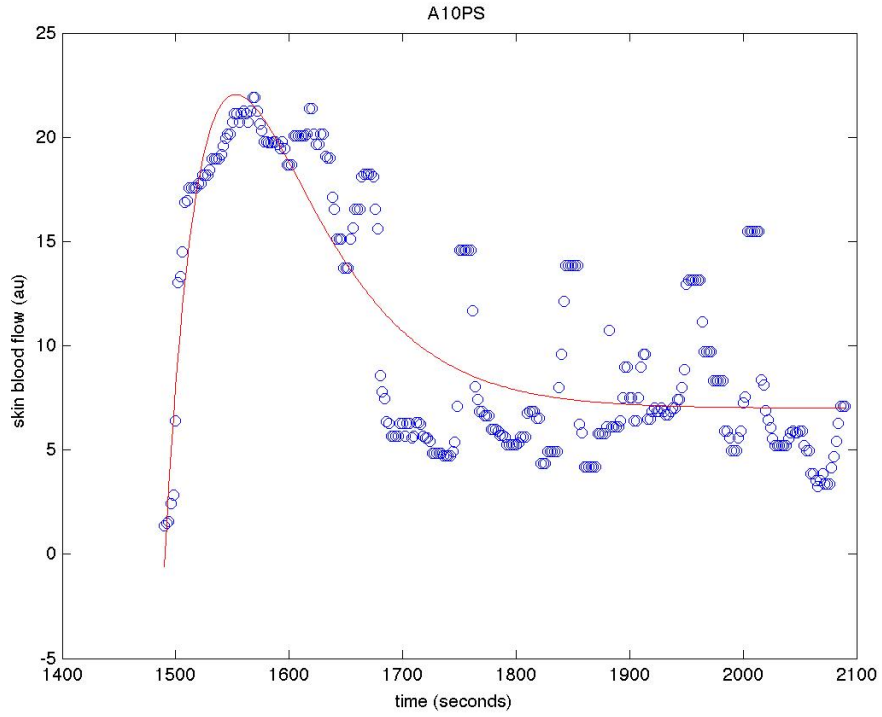
Subject T6A_09: baseline SBF: PF=7.68, PO= 8.15, PS= 10.00



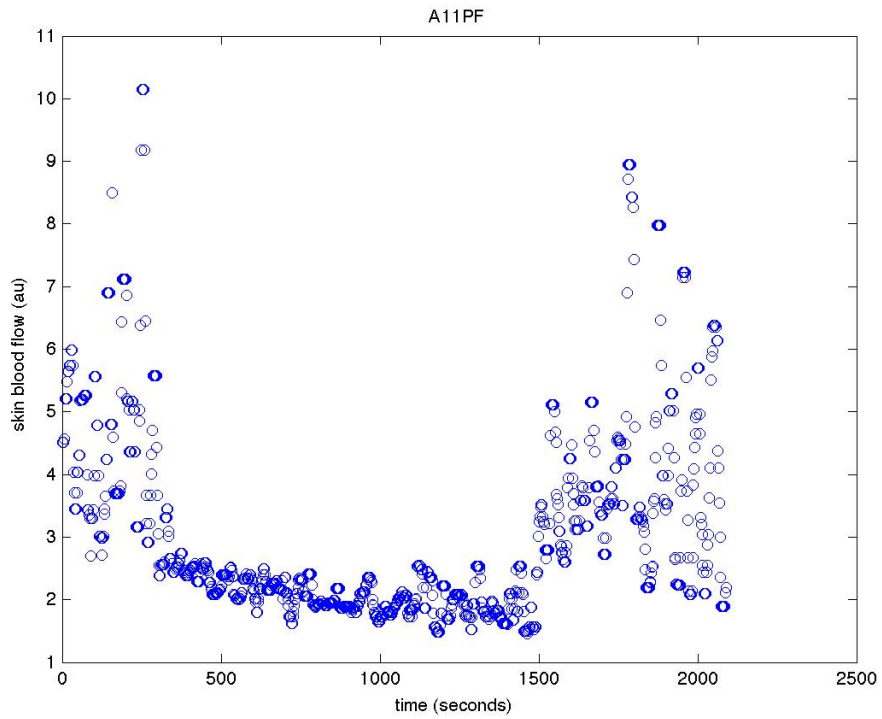


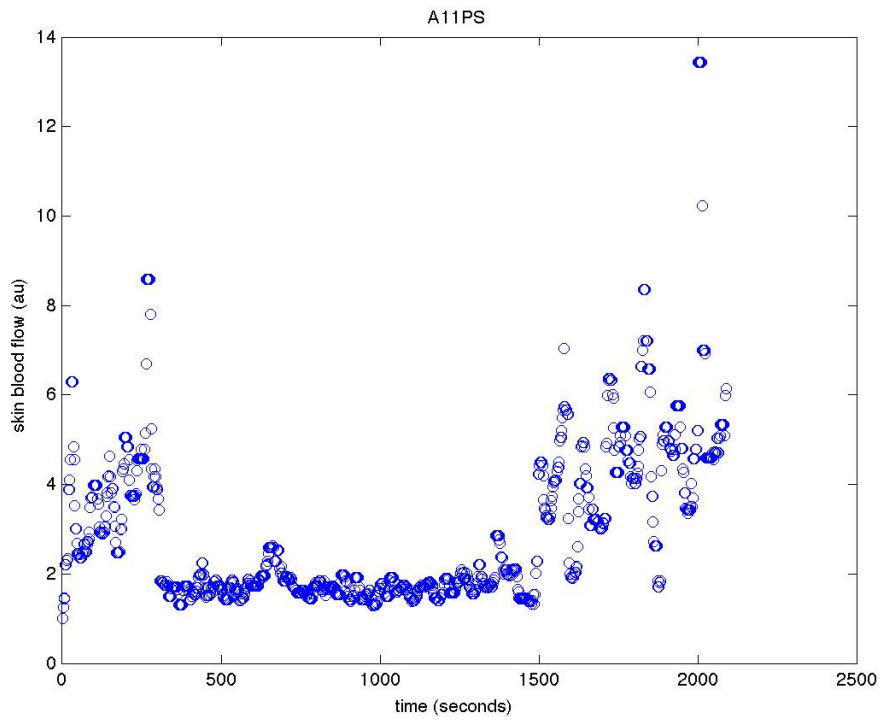
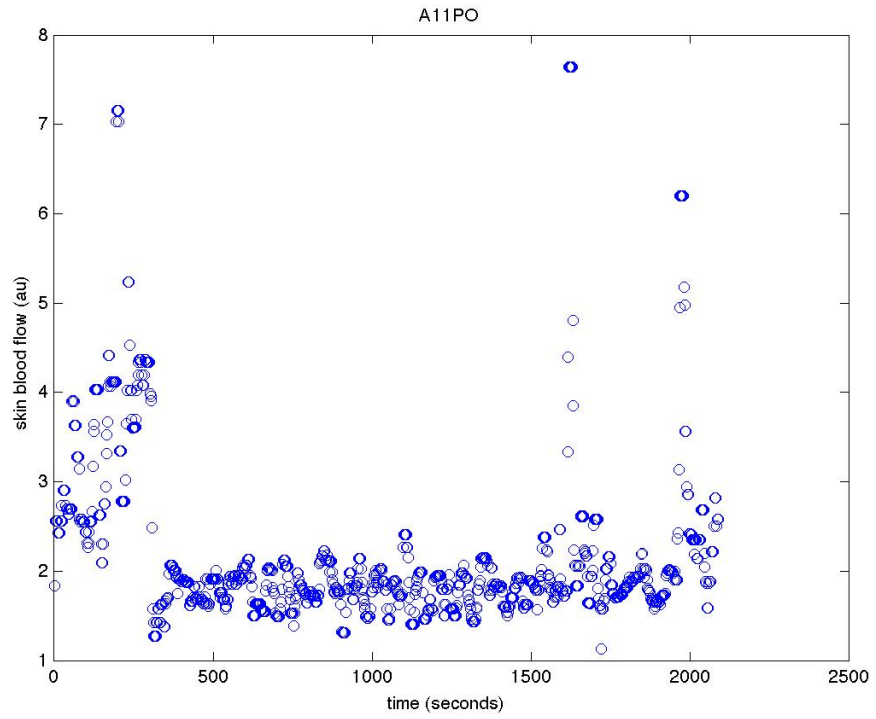
Subject T6A_10: baseline SBF: PF=4.00, PO= 4.55, PS= 5.49



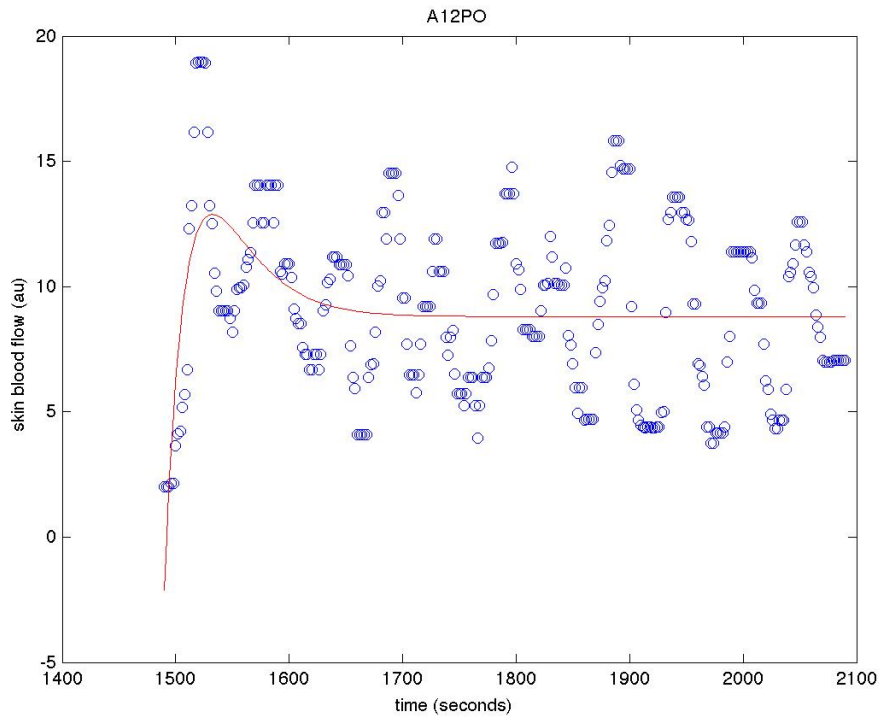
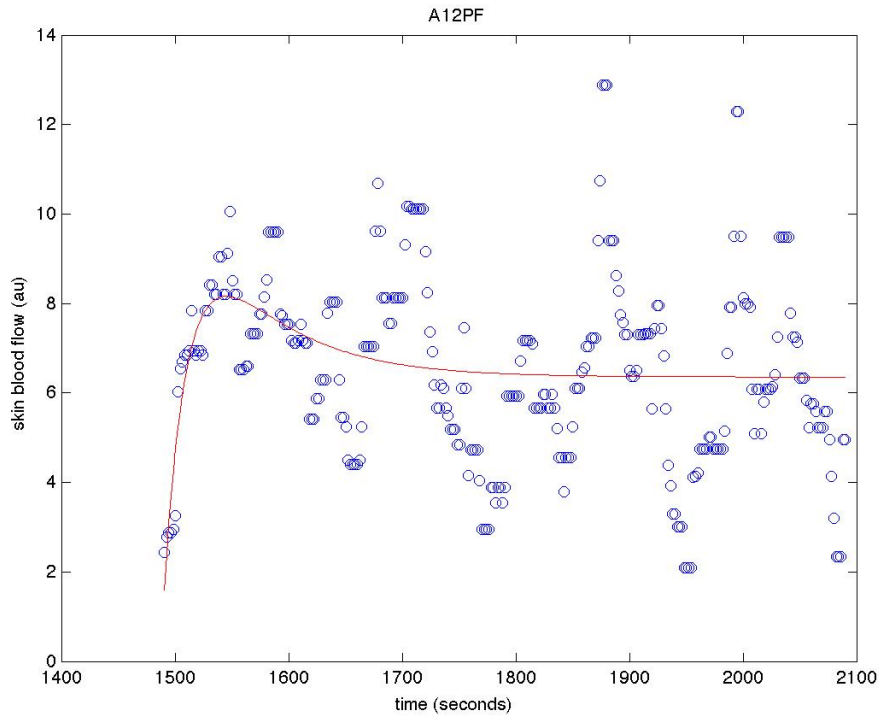


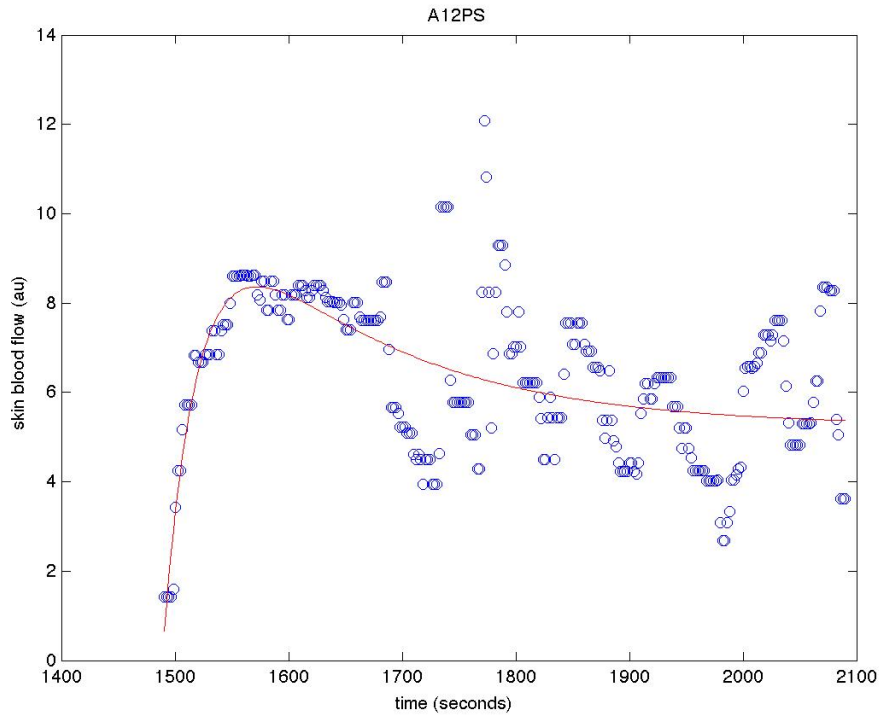
Subject T6A_11: baseline SBF: PF=4.87, PO= 3.44, PS= 3.57



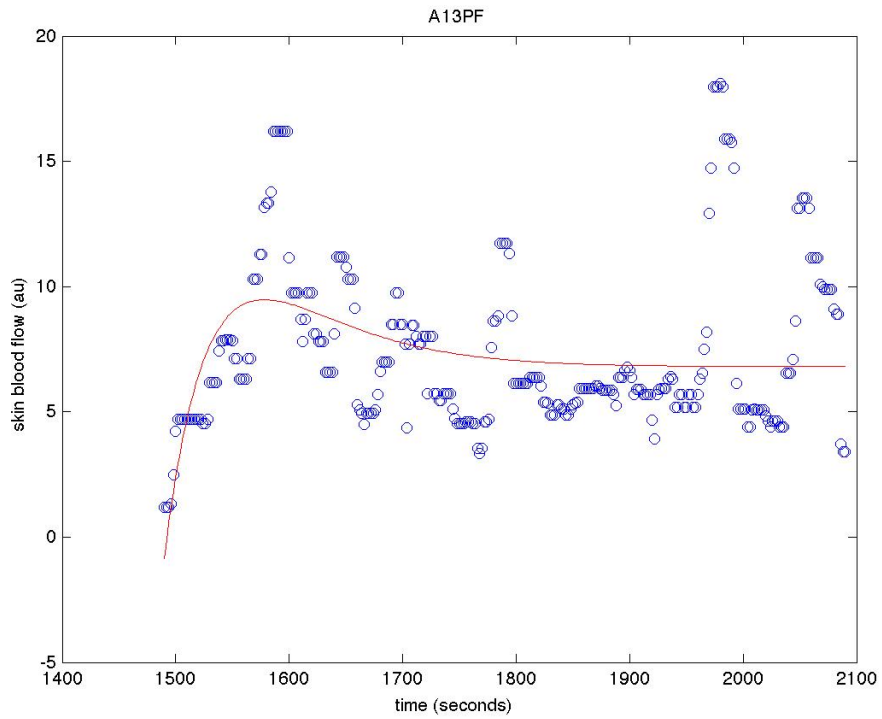


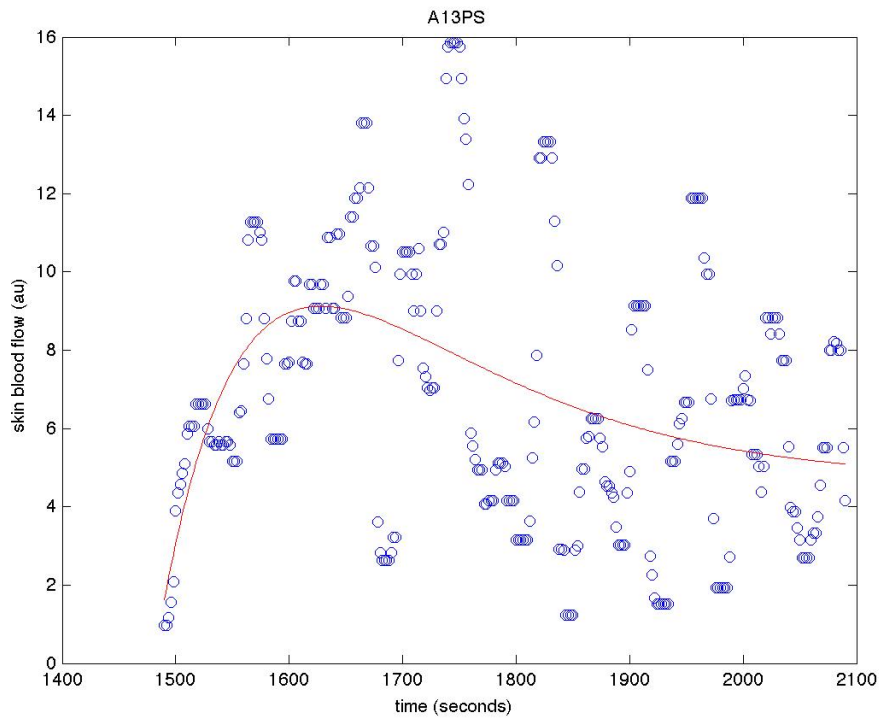
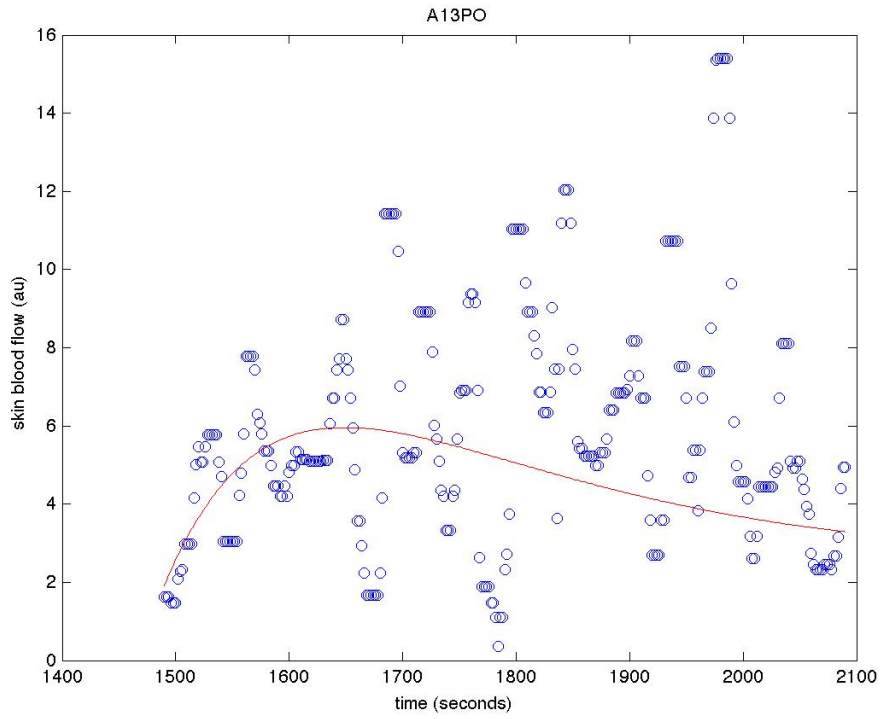
Subject T6A_12: baseline SBF: PF=4.44, PO= 4.82, PS= 4.80



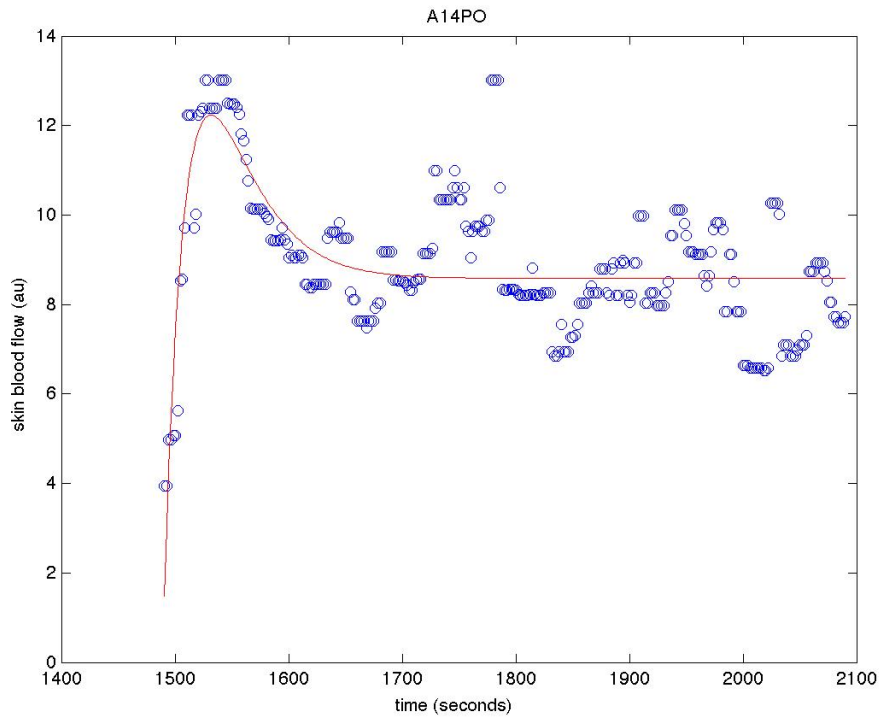
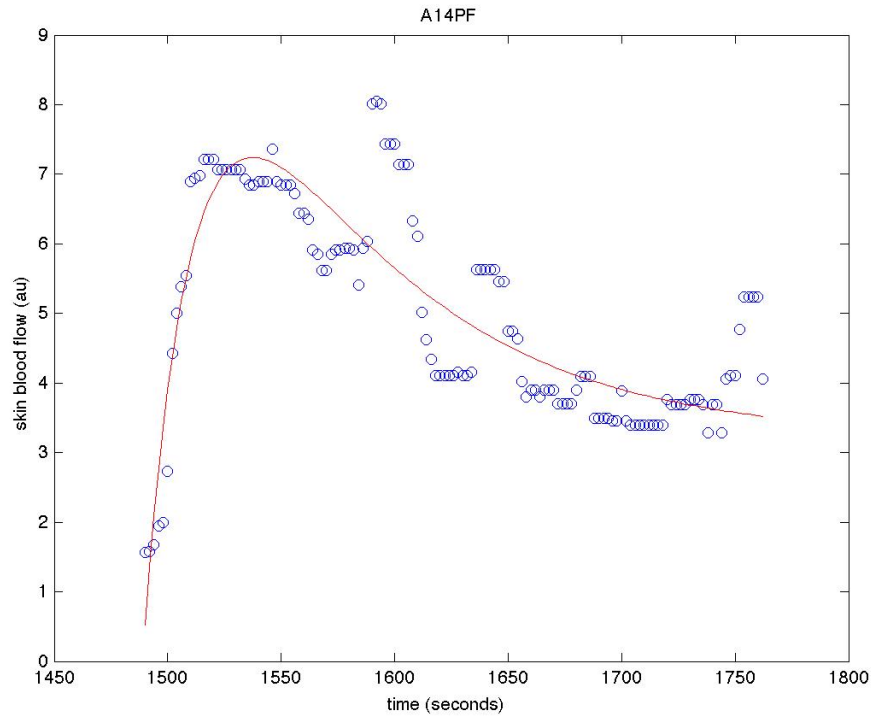


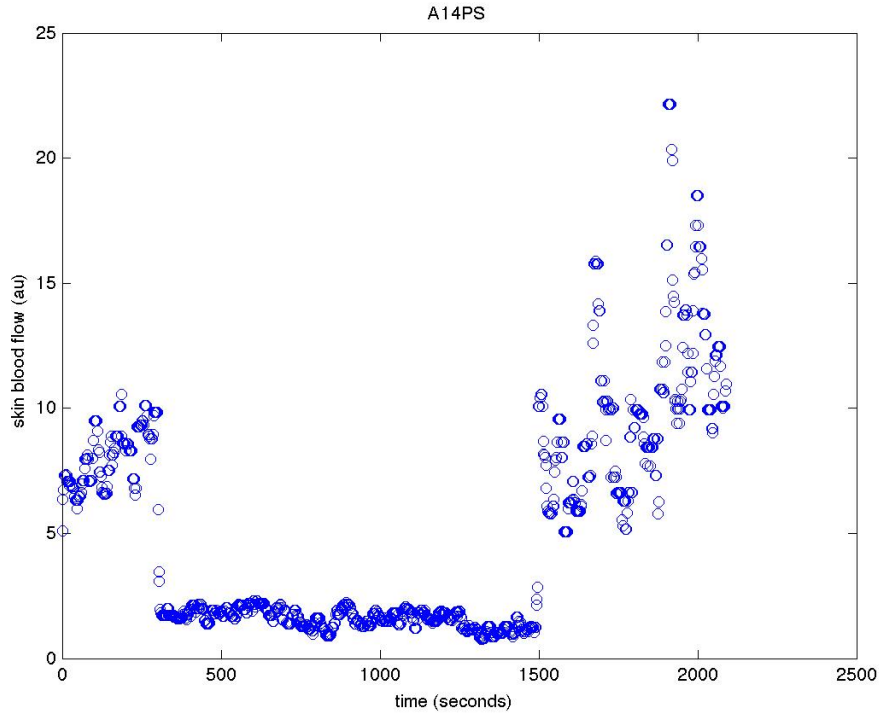
Subject T6A_13: baseline SBF: PF=6.26, PO= 3.75, PS= 3.26



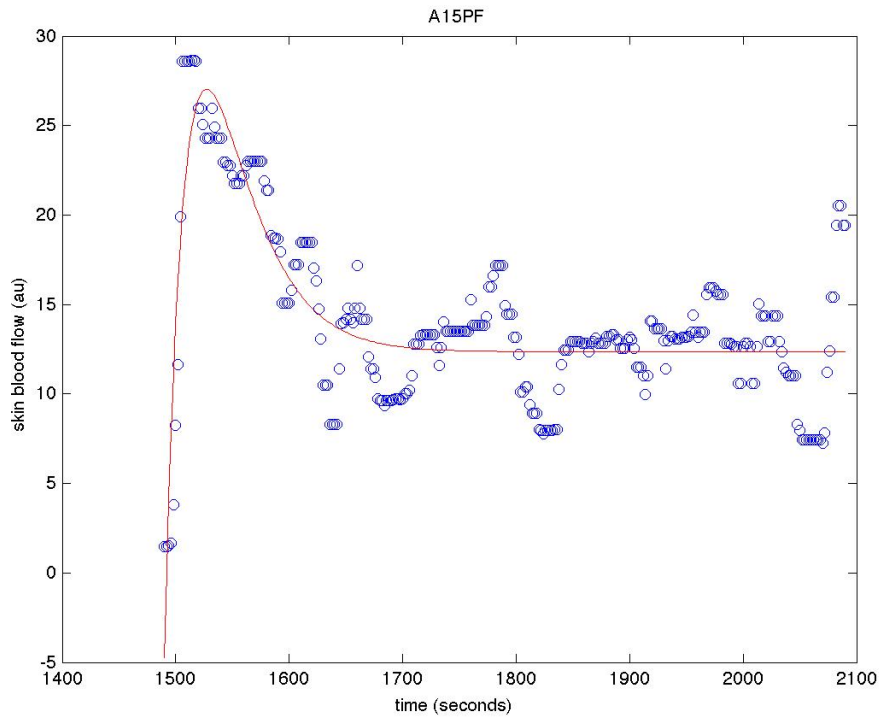


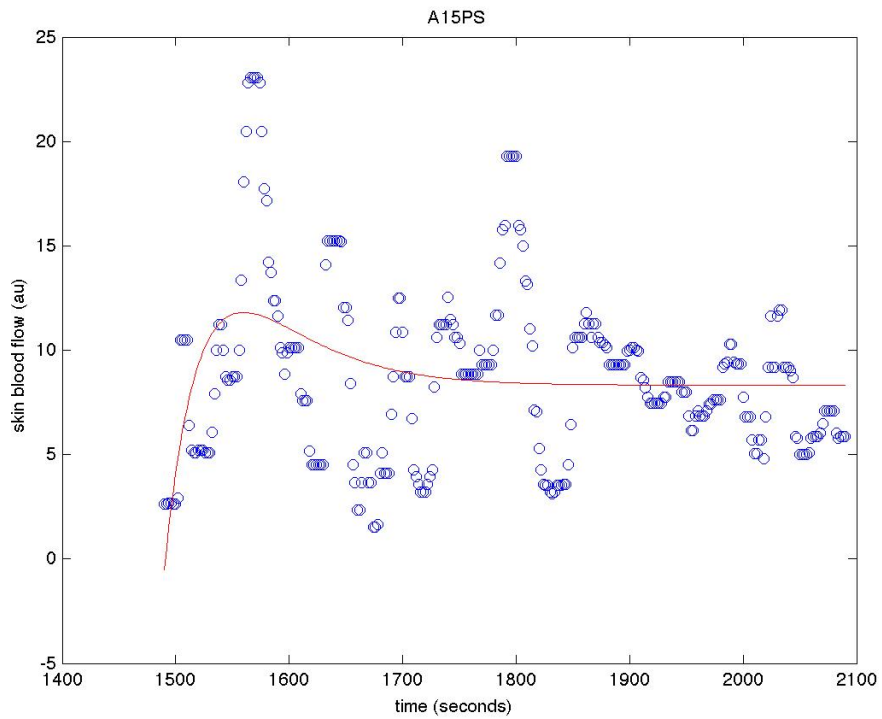
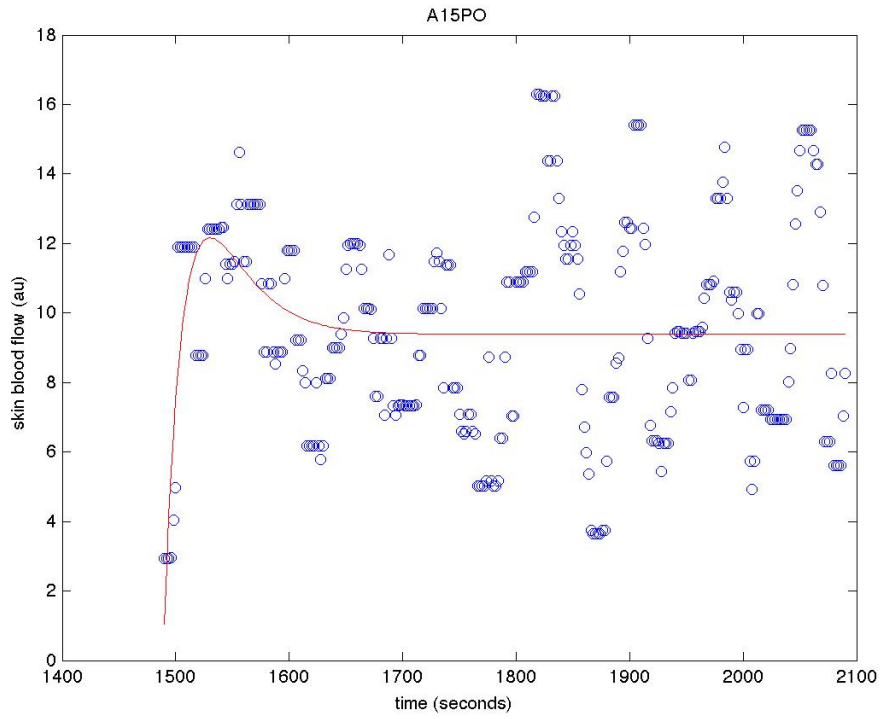
Subject T6A_14: baseline SBF: PF=4.21, PO= 8.16, PS= 8.07



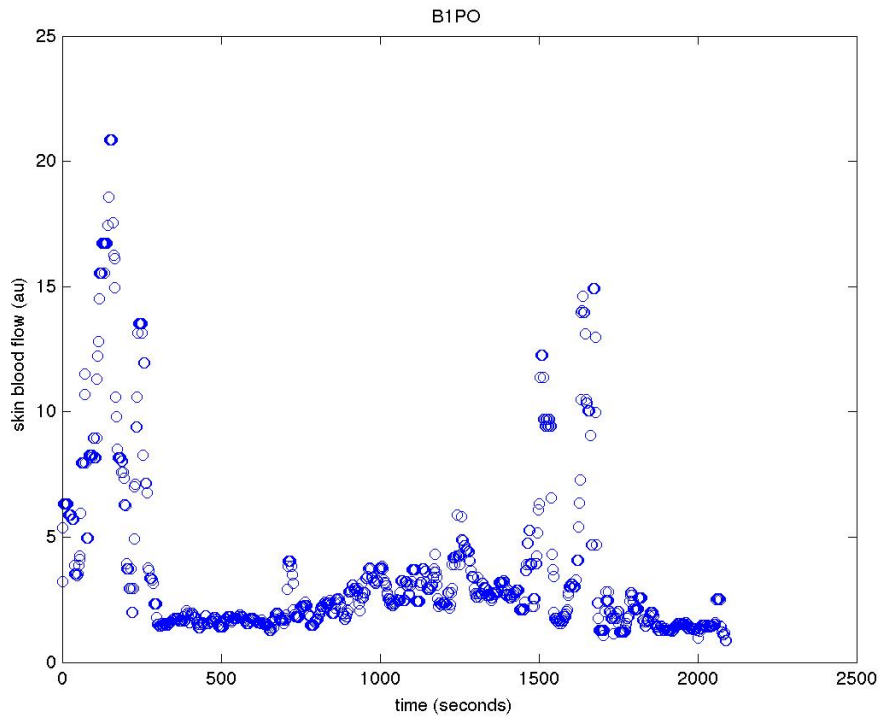
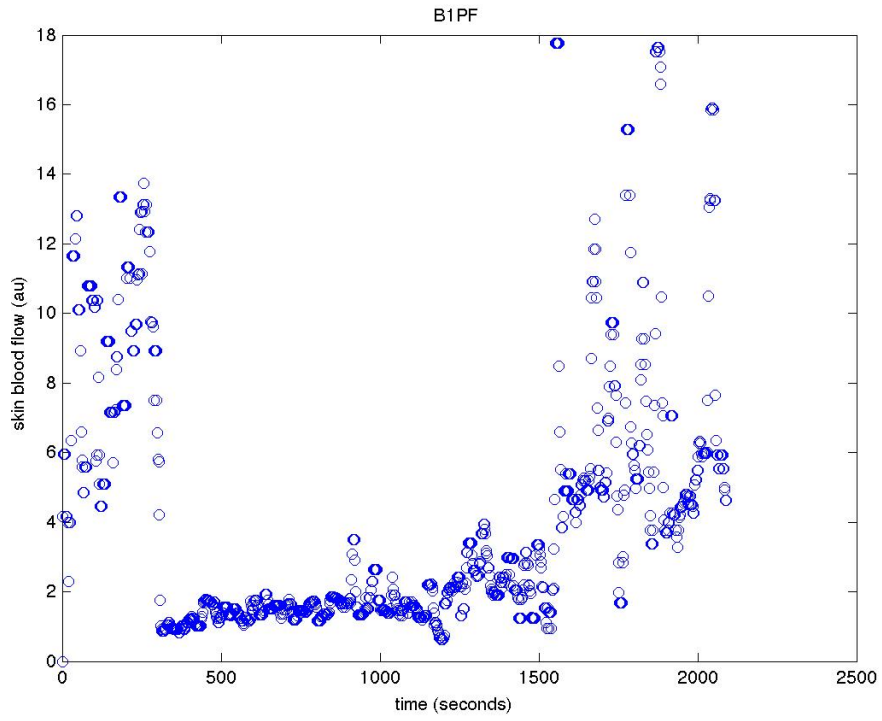


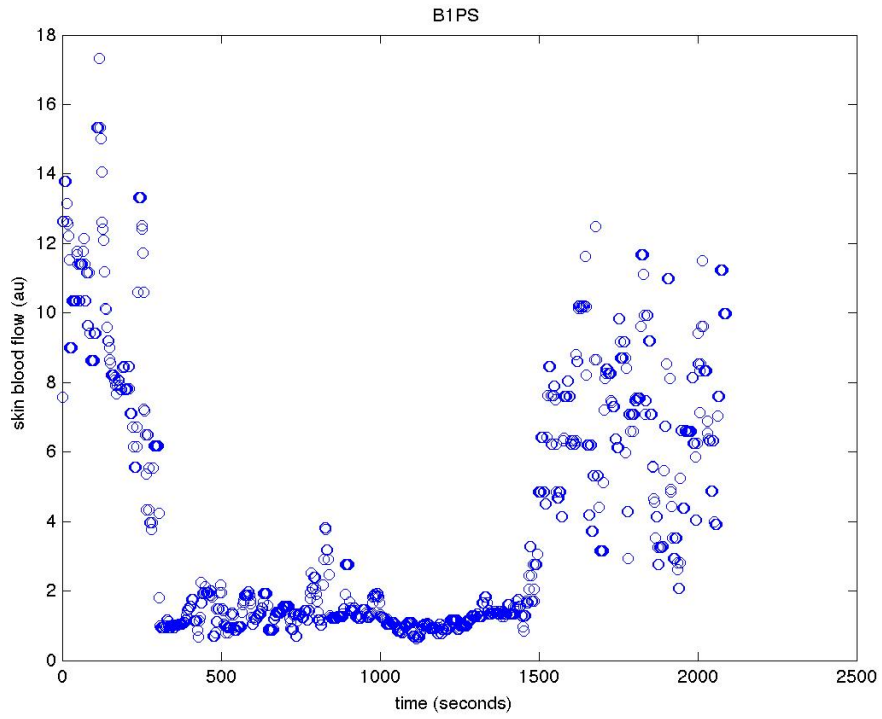
Subject T6A_15: baseline SBF: PF=5.42, PO= 9.96, PS= 10.30



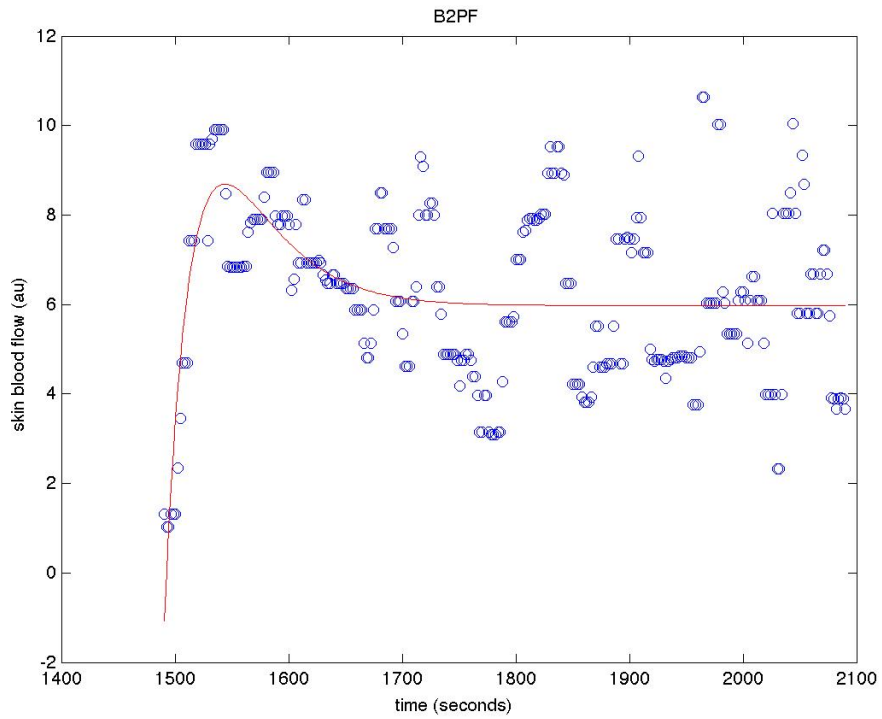


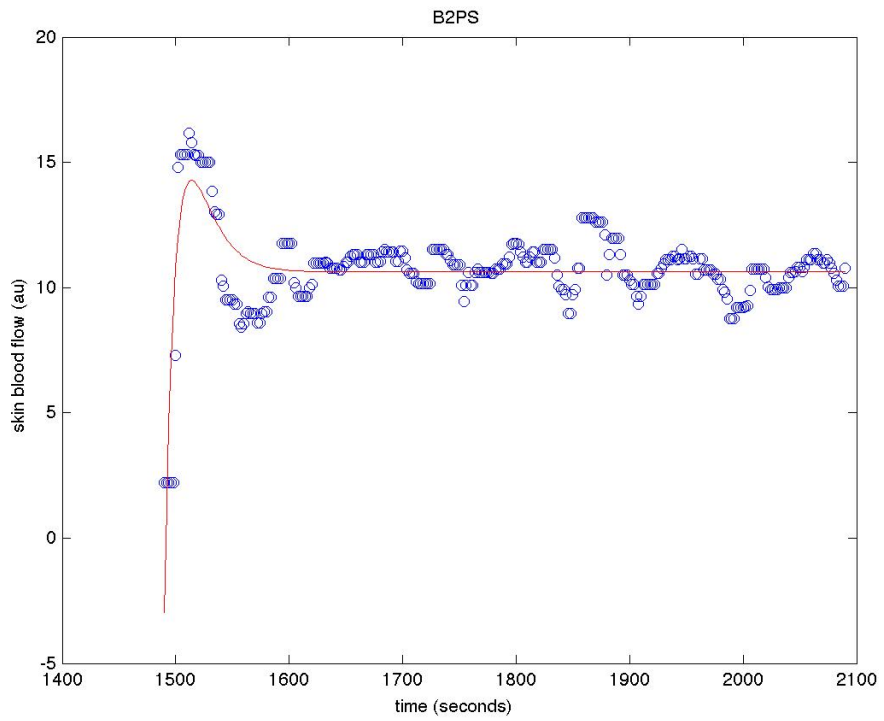
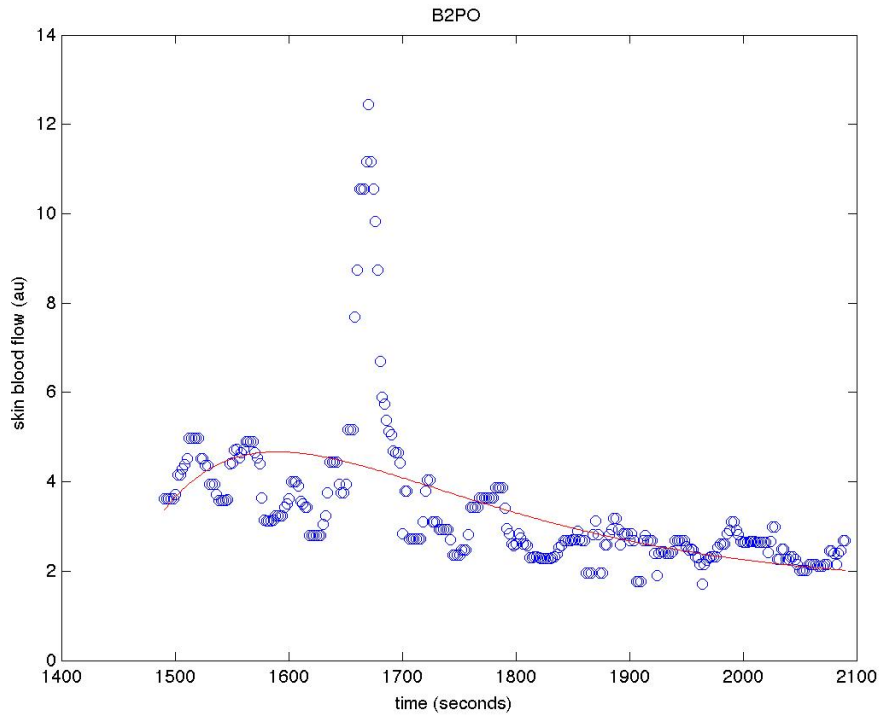
Subject T6B_01: baseline SBF: PF=8.96, PO= 8.60, PS= 9.48



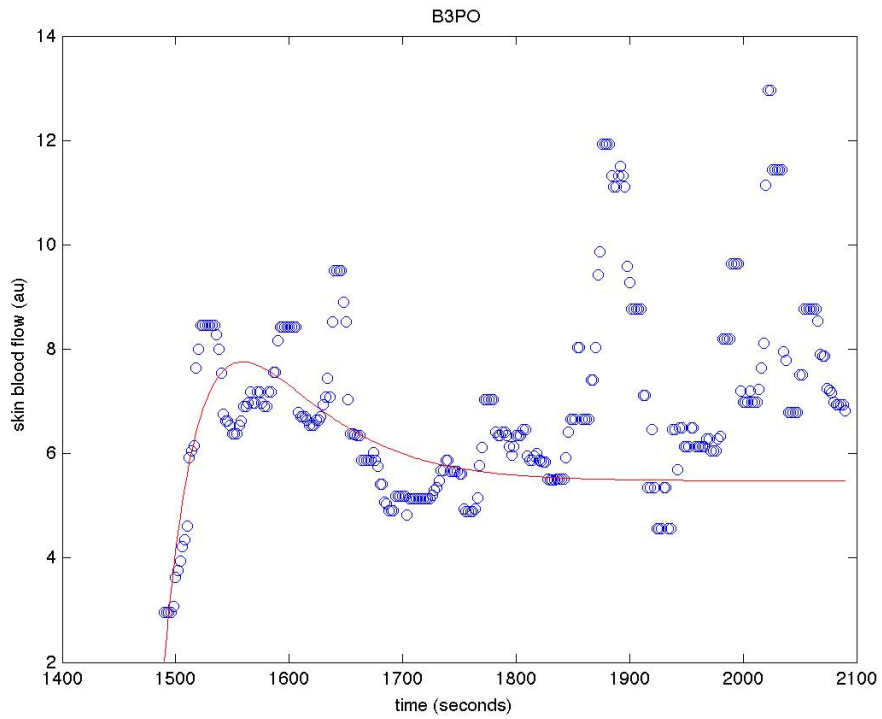
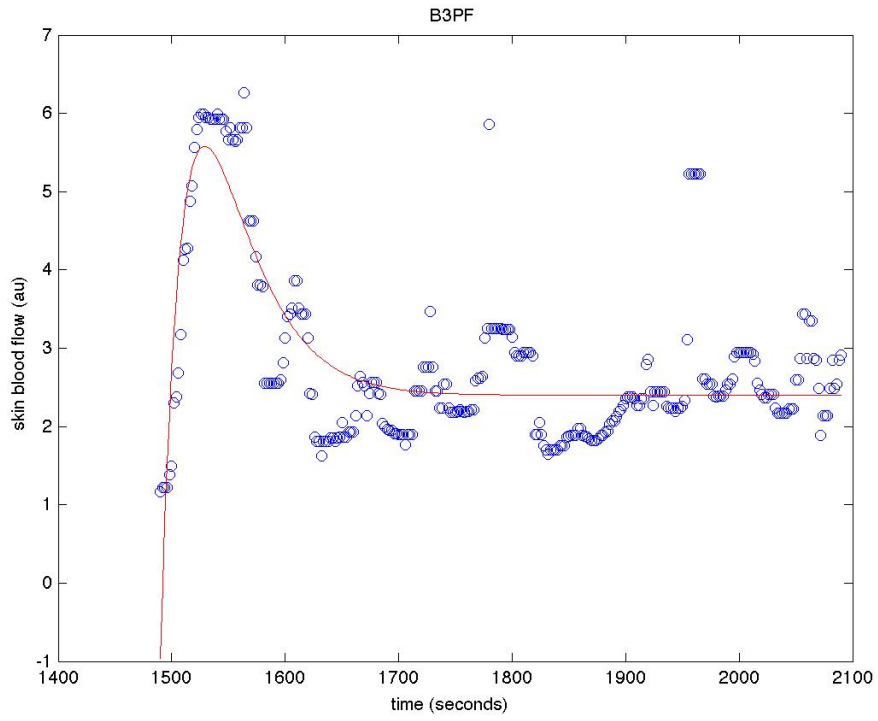


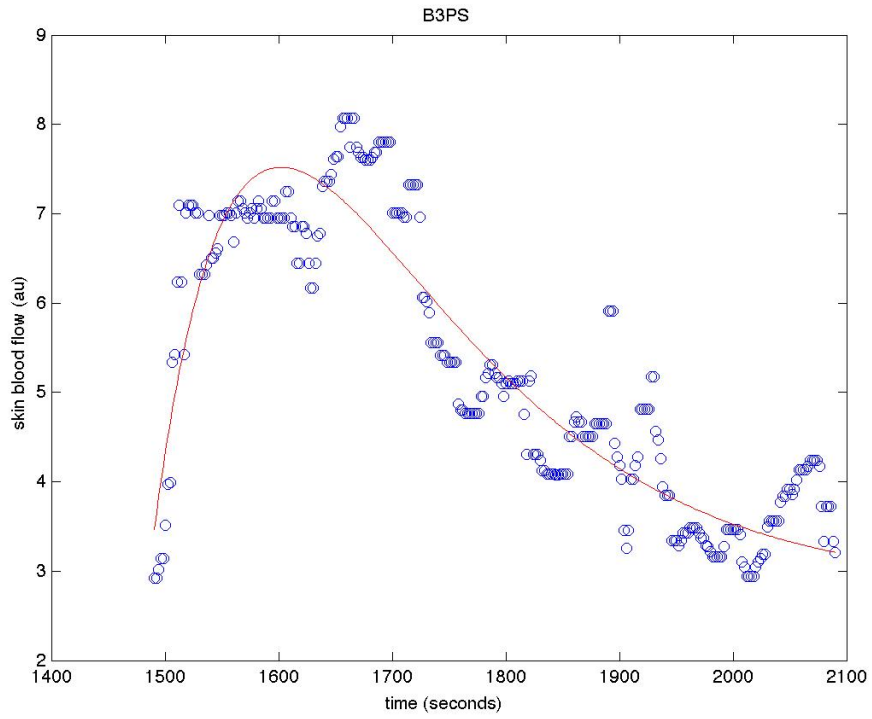
Subject T6B_02: baseline SBF: PF=3.57, PO= 2.87, PS= 4.33



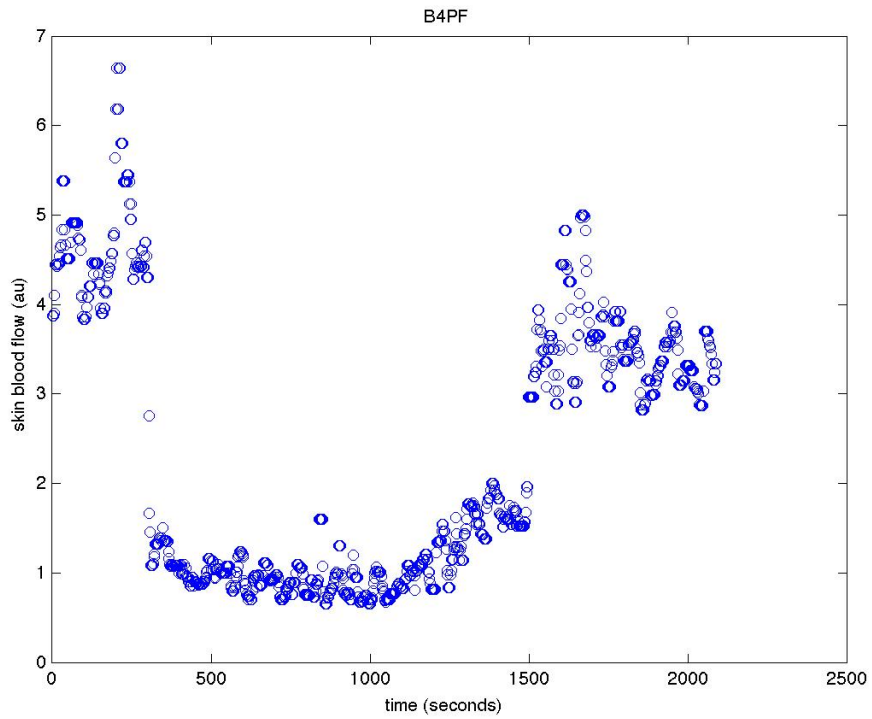


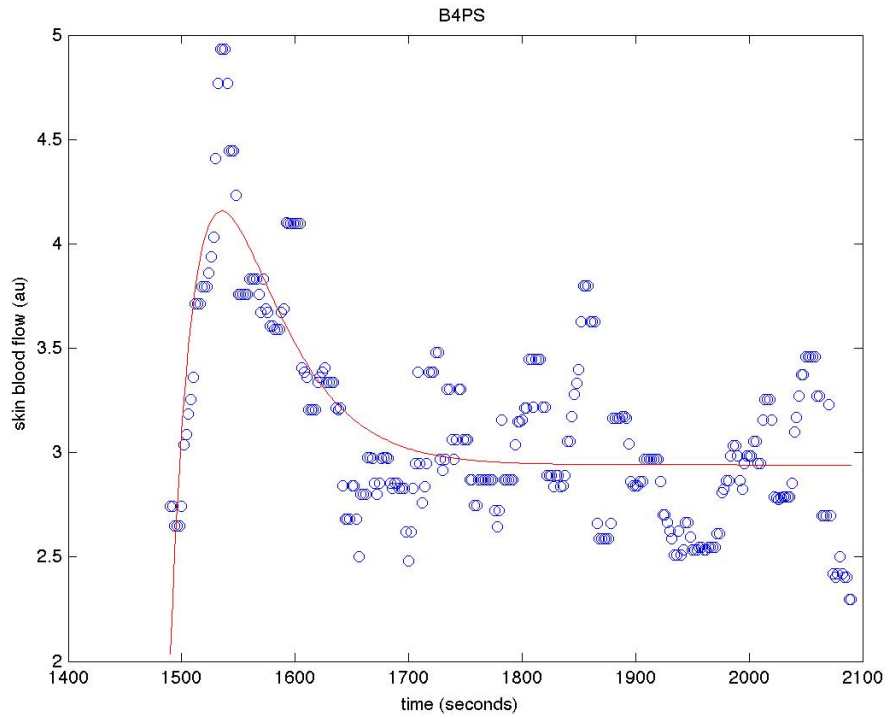
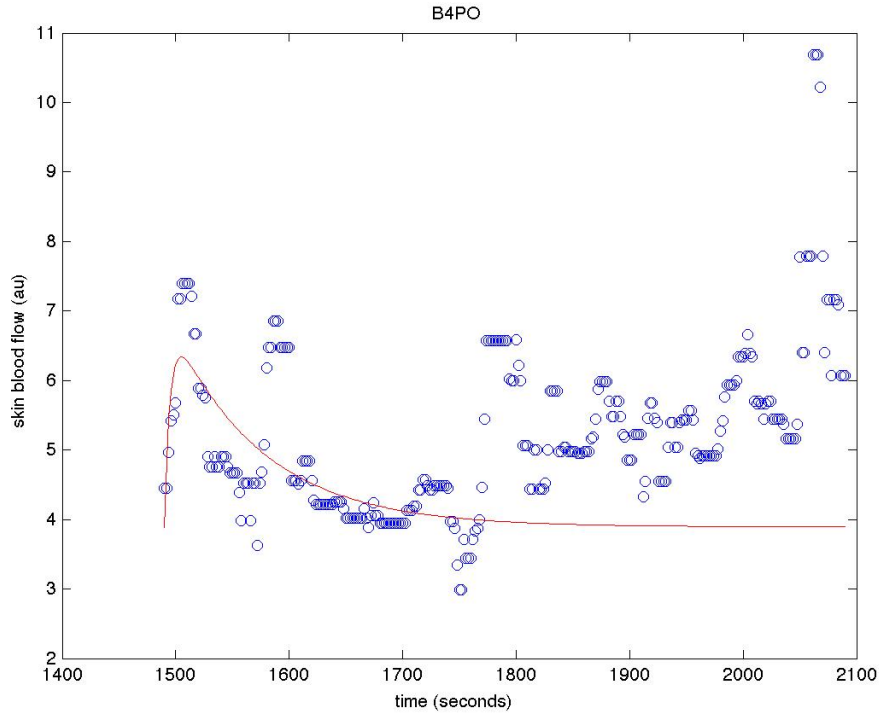
Subject T6B_03: baseline SBF: PF=4.35, PO= 4.55, PS= 4.60



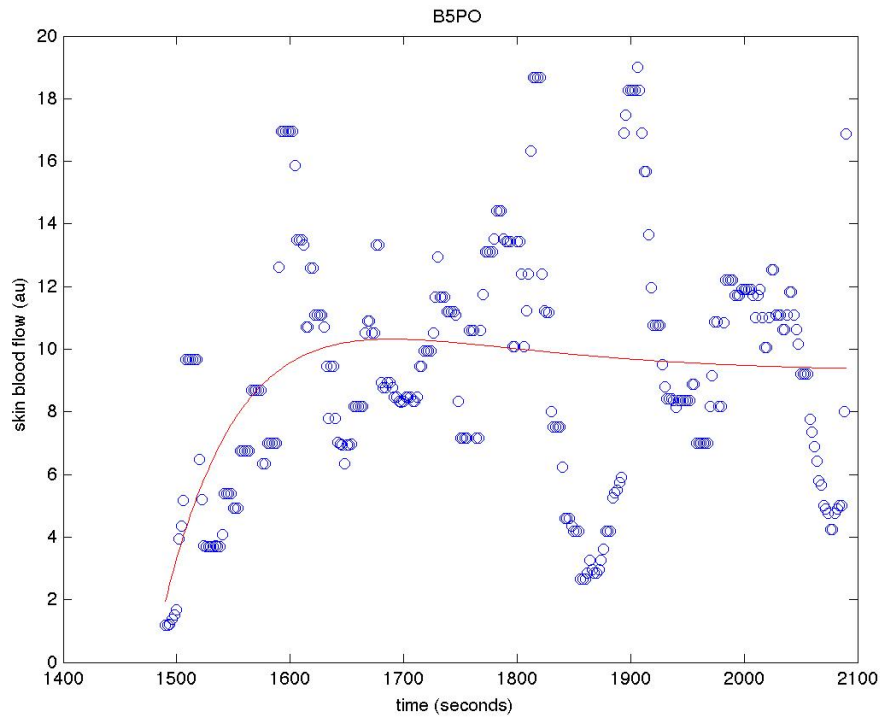
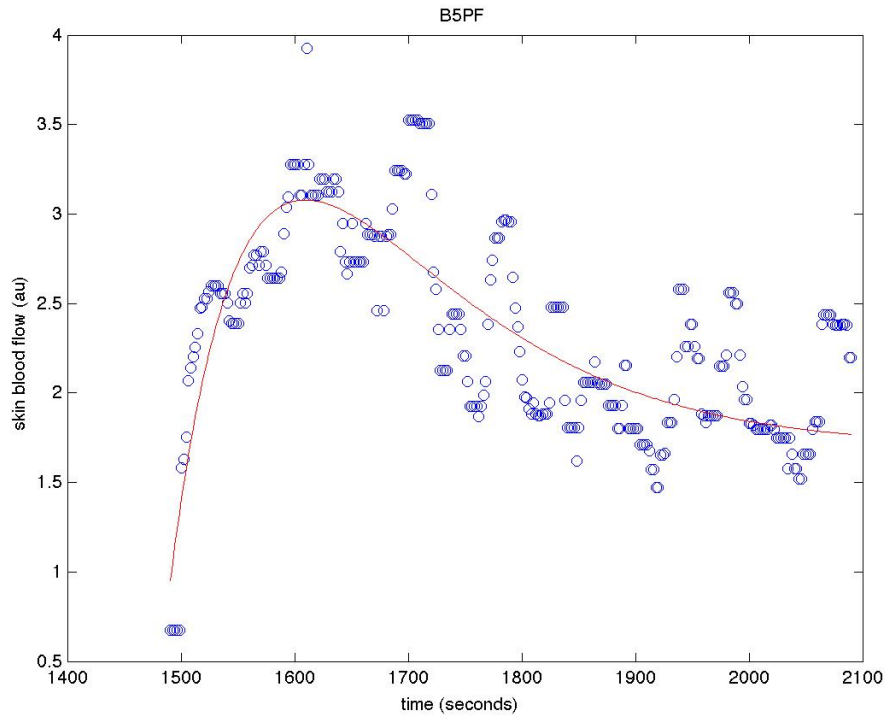


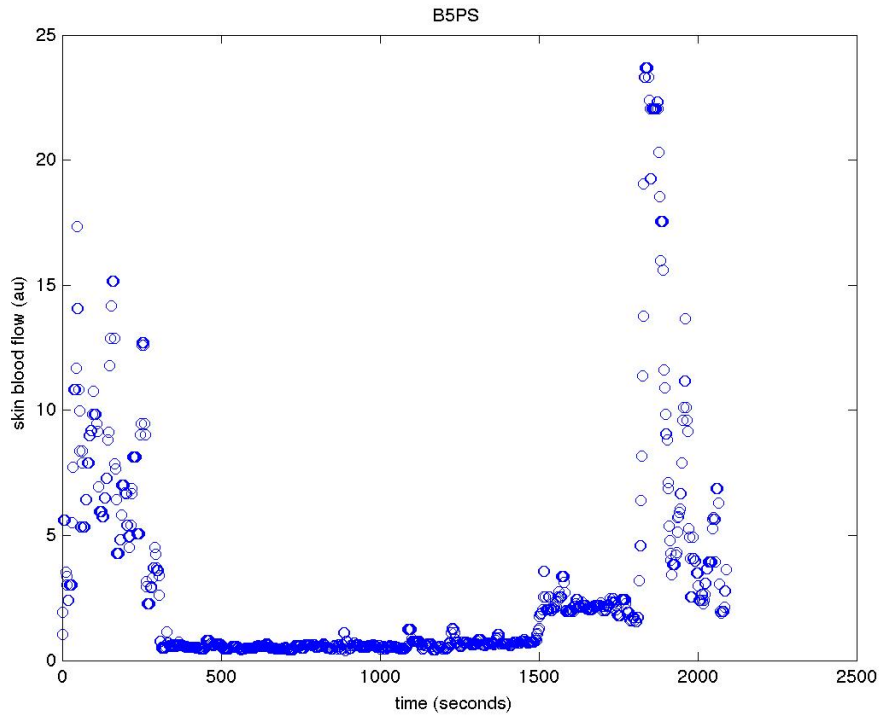
Subject T6B_04: baseline SBF: PF=4.44, PO= 5.44, PS= 3.73



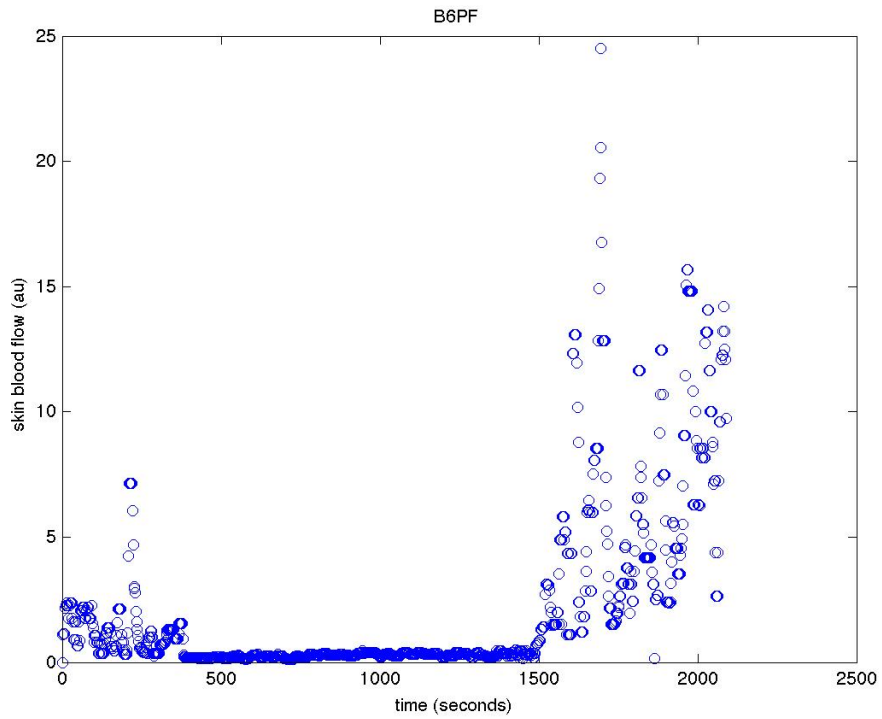


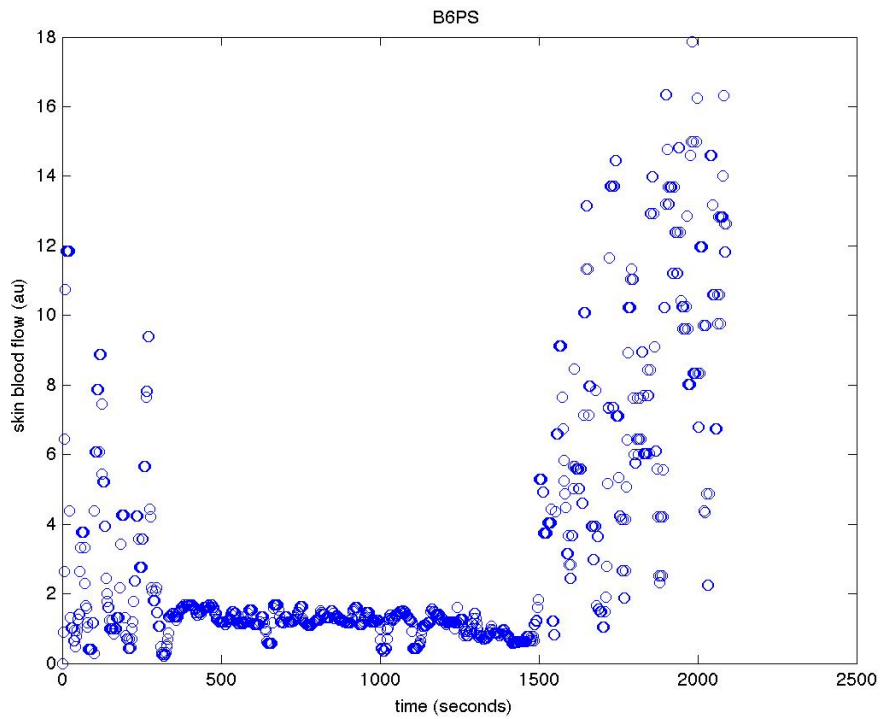
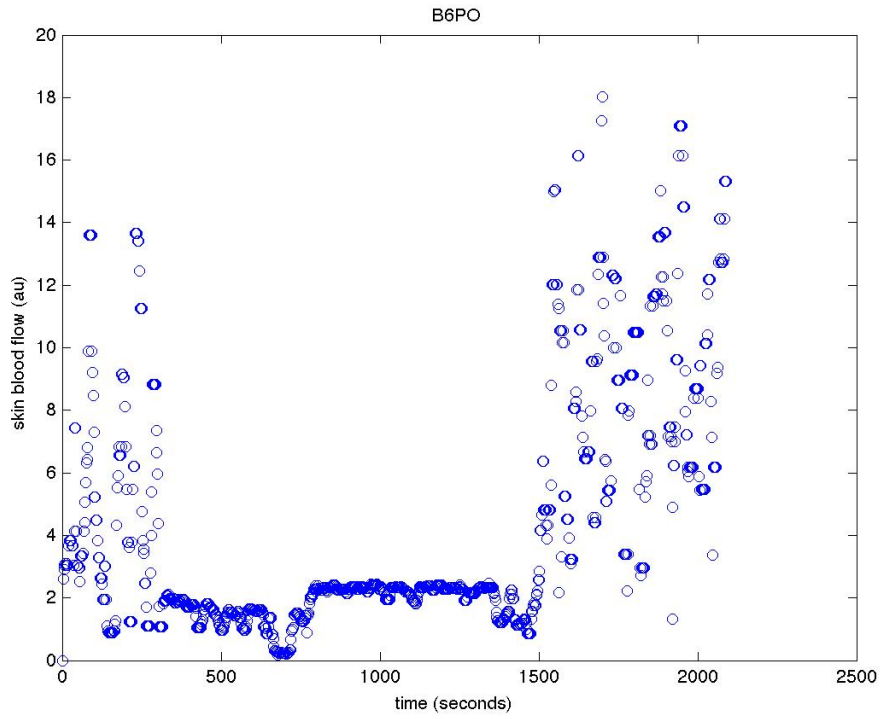
Subject T6B_05: baseline SBF: PF=2.27, PO= 2.61, PS= 7.07



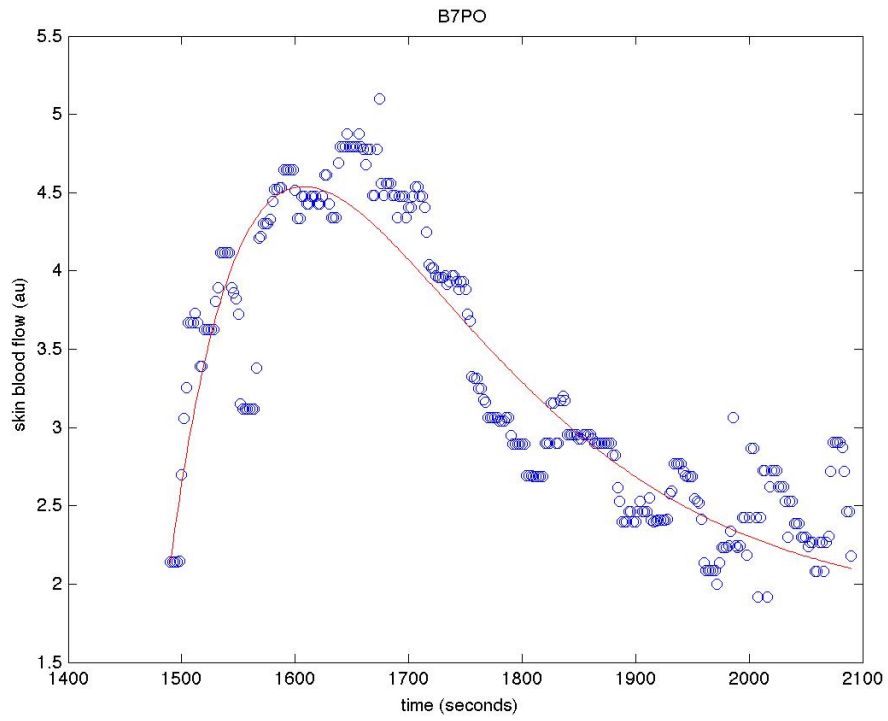
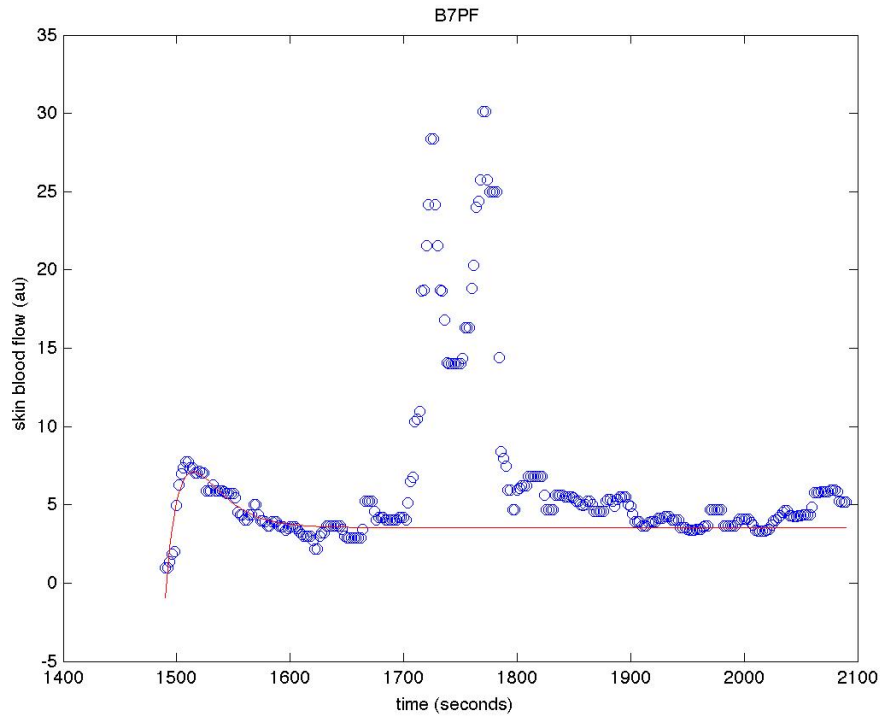


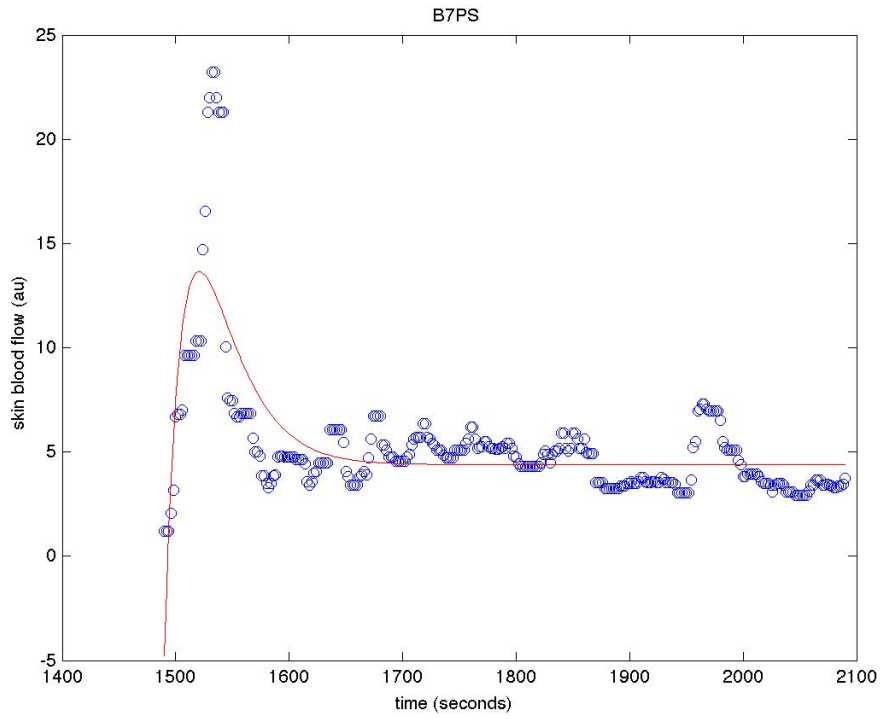
Subject T6B_06: baseline SBF: PF=1.32, PO= 4.88, PS= 3.26



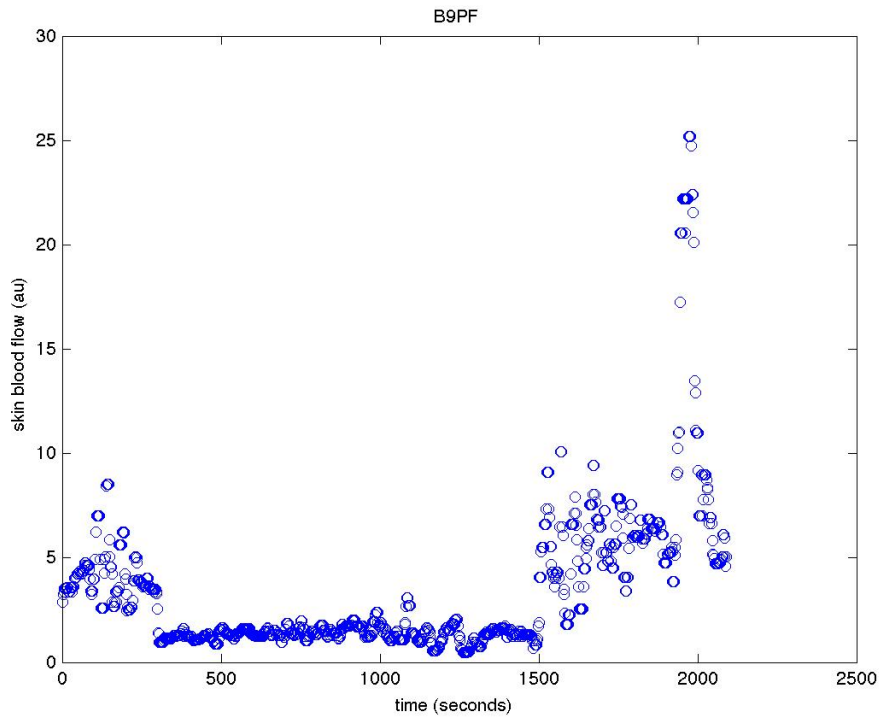


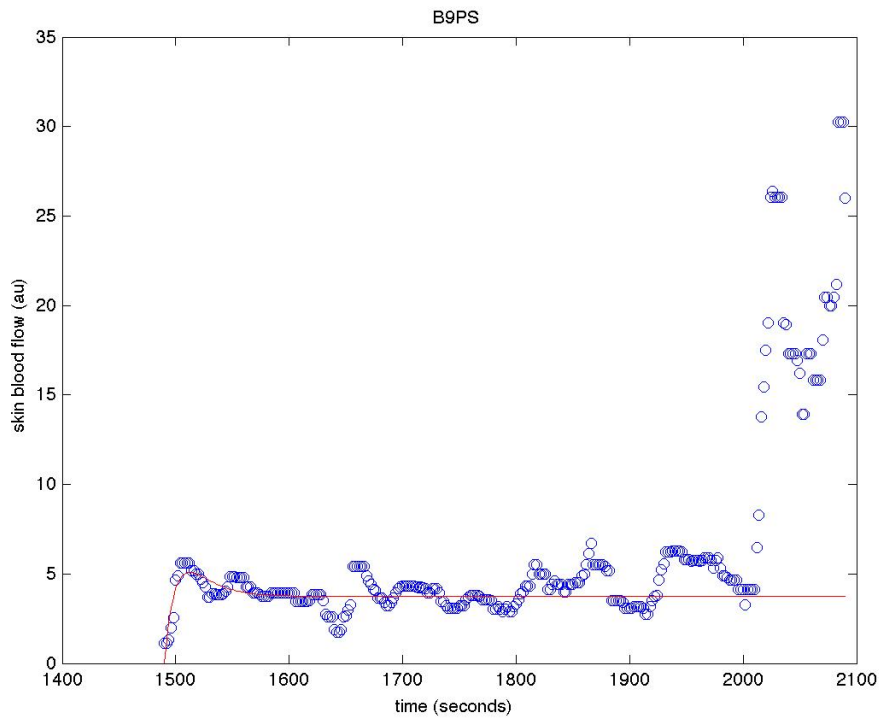
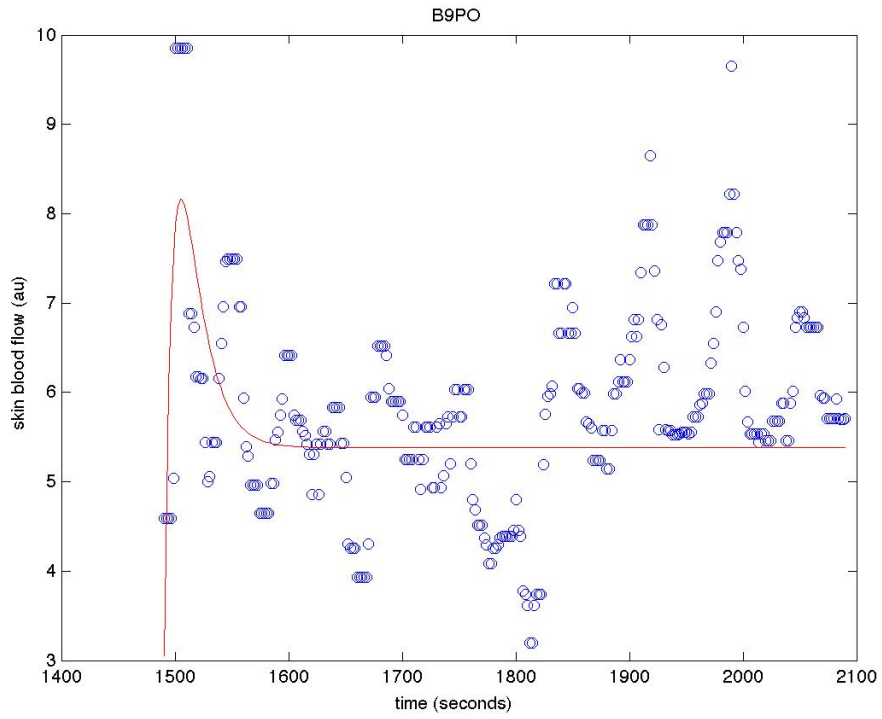
Subject T6B_07: baseline SBF: PF=3.05, PO= 3.32, PS= 6.39





Subject T6B_09: baseline SBF: PF=3.86, PO= 2.46, PS= 2.92





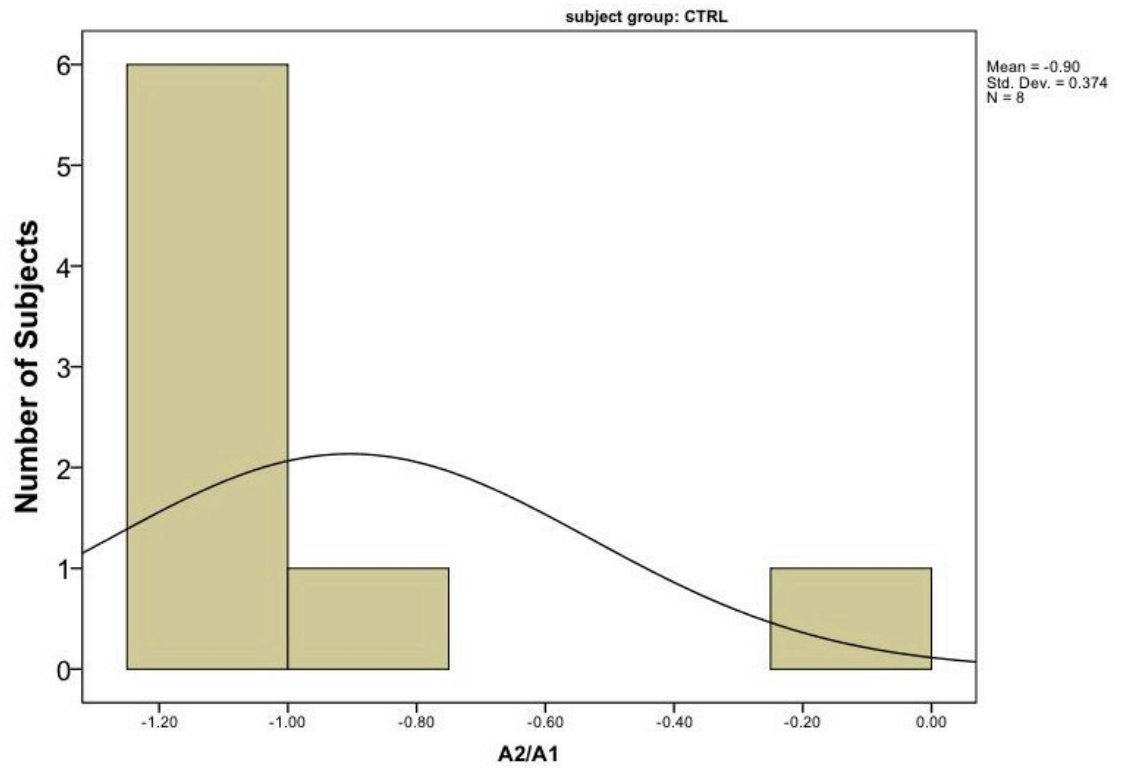
APPENDIX B

HISTOGRAMS OF CURVE FIT PARAMETERS IN ALL THREE GROUPS

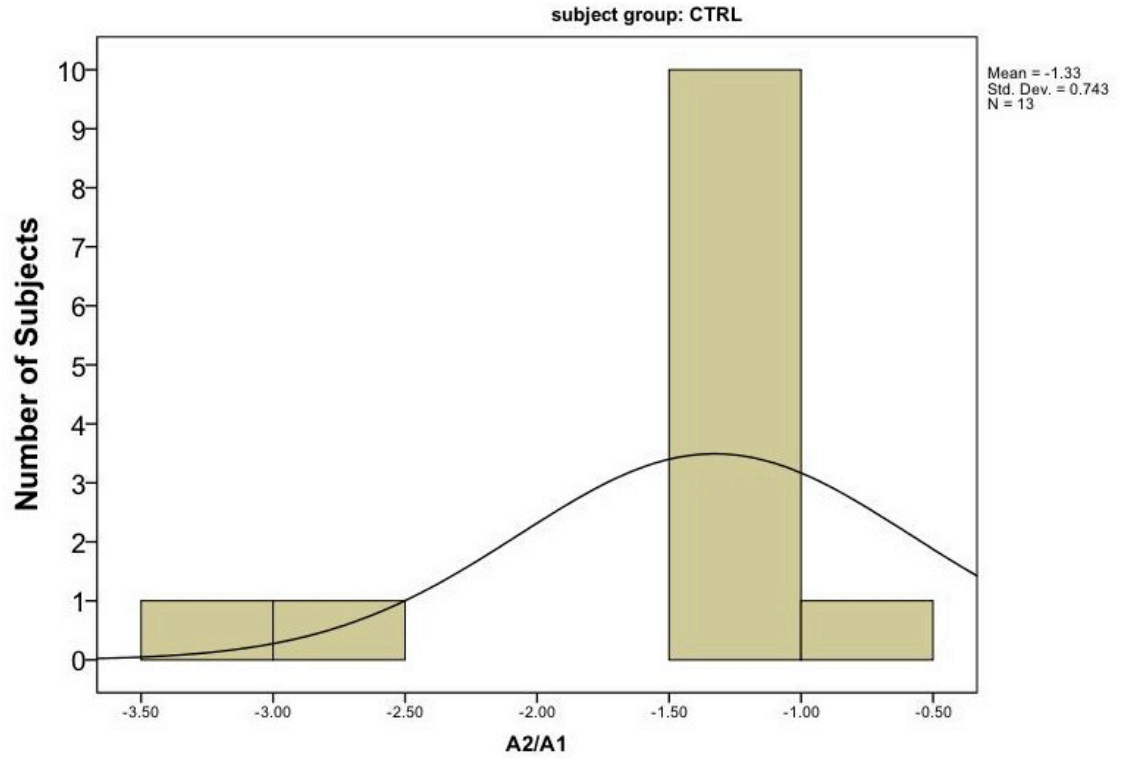
All histograms here show the distribution of each curve-fit parameter by test sessions and by subject groups. The purpose of this appendix is to show the different distribution among subject groups. The parameters were from equation: $y(t) = A_1e^{-t/\tau_1} + A_2e^{-t/\tau_2} + B$.

B.1 A_1/A_2

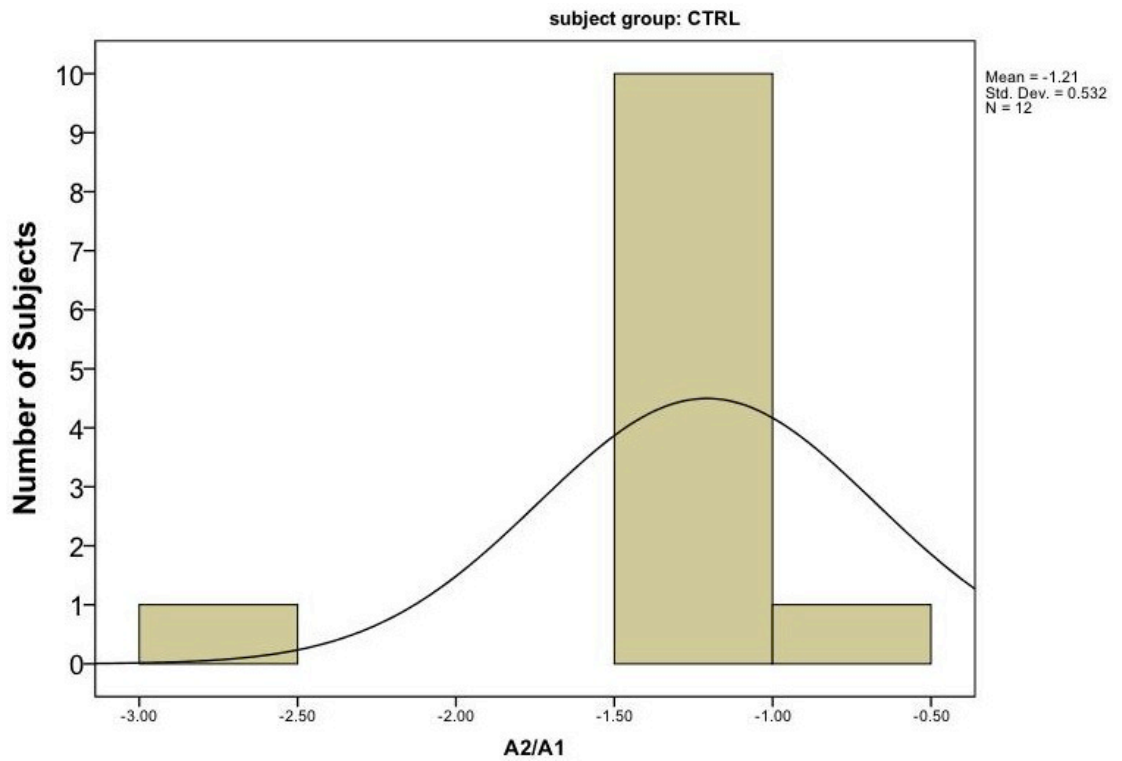
Control group: pressure with fast cooling



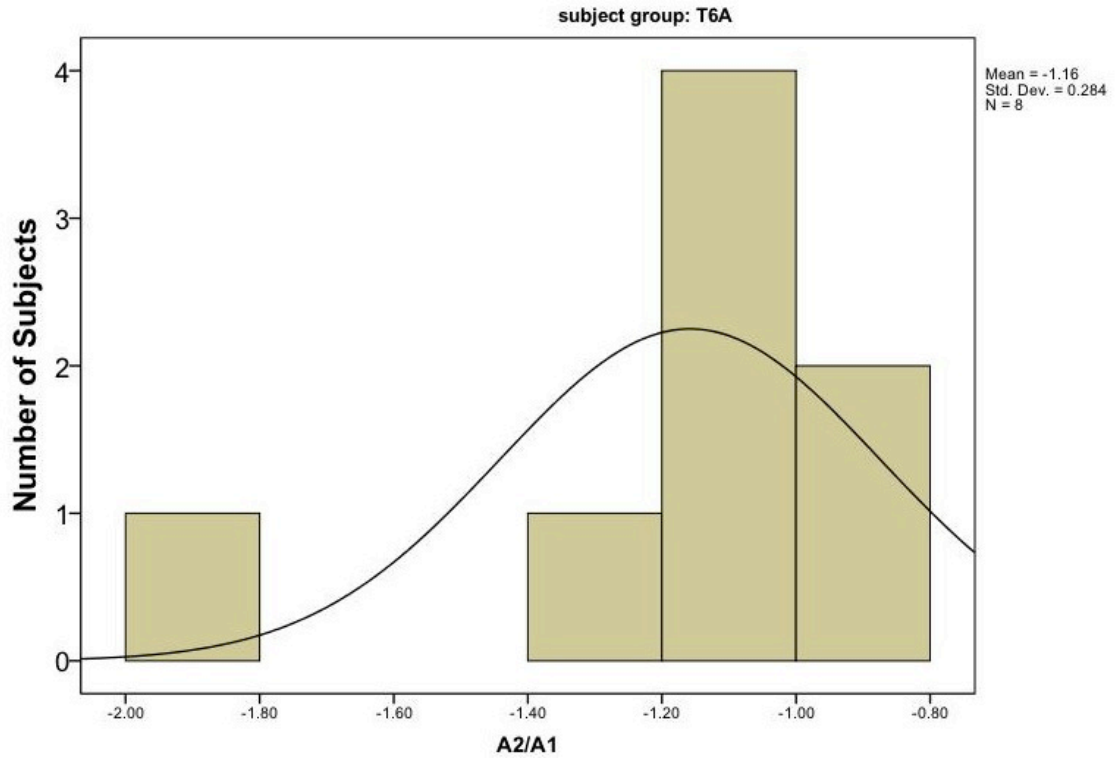
Control group: pressure only



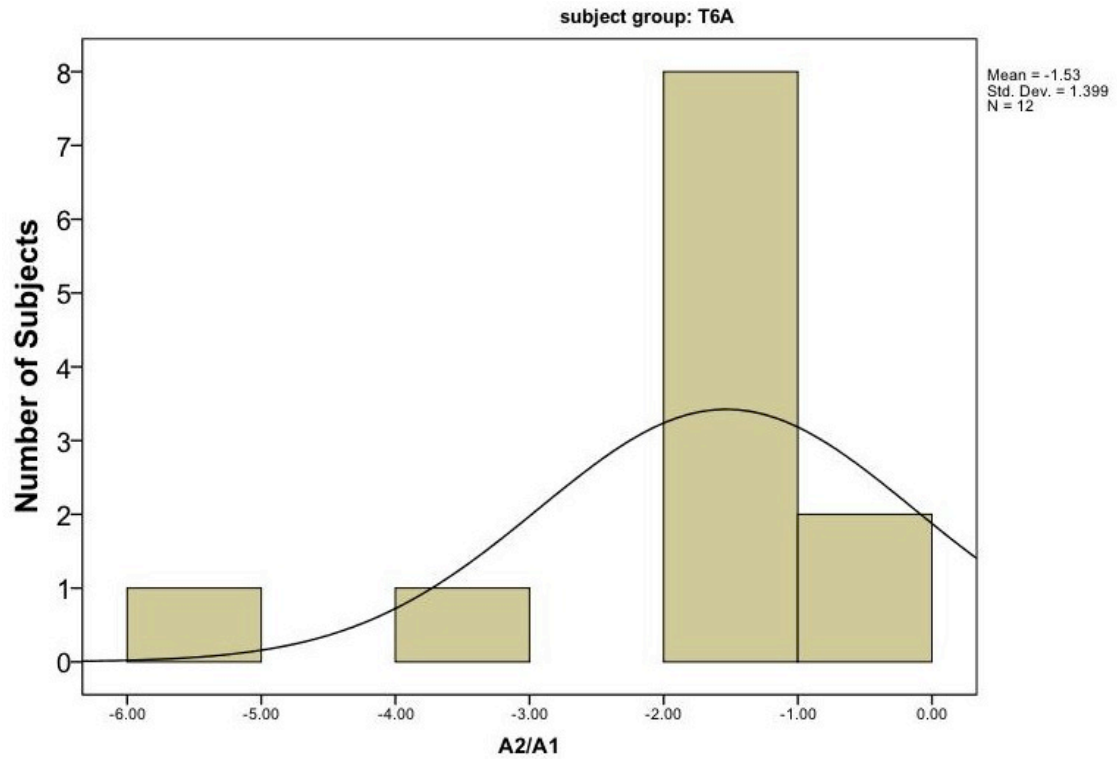
Control group: pressure with slow cooling



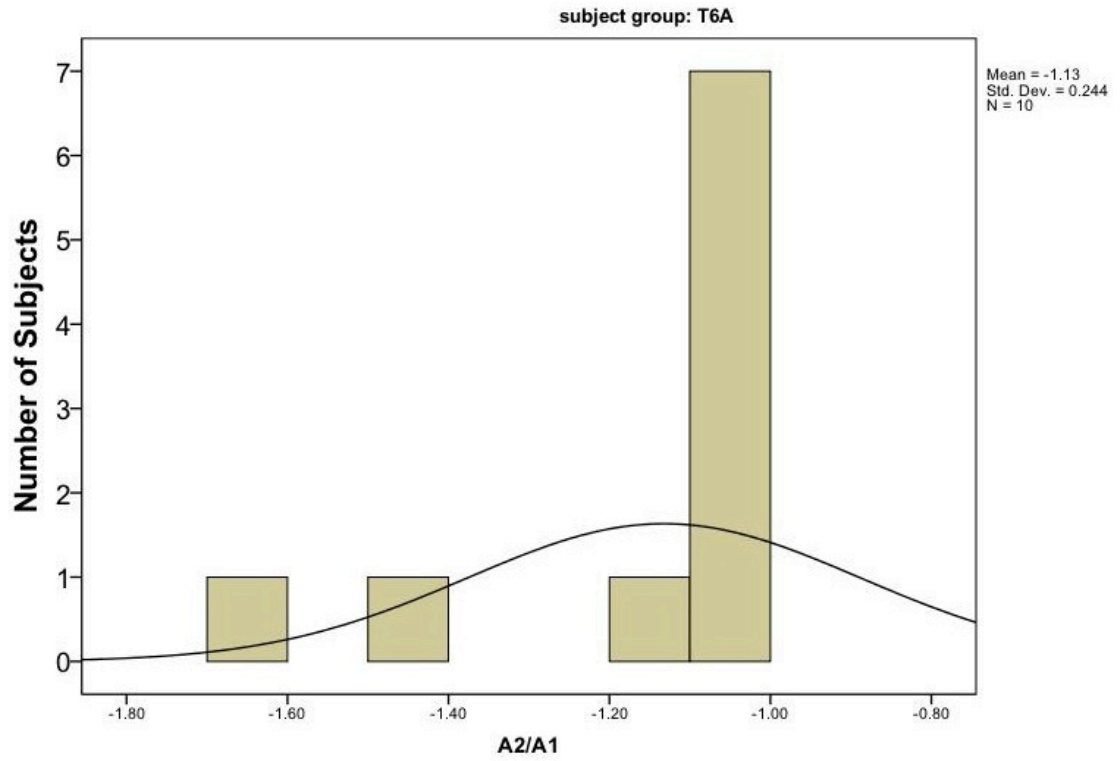
T6A group: pressure with fast cooling



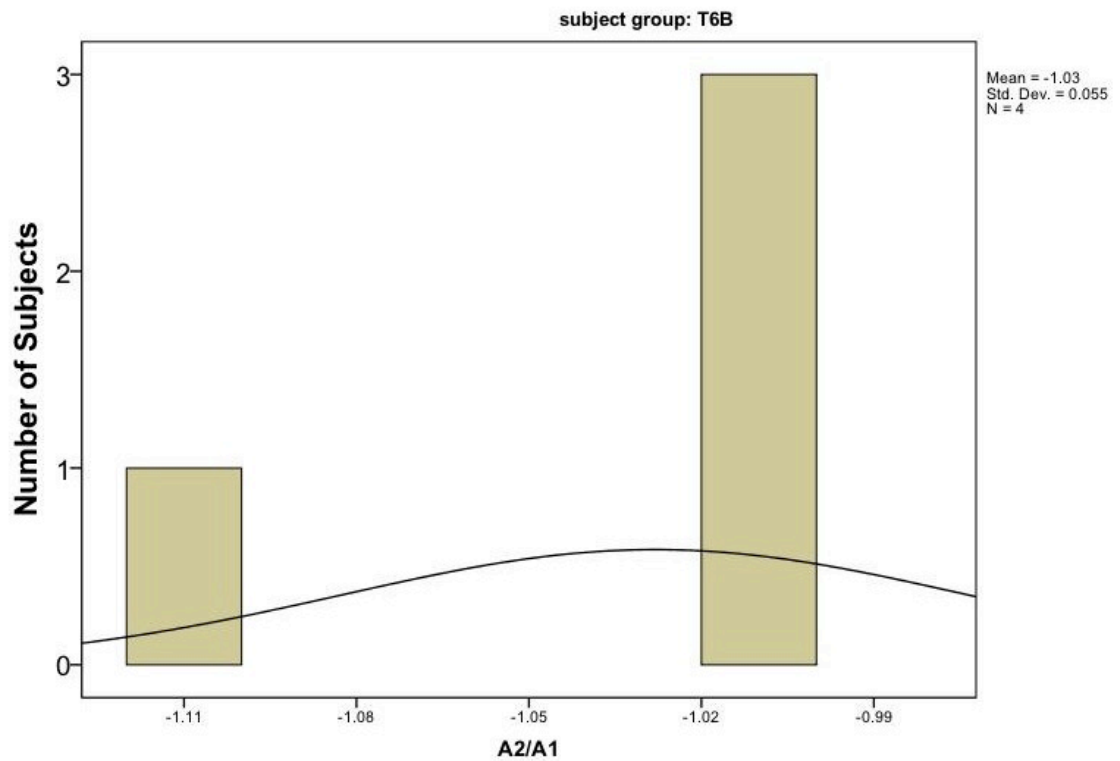
T6A group: pressure only



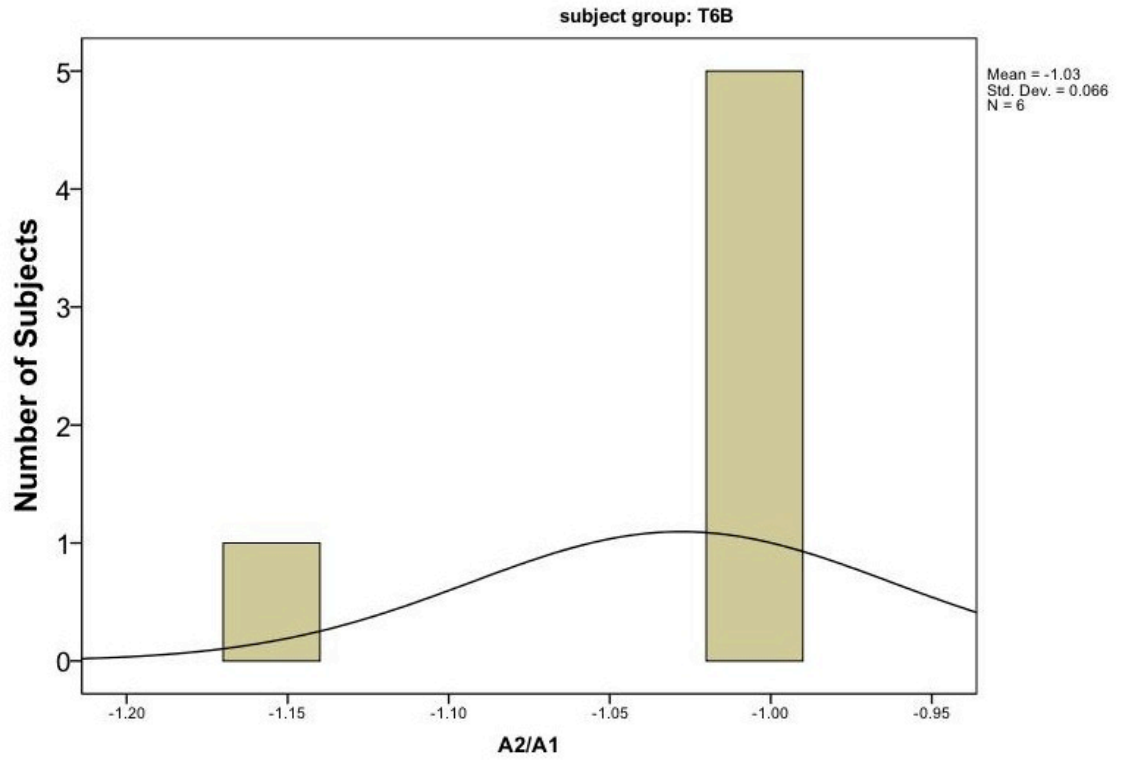
T6A group: pressure with slow cooling



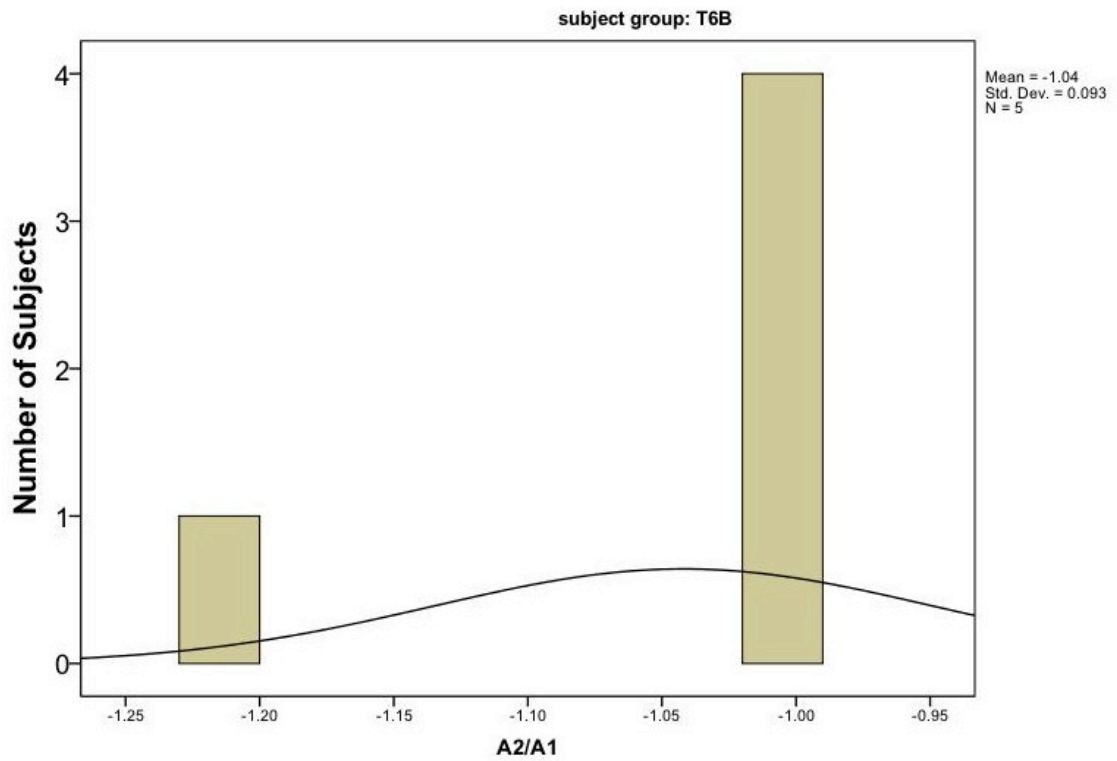
T6B group: pressure with fast cooling



T6B group: pressure only

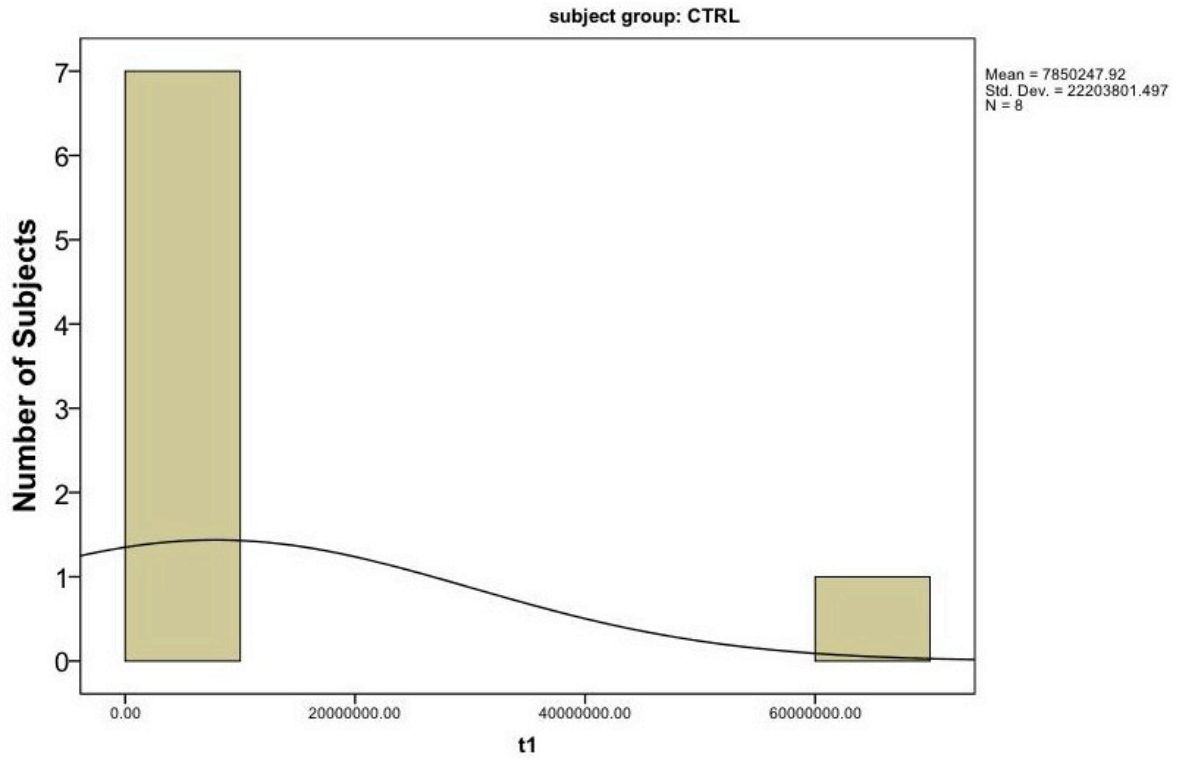


T6B group: pressure with slow cooling

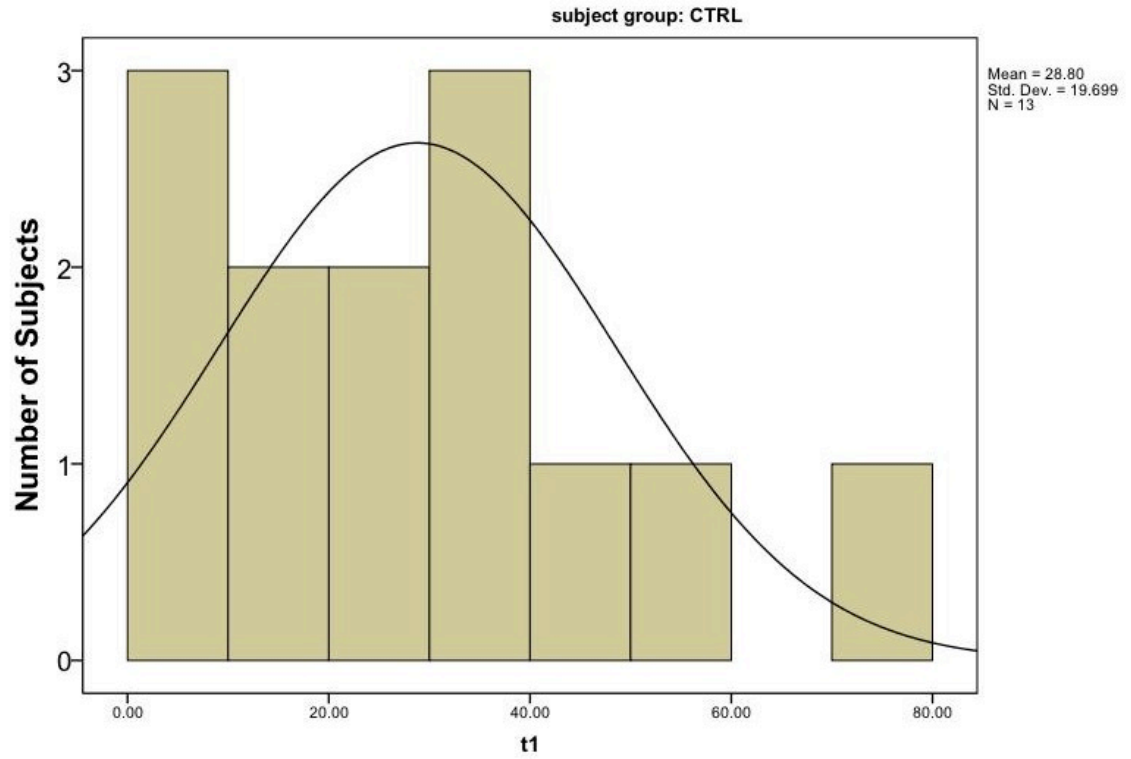


B.2 T₁

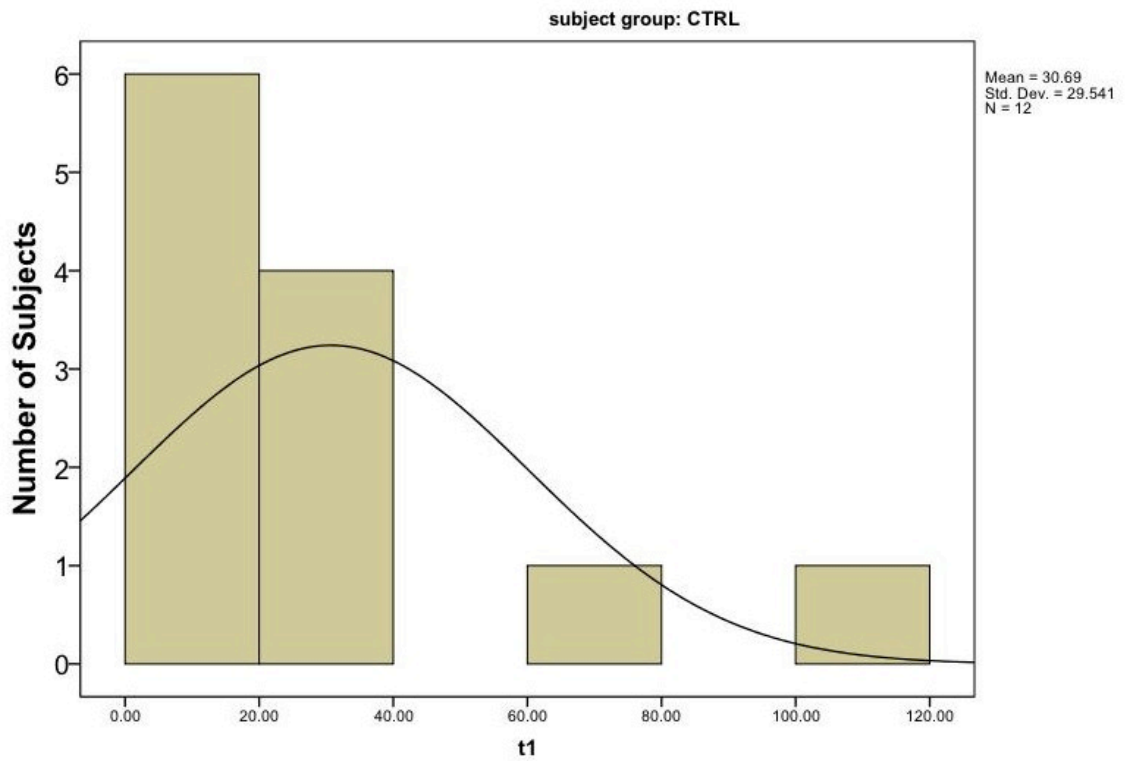
Control group: pressure with fast cooling



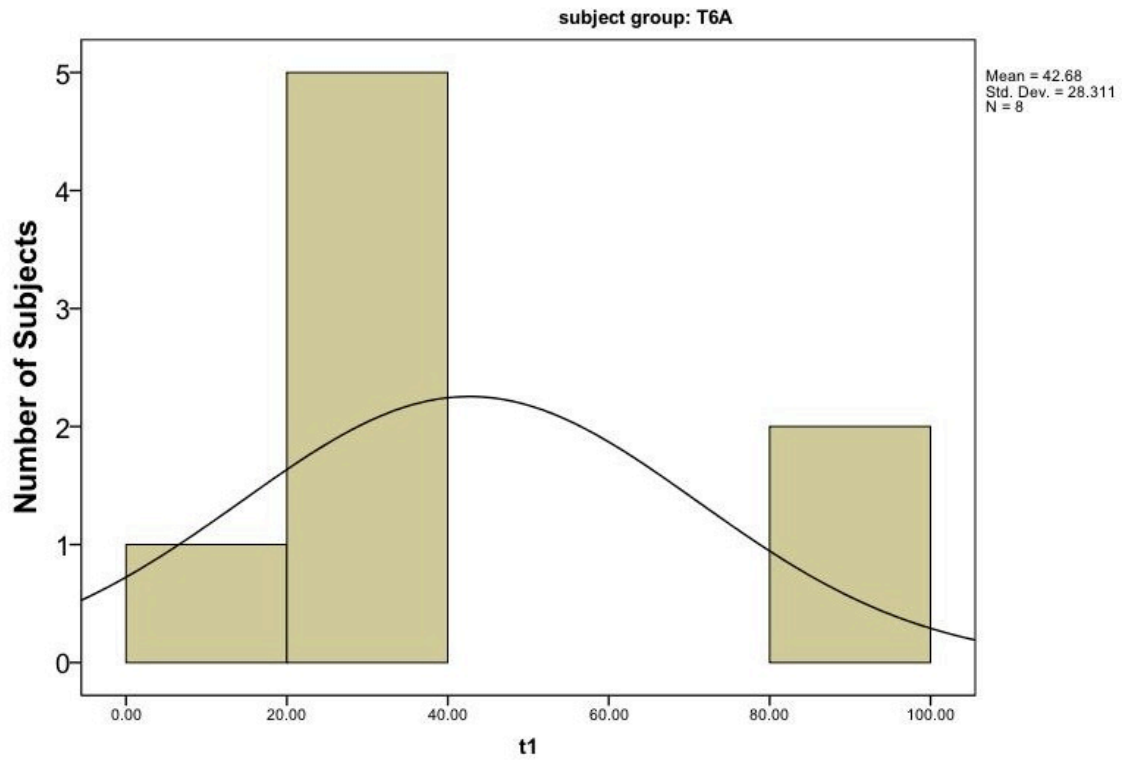
Control group: pressure only



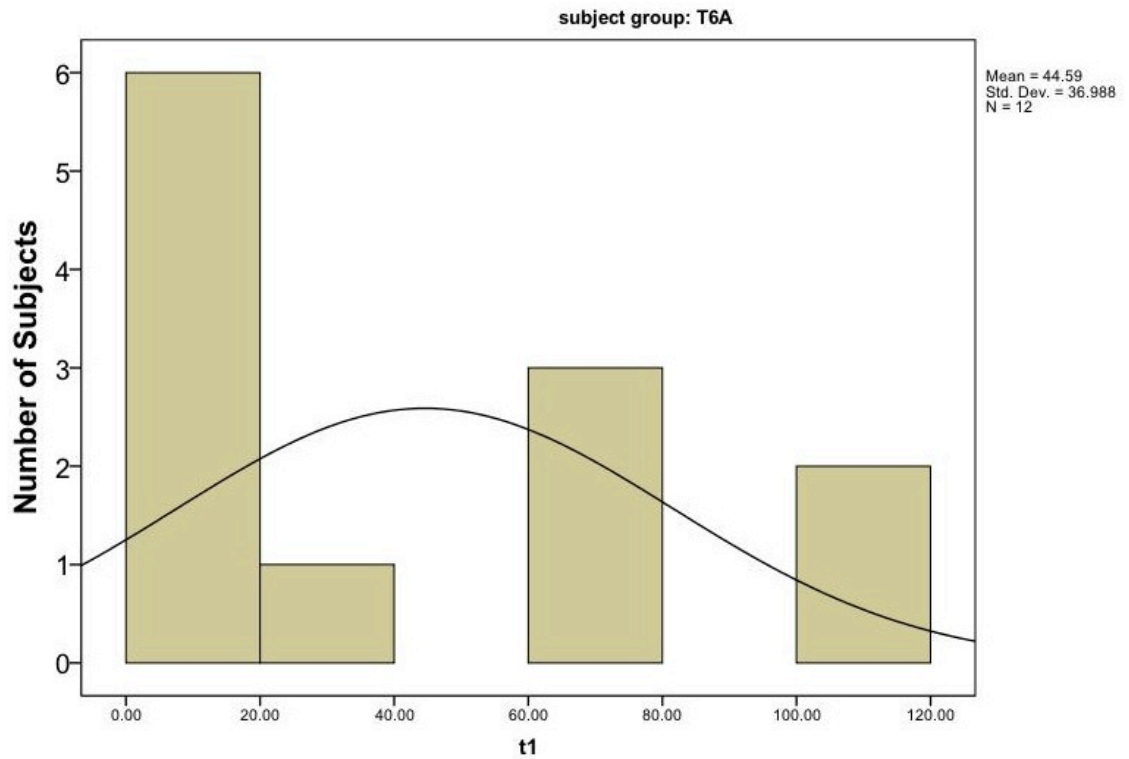
Control group: pressure with slow cooling



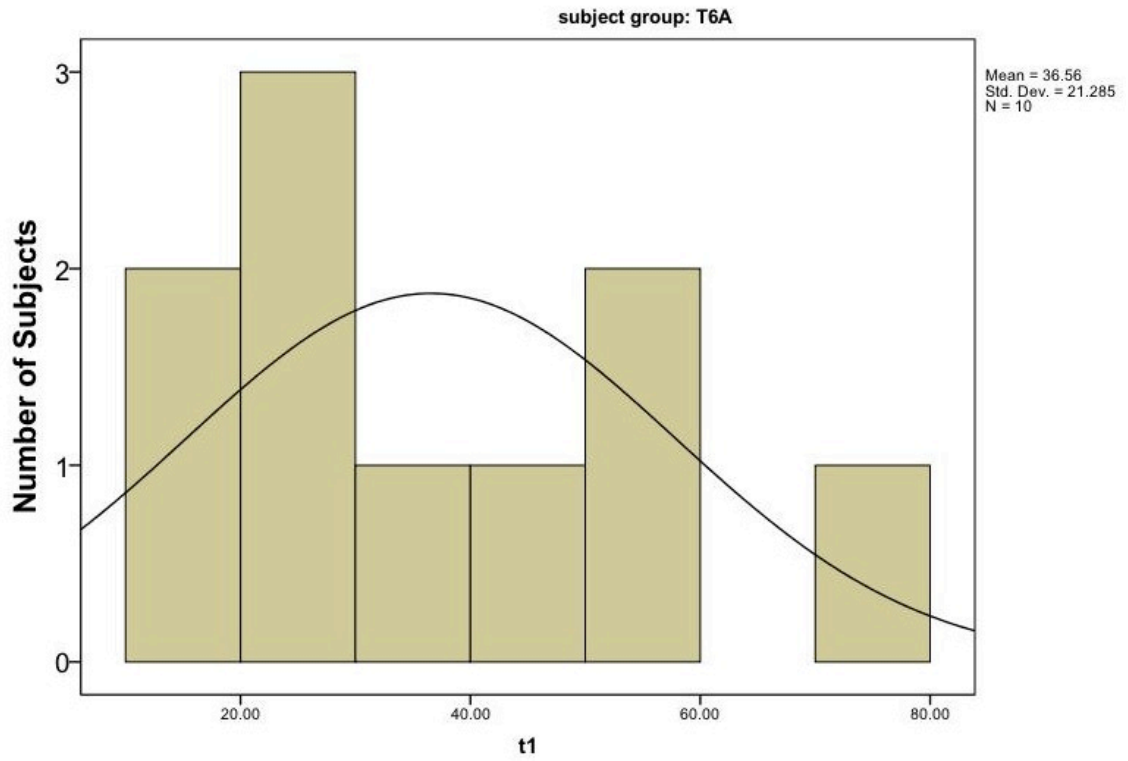
T6A group: pressure with fast cooling



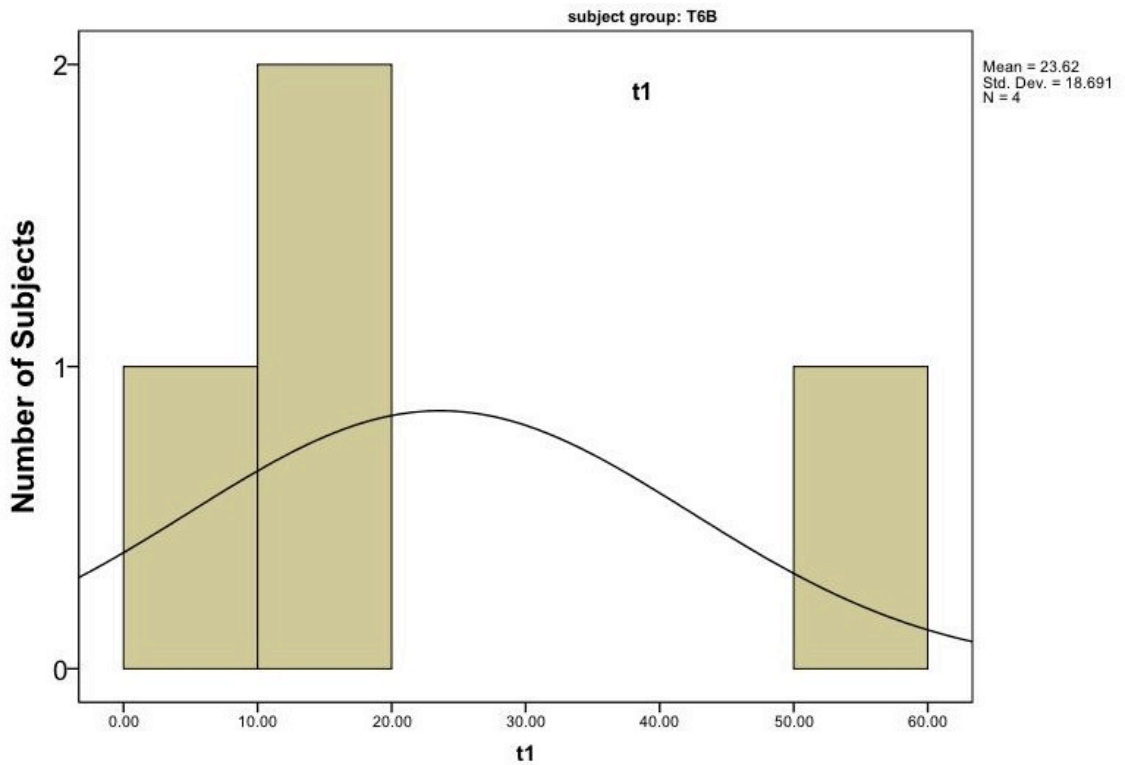
T6A group: pressure only



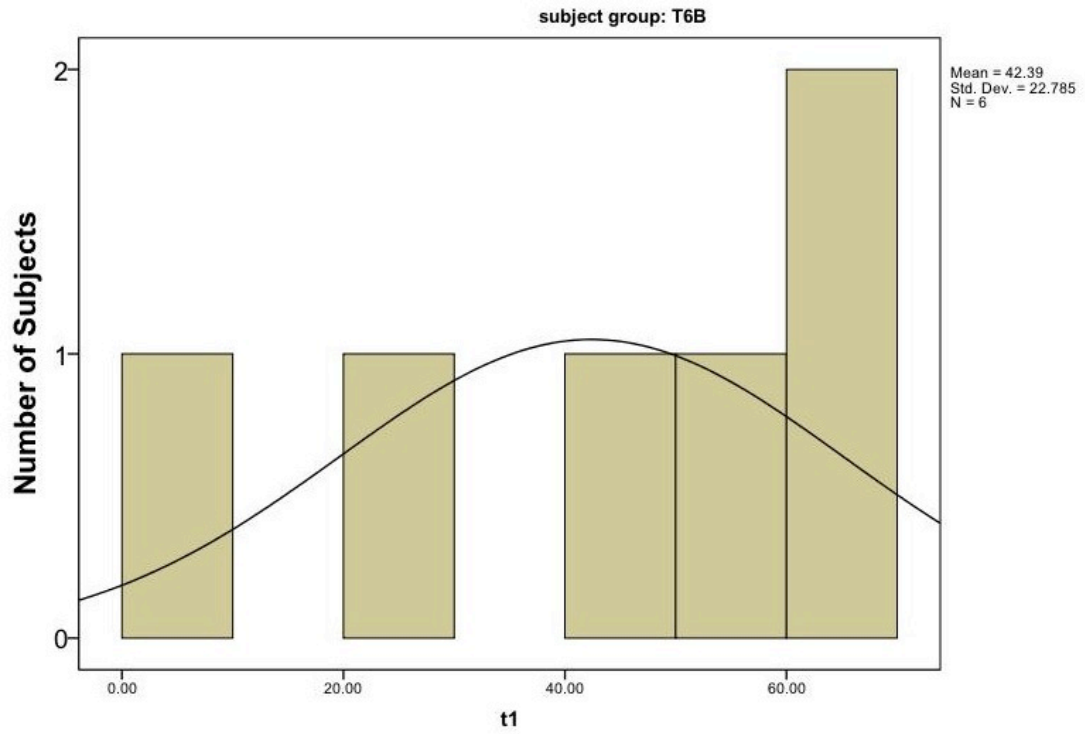
T6A group: pressure with slow cooling



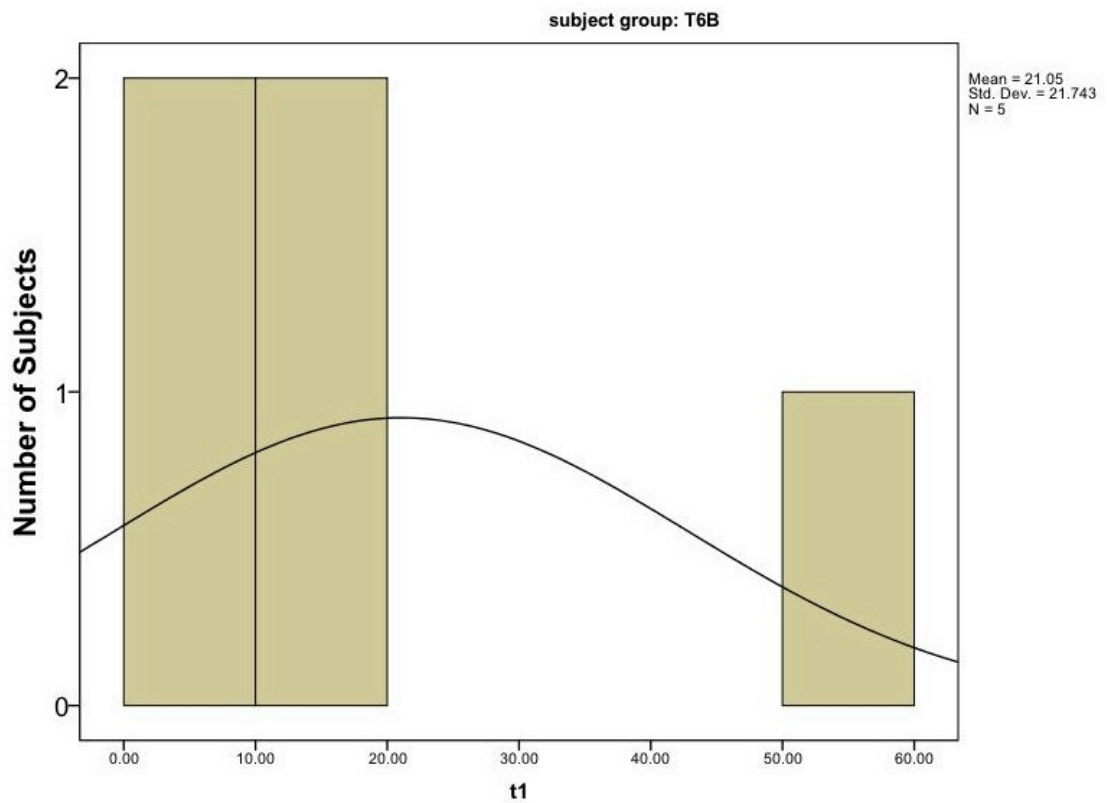
T6B group: pressure with fast cooling



T6B group: pressure only

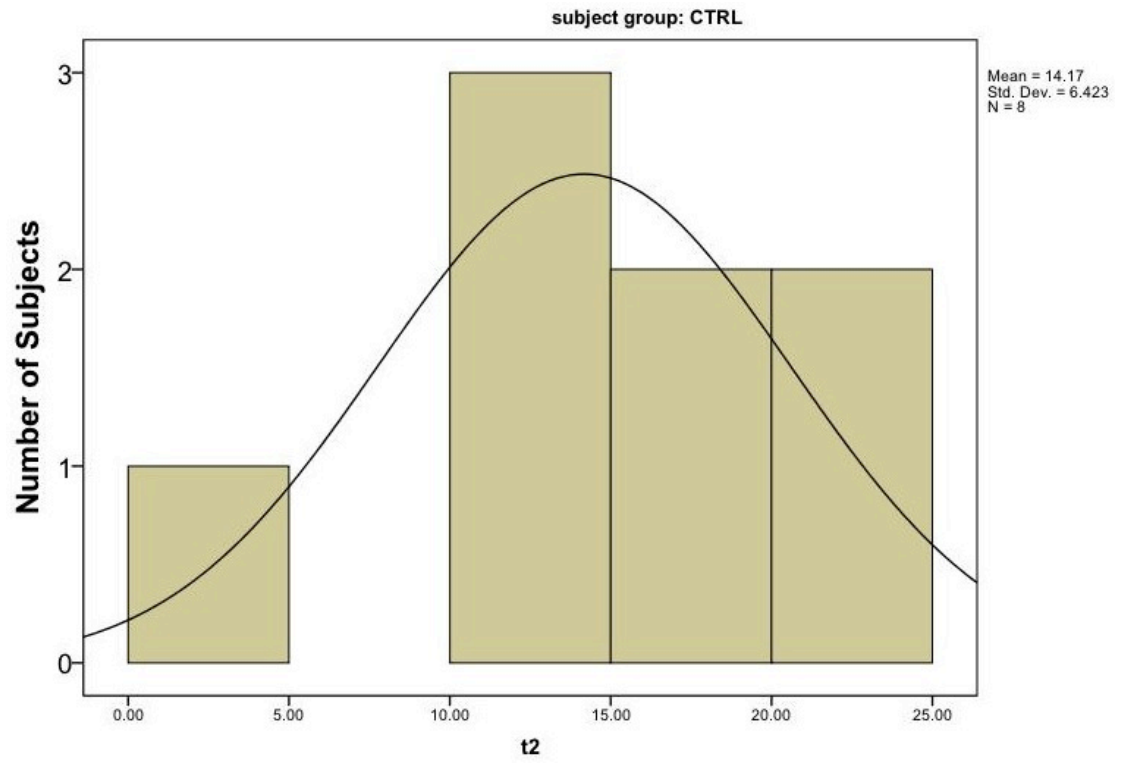


T6B group: pressure with slow cooling

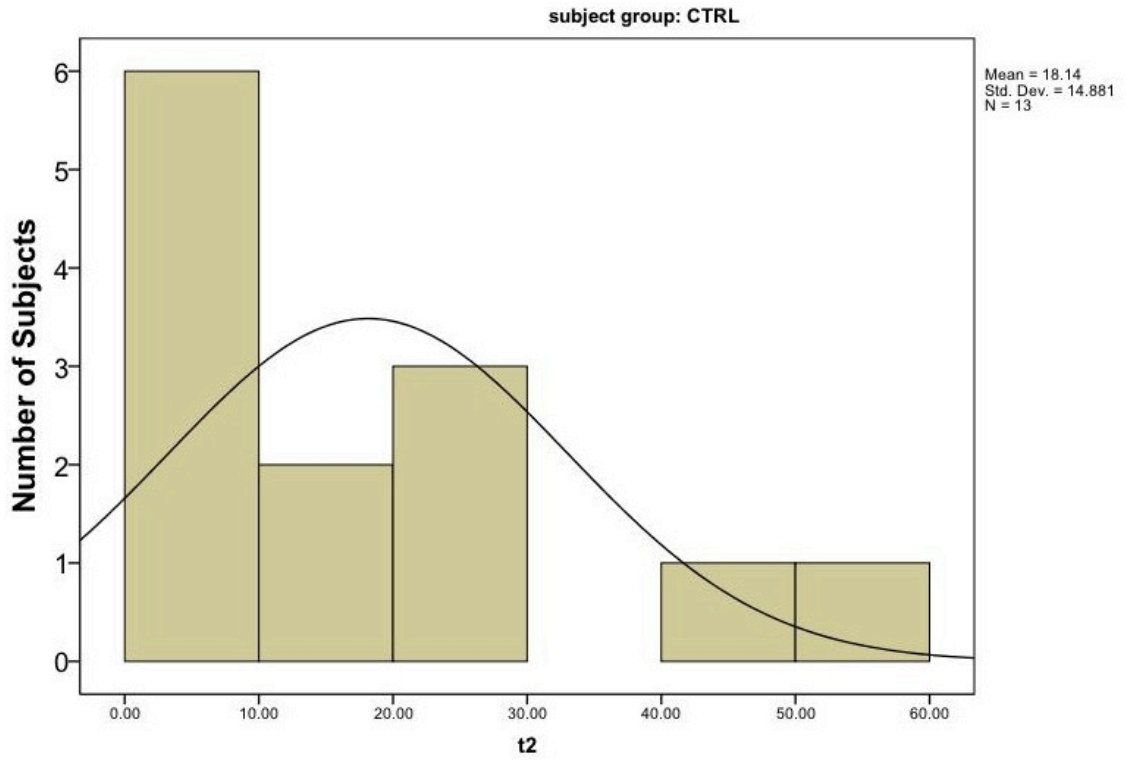


B.3 T₂

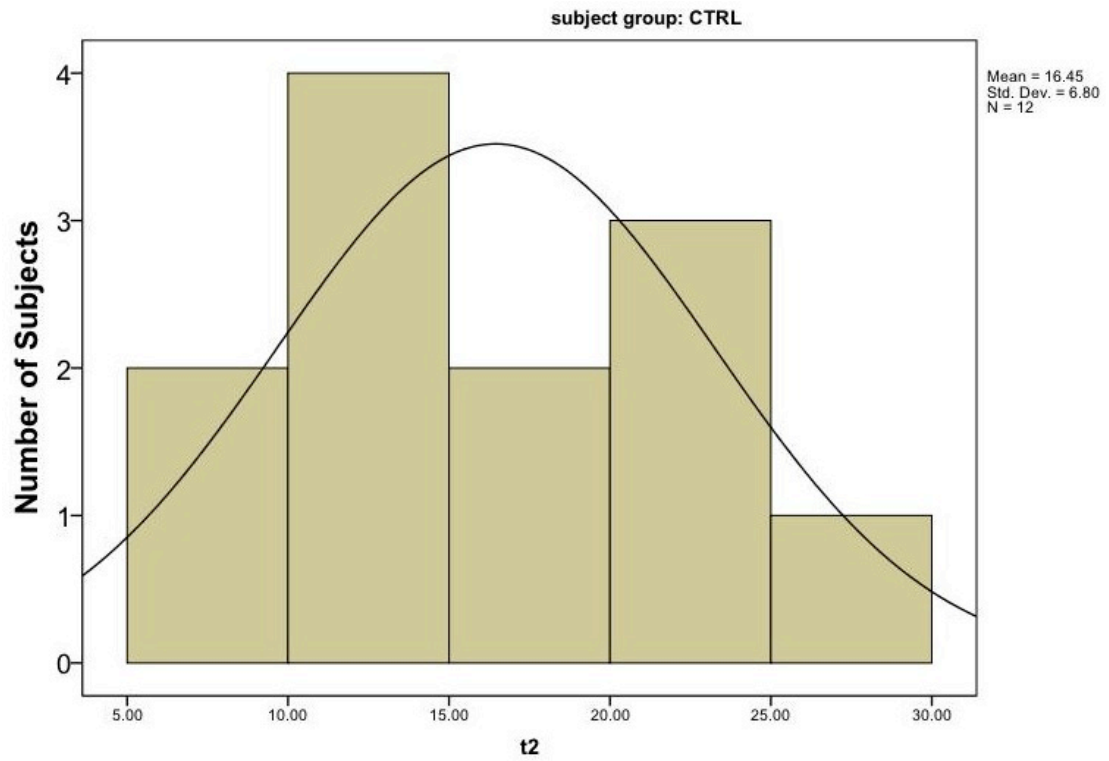
Control group: pressure with fast cooling



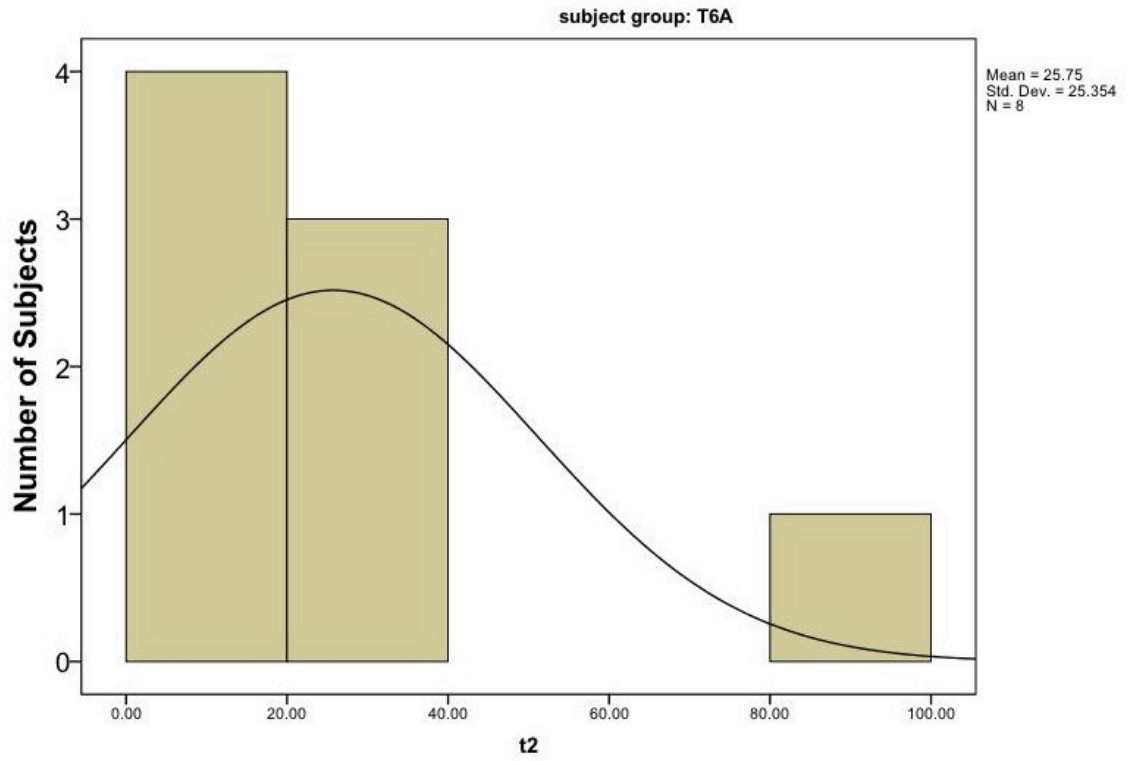
Control group: pressure only



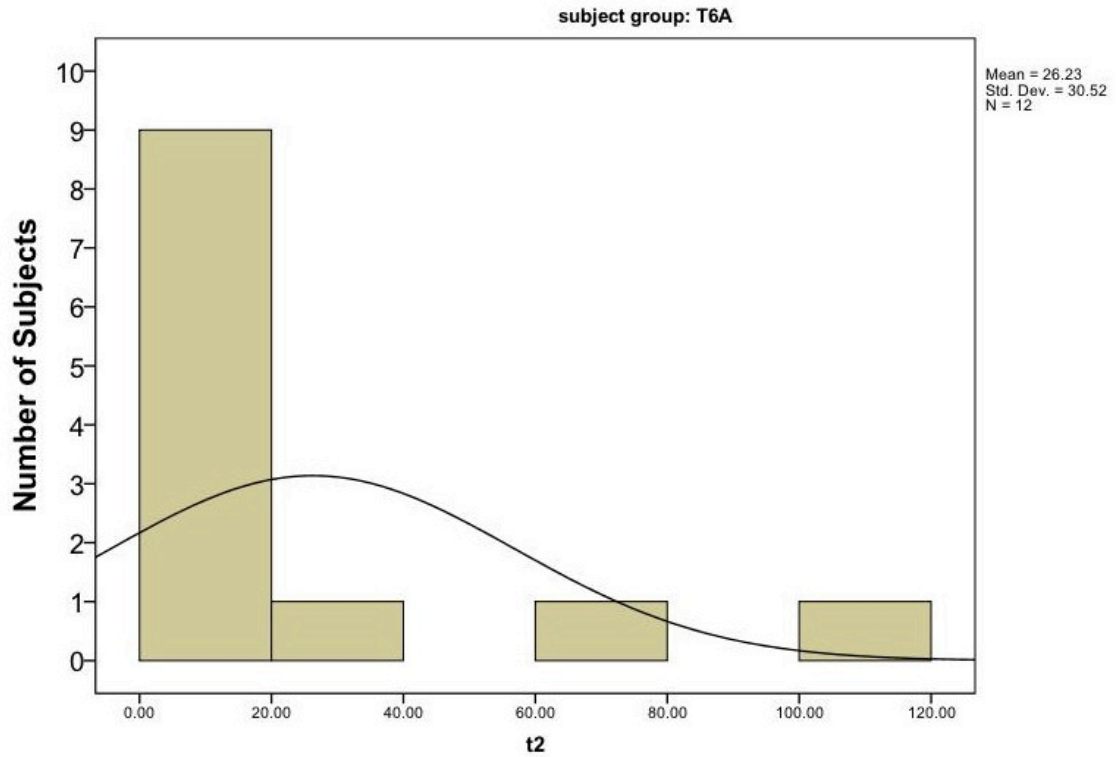
Control group: pressure with slow cooling



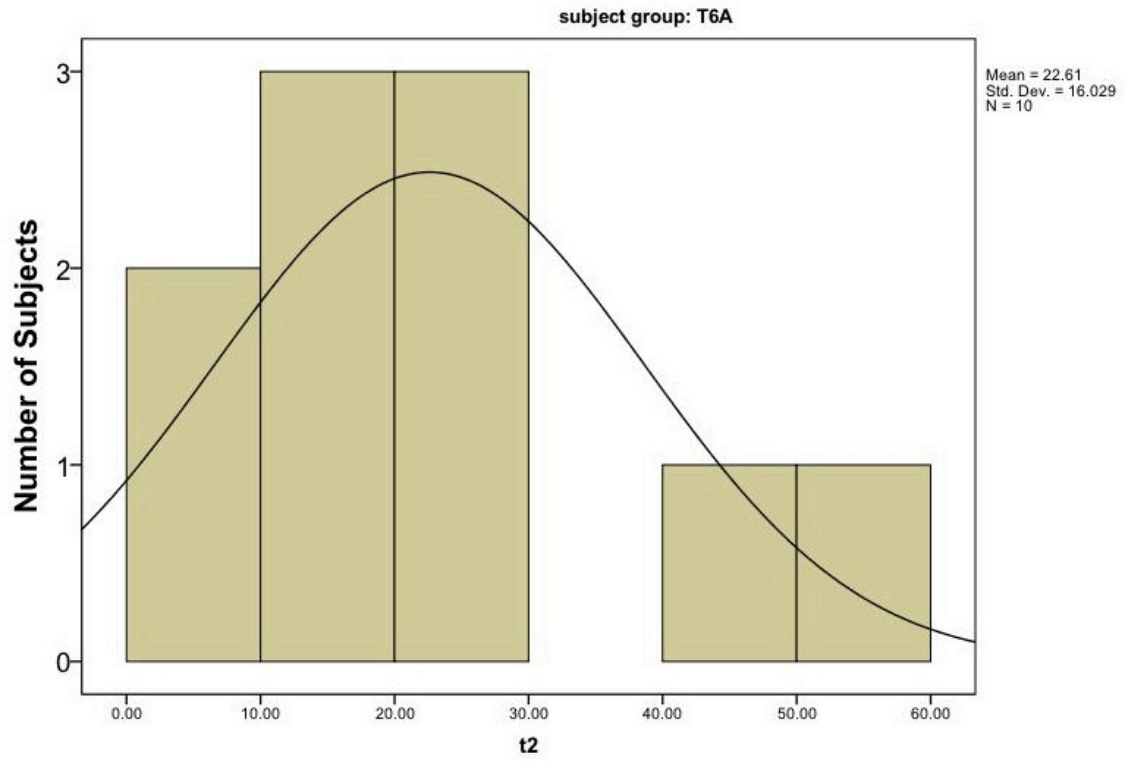
T6A group: pressure with fast cooling



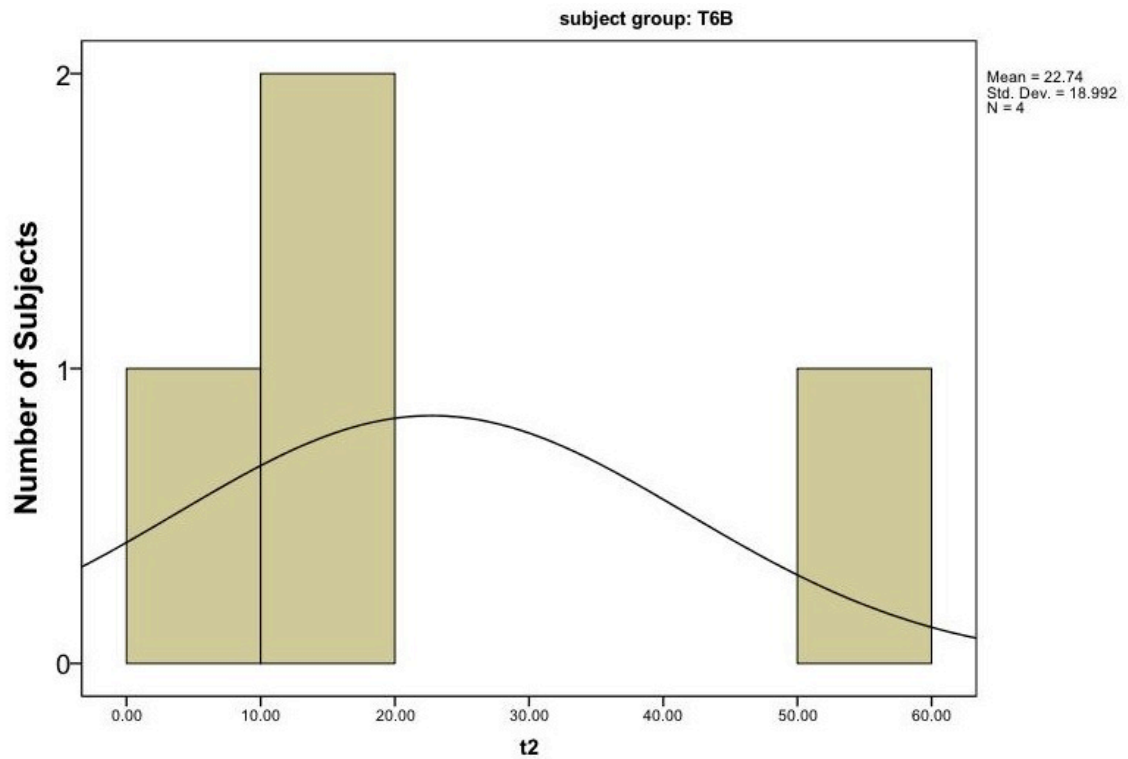
T6A group: pressure only



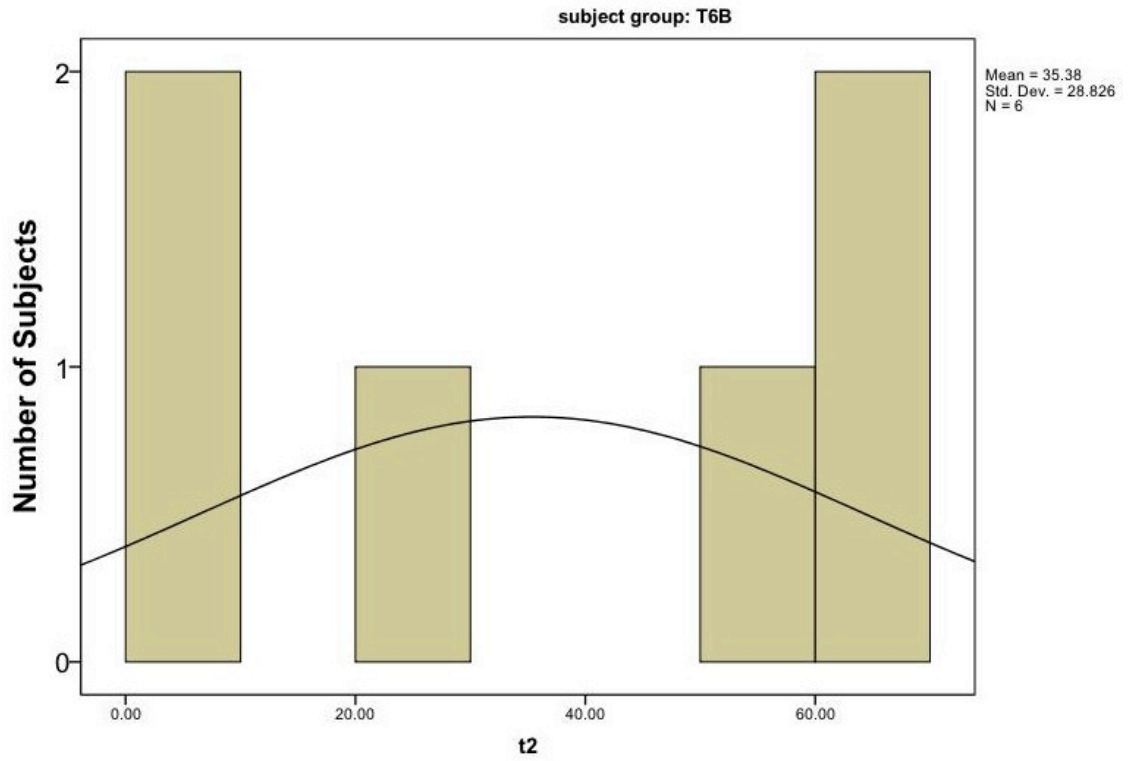
T6A group: pressure with slow cooling



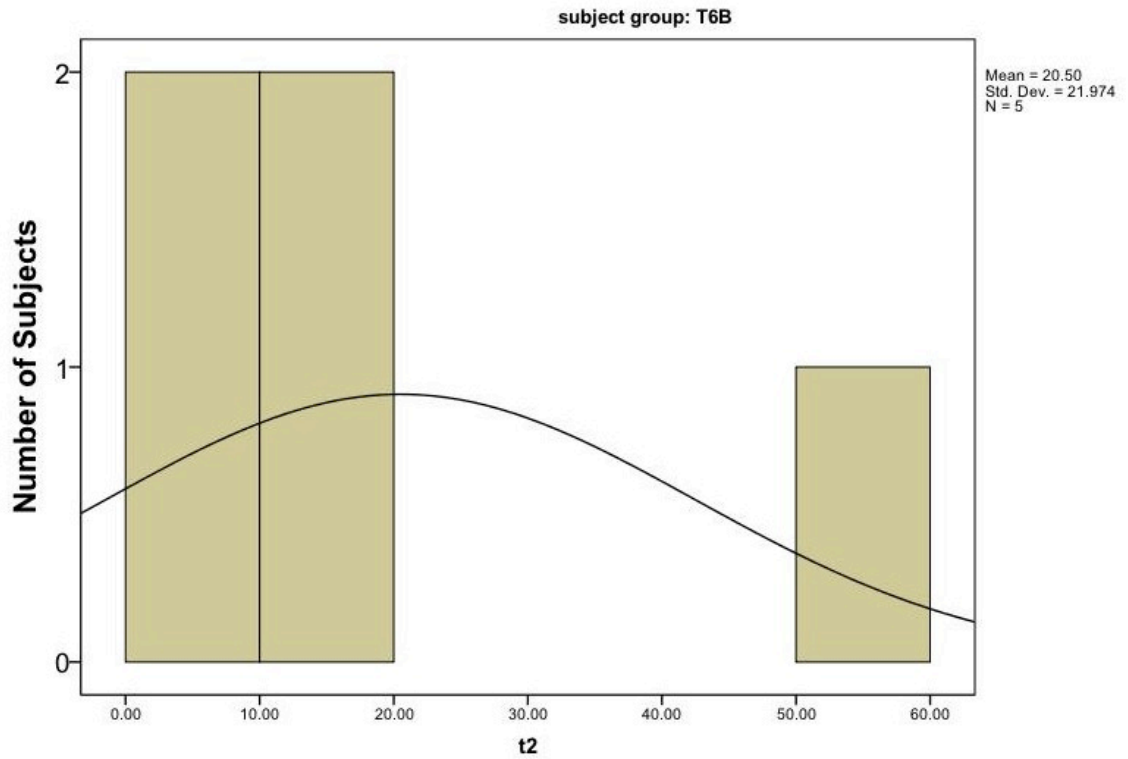
T6B group: pressure with fast cooling



T6B group: pressure only



T6B group: pressure with slow cooling



BIBLIOGRAPHY

- Alexander, L. R., Spungen, A., Liu, M., Losada, M., & Bauman, W. (1995). Resting metabolic rate in subjects with paraplegia: the effect of pressure sores. *Arch Phys Med Rehabil*, *76*, 819-822.
- Allman, R. M. (1989). Pressure ulcers among the elderly. *N Engl J Med*, *320*, 850-853.
- Allman, R. M. (1997). Pressure ulcer prevalence, incidence, risk factors, and impact. *Clin Geriatr Med*, *13*(3), 421-436.
- American Spinal Injury Association. (2006). Standard neurological classification of spinal cord injury. Retrieved July, 2009, from http://www.asia-spinalinjury.org/publications/2006_Classif_worksheet.pdf
- Amlung, S. R., Miller, W. L., & Bosley, L. M. (2001). The 1999 national pressure ulcer prevalence survey: a benchmarking approach. *Adv Skin Wound Care*, *14*(6), 297-301.
- Azman-Juvan, K., Bernjak, A., Urbancic-Rovan, V., Stefanovska, A., & Stajer, D. (2007). Skin blood flow and its oscillatory components in patients with acute myocardial infarction. *J Vasc Res*, *45*, 164-172.
- Bader, D. L. (1990). The recovery characteristics of soft tissues following repeated loading. *J Rehabil Res Dev*, *27*(2), 141-150.
- Bansal, C., Scott, R., Stewart, D., & Cockerell, C. J. (2005). Decubitus ulcers: A review of the literature. *Int J Dermatol*, *44*, 805-810.
- Bayliss, W. (1902). On the local reactions of the arterial wall to changes of internal pressure. *J Physiol*, *28*, 220-231.
- Bellien, J., Iacob, M., Gutierrez, L., Isabelle, M., Lahary, A., Thuillez, C., et al. (2006). Crucial role of NO and endothelium-derived hyperpolarizing factor in human sustained conduit artery flow-mediated dilatation. *Hypertension*, *48*, 1088-1094.
- Bennett, L., Kavner, D., Lee, B. K., & Trainor, F. A. (1979). Shear vs pressure as causative factors in skin blood flow occlusion. *Arch Phys Med Rehabil*, *60*, 309-314.
- Bergstrom, N. (2005). Patients at risk for pressure ulcers and evidence-based care for pressure ulcer prevention. In D. L. Bader, C. V. Bouten, D. Colin & C. W. Oomens (Eds.), *Pressure ulcer research* (pp. 35-50). Berlin: Springer-Verlag.
- Berlowitz, D. R., & Wilking, S. V. (1989). Risk factors for pressure sores. A comparison of cross-sectional and cohort-derived data. *J Am Geriatr Soc*, *37*(11), 1043-1050.
- Bogie, K., & Bader, D. L. (2005). Susceptibility of spinal cord-injured individuals to pressure ulcers. In D. L. Bader, C. V. Bouten, D. Colin & C. W. Oomens (Eds.), *Pressure ulcer research* (pp. 73-88). Berlin: Springer-Verlag.

- Bongard, O., & Bounameaux, H. (1993). Clinical investigation of skin microcirculation. *Dermatology*, *186*(1), 6-11.
- Bouten, C. V., Knight, M. M., Lee, D. A., & Bader, D. L. (2001). Compressive deformation and damage of muscle cell subpopulations in a model system. *Ann Biomed Eng*, *29*, 153-163.
- Bouten, C. V., Oomens, C. W., Colin, D., & Bader, D. L. (2005). The aetiopathology of pressure ulcers: a hierarchical approach. In D. L. Bader, C. V. Bouten, D. Colin & C. W. Oomens (Eds.), *Pressure ulcer research* (pp. 1-10). Berlin: Springer-Verlag.
- Bracic, M., & Stefanovska, A. (1998). Wavelet-based analysis of human blood flow dynamics. *B Math Biol*, *60*, 919-935.
- Bracic, M., & Stefanovska, A. (1999). Wavelet analysis in studying the dynamics of blood circulation. *NPCS*, *2*(1), 68-77.
- Braden, B., & Bergstrom, N. (1988). Braden scale for predicting pressure sore risk. 2007, from <http://www.bradenscale.com/braden.PDF>
- Braden, B., & Bergstrom, N. (2000). A conceptual schema for the study of the etiology of pressuresores. *Rehab Nurs*, *25*, 105-110.
- Breuls, R. G. M., Bouten, C. V., Oomens, C. W., Bader, D. L., & Baaijens, F. P. (2003). Compression induced cell damage in engineered muscle tissue: an in vitro model to study pressure ulcer aetiology. *Ann Biomed Eng*, *31*, 1357-1364.
- Brienza, D. M., & Karg, P. E. (1998). Seat cushion optimization: a comparison of interface pressure and tissue stiffness characteristics for spinal cord injured and elderly patients. *Arch Phys Med Rehabil*, *79*, 388-394.
- Brienza, D. M., Karg, P. E., Geyer, M. J., Kelsey, S., & Treffler, E. (2001). The relationship between pressure ulcer incidence and buttock-seat cushion interface pressure in at-risk elderly wheelchair users. *Arch Phys Med Rehabil*, *82*(4), 529-533.
- Byrne, D. W., & Salzberg, C. A. (1996). Major risk factors for pressure ulcers in the spinal cord disabled: a literature review. *Spinal Cord*, *34*, 255-263.
- Cardenas, D. D., Hoffman, J. M., Kirshblum, S., & McKinley, W. (2004). Etiology and incidence of rehospitalization after traumatic spinal cord injury: a multicenter analysis. *Arch Phys Med Rehabil*, *85*(11), 1757-1763.
- Carlsson, I., Sollevi, A., & Wennmalm, A. (1987). The role of myogenic relaxation, adenosine, and prostaglandins in human forearm reactive hyperemia. *J Physiol*, *389*, 147-161.
- Castro, M. J., Apple Jr., D. F., Staron, R. S., Campos, G. E., & Dudley, G. A. (1999). Influence of complete spinal cord injury on skeletal muscle within 6 mo of injury. *J Appl Physiol*, *86*(1), 350-358.
- Centers for Disease Control and Prevention. (1998). Spinal cord injury: fact sheet. Retrieved July, 2010: <http://www.cdc.gov/TraumaticBrainInjury/scifacts.html>
- Chen, Q., Carmara, A. K. S., An, J., Riess, M. L., Novalija, E., & Stowe, D. F. (2002). Cardiac preconditioning with 4-h, 17°C ischemia reduces [Ca²⁺]_i load and damage in part via KATP channel opening. *Am J Physiol Heart Circ Physiol*, *282*, 1961-1969.
- Chen, Y., DeVivo, M. J., & Jackson, A. B. (2005). Pressure ulcer prevalence in people with spinal cord injury: age-period-duration effects. *Arch Phys Med Rehabil*, *86*, 1208-1213.
- Chitwood, J., W. Randolph, Sink, J. D., Hill, R. C., Wechsler, A. S., & Sabiston, J., David C. (1979). The effects of hypothermia on myocardial oxygen consumption and transmural coronary blood flow in the potassium-arrested heart. *Ann Surg*, *190*(1), 106-116.

- Choi, S., Noh, J., Hirose, R., Ferrell, L., Bedolli, M., Roberts, J. P., et al. (2005). Mild Hypothermia provides significant protection against ischemia/ reperfusion injury in livers of obese and lean rats. *Ann Surg*, 241, 470-476.
- Cochran, G. V. B. (1985). *Measurement of pressure and other environmental factors at the patient-cushion interface*. New York: McGraw-Hill.
- Cohen, L. (1995a). The need for time-frequency analysis *Time-frequency analysis* (pp. 70-81). Englewood Cliffs, NJ: Prentice-Hall, Inc. .
- Cohen, L. (1995b). The short-time Fourier transform *Time-frequency analysis* (pp. 93-112). Englewood Cliffs, NJ: Prentice-Hall, Inc. .
- Cohen, L. (1995c). The time and frequency description of signals *Time-frequency analysis* (pp. 1-26). Englewood Cliffs, NJ: Prentice-Hall, Inc. .
- Cracowski, J.-L., Minson, C. T., Salvat-Melis, M., & Halliwill, J. R. (2006). Methodological issues in the assessment of skin microvascular endothelial function in humans. *Trends Pharmacol Sci*, 27, 503-508.
- de Mul, F. F. M., Morales, F., Smit, A. J., & Graaff, R. (2005). A model for post-occlusive reactive hyperemia as measured with laser-Doppler perfusion monitoring. *IEEE T Bio-med Eng*, 52(2), 184-190.
- Di Renzo, M., Marnica, G., Parati, A., Pedott, A., & Zanchetti, A. (1995). *Computer analysis of cardiovascular signals*. Amsterdam: IOS press.
- Diederich, R., Mowlavi, A., Meldrum, G., Medling, B., Bueno, R., & M, N. (2009). Local cooling provides muscle flaps protection from ischemia-reperfusion injury in the event of venous occlusion during the early reperfusion period. *Hand*, 4, 19-23.
- Dinsdale, S. M. (1974). Decubitus ulcers: role of pressure and friction in causation. *Arch Phys Med Rehabil*, 55, 147-152.
- Engelke, K., Halliwill, J., Proctor, D., Dietz, N., & Joyner, M. (1996). Contribution of nitric oxide and prostaglandins to reactive hyperemia in the human forearm. *J Appl Physiol*, 81(4), 1807-1814.
- Erecinska, M., Thoresen, M., & Silver, I. (2003). Effects of hypothermia on energy metabolism in mammalian central nervous system. *J Cerebr Blood F Met*, 23, 513-530.
- Exton-smith, A. N., & Sherwin, R. W. (1961). The prevention of pressure sores: significance of spontaneous bodily movements. *Lancet*, 2, 1124-1125.
- Fisher, S. V., Szymke, T. E., Aptem, S. Y., & Kosiak, M. (1978). Wheelchair cushion effect on skin temperature. *Arch Phys Med Rehabil*, 59, 68-71.
- Flavahan, N. A. (1991). The role of vascular $\alpha 2$ -adrenoceptors as cutaneous thermosensors. *News Physiol Sci*, 6, 251-255.
- Garber, S. L., & Rintala, D. H. (2003). Pressure ulcers in veterans with spinal cord injury: a retrospective study. *J Rehabil Res Dev*, 40(5), 433-442.
- Garcia, A. e. D., & Thomas, D. R. (2006). Assessment and management of chronic pressure ulcers in the elderly. *Med Clin North Am*, 90(5), 925-944.
- Gelis, A., Dupeyron, A., Legros, P., Benaim, C., Pelissier, J., & Fattal, C. (2009). Pressure ulcer risk factors in persons with spinal cord injury part 2: the chronic stage. *Spinal Cord*, 47(9), 651-661.
- Geyer, M. J., Jan, Y.-K., Brienza, D. M., & Boninger, M. L. (2004). Using wavelet analysis to characterize the thermoregulatory mechanisms of sacral skin blood flow. *J Rehabil Res Dev*, 41(6A), 797-806.

- Ghazanfari, M., Vogt, L., Banzer, W., & Rhodius, U. (2002). Reproducibility of non-invasive blood flow measurements using laser Doppler Spectroscopy. *Phys Med Rehab Kuror*, *12*, 330-336.
- Giangregorio, L., & McCartney, N. (2006). Bone loss and muscle atrophy in spinal cord injury: epidemiology, fracture prediction, and rehabilitation strategies. *J Spinal Cord Med*, *29*, 489-500.
- Goldstein, B., & Sanders, J. (1998). Skin response to repetitive mechanical stress: a new experimental model in pig. *Arch Phys Med Rehabil*, *79*(3), 265-272.
- Goossens, R. H. M., Zegers, R., Hoek van Dijke, G. A., & Snijders, C. J. (1994). Influence of shear on skin oxygen tension. *Clin Physiol*, *14*, 111-118.
- Hagisawa, S., Ferguson-Pell, M., Cardi, M., & Miller, D. (1994). Assessment of skin blood content and oxygenation in spinal cord injured subjects during reactive hyperemia. *J Rehabil Res Dev*, *31*(1), 1-14.
- Haisma, J. A., van der Woude, L. H., Stam, H. J., Bergen, M. P., Sluis, T. A., Post, M. W., et al. (2007). Complications following spinal cord injury: occurrence and risk factors in a longitudinal study during and after inpatient rehabilitation. *J Rehabil Med*, *39*(5), 393-398.
- Hochachka, P. W. (1986). Defense strategies against hypoxia and hypothermia. *Science*, *231*(234-41).
- Hokfelt, T. M., Johansson, O., Ljungdahl, A., Lundberg, J. M., & Schultzberg, M. (1980). Peptidergic neurones. *Nature*, *284*, 515-521.
- Holowatz, L. A., Houghton, B. L., Wong, B. J., Wilkins, B. W., Harding, A. W., Kenney, W. L., et al. (2003). Nitric oxide and attenuated reflex cutaneous vasodilation in aged skin. *Am J Physiol Heart Circ Physiol*, *284*(5), H1662-1667.
- Holzle, F., Loeffelbein, D. J., Nolte, D., & Wolff, K.-D. (2006). Free flap monitoring using simultaneous non-invasive laser Doppler flowmetry and tissue spectrophotometry. *J Craniomaxillofac Surg*, *34*, 25-33.
- Humeau, A., Saumet, J. L., & L'Huillier, J. P. (2000). Use of wavelets to accurately determine parameters of laser Doppler reactive hyperemia. *Microvasc Res*, *60*, 141-148.
- Iaizzo, P. A., Kveen, G. L., Kokate, J. Y., Leland, K. J., Hansen, G. L., & Sparrow, E. M. (1995). Prevention of pressure ulcers by focal cooling: histological assessment in a porcine model. *Wounds*, *7*(5), 161-169.
- Jackson, W. F. (2000). Ion channels and vascular tone. *Hypertension*, *35*(1 Pt 2), 173-178.
- Jan, Y.-K., & Brienza, D. M. (2006). Technology for pressure ulcer prevention. *Top Spinal Cord Inj Rehabil*, *11*(4), 30-41.
- Jan, Y.-K., Brienza, D. M., & Geyer, M. J. (2005). Analysis of week-to-week variability in skin blood flow measurements using wavelet transforms. *Clin Physiol Funct Imaging*, *25*, 253-262.
- Jan, Y.-K., Brienza, D. M., Geyer, M. J., & Karg, P. E. (2008). Wavelet-based spectrum analysis of sacral skin blood flow response to alternating pressure. *Arch Phys Med Rehabil*, *89*, 137-145.
- Johnson, J. M. (2007). Mechanisms of vasoconstriction with direct skin cooling in humans. *Am J Physiol Heart Circ Physiol*, *292*, H1690-1691.
- Johnson, J. M., Yen, T. C., Zhao, K., & Kosiba, W. A. (2005). Sympathetic, sensory, and nonneuronal contributions to the cutaneous vasoconstrictor response to local cooling. *Am J Physiol Heart Circ Physiol*, *288*(4), 1573-1579.

- Kanemoto, S., Matsubara, M., Noma, M., Leshnower, B., Parish, L., Jackson, B., et al. (2009). Mild hypothermia to limit myocardial ischemia-reperfusion injury: importance of timing. *Ann Thorac Surg*, *87*, 157-163.
- Kastrup, J., Bülow, J., & Lassen, N. A. (1989). Vasomotion in human skin before and after local heating recorded with laser Doppler flowmetry. A method for induction of vasomotion. *Int J Microcirc Clin Exp*, *8*(2), 205-215.
- Kellogg, D. L. (2006). In vivo mechanisms of cutaneous vasodilation and vasoconstriction in humans during thermoregulatory challenges. *J Appl Physiol*, *100*(5), 1709-1718.
- Kellogg, D. L., Crandall, Y. L., Chrarkoudian, N., & Johnson, J. M. (1998). Nitric oxide and cutaneous active vasodilation during heat stress in humans. *J Appl Physiol*, *85*(3), 824-829.
- Kellogg, D. L., Liu, Y., Kosiba, I. F., & O'Donnell, D. (1999). Role of nitric oxide in the vascular effects of local warming of the skin in humans. *J Appl Physiol*, *86*, 1185-1190.
- Kellogg, D. L., Pergola, P. E., Piest, K. L., Kosiba, W. A., Crandall, C. G., Grossmann, M., et al. (1995). Cutaneous active vasodilation in humans is mediated by cholinergic nerve cotransmission. *Circ Res*, *77*(6), 1222-1228.
- Kilbom, A., & Wennmalm, A. (1976). Endogenous prostaglandins as local regulators of blood flow in man: effect of indomethacin on reactive and functional hyperemia. *J Physiol*, *257*, 109-121.
- Kind, G., Buntic, R., Buncke, G., Cooper, T., Siko, P., & Buncke Jr, H. (1998). The effect of an implantable Doppler probe on the salvage of microvascular tissue transplants. *Plast Reconstr Surg*, *101*, 1268-1273.
- Knight, S. L., Taylor, R. P., Polliack, A. A., & Bader, D. L. (2001). Establishing predictive indicators for the status of loaded soft tissues. *J Appl Physiol*, *90*, 2231-2237.
- Kokate, J. Y., Leland, K. J., Held, A. M., Hansen, G. L., Kveen, G. L., Johnson, B. A., et al. (1995). Temperature-modulated pressure ulcers: a porcine model. *Arch Phys Med Rehabil*, *76*, 666-673.
- Koller, A., & Bagi, Z. (2002). On the role of mechanosensitive mechanisms eliciting reactive hyperemia. *Am J Physiol Heart Circ Physiol*, *283*, H2250-2259.
- Kooijman, M. (2008). *Regulation of peripheral vascular tone in spinal cord-injured individuals*. Radboud University Nijmegen, Nijmegen, The Netherlands.
- Kooijman, M., de Hoog, M., Rongen, G. A., van Kuppevelt, H. J., Smits, P., & Hopman, M. T. E. (2007). Local vasoconstriction in spinal cord-injured and able-bodied individuals. *J Appl Physiol*, *103*(3), 1070-1077.
- Kooijman, M., Rongen, G. A., Smit, A. J., & Hopman, M. T. E. (2003). Preserved alpha-adrenergic tone in the leg vascular bed of spinal cord-injured individuals. *Circulation*, *108*(19), 2361-2367.
- Kosiak, M. (1961). Etiology of decubitus ulcers. *Arch Phys Med Rehabil*, *42*, 19-29.
- Lachenbruch, C. (2005). Skin cooling surfaces: estimating the importance of limiting skin temperature. *Ostomy Wound Manage*, *51*(2), 70-79.
- Larkin, S. W., & Williams, T. J. (1993). Evidence for sensory nerve involvement in cutaneous reactive hyperemia in humans. *Circ Res*, *73*, 147-154.
- Levick, J. R. (2003). *Control of blood vessels I: intrinsic control* (4th ed.). New York: Oxford University Pr.

- Li, Z., Leung, J. Y., Tam, E. W., & Mak, A. F. (2006). Wavelet analysis of skin blood oscillations in persons with spinal cord injury and able-bodied subjects. *Arch Phys Med Rehabil*, *87*, 1207-1212.
- Linder-Ganz, E., & Gefen, A. (2007). The effects of pressure and shear on capillary closure in the microstructure of skeletal muscles. *Ann Biomed Eng*, *35*(12), 2095-2107.
- Linder-Ganz, E., Shabshin, N., Itzchak, Y., & Gefen, A. (2007). Assessment of mechanical conditions in sub-dermal tissues during sitting: a combined experimental-MRI and finite element approach. *J Biomech*, *40*(7), 1443-1454.
- Linder-Ganz, E., Shabshin, N., Itzchak, Y., Yizhar, Z., Siev-Ner, I., & Gefen, A. (2008). Strains and stresses in sub-dermal tissues of the buttocks are greater in paraplegics than in healthy during sitting. *J Biomech*, *41*, 567-580.
- Lindgren, M., Unosson, M., Fredrikson, M., & Ek, A. C. (2004). Immobility--a major risk factor for development of pressure ulcers among adult hospitalized patients: a prospective study. *Scand J Caring Sci*, *18*(1), 57-64.
- Lorenzo, S., & Minson, C. T. (2007). Human cutaneous reactive hyperaemia: role of BKCa channels and sensory nerves. *J Physiol*, *585*, 295-303.
- Matsubara, J., Narumi, J., Nagasue, M., Sakamoto, S., Yuasa, K., & Shimizu, T. (1998). Postocclusive reactive hyperemia during vascular reconstruction. *Int J Angiol*, *7*, 222-227.
- McCord, J. M. (1985). Oxygen-derived free radicals in postischemic tissue injury. *N Engl J Med*, *312*(3), 159-163.
- McKinley, W. O., Jackson, A. B., Cardenas, D. D., & DeVivo, M. J. (1999). Long-term medical complications after traumatic spinal cord injury: a regional model systems analysis. *Arch Phys Med Rehabil*, *80*(11), 1402-1410.
- Michenfelder, J., & Milde, J. (1991). The relationship among canine brain temperature, metabolism, and function during hypothermia. *Anesthesiology*, *75*, 130-136.
- Minson, C. T., Berry, L. T., & Joyner, M. (2001). Nitric oxide and neurally mediated regulation of skin blood flow during local heating. *J Appl Physiol*, *91*, 1619-1626.
- Mowlavi, A., Neumeister, M. W., Wilhelmi, B. J., Song, Y.-H., Suchy, H., & Russell, R. C. (2003). Local hypothermia during early reperfusion protects skeletal muscle from ischemia-reperfusion injury. *Plast Reconstr Surg*, *111*, 242-250.
- National Pressure Ulcer Advisory Panel. (2007a). Pressure ulcer definition and stages. 2007, from http://www.npuap.org/documents/PU_Definition_Stages.pdf
- National Pressure Ulcer Advisory Panel. (2007b). Support surface standards initiative terms and definitions. from http://www.invisiblecaregiver.com/docs/NPUAP_Standards.pdf
- Newson, T. P., & Rolfe, P. (1982). Skin surface PO₂ and blood flow measurements over the ischial tuberosity. *Arch Phys Med Rehabil*, *63*(11), 553-556.
- Niazi, Z. B., Salzberg, C. A., Byrne, D. W., & Viehbeck, M. (1997). Recurrence of initial pressure ulcer in persons with spinal cord injuries. *Adv Wound Care*, *10*, 38-42.
- Nicholson, P. W., Leeman, A. L., Dobbs, S. M., Denham, M. J., & Dobbs, R. J. (1988). Pressure sores: effect of parkinson's disease and cognitive function on spontaneous movement in bed. *Age Ageing*, *17*, 111-115.
- Noble, M., Voegeli, D., & Clough, G. F. (2003). A comparison of cutaneous vascular responses to transient pressure loading in smokers and nonsmokers. *J Rehabil Res Dev*, *40*(3), 283-288.

- Olive, J. L., McCully, K. K., & Dudley, G. A. (2002). Blood flow response in individuals with incomplete spinal cord injuries. *Spinal Cord*, 40, 639-645.
- Olivecrona, G. K., Gotberg, M., Harnek, J., Van der Pals, J., & Erlinge, D. (2007). Mild hypothermia reduces cardiac post-ischemia reactive hyperemia. *BMC Cardiovasc Disord*, 7, 5.
- Paker, N., Soy, D., Kesiktas, N., Nur Bardak, A., Erbil, M., Erson, S., et al. (2006). Reasons for rehospitalization in patients with spinal cord injury: 5 years' experience. *Int J Rehabil Res*, 29, 71-76.
- Patel, S., Knapp, C. F., Donofrio, J. C., & Salcido, R. (1999). Temperature effects on surface pressure-induced changes in rat skin perfusion: implications in pressure ulcer development. *J Rehabil Res Dev*, 36(3), 189-201.
- Peirce, S. M., Skalak, T. C., & Rodeheaver, G. T. (2000). Ischemia-reperfusion injury in chronic pressure ulcer formaion: A skin model in the rat. *Wound Repair Regen*, 8(1), 68-76.
- Pergola, P. E., Johnson, J. M., Kellogg, D. L., & Kosiba, W. A. (1996). Control of skin blood flow by whole body and local skin cooling in exercising humans. *Am J Physiol*, 270(1 Pt 2), H208-215.
- Pergola, P. E., Kellogg, D. L., Johnson, J. M., Kosiba, W. A., & Solomon, D. E. (1993). Role of sympathetic nerves in the vascular effects of local temperature in human forearm skin. *Am J Physiol*, 265(34), H785-792.
- Petrofsky, J. S. (1992). Thermoregulatory stress during rest and exercise in heat in patients with spinal cord injury. *Eur J Appl Physiol*, 64, 503-507.
- Preto, E. A. (1991). Reperfusion injury of the liver. *Transplant Proc*, 23, 1912-1914.
- Price, M. J. (2006). Thermoregulation during exercise in individuals with spinal cord injuries. *Sports Med*, 36(10), 863-870.
- Raghavan, P., Raza, W., Ahmed, Y., & Chamberlain, M. (2003). Prevalence of pressure sore in a community sample of spinal injury patients. *Clin Rehabil*, 17, 879-884.
- Reuler, J. B., & Cooney, T. G. (1981). The pressure sore: pathophysiology and principles of management. *Ann Intern Med*, 94, 661-666.
- Riess, M. L., Camara, A. K. S., Kevin, L. G., An, J., & Stowe, D. F. (2004). Reduced reactive O₂ species formation and preserved mitochondrial NADH and [Ca²⁺] levels during short-term 17°C ischemia in intact hearts. *Cardiovasc Res*, 61(3), 580-590.
- Rosomoff, H. L., & Holaday, D. A. (1954). Cerebral blood flow and cerebral oxygen consumption during hypothermia. *Am J Physiol*, 179(1), 85-88.
- Rossi, M., Carpi, A., Maria, C. D., Franzoni, F., Galetta, F., & Santoro, G. (2007). Post-ischemic peak flow and myogenic flowmotion component are independent variables for skin post-ischemic reactive hyperaemia in healthy subjects. *Microvasc Res*, 74, 9-14.
- Rowell, L. B. (1974). *The cutaneous circulation* (20th ed.). Philadelphia: Saunders Pr.
- Ruano, J., Lopez-Miranda, J., Fuentes, F., Moreno, J. A., Bellido, C., Perez-Martinez, P., et al. (2005). Phnolic content of virgin olive oil improves ischemic reactive hyperemia in hypercholesterolemic patients. *J Am Coll Cardiol*, 46(10), 1864-1868.
- Ruch, R. C., & Patton, H. D. (1965). *Energy metabolism* (19th ed.). Philadelphia: Saunders Pr.
- Sae-Sia, W., Wipke-Tevis, D. D., & Williams, D. A. (2007). The effect of clinically relevant pressure duration on sacral skin blood flow and temperature in patients after acute spinal cord injury. *Arch Phys Med Rehabil*, 88, 1673-1680.

- Salcido, R., Fisher, S. B., Donofrio, J. C., Bieschke, M., Knapp, C., Liang, R., et al. (1995). An animal model and computer-controlled surface pressure delivery system for the production of pressure ulcers. *J Rehabil Res Dev*, 32(2), 149-161.
- Salzberg, C. A., Byrne, D. W., Cayten, C. G., van Niewerburgh, P., Murphy, J. G., & Viehbeck, M. (1996). A new pressure ulcer risk assessment scale for individuals with spinal cord injury. *Am J Phys Med Rehab*, 75, 96-104.
- Salzberg, C. A., Byrne, D. W., Kabir, R., van Niewerburgh, P., & Cayten, C. G. (1999). Predicting pressure ulcers during initial hospitalization for acute spinal cord injury. *Wounds*, 11(1), 45-57.
- Schubert, R., & Mulvany, M. (1999). The myogenic response: established facts and attractive hypotheses. *Clin Sci*, 96, 313-326.
- Schubert, V., & Fagrell, B. (1991a). Evaluation of the dynamic cutaneous post-ischaemic hyperaemia and thermal response in elderly subjects and in an area at risk for pressure sores. *Clin Physiol*, 11(2), 169-182.
- Schubert, V., & Fagrell, B. (1991b). Postocclusive reactive hyperemia and thermal response in the skin microcirculation of subjects with spinal cord injury. *Scand J Rehab Med*, 23, 33-40.
- Scremin, G., & Kenney, L. (2004). Aging and the skin blood flow response to the unloading of baroreceptors during heat and cold stress. *J Appl Physiol*, 96(3), 1019-1025.
- Segal, S. S., & Faulkner, J. A. (1985). Temperature-dependent physiological stability of rat skeletal muscle in vitro. *Am J Physiol*, 248(3 Pt 1), C265-270.
- Seiyama, A., Kosaka, H., Maeda, N., & Shiga, T. (1996). Effect of hypothermia on skeletal muscle metabolism in perfused rat hindlimb. *Cryobiology*, 33, 338-346.
- Seymour, R. J., & Lacefield, W. E. (1985). Wheelchair cushion effect on pressure and skin temperature. *Arch Phys Med Rehabil*, 66, 103-108.
- Shastry, S., Dietz, N. M., Halliwill, J. R., Reed, A. S., & Joyner, M. J. (1998). Effects of nitric oxide synthase inhibition on cutaneous vasodilation during body heating in humans. *J Appl Physiol*, 85(3), 830-834.
- Shibasaki, M., Wilson, T. E., Cui, J., & Crandall, C. G. (2002). Acetylcholine released from cholinergic nerves contributes to cutaneous vasodilation during heat stress. *J Appl Physiol*, 93, 1947-1951.
- Skrha, J., Prazn, M., Haas, T., Kvasnicka, J., & Kalvodova, B. (2001). Comparison of laser-Doppler flowmetry with biochemical indicators of endothelial dysfunction related to early microangiopathy in Type 1 diabetic patients. *J Diabetes Complicat*, 15, 234-240.
- Sprigle, S., Linden, M., & Riordan, B. (2002). Characterizing reactive hyperemia via tissue reflectance spectroscopy in response to an ischemic load across gender, age, skin pigmentation and diabetes. *Med Eng Phys*, 24(10), 651-661.
- Stefanovska, A., Bracic, M., & Kvernmo, H. (1999). Wavelet analysis of oscillations in the peripheral blood circulation measured by laser Doppler technique. *IEEE T Bio-med Eng*, 46(10), 1230-1239.
- Stekelenburg, A., Oomens, C. W., Strijkers, G. J., Nicolay, K., & Bader, D. L. (2006). Compression-induced deep tissue injury examined with magnetic resonance imaging and histology. *J Appl Physiol*, 100(6), 1946-1954.
- Stephens, D. P., Aoki, K., Kosiba, W. A., & Johnson, J. M. (2001). Nonnoradrenergic mechanism of reflex cutaneous vasoconstriction in men. *Am J Physiol Heart Circ Physiol*, 280, H1496-1504.

- Stephens, D. P., Saad, A. R., Bennett, L. a. T., Kosiba, W. A., & Johnson, J. M. (2004). Neuropeptide Y antagonism reduces reflex cutaneous vasoconstriction in humans. *Am J Physiol Heart Circ Physiol*, 287, H1404-1409.
- Stewart, J., Kohen, A., Brouder, D., Rahim, F., Adler, S., Garrick, R., et al. (2004). Noninvasive interrogation of microvasculature for signs of endothelial dysfunction in patients with chronic renal failure. *Am J Physiol Heart Circ Physiol*, 287, H2687-2696.
- Stewart, S. F. C., Palmieri, V., & Cochran, G. V. B. (1980). Wheelchair cushion effect on skin temperature, heat flux, and relative humidity. *Arch Phys Med Rehabil*, 61, 229-233.
- Taylor, R., & James, T. (2005). The role of oxidative stress in the development and persistence of pressure ulcers. In D. L. Bader, C. V. Bouten, D. Colin & C. W. Oomens (Eds.), *Pressure ulcer research* (pp. 205-232). Berlin: Springer-Verlag.
- Thompson, C. S., Holowatz, L. A., Flavahan, N. A., & Kenney, L. (2007). Cold-induced cutaneous vasoconstriction is mediated by Rho kinase in vivo in human skin. *Am J Physiol Heart Circ Physiol*, 292, H1700-1705.
- Togawa, T., Tamura, T., & Öberg, P. Å. (1997a). *Chemical Measurement*. Boca Raton, Florida: CRC Press LLC.
- Togawa, T., Tamura, T., & Öberg, P. Å. (1997b). *flow measurement*. Boca Raton, Florida: CRC Press LLC.
- Tsuji, S., Ichioka, S., Sekiya, N., & Nakatsuka, T. (2005). Analysis of ischemia-reperfusion injury in a microcirculatory model of pressure ulcers. *Wound Repair Regen*, 13, 209-215.
- Tzen, Y., Brienza, D., Karg, P., & Loughlin, P. (2010). Effects of local cooling on sacral skin perfusion response to pressure: implications for pressure ulcer prevention. *J Tissue Viability*, *In press*.
- Wang, Y.-N., & Sanders, J. (2005). Skin model studies. In D. L. Bader, C. V. Bouten, D. Colin & C. W. Oomens (Eds.), *Pressure ulcer research* (pp. 263-285). Berlin: Springer-Verlag.
- Whittington, K. T., & Briones, R. (2004). National prevalence and incidence study: 6-year sequential acute care data. *Adv Skin Wound Care*, 17, 490-494.
- Wilkin, J. K. (1987). Cutaneous reactive hyperemia: viscoelasticity determines response. *J Invest Dermatol*, 89, 197-200.
- Witkowski, J. A., & Parish, L. C. (2000). The decubitus ulcer: skin failure and destructive behavior. *Int J Dermatol*, 39(12), 894-896.
- Yamazaki, F., Sone, R., Zhao, K., Alvarez, G. E., Kosiba, W. A., & Johnson, J. M. (2006). Rate dependency and role of nitric oxide in the vascular response to direct cooling in human skin. *J Appl Physiol*, 100, 42-50.
- Yarkony, G. M. (1994). Pressure ulcers: a review. *Arch Phys Med Rehabil*, 75, 908-917.
- Yuen, J., & Feng, Z. (2000). Monitoring free flaps using the laser Doppler flowmeter: five-year experience. *Plast Reconstr Surg*, 105, 55-61.
- Yvonne-Tee, G. B., Rassol, A. H. G., Halim, A. S., & Rahman, A. R. A. (2005). Reproducibility of different laser Doppler fluximetry parameters of postocclusive reactive hyperemia in human forearm skin. *J Pharmacol Toxicol*, 52, 286-292.
- Zhao, H., Steinberg, G. K., & Sapolsky, R. M. (2007). General versus specific actions of mild-moderate hypothermia in attenuating cerebral ischemic damage. *J Cerebr Blood F Met*, 27, 1879-1894.

